Review

International Journal of Modern Physics A
Vol. 23, No. 1 (2008) 1–141

World Scientific
www.worldscientific.com

ASTROPHYSICAL ASPECTS IN THE STUDIES OF SOLAR COSMIC RAYS

L. I. MIROSHNICHENKO*,†,‡,§ and J. A. PEREZ-PERAZA*,¶

Instituto de Geofísica, Universidad Nacional Autónoma de México (UNAM), C.U., Coyoacán, 04510, México, D.F., Mexico

and

†*N. V. Pushkov Institute of Terrestrial Magnetism, Ionosphere and Radio Wave Propagation (IZMIRAN), Russian Academy of Science, Troitsk, Moscow Region, 142190, Russia*

‡*leonty@geofisica.unam.mx*

§*leonty@izmiran.ru*

¶*perperaz@igeofcu.unam.mx*

Received 31 July 2007
Revised 4 October 2007

This review paper comprises main concepts, available observational data and recent theoretical results related to astrophysical aspects of particle acceleration at/near the Sun and extreme capacities of the solar accelerator(s). We summarize underground and ground-based observations of solar cosmic rays (SCR) accumulated since 1942, direct spacecraft measurements of solar energetic particles (SEP) near the Earth's orbit, indirect information on the SCR variations in the past, and other relevant astrophysical, solar and geophysical data. The list of the problems under discussion includes: upper limit spectrum (ULS) for solar cosmic rays; maximum energy (rigidity), E_m (R_m), of particles accelerated at/near the Sun; production of the flare neutrinos; energetics of SCR and solar flares; production of flare neutrons and gamma rays; charge states and elemental abundances of accelerated solar ions; coronal mass ejections (CME's) and extended coronal structures in acceleration models; magnetic reconnection in acceleration scenarios; size (frequency) distributions of solar proton events (SPE) and stellar flares; occurrence probability of giant flares; archaeology of solar cosmic rays. The discussion allows us to outline a series of interesting conceptual and physical associations of SCR generation with the high-energy processes at other stars. The most reliable estimates of various parameters are given in each of research fields mentioned above; a set of promising lines of future studies is highlighted. A great importance of SCR data for resolving some general astrophysical problems is emphasized.

Keywords: Solar flares; particle acceleration; cosmic rays; astroparticles; neutrino; magnetic reconnection.

Contents

1. Introduction

Flares on the Sun and other stars are important to astrophysics because they originate in out-of-equilibrium magnetic field-plasma interactions rather than in gravitational, thermonuclear, or radiative processes in near equilibrium. According to Haisch *et al.*,[129] flaring stars constitute about 10% of the stars in the Galaxy. In spite of its rather modest place in star hierarchy, the Sun is an invaluable proving ground to test predictions of flare theories and to develop analytical techniques for future stellar application. In turn, extreme flare star conditions impose the limits of models.

In this context, a flare may be defined as a catastrophic release of magnetic energy leading to particle acceleration and electromagnetic radiation, bearing in mind that the magnetic energy release has never been directly observed. Since flare-like physical processes occur in diverse astrophysical regimes, the field of solar and stellar flares can serve as an astrophysical "touchstone" (e.g. Refs. 128, 314 and 129). On the other hand, solar flares release a considerable portion of their energy (up to $\sim$10%) in the form of solar cosmic rays (SCR), mainly protons with the energy range 1 MeV–10 GeV.

These particles are observed near the Earth's orbit as a solar particle event (SPE). Spectral characteristics, elemental abundances and some other features of solar cosmic rays are quite different from those for galactic cosmic rays (GCR). Nevertheless, in many other respects, SCR are consistent with more extended panorama of astrophysics of cosmic rays (e.g. Ref. 35).

Historically, over the years the solar particle occurrences have been referred to by a number of descriptive names such as solar cosmic ray (SCR) events, solar proton events (SPE), solar energetic particle (SEP) events, Ground Level Enhancements, or Ground Level Events (GLE), and polar cap absorption (PCA) events (e.g. Refs. 334, 228 and 229). It is widely recognized now that SCR events are time associated with fast coronal mass ejections (CME's) that drive shocks and may be a significant (and perhaps the dominant) source of MeV ions observed in the interplanetary space (e.g. Ref. 292). There are also compelling evidences that both flares and CME's are products of magnetic reconnection process, usually occurring at the Sun in active magnetic field regions of great complexity.

In general, the energy release of solar energetic phenomena occurs partly in electromagnetic radiation (e.g. X-rays), partly in kinetic energy of ejecta, and partly in energetic particles. Each form affects the terrestrial environment differently, but in a crude first approximation they can be compared either on the basis of total energy release (energy fluence) in individual events, or in terms of peak fluxes measured (estimated) at the boundary of the terrestrial magnetosphere.

From another point of view, it is worth to remind that in space research we deal with the four groups of fundamental factors — physical fields, particles, waves and electromagnetic emissions of different frequencies. Heaving been involved in different processes, SCR contribute valuable information into all four branches of investigations. For example, they allow probing the magnitude, structure and dynamics of magnetic fields in the Sun's environment. Some results of SEP investigation (composition and spectrum of accelerated solar particles, their maximum energy, charge states, etc.) may be very helpful for the theory of acceleration and particle astrophysics. Finally, recent findings in the study of particle acceleration by coronal and interplanetary shocks are of common interest for astrophysical plasma physics (for a recent review see, e.g. Refs. 292 and 228).

The discussion below allows outlining a series of interesting conceptual and physical associations, common features and close analogies of SCR generation with the high-energy physical processes at other stars and in the astrophysical plasmas. The most reliable estimates of various parameters are given in each of research fields mentioned above; a set of promising lines of future studies (though disputable at present time) is highlighted. It is emphasized a great importance of SCR data for resolving some general problems of astrophysics and plasma physics.

2. The Sun as a Source of Cosmic Rays

Due to spacecraft measurements, at present it became possible to observe solar energetic particles (SEP's) near the Earth's orbit (at 1 AU) in the range of $E \geq 0.5$ MeV/nucleon, and an occurrence rate of the SPE's turned out to raise drastically with decreasing of the threshold energy of their detection. An average rate of the SPE occurrence is about 1.1 y^{-1} (events per year) at $E \geq 433$ MeV/nucleon (or magnetic rigidity $R \geq 1$ GV), about 2.0 y^{-1} at $E \geq 100$ MeV/nucleon, and ≥ 250 y^{-1} at $E \leq 10$ MeV/nucleon (for protons). Decreasing of the threshold energy of registration, increasing of the detector sensitivity and duration of spacecraft measurements allowed to conclude that the Sun is, in fact, a permanent source of SEP's with the energies of $E \geq 1$ MeV/nucleon.

2.1. *Brief history and detection technique*

Continuous measurements of sea level ionizing radiation using ionization chambers began in the 1920's, but the validity of the observed intensity variations was doubtful because of atmospheric effects and instrument instability (e.g. Ref. 329). Some later, Compton *et al.*[58] developed an ionization chamber (IC) of general purpose

wherein the average cosmic ray background ionization was nulled out, so current variations above and below the ambient null were represented as time-intensity variations. Just this improved installation has played a crucial role in a discovery of SCR at the beginning of 1940's. Although there was evidence that observers in the 1920–1930's had recorded intensity increases, which were due to solar flares (e.g. Ref. 51), the intensity increases of 28 February and 7 March 1942 associated with solar flares first drew attention to the importance of high-energy particles from the Sun.

The observations of solar activity (manifested as interference in detection and surveillance equipment), however, were shrouded in secrecy by the antagonists of the Second World War (e.g. Ref. 334). Only several years after, when two similar events occurred — on 25 July 1946 and 19 November 1949[102,104] — the explanation of solar flare association of observed relativistic particles was given respectable scientific credence.

Similar observations and research work were going on in Europe, and they have reached similar conclusions (e.g. Ref. 82). In fact, due to these observations two important astrophysical phenomena, namely, Ground Level Events of two kinds were discovered for the first time. According to Simpson,[329] the first kind is rapid intensity increase of SCR (Ground Level Enhancement, or GLE's), and the second one is rapid GCR intensity decrease (or Forbush-decrease, FD), both of them being caused by energetic solar phenomena.

The initial observations of SCR relied upon measurements of secondary particles (muons) generated at the top of the Earth's atmosphere. The original ionization chambers (IC) and counter telescopes are now classified as muon detectors (in particular, standard muon telescope (MT)). These detectors respond to primary high-energy (> 4 GeV) protons interacting at the top of the atmosphere. In the 1950's, development of the cosmic-ray neutron monitor (NM) lowered the detection threshold to > 450 MeV primary protons.[328] A number of standard neutron monitors (NM of IGY type) were deployed for the International Geophysical Year — IGY (1957–1958), and due to those instruments, in particular, an outstanding SCR event of 23 February 1956 has been recorded. Some later the design was improved[47] with the development of the so-called "super" neutron monitor (SNM-1964).

Concurrently, more sensitive instruments were developed that could directly measure the incident particles. These detectors were initially carried by balloons to get above as much of the Earth's atmospheric shielding as possible; later these detectors were adapted for the initial man-made Earth-orbiting satellites. While cosmic-ray researchers were developing their instruments, high-frequency communication engineers, particularly those involved in the propagation of electromagnetic signals in the polar regions, noted interference that seemed to be associated with solar activity. It is now well known that charged particles interacting with the Earth's ionosphere enhance the ionization and change the electromagnetic propagation characteristics of the medium.

In the late 1950's, the development of the riometer (radio ionosphere opacity meter) proved to be very sensitive to particle deposition in the ionosphere directly above the instrument.[184] Even though the riometer could not uniquely distinguish the type of particle, its sensitivity was equivalent to the early satellite instruments. Most of the solar particle flux and fluence data available from the 19th solar cycle (1955–1965) were derived from riometer measurements in the Earth's polar regions (e.g. Ref. 71). Even now the ionosphere can still be used as a very sensitive (but nonlinear) particle detection medium, since very low frequency phase and amplitude changes along transpolar propagation paths have the same approximate detection thresholds as particle detectors on spacecraft.[334] Comprehensive summary of the first studies of SCR was presented by Dorman,[72,73] Dorman and Miroshnichenko,[74] Sakurai,[308] Duggal,[78] Dorman and Venkatesan.[75]

Figure 1 gives a summary of observational technique for SCR study. It illustrates very visually the evolution of detection energy thresholds and detector techniques since 1933.[334] In particular, regular balloon observations of SEP's in the energy interval of 100–500 MeV are being performing since 1958 by Lebedev Physical Institute (LPI, Moscow) at high and mid-latitudes (e.g. Refs. 24, 28 and 22). Since

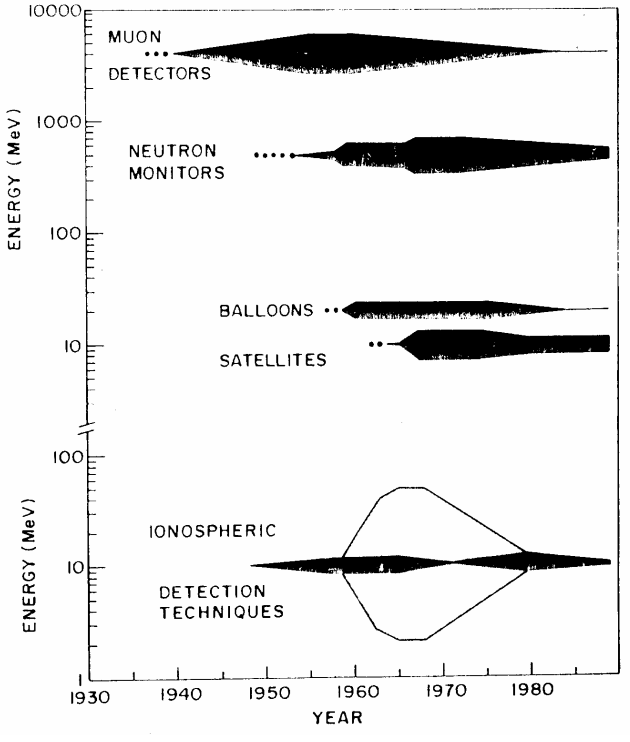

Fig. 1. Conceptual history of the detection thresholds of solar proton events. The thickness of the lines indicates the relative number of each type of detector in use. The difference in shading in the ionospheric section indicates changes in detection technique.[334]

the beginning of 1990's, regular observations of high-energy solar neutrons started with special Solar Neutron Telescopes (SNT) (e.g. Ref. 101) by the "World Neutron Network" (for details and references, see e.g. Ref. 228).

2.2. *Observation database*

From the beginning of the 1980's, for the SCR studies it became possible to use also the data of some large nonstandard detectors, LNSD (for instance, Baksan Underground Scintillation Telescope (BUST), Extensive Air Shower (EAS) Arrays like Carpet and Andyrchy, Baksan Muon Detector, Project GRAND Array, Milagrito and others). Even though those detectors have been designed for resolving quite different nuclear and astrophysical problems, nevertheless, they proved to be sensible to the effects caused by powerful sporadic manifestations of the solar activity (e.g. Refs. 146, 147 and 63). These observations allow to advance into the energy range far above 10 GeV (probably, up to ≥ 100 GeV) and understand more distinctly the extreme potentialities of solar accelerators (e.g. Refs. 228, 230 and 232).

Historical review shows that many other intensity increases of cosmic rays were also observed between 1941 and 1943 (e.g. Ref. 51, and references therein). It is considered, nevertheless, that a historical beginning of SCR observations was a GLE of solar cosmic rays on 28 February 1942. Since then up to now (July 2007) 70 similar events have been recorded by the worldwide network of cosmic ray stations (the last one was observed on 13 December 2006). These events characterize only one, relativistic part of entire energy spectrum of SCR (kinetic energy $E \geq 433$ MeV/nucleon, or magnetic rigidity $R \geq 1$ GV). If the energy of primary protons is < 100 MeV ($R < 0.44$ GV), neutron monitors are practically do not respond them due to atmospheric absorption of neutrons (the so-called "atmospheric cutoff," R_a), a maximum of the NM response being within 1–5 GV. It means that all high-latitude (polar) NM stations start to record secondary neutrons efficiently from the same rigidity of the primary protons about 1 GV, irrespective of the NM nominal (calculated) "geomagnetic cutoff rigidity," R_c.

As it fortunately happened, a rigidity 1.0 GV ($\sim$433 MeV) is approximately midway between the low rigidity and ultrarelativistic rigidity range, and it turned out to be a convenient reference point as a characteristic rigidity threshold at the polar NM stations.[337]

Surface detectors of the secondary muons have their detection threshold R_a about 4 GV determined by air mass absorption for muons. Underground muon telescopes have their own rigidity thresholds, R_u, quite different from the first two and determined by rock mass above the instruments. For a comparison, we cite here the threshold rigidities of 19 GV and 500 GV, respectively, for two underground telescopes located in Embudo Cave near Albuquerque, New Mexico, USA[350] at the depth of 35 meters of water equivalent (m.w.e.) and in Baksan Valley, Russia, at the depth of 850 m.w.e. under the mountain Andyrchi, Northern Caucasus (e.g. Ref. 146.

Space does not allow discussing here in detail each of 70 relativistic SPE's, or GLE's, compiled for the entire period of SCR observations (since February 1942 up to July 2007). In Table 1 we only show a complete list of observed GLE's in their modern numeration. Some of them are discussed in more detail by Miroshnichenko.[228] There were also mentioned several Catalogues of Solar Proton Events since 1955 up to 1997.[71,6,26,27,332] Electronic version of the SPE Catalogue data has been prepared by Sladkova.[331] Very important work was carried out by Gentile[115] who has compiled a database of the GLE's observed during the 22nd solar activity cycle. A database for SCR measurements carried out on board a series of Soviet space vehicles in 1964–1989 has been elaborated by Getselev *et al.*[116]

An extended catalogue of the source proton spectra (SPS) for 80 proton events has been prepared by Miroshnichenko *et al.*[238] In some recent publications one can find also a number of other catalogues (or lists) of proton, electron, neutron, gamma ray and other energetic solar events. The most of them were compiled by the data of different spacecraft measurements (IMP, Meteor, GOES, SMM, Compton Gamma Ray Observatory, GRANAT Observatory and many others). For example, we mention the energy spectra for 55 electron events of the period 1978–1982,[246] the list of solar proton events 1980–1985 by Cliver *et al.*,[54] the data sets of the IMP-8[14] and GOES,[388] the table of GRANAT solar flare data of 1990–1994 by Terekhov *et al.*[352] and the Atlas of the SMM gamma-ray bursts of 1980–1989 by Vestrand *et al.*[383] As a summary of the early solar proton events the *Solar Proton Manual* edited by McDonald[208] is also very helpful. All these collections of data form a very solid base for different kind of fundamental and applied research in the field of solar and solar-terrestrial physics.

2.3. *Classification systems for solar energetic particles*

A great variety of the SPE's observed near the Earth's orbit, in their energy spectra, intensities, elemental abundances, charge states, spatial and temporal properties make serious difficulties of the classification and analysis of the events. The best classification system remains up to now that one proposed by Smart and Shea.[333] This system relies upon three intensity digits: integral (peak) flux of protons at the energy $E_p > 10$ MeV by spacecraft measurements; daylight polar cap absorption at 30 MHz (PCA effect); sea level neutron monitor increase. According to this system, any SCR increase may be characterized by three indexes.

For example, the GLE of 23 February 1956 — the biggest one during the entire period of SCR observations — has an importance X34, where X means that there were no space observations of SCR in 1956; Fig. 3 corresponds to the PCA in the interval of 4.6–15 dB, and Fig. 4 indicates to strong ($> 100\%$) increase of counting rate at sea level neutron monitor. Based on this system, several SPE catalogues have been compiled.[71,6,26,27,331,332] To characterize a SPE flux a special unit is often used: 1 proton flux unit (pfu) = 1 particle cm^{-2} s^{-1} sr^{-1} = 10^4 particle m^{-2} s^{-1} sr^{-1}.

Table 1. Ground-level enhancements (1942–2006).

GLE number	Observation date	Flare position	Onset UT	Flare $H\alpha/X$	Data reference
1	28 Feb 1942	07N 04E	N.O.	3+	78
2	07 Mar 1942	07N 90W	N.O.	—	78
3	25 Jul 1946	22N 15E	1615	3+	78
4	19 Nov 1949	03S 72W	1029	3+	78
5	29 Feb 1956	23N 80W	$<$ 0334	3	S. & S. 1975
6	31 Aug 1956	15N 15E	1226	3	S. & S. 1975
7	17 Jul 1959	16N 31W	2114	3+	S. & S. 1975
8	04 May 1960	13N 90W	1000	3	S. & S. 1975
9	03 Sep 1960	18N 88E	0037	2+	S. & S. 1975
10	12 Nov 1960	27N 04W	1315	3+	S. & S. 1975
11	15 Nov 1960	25N 35W	0207	3+	S. & S. 1975
12	20 Nov 1960	28N $\sim$ 112W	2017	2	S. & S. 1975
13	18 Jul 1961	07S 59W	0920	3+	S. & S. 1975
14	20 Jul 1961	06S 90W	1553	3	S. & S. 1975
15	07 Jul 1966	35N 48W	0025	2B	S. & S. 1975
16	28 Jan 1967	22N $\sim$ 150W	$<$ 0200	—	S. & S. 1975
17	28 Jan 1967	22N $\sim$ 150W	$<$ 0800	—	S. & S. 1975
18	29 Sep 1968	17N 51W	1617	2B	S. & S. 1975
19	18 Nov 1968	21N 87W	$<$ 1026	1B	S. & S. 1975
20	25 Feb 1969	13N 37W	0900	2B/X2	S. & S. 1975
21	30 Mar 1969	19N 103W	$<$ 0332	1N	S. & S. 1975
22	24 Jan 1970	18N 49W	2215	3B/X5	SGD 323B 19
23	01 Sep 1971	11S 120W	$<$ 1934	—	SGD 327A 82
24	04 Aug 1972	14N 08E	0617	3B/X4	SGD 342B 06
25	07 Aug 1972	14N 37W	1449	3B/X4	SGD 342B 09
26	29 Apr 1973	14N 73W	2056	2B/X1	SGD 350B 23
27	30 Apr 1976	08S 46W	2047	1B	SGD 386B 11
28	19 Sep 1977	08N 57W	$<$ 0955	3B/X2	SGD 403B 14
29	24 Sep 1977	10N 120W	$<$ 0552	—	SGD 399A109
30	22 Nov 1977	24N 40W	0945	2B/X1	SGD 405B 13
31	07 May 1978	23N 72W	0327	1N/X2	SGD 411B 11
32	23 Sep 1978	35N 50W	0944	3B/X1	SGD 415B 26
33	21 Aug 1979	17N 40W	0550	2B	SGD 436B 70
34	10 Apr 1981	07N 36W	1632	2B/X2.3	SGD 474B 53
35	10 May 1981	03N 75W	0715	1N	SGD 475B 31
36	12 Oct 1981	18S 31E	0615	2B/X3.1	SGD 481B 54
37	26 Nov 1982	12S 87W	0230	1N	SGD 487B173
38	07 Dec 1982	19S 86W	2341	1B/X2.8	SGD 488B 26
39	16 Feb 1984	$-$S $\sim$ 130W	$<$ 0858	—	SGD 476A 99
40	25 Jul 1989	26N 85W	0839	1B	SGD 545B 22
41	16 Aug 1989	15S 85W	0058	2N	SGD 546B 26
42	29 Sep 1989	24S $\sim$ 105W	1141	1B/X9	SGD 547B 38

Table 1. (*Continued*)

GLE number	Observation date	Flare position	Onset UT	Flare $H\alpha/X$	Data reference
43	19 Oct 1989	25S 09E	1229	3B	SGD 548B 19
44	22 Oct 1989	27S 32W	1708	1N	SGD 548B 24
45	24 Oct 1989	29S 57W	1738	2N	SGD 548B 27
46	15 Nov 1989	11N 28W	0638	2B	SGD 449B 20
47	21 May 1990	34N 37W	2212	2B	SGD 555B 23
48	24 May 1990	36N 76W	2046	1B	SGD 555B 25
49	26 May 1990	$\sim$35N $\sim$103W	2045	—	SGD 555B 61
50	28 May 1990	$\sim$35N $\sim$120W	$<$0516	—	SGD 555B 63
51	11 Jun 1991	32N 15W	0105	2B/X12	SGD 568B 14
52	15 Jun 1991	36N 70W	0633	3B/X12	SGD 568B 20
53	25 Jun 1992	09N 69W	1947	2B	SGD 580B 17
54	02 Nov 1992	$\sim$25S $\sim$100W	0231	−/X9	SGD 580A 28
55	06 Nov 1997	18S 68W	1149	2B/X9.4	SGD 640A 29
56	02 May 1998	15S 15W	1334	3B/X1.1	SGD 646A 28
57	06 May 1998	11S 65W	0758	1N/X2.7	NM Database
58	24 Aug 1998	18N 09E	2148	3B/M7.1	NM Database
59	14 Jul 2000	22N 07W	1003	3B/X5.7	NM Database
60	15 Apr 2001	20S 85W	1319	2B/X14.4	NM Database
61	18 Apr 2001	23S W117	0211	−/−	NM Database
62	04 Nov 2001	06N 18W	1603	3B/1.3	NM Database
63	26 Dec 2001	08N 54W	0432	−/M7.1	NM Database
64	24 Aug 2002	02S 81W	0049	−/X3.1	NM Database
65	28 Oct 2003	20S 02E	1100	4B/X17	NM Database
66	29 Oct 2003	19S 09W	2037	−/X10	NM Database
67	02 Nov 2003	18S 59W	1718	2B/X8.3	NM Database
68	17 Jan 2005	15N 25W	0659	3B/X3.8	NM Database
69	20 Jan 2005	14N 61W	0639	2B/X7.1	NM Database
70	13 Dec 2006	06S 23W	0217	4B/X3.4	NM Database

Notes:

(1) SGD XXXB PG refers to Solar-Geophysical Data, v. XXX, part Y, p. ZZ.
(2) S. & S. refers to the Catalogue of Solar Proton Events 1955–1969[71] edited by Z. Svestka and P. Simon.
(3) N.O. stands for No optical observations. Positions of some behind-the-limb flares have been estimated from location of assumed associated active region.
(4) In recent years, many researchers use a new ordinal numeration for GLE's. For example, the events of 23 February 1956 and 20 January 2005 have now the numbers GLE05 and GLE69, respectively.

During the three last decades, due to regular spacecraft observations of X-ray emissions from solar flares, a new classification of SEP events raised, depending on the features of originating flare, namely, on the duration of soft X-ray burst (e.g. Ref. 291). In the light of a current paradigm of particle acceleration (see Subsec. 6.3) in different sources at/or near the Sun (impulsive or gradual flares, CME-driven

Table 2. Properties of impulsive and gradual events.[291]

Parameters of particles, observation method	Impulsive events	Gradual events
Particles	Electron-rich	Proton-rich
^{3}He/^{4}He	~ 1	~ 0.0005
H/He	~ 1	~ 0.1
Fe/O	~ 10	~ 100
Q(Fe)	~ 20	~ 14
Duration	Hours	Days
Longitude cone	< 30 degrees	~ 180 degrees
Radio type	III, V (II)	II, IV
X-rays	Impulsive	Gradual
Coronograph	—	CME's (96%)
Solar wind	—	IP Shock
Events/year	~ 1000	~ 10

shocks, etc.) it becomes a very keen problem of SPE identification with different sources.

Historically, the terms *impulsive* and *gradual* referred to the time duration of the soft X-rays in the event (namely, < 1 h and > 1 h, respectively). However, it became clear later that there are other differences as well, in both the radiations that are emitted and the particles that are observed in space. In particular, the X-ray duration gives only a poor, statistical distinction of the underlying mechanisms, while the particle abundances, for example, distinguish them clearly.

The properties of gradual and impulsive events as they were summarized by Reames[291] are given in Table 2. This author suggested using the terms impulsive and gradual to refer to the underlying acceleration mechanisms, irrespective of the actual X-ray duration in an event. Of course, there are events in which *both*, impulsive and gradual, phenomena occur (e.g. Ref. 53). It is important that more recent observations seem to allow one to extend this concept to particles of very high energy. In particular, Kahler[138] argued that even in GLE's, particles of ~ 20 GeV have a clear association with CME-driven shocks. At the same time, some open questions of this classification, as well as of the current paradigm of SEP acceleration in the whole, still exist (see Subsec. 6.3).

Cliver[53] has expanded Table 2 to include characteristics of the particles that interact at the Sun to produce gamma-ray emission. This addition underscores the contributions of gamma-ray observations to our current understanding. The broad picture that is emerging is remarkable for its simplicity: while SEP events come in two basic types depending on the duration of the associated flares, the interacting particles in impulsive and gradual flares appear to be indistinguishable and resemble the SEP's observed in space following impulsive flares. The Expanded Classification System by Cliver[53] includes also the so-called "hybrid" events, i.e. flares in which

the gradual/impulsive distinction is blurred and for which the SEP events contain a *mixture* of flare-accelerated and CME/shock-accelerated particles. It is suggested that SEP events associated with long duration flares can be expected to have a temporally and spatially confined "core" of flare-accelerated particles surrounded by a "halo" of CME/shock particles.

Proton events can also be classified in terms of fluence (i.e. event-integrated flux in units of cm^{-2}, or proton cm^{-2}). For example, Nymmik[256] suggested to separate the SEP events into several classes, according to fluence of protons $F_s\,(>30$ MeV). Studies of the dependence of event occurrence rate on proton fluence brought conclusion (e.g. Refs. 394, 94 and 95) that this distribution is described by log–normal function

$$\Psi(f) = \frac{1}{(2\pi\sigma)} \exp\left[-0.5\left\{\frac{(f-f_0)}{\sigma}\right\}\right], \tag{1}$$

where $f = \log[F_s(E)]$ is the logarithm of fluence magnitudes, and f_0 and σ are parameters of the normal distribution which, for protons with energies ≥ 30 MeV, have the values $f_0 = 6.93$ and $\sigma = 1.19$.[94,95] It appears logical to separate this set into groups (classes), according to fluence magnitudes,[256]

$$F_k = 10^{(f+k\sigma/2)}, \tag{2}$$

where $k = -1, 1, 3, 5$. The distribution function in fluence of protons $F_s\,(>30$ MeV) with the proposed classification is shown in Fig. 2. The group names, symbols, and mean fluence values in the different groups (with account for the probability density) for the suggested classification are given in Table 3.

This classification contains the VL and EL events that are analogues of "anomalously large" events used in some other models (e.g. Refs. 2 and 334). The only difference is that Nymmik[256] suggests precise quantitative criteria to analyze the

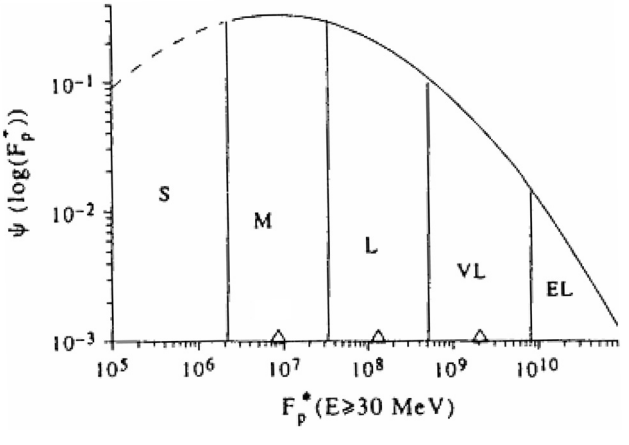

Fig. 2. Logarithmic normal distribution of SCR events on fluence magnitude of protons F_s (>30 MeV), according to Feynman *et al.*,[94,95] and the event classification of Nymmik.[256]

Table 3. Proton events classification by fluence, F_s (> 30 MeV), cm^{-2}.[256]

Name	Symbol	Interval	Mean value
Small	S	$< 2.0 \times 10^6$	5.50×10^5
Medium	M	2.0×10^6–3.3×10^7	8.60×10^6
Large	L	3.3×10^7–5.2×10^8	1.05×10^8
Very large	VL	5.2×10^8–8.0×10^9	1.34×10^9
Extremely large	EL	$> 8.0 \times 10^9$	(3.30×10^{10})

SCR phenomena development. As one can see, in the range of smaller fluences an evident upturn takes place. This can be explained by the fact that a log–normal distribution will underestimate such minor events since, empirically, the number of smaller events increases as fluence decreases,[94,95] whereas an inherent property of the distribution function requires that the opposite be true below the mean value. Thus, a second contributing factor is the fact that an upturn is an unavoidable consequence of truncating a data set.

In conclusion of this section, it is necessary to note some issues which still remain rather disputable. In particular, unlike a log–normal distribution used by Feynman *et al.*[96] for the > 10 MeV proton events, Nymmik[256,257] proposed for the > 30 MeV protons a power-law function with exponential steepening at large fluences. His model predicts the > 30 MeV proton fluence range from 10^6 to 10^{11} cm^{-2}. Meanwhile, according to Lingenfelter and Hudson[182] and Gabriel and Feynman,[425] the corresponding distributions become considerably steeper starting from fluences about 10^9 cm^{-2}. Also, the threshold effects of detection and separation of proton events may be important at low fluences.

3. Solar Cosmic Rays at High Rigidity

Proceeding from physical or practical reasons, some researchers distinguish the most powerful SPE's into a special group. The event data with large fluxes of relativistic protons (for example, two GLE's of 23 February 1956 and 29 September 1989) are used then for evaluation of the extreme possibilities of a solar accelerator.[224,373] This list may now be complemented by the recent very large GLE event of 20 January 2005 (or GLE69). If the main increase is observed in the nonrelativistic range (for example, in July 1959, August 1972, October 1989) then such an event is most suitable for modeling of "a worst case" from the point of view of radiation hazard.[2,334,229]

In this context, data on the most powerful proton events are summarized below (Subsec. 3.1), and a concept of the upper limit spectrum (ULS) is grounded (Subsec. 3.2). As the basis for the concept it was suggested to synthesize the proton spectra obtained for different energy intervals during the largest SPE's.[226] The data on maximum rigidity of SCR are considered in Subsec. 3.3. We also briefly discuss existing constraints on maximum energy of solar cosmic rays (Subsec. 3.4).

3.1. *Largest proton events since 1942*

We selected the maximum proton intensities, $I_m\,(>E_p, t_m)$, obtained for different energy intervals by various methods of observations at the Earth, in the stratosphere, ionosphere and near-Earth space environment since 1942 till 2007 (till the end of the 23rd solar cycle). As a result, a set of the 30 largest events was formed (Table 4). In total, in 1987–1996 (during the 22nd solar cycle) 18 events with a magnitude $\geq$ 1000 pfu at $>$ 10 MeV have been detected near the Earth's orbit including three events with the proton intensity above 10^4 pfu.[332]

More recently, Reedy[300] has published the event-integrated fluences of solar protons $>$ 10 to $>$ 100 MeV for 21 events since 1996 up to the end of 2001. Minimum fluence of the $>$ 10 MeV protons, 5.0×10^6 cm^{-2}, was obtained for the event of 20 May 2001, the largest fluences, 1.10×10^{10} and 1.5×10^{10} cm^{-2}, were fixed during the events of 14 July 2000 (Bastille Day Event, or BDE) and 5 November 2001, respectively. The events of February 1956, August 1972, September and October 1989 are of special interest. Quite recently, on 20 January 2005, a new very large GLE occurred. According to recently revised data by P. Lantos (Observatoire de Paris-Meudon), the magnitude of increase at the NM Terre Adelie (Antarctic) was 4527.4% by 1-minute data.

Table 4 demonstrates extreme possibilities of the Sun's proton production for the entire period of SCR observations (since 1942). For example, the GLE05 of 23 February 1956 is very likely the most intense event as to total number of relativistic protons (4554% by 15-minute data of neutron monitors). As to nonrelativistic energies the largest events range over a rather narrow intensity interval, mainly between well-known events of 23 February 1956 and 4 August 1972, with the exception of 20 October 1989 event.

However, since October 1989 the event of 4 August 1972 would not be considered any longer as "the worst case" from the point of view of radiation hazard, as it was proposed earlier.[2,334] As to the GLE69 of 20 January 2005, obviously, this event would become No. 2 in the "hierarchy" of the GLE's since 1942, after the event of 23 February 1956 (see also Table 5 below).

At the same time, it would be erroneous to ignore some indirect (the so-called "archaeological") evidence of the Sun producing a greater amount of nonrelativistic protons than was observed, for example, in August 1972 or in October 1989. Thus, for instance, the high-resolution analysis of the content of different nitrogen oxides NO_x in the cores of Antarctic ice (the so-called "nitrate method," see Subsec. 13.2) have revealed several anomalously large concentration peaks.[76] The peaks have been dated with confidence and found to correlate with the white-light flare of July 1928 and with two major solar proton events of 25 July 1946 and 4 August 1972. The magnitudes of the peaks were about 4, 11 and 7 of standard deviations, respectively.

If solar protons with the energies up to 500 MeV are considered to give the main contribution to the concentration jumps, then from the data of Dreschhoff and Zeller[76] it follows that the fluence F_s (i.e. total event-integrated flux) of low-energy

Table 4. Largest solar proton events of 1942–2006.

Event number	SPE date	Flare importance	Energy, E_p, MeV	Flux, $I_m\,(>E_p)$, $\mathrm{cm^{-2}\ s^{-1}\ sr^{-1}}$	Observation technique
1	19 Nov 1949	3+	>435	4.1×10^{1}	IC
2	23 Feb 1956	3+	>435	2.5×10^{2}	IC, NM
3	15 Jul 1959	3+	>88	2.4×10^{2}	Balloon
4	12 Nov 1960	3+	>10	2.1×10^{4}	PCA
5	15 Nov 1960	3+	>10	2.1×10^{4}	PCA
6	12 Jul 1961	3	>10	2.5×10^{4}	PCA
7	18 Jul 1961	3+	>10	6.3×10^{3}	PCA
8	04 Aug 1972	3B/X5	>25	1.0×10^{4}	Meteor
9	09 Jul 1982	3B/X9.8	>10	5.8×10^{3}	Meteor
10	12 Aug 1989	2B/X2	>10	6.6×10^{3}	Meteor, GOES
11	29 Sep 1989	$-$?/X9.8	>10	3.2×10^{3}	Meteor, GOES
			>600	1.5×10^{0}	Meteor
12	19 Oct 1989	4B/X13	>10	2.9×10^{3}	Meteor, GOES
13	20 Oct 1989	The same	>10	4.0×10^{4}	Meteor, GOES
		flare	>25	2.2×10^{4}	Meteor
14	22 Oct 1989	The same	>10	5.7×10^{3}	Meteor, GOES
15	24 Oct 1989	The same	>10	3.3×10^{3}	Meteor, GOES
16	30 Nov 1989	3B/X2	>10	4.4×10^{3}	Meteor, GOES
17	22 Mar 1991	3B/X9	>10	5.0×10^{4}	Meteor, GOES
18	11 Jun 1991	3B/X12	>10	8.0×10^{3}	GOES, Meteor
19	15 Jun 1991	3B/X12	>10	1.2×10^{3}	Meteor, GOES
20	07 Jul 1991	2B/X1	>10	2.0×10^{3}	Meteor, GOES
21	08 May 1992	4B/M7	>10	4.5×10^{3}	Meteor, GOES
22	30 Oct 1992	2B/X1	>10	1.4×10^{4}	Meteor, GOES
23	02 Nov 1992	2B/X9	>10	1.8×10^{3}	Meteor, GOES
24	20 Feb 1994	3B/M4	>10	7.0×10^{3}	Meteor, GOES
25	06 Nov 1997	2B/X9	>10	5.0×10^{2}	GOES
26	14 Jul 2000	3B/X5	>10	2.2×10^{4}	GOES
27	15 Apr 2001	2B/X14	>10	7.8×10^{2}	GOES
28	28 Oct 2003	4B/X17	>10	3.0×10^{4}	GOES
29	02 Nov 2003	2B/X8.3	>10	1.6×10^{3}	GOES
30	20 Jan 2005	2B/X7.1	>10	1.9×10^{3}	GOES

Notes: IC: ionization chamber; NM: neutron monitor; PCA: polar cap absorption. Flare importance since 1966 is estimated in optical and X-ray ranges.

(nonrelativistic) protons in July 1946 could be 1.5 times or more the fluence of August 1972. Meanwhile, in the relativistic region, the event magnitude in July 1946 was about 15 times less than in February 1956, according to ionization chamber data compiled by Smart and Shea.[336] It implies that the July 1946 event was similar to (and exceeded) the event of 4 August 1972. On the whole, three major SPE's (July 1946, August 1972, and October 1989) observed in different solar cycles turned out to produce the comparable amounts of nonrelativistic protons.

Table 5. Magnitudes of GLE's (in %) in solar cycles 17–23 (adapted after Smart and Shea,[336]).

Rank	Date	Ion chamber	Muon telescope	Neutron monitor
1	23 Feb 1956	300	280	4554 (15-min)
2	20 Jan 2005	N.O.	No increase?	4527.4 (1-min)
3	19 Nov 1949	41	70	563
4	29 Sep 1989	N.O.	41	373
5	25 Jul 1946	20	N.O.	N.O.
6	28 Feb 1942	15	N.O.	N.O.
7	07 Mar 1942	14	N.O.	N.O.

Notes: N.O.: no observations. It seems there was no increase at the standard MT's on 20 January 2005, but some nonstandard muon detectors registered statistically significant effects in muon component.

The first three GLE's (28 February 1942, 07 March 1942, and 25 July 1946) have been detected only by ionization chambers; one nonstandard neutron monitor was also in operation to record the fourth event of 19 November 1949. Using these measurements, Smart and Shea[336] evaluated relative amplitude of these early events. The GLE42 of 29 September 1989 which Smart and Shea[336] have used as a calibration event would rank third in this "hierarchy." However, at present, the GLE69 of 20 January 2005 seems to be ranked as No. 2, in spite of the absence of discernible increase at standard surface muon telescopes. Statistically significant effects in muon component, however, have been registered by two *nonstandard muon detectors*, Carpet and BMD, at the Baksan Neutrino Observatory,[147] and by an array of *proportional wire chamber* stations, Project GRAND.[63] According to the Project GRAND data, in the interval from 06:51 to 06:57 UT a peak intensity of $13 \pm 1\%$ occurred at the same time as the Newark NM signal and preceded the peak for the Oulu NM by nine minutes.

The "magnitude" distribution of GLE's is illustrated by Table 5. Based on both the muon and neutron monitor data, the GLE of 19 November 1949 is larger than the event of 29 September 1989; however, the well-known GLE of 23 February 1956 will rank No. 1. Note, meanwhile, that any kind of SPE classifications depends strongly of the key parameters used (spectrum shape, intensity or fluence, energy or rigidity range under consideration, etc.).

3.2. *Upper limit spectrum*

One of the previous attempts to construct an upper limit spectrum (ULS) was undertaken by Adams and Gelman[2] based on the data of two largest SPE's (23 February 1956 and 4 August 1972). Relying upon more extended set of data of Table 4, Miroshnichenko[226,228–232] has suggested and developed an improved model of ULS (shadowed line 15 in Fig. 3). All points of this ULS are situated about one order of magnitude above the largest observed (or estimated) values of integral

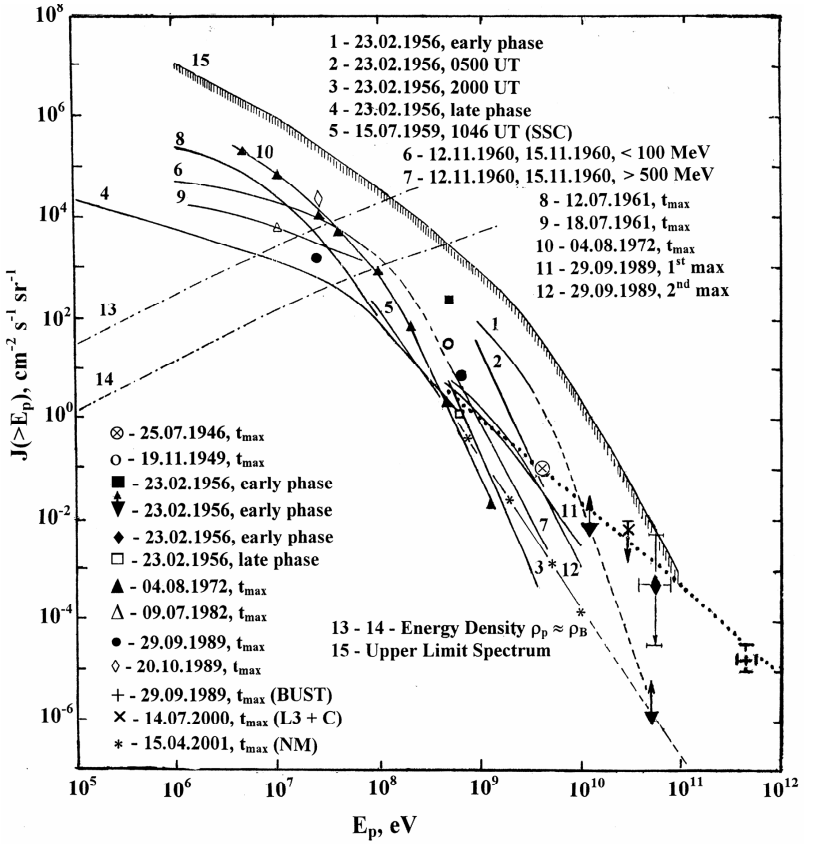

Fig. 3. Integral energy spectra of solar protons for the largest SPE's observed near the Earth in the solar activity cycles 18–23 (this work). Curve 15 corresponds to the Upper Limit Spectrum proposed earlier.[226] Integral spectrum for galactic cosmic rays above 10^9 eV is also shown (dotted line). For details see Refs. 224, 226, 228–232.

proton intensity at each energy threshold. In the right lower corner we show, in particular, absolute intensity of the $\sim$ 500 GeV protons estimated by the BUST data for the event of 29 September 1989.[146] Integral spectrum for galactic cosmic rays above 10^9 eV is also shown (dotted line).

The ULS may be fitted by a power law function with the exponent depending on proton energy, namely, $\gamma = \gamma_0 E^{\alpha}$, where $\alpha = 1.0$ at $E > 1$ MeV. Remaining parameters of the upper limit spectrum are given in Table 6.

The uncertainties of exponent values are estimated to be from ± 0.2 to ± 0.5 at the energies below 10^9 eV and above 10^{10} eV, respectively. The factor of 10 was chosen to provide a necessary "reserve" of particle intensity for overlapping the established and/or assumed range of uncertainties in the measured (or estimated) values of $I_p(t_m)$. Such an empirical approximation of the ULS is far from being a complete model suitable for direct application. However, we believe this

Table 6. Parameters of the upper limit spectrum (ULS) for SCR.

Energy, eV	$> 10^6$	$> 10^7$	$> 10^8$	$> 10^9$	$> 10^{10}$	$> 10^{11}$
Exponent, γ	1.0	1.45	1.65	2.2	3.6	> 4.0
$I\,(> E_p)$, pfu	10^7	10^6	3.5×10^4	8×10^2	1.2×10^0	7×10^{-4}

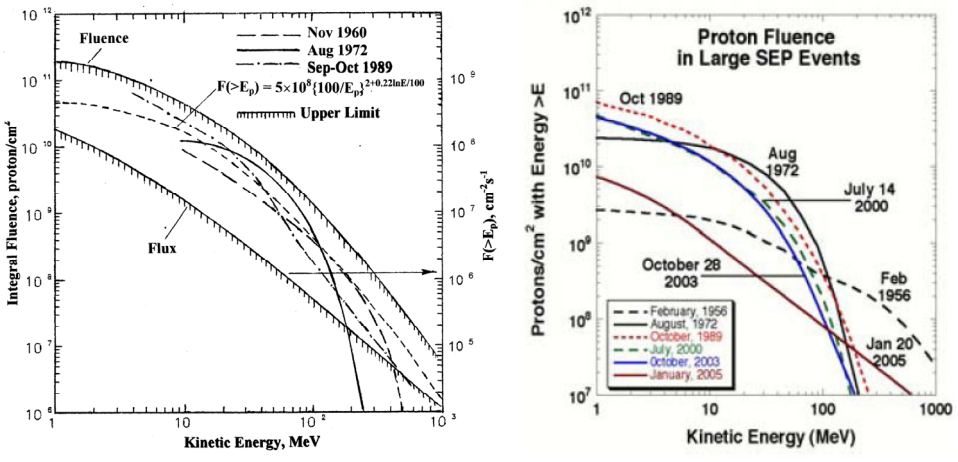

Fig. 4. Upper limit spectrum and fluence as a function of particle kinetic energy for several largest proton events of 1960–1989 (left panel, by courtesy of I. V. Getselev[395]). Fluence spectra of some of the largest SEP events of the last 50 years (right panel, Mewaldt *et al.*[210,211]).

model spectrum poses clear observational limits on expected extreme intensities of energetic solar particles near the Earth's orbit.

Figure 4 shows observed fluence spectra of some of the largest SEP events of the last 50 years,[395,210,211] including the GLE of 20 January 2005. Estimated upper limit for the fluence spectrum is also depicted at the left panel. Note that the fluence spectrum in Fig. 4 (left) declines smoothly at large fluences, and the upper limit fluences proposed for the > 10 MeV and > 30 MeV protons are about 3×10^{11} and 10^{10} cm^{-2}, respectively. Four of the six events at the right panel have very similar spectral shapes; only the February 1956 and January 2005 events stand out because of their much harder spectra.

3.3. *Maximum rigidity of accelerated particles*

Relativistic solar particles are of special interest to understand the maximum capacities of solar accelerators. In particular, a series of the GLE's of solar cycle 22 have renewed interest in the effects of those particles. Below we present a summary of the essential observations of accelerated particles that *any* theoretical model of flares must account for. It is convenient to approach this by posing the following questions. (1) To what energies (rigidities), $E_{\max}$ (or $R_{\max}$), are particles accelerated? (2) How quickly (acceleration rate, dE/dt, and total acceleration time, T_{ac}) do they

reach these energies? (3) How many particles are accelerated per second, dN/dt? These questions can be asked of both electrons and ions.[217]

If the low-energy threshold of the SCR spectrum turns out to be conditioned by intimate micro-processes in solar flare plasma, then the upper one, R_m, seems to be determined mainly by the structure, extension and dynamics of the coronal magnetic fields (e.g. Refs. 271 and 185) or by the parameters of CME-driven coronal shock (e.g. Ref. 55). Maximum rigidity, R_m, is one of decisive parameters to test different models of particle acceleration at the Sun. For example, in one of the earliest works on this subject where the upper cutoff was determined at the source by a stochastic mechanism of acceleration,[260] the theoretical high-energy cutoff was estimated to be $E_m \cong 15.1$ GeV.

The possibilities of observational discovery of the upper rigidity boundary for SCR, however, are limited, in particular, by large statistical errors of measurements (Fig. 3) at the galactic cosmic ray (GCR) background and anisotropic arrival of relativistic solar protons (e.g. Refs. 230 and 232). Routine observations by the standard surface detectors allowed to estimate, for example, the magnitude of $R_m = 20.0\ (+10 - 4)$ GV by the data on the 23 February 1956 event.[130] Meanwhile, due to the observations by nonstandard surface muon telescopes Sarabhai *et al.*[310] have registered solar proton with the energies of 35–67.5 GeV during initial stage of the same event.

Observations by underground muon detectors oriented towards the Sun allow advancing into the energy range of 100–200 GeV. In particular, on the data of narrow-angle scintillation muon telescope (at a nominal depth of 200 meters of water equivalent, m.w.e., in the Experimental Mine of the Colorado School of Mines, Idaho Springs, Colorado) Schindler and Kearney[312] have separated by the superposed epoch method (Chree technique) 24 increases of secondary muon intensity with the amplitudes from 60 ± 30 to $230 \pm 80\%$ within 10 min before the beginning of the proper flare in $H\alpha$ line. These results pointed out a possibility of the particle acceleration at the Sun up to the energy of $E_m = 200$ GeV. However, these evidences still needed to be confirmed by more reliable observations because the above data were, in essence, within the limits of 3σ.

This deficiency seems to be overcome due to the observations by the BUST since 1981.[8] Note that a research interest to the problem under consideration was extremely enhanced due to the first reliable registration of underground effects of solar flares. It happened on 29 September 1989 when solar protons have been accelerated, according to different estimations, to the energies from quite reasonable values of $E_m \geq 20$ GeV up to, probably, ≥ 100 GeV. Underground increases have been observed not only by the BUST, but also by standard MT's in Embudo Cave near Albuquerque, New Mexico, USA[350] at the depth of 35 m.w.e. with the threshold rigidity of 19 GV and in Yakutsk (USSR) at the depths of 7, 20, and 60 m.w.e., with the threshold energies 8.2, 16.0, and 39.0 GeV, respectively.[171] However, some estimated values of 900–1000 GeV seem to be absolutely unrealistic ones (e.g. Ref. 239).

Alexeyev *et al.*[8] described the first (and the largest) burst of muon intensity at the level of 5σ recorded at the BUST during the GLE of 29 September 1989. A preliminary search for the similar bursts in the other GLE's (during the BUST operation) was undertaken by Alexeyev and Karpov.[9] Using the statistical analysis it was shown that at least three bursts (29 September 1989, 15 June 1991 and 12 October 1981) with a high probability might be connected with the certain solar phenomena. These short-term (< 15 min) bursts were concentrated in a small solid angle (0.03 sr on the average) and recorded in 1–2 hours after the soft X-ray maximum. The energy of the muons is $E_\mu > 200$ GeV, which corresponds to the primary proton energy $E_m > 500$ GeV. The connection with GLE's for the other 15 bursts (from 18 in all) is not quite certain.

After these first studies (Refs. 8 and 9), analysis of the same data was performed[146] with allowance for the angular characteristics of bursts and sensitivity diagram of the BUST, as well as for the position and importance of the proper flares, direction of interplanetary magnetic field (IMF), anisotropy and spectrum hardness of relativistic solar protons. The muon bursts associated with the other 15 GLE's had smaller amplitudes. Many of those 15 bursts maybe also associated with powerful solar phenomena; otherwise it is difficult to explain significant distinctions of their spatial and temporal properties from the noise ones.

Karpov *et al.*[146] carefully revised previous findings with the purpose to confirm a solar origin (or, at least, solar association) of the muon bursts at the BUST. In particular, for the event of 29 September 1989 absolute intensity of the ~ 500 GeV protons has been estimated by the BUST data (see Fig. 3, right lower corner) and SCR rigidity spectrum has been constructed by the NM and MT data in relativistic range. The results give no final answer, and the problem of R_m determination or this GLE remains open.

Up to 1990 it has been possible to determine the quantity E_m (R_m) for 18 events only. Toward the end of 2005 the list of the BUST muon bursts has been extended up to 34.[147] It is still under discussion, however, several estimates of E_m for the event of 29 September 1989.[239] In order to verify a possible relation between R_m and the number of accelerated protons, N_a, we have compiled the Table 7 that includes the values of R_m, N_a (> 0.24 GV) and N_a (> 1.0 GV) ($E_p > 30$ and > 433 MeV, respectively) for all 19 proton events. The estimates of N_a have been obtained by involving the data of 1949–1991 on source proton spectra (SPS) of SCR.[238]

3.4. *Constraints of maximum energy*

Based on the data of Table 7, it would be interesting to study a very peculiar problem of upper rigidity limit, R_m, for solar cosmic rays. Preliminary examination[23] reveals a slight tendency of the R_m increasing for large SPE's; however, a total statistics of available estimates (19 events) prevents of definitive conclusion. In this context, a very important question arises about the restrictions of the accuracy in the E_m determination. The statistical accuracy of modern neutron monitors (NM)

Table 7. Maximum rigidity and number of accelerated protons.

No.	Date	N (> 0.24 GV)	N (> 1 GV)	R_m, GV	Reference
1	23.02.1956	1.9×10^{34}	2.3×10^{33}	$20(+10, -4)$	HTP-1976
2	04.05.1960	1.8×10^{31}	2.0×10^{26}	7.0 ± 1.0	HTP-1976
3	03.09.1960	1.7×10^{31}	6.5×10^{29}	5.0 ± 2.0	HTP-1976
4	15.11.1960	4.6×10^{33}	6.5×10^{31}	4.1 ± 0.8	HTP-1976
5	18.07.1961	1.7×10^{33}	6.5×10^{30}	4.3 ± 0.9	HTP-1976
6	07.07.1966	2.0×10^{31}	2.7×10^{30}	3.2 ± 0.7	HTP-1976
7	28.01.1967	7.8×10^{31}	1.0×10^{31}	5.7 ± 0.7	HTP-1976
8	18.11.1968	2.9×10^{32}	4.0×10^{30}	5.7 ± 1.5	HTP-1976
9	25.02.1969	4.8×10^{31}	1.8×10^{31}	5.7 ± 0.9	HTP-1976
10	30.03.1969	8.9×10^{30}	2.9×10^{25}	4.5 ± 0.7	HTP-1976
11	24.01.1971	5.2×10^{33}	3.0×10^{30}	4.2 ± 0.6	HTP-1976
12	01.09.1971	1.6×10^{32}	4.3×10^{30}	3.4 ± 0.6	HTP-1976
13	07.08.1972	8.1×10^{33}	4.0×10^{29}	6.6 ± 1.0	HTP-1976
14	22.11.1977	8.0×10^{31}	7.8×10^{26}	6.0 ± 1.0	BM-1988
15	10.04.1981	9.7×10^{31}	2.8×10^{27}	1.2 ± 0.2	K-1983
16	12.10.1981	9.7×10^{32}	6.4×10^{29}	9.0 ± 1.0	BM-1988
17	26.11.1982	4.0×10^{32}	2.6×10^{29}	11.9 ± 2.0	ZS-1989
18	07.12.1982	8.5×10^{32}	2.4×10^{31}	10.4 ± 1.5	ZS-1989
19	29.09.1989	8.0×10^{32}	1.0×10^{32}	> 20.0	Several authors

Notes: The R_m value for the GLE of September 29, 1989 is still under discussion (for a review see Ref. 239. The corresponding references are: HTP-1976;[130] BM-1988;[23] K-1983;[158] and ZS-1989.[393]

amounts to $\sim 0.15\%$ in terms of hourly data and $\sim 0.5\%$ in terms of 5-min readings. The actual width of the distribution of hourly values under undisturbed geomagnetic conditions exceeds the width of the Poisson distribution by a factor of ~ 1.5. This means that the accuracy of the E_m determination is limited significantly by the sensitivity of the monitors to the minimum measurable fluxes of SCR near the energy of $E_p \geq 500$ MeV.

As shown by Bazilevskaya and Makhmutov,[23] this sensitivity, on the one hand, is comparable to the sensitivity of the stratospheric experiment of FIAN (Physical Lebedev Institute), where the fluxes $I\,(> E_p) = 0.03$ pfu in the $E_p = 100$–500 MeV interval are the minimum measurable values. On the other hand, it is inferior to the best measurements in interplanetary space, where for the same spectral indices the measurable particle fluxes with $E_p = 10$–400 MeV are $\sim 10^{-3}$ pfu (see, e.g. Ref. 84). Thus, the absence of an increase in the counting of the neutron monitors does not yet indicate the presence of an upper limit to the energy of SCR in the range of $E_m = 500$–1000 MeV.

Another fundamental restriction is due to the uncertainty of the integral multiplicity $m(R)$ values, used in the iteration method for determining E_m. As shown by Dorman and Miroshnichenko,[423,74] the accuracy of the $m(R)$ calculation from NM data, due to the presence of different nuclei in the primary flux of galactic cosmic rays, does not exceeds a factor ~ 2 (for details see Ref. 228). Bazilevskaya

and Makhmutov[23] used the multiplicity values $S(E)$ that had been calculated[186] with the elemental composition of the SCR taken into account. Nevertheless, when comparing their calculations with the results of other works, Lockwood *et al.*[186] also found discrepancies from 50% to an order of magnitude in the $S(E)$ values.

Similar problem also exists when interpreting the data of underground muon telescopes (MT), for example, in the case of GLE of 29 September 1989.[170] If one uses so-called coupling coefficients $W(E)$ between the intensity of primary GCR and intensity of secondary muons, then a possibility exists to determine a cutoff energy E_c in the SCR spectrum by the data of MT's located at different depths. With this approach to the data of Yakutsk detectors, the author concluded that this event had extremely hard energy spectrum ($\gamma = 3.2$) with the cutoff energy $E_c \cong 20$ GeV (see also Table 7). Therefore, in spite of very hard spectrum, the energy cutoff in the GLE of 29 September 1989 did not exceed too much the E_c values derived for a number of previous events. It is emphasized, however, that if the spectrum cutoff is preceded by spectrum softening (steepening), then the maximum energy of accelerated particles should be higher than given by the author.

Finally, let us point out the distinct tendency of the SCR spectra to become steeper in the range of proton energies $E_p > 100$ MeV. Such a tendency was confirmed, in particular, by Bazilevskaya and Makhmutov[23] based on the data from the SPE catalogue of 1970–1979[6] for 59 events, which were reliably identified with solar flares. In their study, however, the effect of increase in the counting rate at neutron monitors after faint flares at the Sun, pointed earlier,[396] was not confirmed. Moreover, it is impossible to exclude the possibility for the formation of extremely hard spectrum of protons with an upper limit of $E_m \gg 10$ GeV at the Sun.

Some evidences of such a possibility have been obtained in the event of 29 September 1989. If such particles arrived at the Earth in the form of a narrow (anisotropic) beam and experienced a deflection in the geomagnetic field, then they could give a ground increase effect event at night. Such an increase with an amplitude greater than 3σ was found[397] from the data of the Chacaltaya neutron monitor ($R_c = 13.1$ GV, 5220 m above sea level) by the Chree method for 16 X-ray and gamma flares, only one of them having been accompanied by a weak enhancement of the flux of protons with $E_p > 100$ MeV.[398] The arrival of the prompt component of SCR at the Earth in some events (e.g. Ref. 271) seems to corroborate the existence of narrow beams of relativistic protons.

Although the value of R_m in Table 7 changes from one event to another, no distinct relationships has not yet been found between this parameter and the amplitude of the proton event near the Earth and the amplitude and time profile of X-ray and microwave bursts.[130] On the other hand, from the data of Table 7 one can see a slight tendency for R_m to increase in the case of the most powerful SPE's. In our opinion, the accuracy of the determination of the values of E_m and limited statistics of Table 7 are not yet adequate for investigating the correlation or physical relationship between this parameter and other parameters of the flares and the solar activity indices.

Nevertheless, some attempts seems to deserve attention (Refs. 192 and 23) to compare the occurrence rate of GLE's with the largest value of E_m in a year and the values of the exponent of the integral spectrum of protons with $E_p = 100$–500 MeV with the smoothed values of the number of sunspots W during the period of 1956–1985. It was shown that the slope of the spectrum is practically independent of the phase of the solar cycle, whereas the largest values of E_m for each year have double-hump behavior in the solar-activity cycle, reaching values > 5 GeV during the years before and after maximum activity. Such a dependence of E_m on the phase of the solar cycle can be explained by a coronal magnetic field structure that varies during the cycle.

Similar results were obtained by Nagashima *et al.*[253] Using the data of NM's and MT's during the period of 1942–1990, these authors analyzed the well-known tendency of GLE's to be grouped preferentially during the ascending and descending phases of the 11-year solar cycle (e.g. Ref. 228). It was shown that flares causing such increases are essentially forbidden during the transitional phase when a change occurs in the sign of the global magnetic field of the Sun near the periods of solar activity maxima. Nagashima *et al.*[253] suggest that the absence of GLE's near the maximum is explained not by the suppression of proton production by the Sun because of strong magnetic fields but by a deterioration of the efficiency of proton acceleration during the structural rearrangement of the fields in the transitional period. On the whole, however, the question of the magnitude and nature of the parameter R_m remains unanswered. In order to separate the effects of SCR acceleration and their escape from the solar atmosphere it is necessary to investigate the structure of the coronal magnetic fields in individual events.

4. Production and Detection Probability of Flare Neutrinos

Bahcall[18] has paid a special attention to the hypothesis of possible contribution of flare neutrinos to the counting rate of detectors recording the thermonuclear neutrinos from the Sun's interior. He reviewed the capacities of several detectors constructed before 1990 and concluded that no one flare could give a discernible signal in the detectors of Homestake, Kamiokande, SAGE, Baksan and LVD. Nevertheless, from theoretical point of view, it would be very important to estimate, at least, upper limits of expected flare neutrino flux.

4.1. *Early theoretical estimates*

From the parameters given in Tables 6 and 7 one can use, for relativistic protons, in particular, to estimate expected flux of flare neutrinos and their possible contribution to the counting rate of detectors recording the thermonuclear neutrinos from the Sun's core. When estimating it should take into account the different sensitivities to the flare neutrinos of radiochemical detectors (of the type of well-known detector by R. Davis[64]) and direct count detectors (of the Kamiokande type, Japan).

During more than 25-year operation the Davis' detector in Homestake Gold Mine (South Dakota, USA) has registered several peaks with considerable excess of solar neutrino flux, in comparison with the average values. It was suggested[25,64] that some of the peaks could be related to the certain powerful proton events (4 and 7 August 1972, 12 October 1981 and others). However, direct calculations[167] for two large events, 23 February 1956 and 4 August 1972, carried out by the data of source proton spectra (see their summary in Ref. 238) lead to the negative result. For example, calculated flux of the flare neutrinos turned out to be > 2 orders of magnitude low as observed one in August 1972. Also, according to the estimates by Lingenfelter *et al.*[183] for the same event, it would be not realistic to expect that flare neutrinos may cause a significant effect in the Homestake detector. Meanwhile, a number of the counts in the detector of the Kamiokande type could be 2 orders of magnitude higher as in the Davis' detector (see also Ref. 18, and references therein).

In the light of given estimates, it is worth to discuss briefly the probability of recording flare neutrinos by means of existing and projected detectors. Decisive parameters for such recording are, on the one hand, intensity and orientation of relativistic proton beam ($R > 1$ GV) in the Sun's atmosphere and, on the other hand, the sensitivity of the specific detector to high-energy neutrinos. From the generation conditions, flare neutrinos of electron type ν_e have maximum intensity at the energy $E_\nu \sim 10$ MeV under isotropic distribution, and in the range $E_\nu \sim 10$–100 MeV — at various angles θ relative to the orientation of the original proton beam.[159] As a result, the isotropic neutrino flux turns out to be a factor of 5–10 smaller than the anisotropic one. Generation rates and spectra of muon neutrinos ν_μ and antineutrinos ν_μ slightly differ from those of ν_e, and the flux of electron antineutrinos ν_e proves to be much lesser than that of ν_e. The probability of recording will evidently depend on the kind and energy of neutrino and on the value of θ as well.

4.2. *Upper observational limits*

It was not surprisingly that a powerful solar flare of 29 September 1989 has called a steady attention of many researchers of solar neutrinos (see, e.g. Ref. 160, and references therein). In fact, it was a good possibility to testify some theoretical aspects of the production of flare neutrinos and a rare occasion to detect them. For example, background of Kamiokande detector for high energy "events" in the solar direction is extremely small and thus even one "event" within a narrow time gate — between 11:20–11:35 UT of 29 September 1989 — could be a brilliant signature of the solar flare neutrino. However, as far as we know, no positive results were reported since then. Meanwhile, Aglietta *et al.*[3] presented the results of a search for flare neutrinos and antineutrinos during the period August 1988–April 1991, performed by the Mont Blanc Liquid Scintillation Detector (LSD). In all, 27 large flares have been analyzed, including the two powerful ones which occurred on 29 September and 19 October 1989. No significant signal was found in time coincidence with any solar flares.

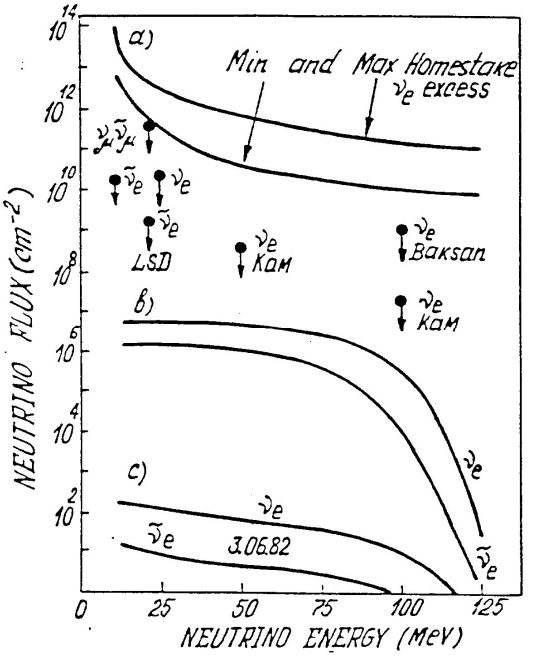

Fig. 5. Estimated fluxes of solar flare neutrinos: (a) upper limits obtained for different detectors;[3] (b) the case of the most restricting suggestions: neutrinos are generated by a beam of relativistic particles moving downwards the Sun; a flare is on the invisible side of the Sun; the energy spectrum of particles is a power law with the spectral index $\gamma = 1.0$; $E_m = 100$ GeV; $N_p\,(> 500\ \text{MeV}) = 3 \times 10^{32}$;[161] (c) results of theoretical considerations for the flare of 3 June 1982.[161]

The obtained upper limits on neutrino fluxes are presented in Fig. 5. As analysis includes two large solar flares (the first of them was located on the hidden solar side), Aglietta *et al.*[3] concluded that obtained results do not support the hypothesis of the Homestake excess being due to solar flare neutrinos with $E_\nu > 25$ MeV. This statement completely confirms the conclusions by Kovaltsov[167] and Lingenfelter *et al.*[183] based on the theoretical considerations.

With the purpose to understand existing experimental possibilities, Kocharov[160] combined in Fig. 5 the observational restrictions of Aglietta *et al.*[3] with theoretical estimates of expected fluxes of flare neutrinos in two large flares — the observed flare on 3 June 1982 and hypothetical one with some specific features.[161] It is seen that the sensitivities of existing radiochemical detectors in South Dakota (^{37}Cl) and Baksan Valley (^{71}Ga), as well as that of direct count detectors (Kamiokande II and LSD) are several orders of magnitude below the threshold necessary for recording flare neutrinos, even in the most "optimistic" conditions of their generation (narrow beam of relativistic protons with a rather hard spectrum from the flare on the invisible side of the Sun). Therefore, recording of flare neutrino depends on the creation of neutrino detectors of a new generation.

4.3. *Prospects of new experiments?*

A possible type of detector of direct registration was examined theoretically long ago by Erofeeva *et al.*[88] A water detector with a mass of 10 tons can record muon neutrinos by Cherenkov radiation of muons generated in the interaction between flare neutrinos ν_μ and the target nucleons (H_2O). Estimates by Erofeeva *et al.*[88] show that the necessary number of relativistic protons for recording a significant effect (i.e. for a generation of sufficient neutrino flux at a flare) is $N_p\,(>1\ \mathrm{GV}) > 10^{32}$ (assuming isotropic generation of neutrinos). In the case of an anisotropic generation (narrow proton beam from a flare on the invisible side of the Sun), the estimated required number of protons can be decreased by a factor 5–10.[159]

From the data on the ejection spectrum for the SPE of 23 February 1956, without separating the prompt and delayed SCR components, Miroshnichenko[424] obtained $N_p\,(>1\ \mathrm{GV}) = 6.1\times10^{32}$ (the accuracy of this value is within a factor of ≥ 2). Within the uncertainty limits, this estimate is evidently compatible with the value of $N_p\,(>1\ \mathrm{GV}) < 2.3\times10^{33}$ obtained by Perez-Peraza *et al.*[271] from the calculations for the prompt component only (see also Table 7). As shown by Vashenyuk *et al.*,[373] for the event of 29 September 1989 the value $N_p\,(>1\ \mathrm{GV})$ should be less by 1–2 orders of magnitude. It means that for this detector, a flare of 29 September 1989 still could not be observed, whereas a flare of the 23 February 1956 type would be observed, especially at the "optimum" orientation of the >1 GV proton beam.[424]

In our opinion, the most "efficient" orientation occurs for a strictly antipodal flare (on the Sun's invisible side), provided for the geometry of the coronal magnetic fields near the source of the SCR also satisfies optimal criteria.[271,227] In other words, besides enhanced detector sensitivity for recording flare neutrino, it is also necessary to have a rare auspicious geometry of magnetic fields in the source region. In spite of this pessimistic conclusion, we stress the importance of the search for flare neutrinos. Their detection would answer a number of crucial questions in flare physics, such as the acceleration mechanism, the maximum rigidity, R_m, of accelerated particles, the source location (altitude) in the solar atmosphere, and the time needed for particle acceleration up to relativistic energies.

Several new aspects of the problem under consideration arise due to possible production of medium energy neutrinos (>1 GeV) by relativistic solar protons *in situ* (immediately in the Sun's atmosphere). Recent calculations by Ryazhskaya *et al.*[305] showed that these neutrinos can come to the Earth and be detected with neutrino telescopes of a new generation. Detection of flare neutrinos may answer a number of crucial questions in flare physics and particle acceleration at/near the Sun.[239,240] Theoretical models do not exclude the values of $E_m > 100$ GeV, and the problem reduces to the search for adequate acceleration scenario(s) and magnetic structures in the solar corona. It is important, however, not only to calculate E_m, but also determine a shape of SCR spectrum in the source at extremely high energies.

5. Threshold and Cutoff Effects

As noted above, the problem of SCR generation in relativistic range ($R \geq 1$ GV) was unusually actualized due to first confident observations of underground effects correlated with solar flares. In particular, significant increases of counting rate at several muon telescopes (for example, in Yakutsk and Embudo) were registered during GLE of 29 September 1989,[171,350] including one very peculiar muon burst[8] at the BUST. All these new findings give a challenge to our present understanding of utmost capacities of particle accelerators at the Sun. In this context, SCR spectral data (in absolute units of proton flux) at rigidity $R \geq 1$ GV are of special interest.

Available acceleration models do not exclude large values of SCR maximum energy, and the problem reduces to the search for adequate magnetic configurations (structures) in the solar corona. For example, the model of two SCR sources[271] gives a value of $E_m \cong 250$ GeV for the flare of 23 February 1956 type; in electromagnetic model of solar flare[279,429,430] maximum proton energy may be as unlikely large as 3×10^{12}–10^{15} GeV. In the whole, however, all such estimations depend heavily on the choice of acceleration model. Moreover, to compare the estimated values with observational results it is not only important to calculate E_m, but also to resolve more difficult problem, namely, to determine SCR spectrum shape in the source and a number of accelerated particles of extremely high energy. Observational data on GLE's occurred in the 22nd solar cycle (since September 1986) are of special interest due to unusually high occurrence rate and large energy content of the events.[338]

5.1. *Possible acceleration scenarios*

In above respects, the summary of SCR spectra observed near the Earth (Fig. 3) for the most powerful SPE's imposes certain upper limitations. In the range of energies from several units to several tens GeV the data point to a steepening behavior of SCR spectrum. At any rate, they do not give convincing grounds for its extrapolation (e.g. Ref. 165) by the power-law function with the same (unchanging) slope to the higher energies. A general picture of particle acceleration at the Sun becomes more distinctive if one takes into account also the source proton spectra (SPS) reconstructed from observations in broad range of SCR energies.[238]

Some peculiarities of the SPS, specifically a spectral steepening for high rigidities, are shown to be characteristic of large events. A spectral steepening for high energies is seen in certain large events of the 23 February 1956 type, and this may be useful for separation of acceleration processes responsible for the formation of final source spectrum. Thus, the SPS over broad ranges allow fits with different functional forms, including a broken power law that may be indicative of multiple (at least, two-step) acceleration processes.

As it was mentioned, the event of 29 September 1989, similarly to the largest GLE of 23 February 1956, was not too prominent in the nonrelativistic energy range. Due to high-energy underground effects, however, it is of paramount importance from the point of view of estimates the upper capability of solar accelerator(s).

Moreover, this event turns out to be an excellent pattern for testing of acceleration models. The main features of the 29 September 1989 event are susceptible of different interpretations, taking into account possible impact of extended coronal structures (large loops, streamers, etc.), CME's, heliospheric current sheet (HCS), and coronal/interplanetary shocks. At least, three tentative scenarios have been suggested: (1) acceleration by CME-driven coronal shock; (2) post-eruption (PE) particle acceleration in the corona; and (3) combined two-source acceleration.

The first one (e.g. Ref. 55) is appealing because of its simplicity: particles accelerated on open field lines can either escape to be observed as SPE near the Earth, or precipitate into the photosphere to give rise to gamma-ray line emission. However, a detailed modeling effort is required to determine whether a shock can still efficiently accelerate protons to energies ≥ 20 GeV.

In the second scenario (e.g. Refs. 50 and 5) a large CME, propagating through the corona, strongly disturbs the coronal magnetic field in an extended region. After the passage of a CME, the disturbed magnetic field relaxes to its initial state via magnetic field reconnection in a quasivertical current sheet, in the magnetic field configuration proposed by Martens and Kuin.[199] The PE energy release following large CME's at the late phase of complex flares appears to be an effective source of prolonged particle acceleration[185] up to high energies side by side with the primary flare energy release and coronal/interplanetary shock waves. It may give a considerable contribution to the 10–30 MeV proton fluxes in the interplanetary space as well as to the GLE's with a complicated intensity-time profile. This assertion is grounded, in particular, by the analysis of recent measurements of prolonged and high-energy gamma ray and neutron flare emissions in six very powerful homologous flares occurred during the first half of June 1991.

At last, a set of evidences exists[373,379,237,227] for two separate sources of SCR in the event of 29 September 1989, i.e. for two SCR components (apparently independent) — prompt (PC) and delayed (DC) ones. According to Perez-Peraza *et al.*,[271] increases of the SCR flux in events with a PC are of impulsive nature and have an anomalously hard spectrum, which may indicate the specific mechanism of fast acceleration. A magnetic bottle[247] upon its expansion is evidently a possible source of the DC, and the PC is presumably generated in the region of reconnection of magnetic loops high in the corona, upon the stimulating (driving) action of the expanding magnetic bottle.

As to the BUST muon burst during the event of 29 September 1989, it is difficult to explain, first of all, its delay for a time > 1 h relatively to the first intensity peak at the surface muon telescopes. It is obviously impossible to accept a hypothesis about the trapping and prolonged containment of relativistic protons in magnetic loops of the solar corona during certain SPE's.[194] The presence of the second source high in the corona[373] would be a possible explanation of above fact. A necessity of second source also follows from the result that the proton intensity corresponding to the BUST burst does not agree with the relativistic proton spectrum at the main GLE stage.[146]

In application to the BUST burst the existing two-source model, however, must be modified taking into account either possible additional acceleration of solar particles at the shock front far from the site of proper flare, or eventual modulation of galactic cosmic rays at the energies above 500 GeV.[146] We return to the discussion of those aspects in Subsec. 11.3 (see also Ref. 147), in the context of general theoretical and observational constraints imposed on the maximum energy of SCR.

5.2. *Energetics of flares and solar cosmic rays*

The SCR energetics comprises, at least, three aspects: (1) the total energy of accelerated particles W_a and their relative contribution to the energetics W_f of the solar flare as a whole, $\delta = W_a/W_f$; (2) variations of the number of accelerated particles $N_a\,(> E)$ and of the quantity δ with the total energy of the flare; (3) variations of the Sun's proton productivity, or energy release in the form of SCR, due to the changes of the solar activity level. As regards the study of the solar flare physics, particularly interesting are the first two aspects. The third one is important in connection with the problem of the long-term variations in the Sun's proton emissivity.

The early estimates of W_a and N_a turned out to be rather controversial (see Ref. 228). Nevertheless, it was found that the contribution of SCR at $E_p \geq 10$ MeV to the flare energetics as a whole does not exceed 10%, provided that W_f is $\sim (1\text{–}2) \times 10^{32}$ erg, about half of this energy being carried away by a shock wave.[343] At the modern level of our understanding it is believed that for a large X-class flare, the flux of X-rays above 20 keV at 1 AU can be $\geq 10^4$ photons cm^{-2} s^{-1}, and results from an emission area of $\approx 10^{18}$ cm^2. The nonthermal model then indicates that $\approx 10^{37}$ electrons s^{-1} were accelerated to energies > 20 keV in such a flare.[217] Hence, if the flare lasts ≈ 100 s, the total number of electrons energized above 20 keV is about 10^{39}.

We point out that, while these numbers are quite large, they are dwarfed by those from the so-called "giant flares," in which the energization rate and total number above 20 keV can be 10^{39} s^{-1} and 10^{41}, respectively, as it was estimated by Kane *et al.*[145] for the giant flare of 1 June 1991. These events, however, are relatively rare, and we do not take them in account in obtaining "typical" numbers for flares. Given the steepness of the electron energy distribution, the bulk of the energy in nonthermal electrons resides at low energies (20–50 keV). Below ≈ 20 keV, it becomes harder to distinguish the nonthermal component from a hot thermal component generated by plasma heating. Note several essential papers in this field, such as Ref. 181 on electrons, Ref. 286 on relativistic electrons and energetic protons, Refs. 210 and 211 on protons and the recent works of Emslie and coworkers[85,86] on flare/CME-related energies.

In Table 8 we summarize some extreme properties of the accelerated ions and electrons inferred from various observations. On several reasons, the estimates in Table 8 are limited in their validity and accuracy. The main reason is a dependence on underlying model of the event used for interpreting the data. For example, a

Table 8. Some extreme properties of SEP's (adapted after Ref. 51).

Parameter	Electrons, keV	References	Ions, MeV	References
Number of particles	10^{41} (> 20)	145	3×10^{35} (> 30)	285
	10^{37} (> 100)	213	$\sim 10^{32}$ (> 300)	51
	5×10^{34} (> 300)	213	6×10^{32} (> 500)	424
Risetime, s	10^{-2}		> 1.0	51
Duration, s	10 ⇒		60 ⇒	51
	—		≤ 10 (> 500)	424
Total energy, erg	10^{34} (> 20)	145	10^{30} (> 30)	285
	10^{29} (> 100)	213	3×10^{28} (> 300)	51
	10^{28} (> 300)	213	5×10^{29} (> 500)	424
Power, erg s^{-1}	10^{32} (> 20)	145	2×10^{28} (> 30)	51
			$< 5 \times 10^{28}$ (> 500)	424

number of relativistic protons (> 500 MeV) has been estimated with the uncertainty factor ≥ 2. Some estimates in Table 8 are not consistent with each other, and this reflects different approaches to the modeling of acceleration processes. Nevertheless, in general, they give a certain idea about the upper limit capacities of the solar accelerators. Note that a number of > 20 keV electrons and all estimates for relativistic protons (> 500 MeV) have been obtained by the data for the so-called "giant flares" of 1 June 1991 and 23 February 1956, respectively. Though these events are very rare, they are of great interest from the astrophysical point of view.

Extended observations from the Yohkoh, Compton Gamma Ray Observatory (CGRO), GRANAT, SOHO, and reanalysis of older observations from the Solar Maximum Mission (SMM), have led to important new results concerning the location, timing, and efficiency of particle acceleration in flares. In particular, the review of pertinent observations and their implications[217] allowed to deduce the average rate $\partial N/\partial t$ at which particles are energized above a given energy. These rates are summarized in Table 9, along with the total energy content of the particles. The electron energization rates are for large flares, such as those, which have detectable gamma-ray emission.

As noted by Miller *et al.*,[217] there is evidence that electron acceleration in impulsive flares occurs in small bursts, which have been termed "energy release fragments" (ERF's) the accelerated electron energy content in an ERF being between 10^{26}–10^{27} ergs. In ERF's, the average rate of energization must be sustained for about 400 ms, while in the entire flare it must occur over several tens of seconds. In light of recent observations (see Ref. 217), about 5×10^{34} electron s^{-1} need to be energized above 20 keV over 400 ms in order to account for an ERF. For protons, Miller *et al.*[217] give rates and energy contents obtained by both pre-1995 and present calculations.

Solar flares and coronal mass ejections (CME's) are the most powerful events in the Solar system. In tens of minutes they can convert in excess of 10^{32} ergs

Table 9. Typical energization rates and total energy contents.[217]

	Electrons > 20 keV			Proton > 1 MeV	
Quantity[a]	ERF, Nonth. Mod.	Entire flare, Nonth. Mod.	Entire flare, Hybrid model[b]	Entire flare, Pre-1995[c]	Entire flare, Present
$\partial N/\partial t$, s^{-1}	5×10^{34}	10^{37}	2×10^{35}	3×10^{33}–2×10^{34}	10^{35}
U_p, erg	5×10^{26}	3×10^{31}	6×10^{29}	10^{29}–10^{30}	10^{31}

Notes: ERF: Energy Release Fragments.
[a] The quantities $\partial N/\partial t$ and U_p denote, respectively, the energization rate and the total energy content above either 20 keV (for electrons) or 1 MeV (for protons).
[b] $\partial N/\partial t$ and U_p are taken to be a factor of $\cong 50$ lower than those resulting from the nonthermal model. This factor is based on an application of both thermal and nonthermal models to one flare.
[c] The lower limit results from stochastic acceleration proton spectra (specifically K_2 Bessel function), while upper limit results from power-law proton spectrum.

of magnetic energy into accelerated particles, heated plasma, and ejected solar material. While the order of magnitude of this total energy is not serious doubt, its partition amongst the component parts of the flare and CME has yet to be reliably evaluated for a particular event or set of event. Recently, Emslie *et al.*[85] reported estimates of the energy in the different flare and CME components of two major solar events, 21 April 2002 and 23 July 2002. On the basis of these estimates, it appeared that the summed energy content of the different flare components was significantly lower than the total energy of the CME, leading them to reach the "cautious" conclusion that "in both events the coronal mass ejection has the dominant component of the released energy," amounting to approximately 30% of the available magnetic energy.

One year later, Emslie *et al.*[86] presented revised estimates of the flare thermal energies in the two events and also added a consideration of the total radiant energy of the events obtained by scaling the measured soft X-ray luminosity based on Solar Radiation and Climate Experiment (SORCE) total solar irradiance measurements for the 28 October 2003 event. Recognizing that many of these energetic components are interrelated, they also take care to distinguish between "primary" components of energy (e.g. the magnetic field), "intermediate" components (e.g. accelerated particles and thermal plasma), and "final" components (e.g. kinetic energy of ejecta, radiant energy in various wave bands). The authors note that since the values of these components are not all independent, careful tallying is necessary to arrive at an overall energy budget for the event. The best estimates for the energies of the various components still show that the CME contains the greatest fraction of the released energy in both events. However, given the large uncertainties in the energies of the different flare components and the higher estimates of radiant energy obtained by scaling from the SORCE measurements, the results are also consistent with the flare and CME energies in both events being comparable, with a common value of $\sim 10^{32}$ ergs.

5.3. *Distribution functions for solar and stellar flares*

Energy spectra and maximum energy of SCR are of great significance for the formulation of self-consistent model of particle acceleration in solar flares. In turn, the main problems of fundamental interest in the theory of particle acceleration at the Sun lie now at two boundary domains of SCR spectra, namely, in low-energy (nonrelativistic) and high-energy (relativistic) ranges. The most important of them are: initial acceleration from the thermal background,[384,236] and final stage of acceleration to extremely high energies of $E_p \leq 100$ GeV.[224,226,228,230] The latter is supposed to be determined by coronal magnetic structures (and/or shock waves) and the former by the fundamental properties of solar plasma and most basic problems of flare physics. In particular, Lu and Hamilton[188] and Lu *et al.*[189] developed the idea that the energy release process in flares can be understood as avalanches of small reconnection events. They predict that the power-law flare frequency distributions will be found to continue downward with the same logarithmic slopes to energy of $\sim 3 \times 10^{25}$ erg and duration of ~ 0.3 s.

In search for possible threshold effects in flare processes we first looked at the available data on size (frequency) distributions extensively reported for various solar flare phenomena (parameters). Studies have been done on radio microwave bursts, type III bursts, soft and hard X-rays, interplanetary electron and proton events, etc. (see, e.g. Refs. 60 and 240, and references therein). All these distributions can be represented above the sensitivity threshold by differential power laws as $f(J) = (dN/dJ) = A_j J^{-a}$, where dN is the number of events recorded with the parameter J of interest between J and $J + dJ$, and A_j and a are constants determined from a least-squares fit to the data. Unlike flare electromagnetic emissions, the data on interplanetary particle events are still rather poor and discrepant, their distribution functions being discernibly different from those for flare electromagnetic emissions. Let us consider this problem on the example of distribution functions for relativistic solar protons (RSP).

Since 28 February 1942 (historical beginning of the SCR observations) the generous data have been obtained on the SCR fluxes, and their spectra have been intensively studied in the energy range from ~ 1 MeV to 10 GeV and even more. In particular, there are ground-based data for 69 GLE's, however, spectral data at the rigidities above 1 GV(≤ 435 MeV) are fairly scarce, rather uncertain and/or controversial. Based on GLE observations since 1942 we summarize available data on absolute spectra of relativistic protons[245,240] at the Earth's orbit. A distribution of GLE's by proton fluxes at rigidity above 1 GV was also obtained.

By the present time absolute SCR spectra above 1 GV have been estimated by various researchers for 35 events of 1942–1992 (Table 10). This statistics is not very impressive; however, this problem is of fundamental interest because it clarifies our knowledge of utmost capacity of solar accelerators (maximum rigidity, R_m and a number of accelerated relativistic particles, N_a). Because the statistics of events is rather poor we were able to construct a distribution function only for an integral number of GLE's with the integral flux of solar protons above 1 GV (Fig. 6).

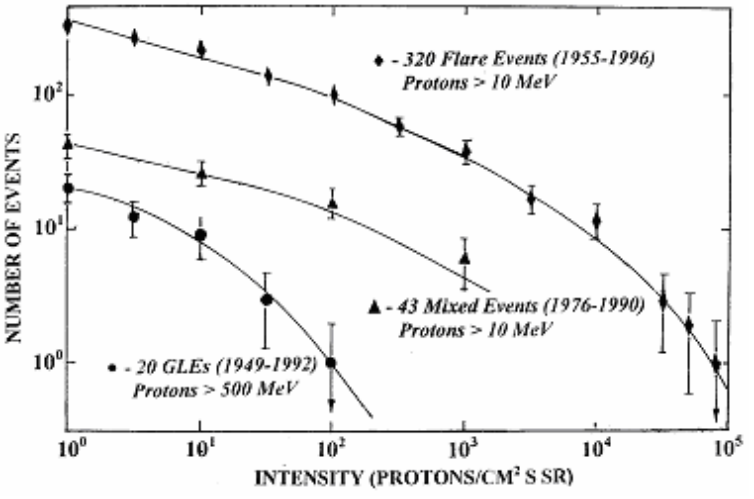

Fig. 6. Integral size distributions constructed by the large database (diamonds, 320 proton events), by the data of Ref. 139 for the $>$ 10 MeV protons (triangles, 43 events), and by the data for the $>$ 500 MeV protons (circles, 20 events) from Ref. 240.

In view of evident distinction between the slopes for the size distributions of proton events detected in differential and integral energy ranges, it is of great interest to compare the distribution slopes at different proton energies.[240] In Fig. 6 we present three integral distributions using the large database of 320 events (diamonds), 43 events from the paper by Kahler *et al.*[139] for the $\geq$ 10 MeV proton events (triangles), and 20 GLE's for the $\geq$ 500 MeV protons (circles) from Table 10. Manifestly, the middle plot (43 events) is similar to the upper one (320 events), and both of them display rather smooth fall over entire range of comparable intensities between 1 pfu and 10^3 pfu. At the same time, the lower curve (20 GLE's) steeply slopes down between 1 pfu and 10^2 pfu. This may point out to a certain dependence of slope on the proton energy range under consideration.

The results by Smart and Shea[324] and, partly, by Miroshnichenko *et al.*[240] are qualitatively consistent with those obtained by Reedy[426] for the fluence distribution, $N\,(> F_s)$, of solar proton events from 1954 to 1991. The integral distribution of the number of events, N, *per year* was shown to have a form of $F_s^{-0.4}$ in the range of low fluences (up to $\sim 10^{10}$ cm^{-2}) and of $F_s^{-0.9}$ at high fluences ($\geq 10^{11}$ cm^{-2}) of the $>$ 10 MeV protons. A similar tendency was found by Nymmik[257,258] for the $>$ 30 MeV protons: their fluence distribution in the solar cycles 20 through 22 can be described by a power-law function with exponential steepening for large fluences.

Obviously, the total statistics of GLE's with estimated maximum flux of RSP is rather poor for more comprehensive study. Nevertheless, it would be interesting to compare a power of their energy release with the suitable distributions of stellar flares on their characteristic parameters (see Ref. 129, and references therein). Here we only note that the energy distributions of stellar flares in the B-band (Balmer

Table 10. Integral fluxes of solar protons at rigidity above 1 GV.

No.	Date of GLE	Time, UT	Rigidity, ΔR, GV	D_0, $\mathrm{sm^{-2}\ s^{-1}\ GV^{-1}}$	γ	I_m, $\mathrm{sm^{-1}\ s^{-1}\ sr^{-1}}$
1	28.02.1942	1300	> 1.0	8.33×10^2	4–5	1.21×10^1
2	07.03.1942	0600	> 1.0	1.04×10^3	4–5	1.53×10^1
3	25.07.1946	1853	> 1.0	Int. IC data	—	2.26×10^1
4	19.11.1949	1200	> 1.0	2.78×10^3	4–5	4.14×10^1
5	23.02.1956	0500	1.5–5.0	1.25×10^4	6.8	2.55×10^2
6	04.05.1960	1050	2.0–5.0	6.30×10^1	3.4	8.27×10^0
7	12.11.1960	2000	1.0–3.5	1.70×10^2	5.2	1.02×10^1
8	15.11.1960	0400	1.5–4.0	1.55×10^2	5.0	1.18×10^1
9	28.01.1967	1200	0.5–10	1.25×10^1	4.5	4.45×10^{-1}
10	18.11.1968	1100	1.6–5.0	1.57×10^1	5.0	1.27×10^0
11	25.02.1969	1000	1.0–4.4	9.50×10^0	4.1	9.86×10^{-1}
12	30.03.1969	1400	1.0–3.0	2.45×10^0	4.0	2.60×10^{-1}
13	24.01.1971	2400	1.0–5.0	1.66×10^1	5.0	1.34×10^0
14	01.09.1971	2200	1.0–5.0	1.57×10^1	5.0	1.14×10^0
15	04.08.1972	1600	1.0–1.6	2.04×10^1	8.0	9.23×10^{-1}
16	07.08.1972	1700	1.0–3.0	7.00×10^0	4.0	1.02×10^0
17	29.04.1973	2215	> 1.0	Int. NM data	—	1.52×10^{-1}
18	30.04.1976	2140	1.0–1.7	1.40×10^0	3.7	5.09×10^{-1}
19	19.09.1977	1400	> 1.0	2.40×10^{-1}	4.0	1.90×10^{-1}
20	24.09.1977	1012	1.0–6.3	4.00×10^0	3.4	5.41×10^{-1}
21	22.11.1977	1200	2.3–4.0	5.00×10^2	5.5	1.05×10^0
24	21.08.1979	0700	> 1.0	5.73×10^0	4.6	5.09×10^{-1}
25	10.04.1981	1730	> 1.0	1.72×10^0	4.5	1.55×10^{-1}
26	10.05.1981	1000	> 1.0	2.00×10^0	4.3	1.90×10^{-1}
27	12.10.1981	1000	> 1.0	1.37×10^1	4.4	1.30×10^0
28	26.11.1982	0455	> 1.0	5.67×10^0	4.1	5.72×10^{-1}
29	08.12.1982	0045	> 1.0	8.62×10^1	5.5	6.05×10^0
30	16.02.1984	0915	> 1.0	7.25×10^0	4.3	1.02×10^1
31	29.09.1989	1217	1.0–4.0	9.33×10^0	2.9	3.02×10^1
32	22.03.1991	0439 (24.03)	> 1.0	Integral meteor data	—	1.10×10^{-1}
33	11.06.1991	0156	1.0–4.0	1.55×10^1	5.5	1.11×10^0
34	15.06.1991	0810	1.0–4.0	6.19×10^1	6.0	4.14×10^0
35	25.06.1992	0032 (26.06)	> 1.0	Integral meteor data	—	1.20×10^{-1}

Notes: Flux estimates for the events Nos. 3, 17, 32 and 35 were obtained by integral data due to measurements by ionization chambers (IC), neutron monitors (NM) and satellite *Meteor*.

emission radiation) are power laws and similar to that for the solar flares, suggesting a similar scenario on other stars.[314] The spectral indices in the energy spectra of star flares have a rather narrow range of values: from 0.4 to 1.4.

To illustrate present situation in this field, Fig. 7 shows energy spectra of flares of 23 red dwarf stars in the solar vicinity, several groups of flare stars in clusters,

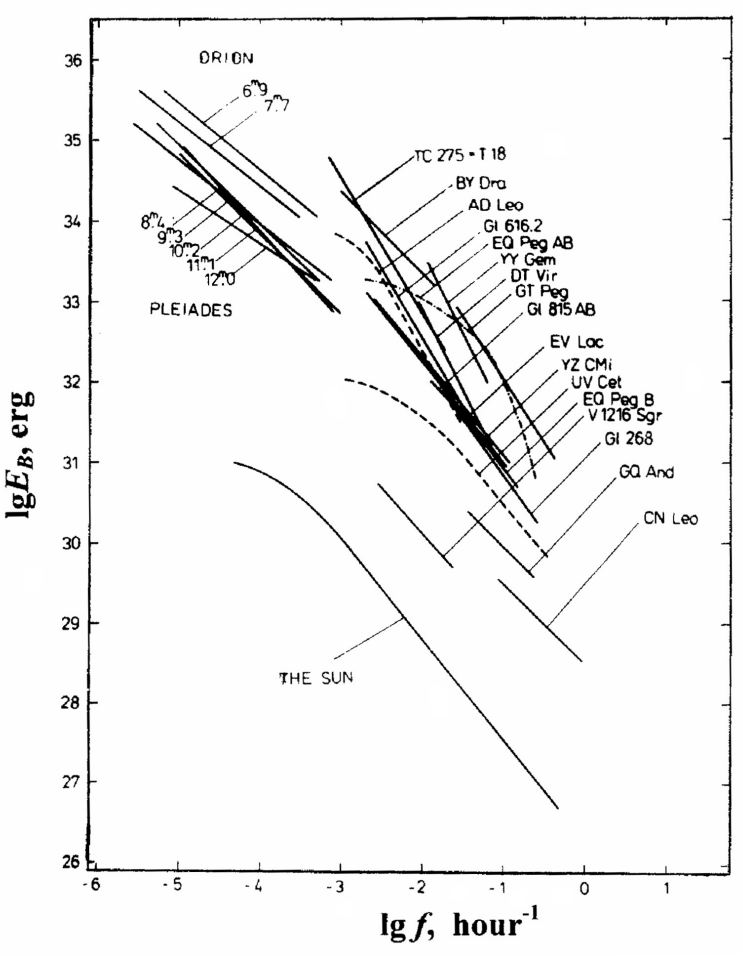

Fig. 7. Energy spectra of flares on red dwarf stars and the Sun.[314] Total energy in the B-band (Balmer emission lines) flare radiation, E_B, is plotted versus frequency, f, of flares with energy exceeding E_B.

and, for comparison, on the Sun (see for details and Ref. 314). In general features, the curves of stellar spectra and solar ones are similar (compare, for example, the curves for the Sun and UV Cet), though a difference in their amplitudes may be of several orders of magnitudes in energy. While this is an interesting similarity (or analogy) the relations between the distributions given in Figs. 6 and 7 is not clear yet.

Note that Figs. 6 and 7 show, respectively, the occurrence frequencies of solar energetic particle events as a function of peak intensity and the occurrence frequency of stellar and solar flares as a function of energy released. The similarity of those distributions, though obvious, is not investigated completely, for example, in terms of the same energy scales. Nevertheless, it is worthy to note that from

physical point of view, potential acceleration sites in the Universe (including the Sun and heliosphere) need to have the appropriate combinations of sizes, magnetic (electric) fields, shock velocities and other relevant parameters. These criteria have been discussed in general astrophysical context by Hillas[131] and Blandford.[38] In application to the solar accelerators, we discuss corresponding problems in Sec. 8 (e.g. Figs. 12 and 14).

5.4. *Energetic protons at other stars*

As one can see from Table 9, the energization rates and total energy contents are very important for understanding of relative role of accelerated ions and electrons in total flare energy budget. Rather long ago, a number of key flare observations and energy arguments were debated by Simnett[325,326] from the viewpoint of protons versus electrons. And the conclusion was that primary nonthermal protons are much more important, in terms of total energy, than nonthermal electrons in flares, the bulk of the energetic electrons being secondary. Although this hypothesis seems to be not proven today, we found it stimulating for the further developments, and we discuss it more profoundly based on our own approach to the initial stage of particle acceleration (see below). Anyway, this hypothesis provides one interesting indirect method to search for energetic protons in the atmosphere of some other stars.

As shown by Simnett,[326] the most sensitive diagnostic of protons in sub-MeV energy range is redshifted $L\alpha$ emission of the relevant excited state of hydrogen. Notice, however, that this method, unfortunately, has never been applied successfully to solar observations (see Ref. 326, and references therein). Although the Ultraviolet Spectrometer and Polarimeter on SMM was designed with a suitable capability, its response degraded before definitive measurements were undertaken. On the other hand, observations by the Goddard High Resolution Spectrograph on the Hubble Space Telescope turned out to be more successful. Woodgate *et al.*[389] have used its data to search for a $L\alpha$ red-wing enhancement during a flare from red dwarf star AU Microscopii on 3 September 1991. They found an event lasting 3 s, supposedly attributed to a low energy proton beam; this occurred a few seconds after the start of observations. From the strength of the $L\alpha$ red-wing they derived an integrated beam power of $> 10^{30}$ erg s^{-1}.

Using simultaneous observations of the Si III line, Woodgate *et al.*[389] estimated the flare energy. If AU Microscopii has an elemental abundance similar to the Sun, the total energy radiated by the plasma from which the Si III line originated was 6×10^{28} erg s^{-1}. In spite of considerable systematic uncertainties involved in these estimates, Simnett[326] believes that, if taking the measurements at face value, this flare was consistent with a dominant energy input from a low-energy proton beam ("proton beam hypothesis"). As he notes, it remains to be seen if these signatures are found in other stellar, or solar, flares.

This discussion reverts us to existing or assumed restrictions in the maximum energy and intensity of SCR, those parameters being of great significance for the

formulation of self-consistent model of particle acceleration at/near the Sun. The main problem of fundamental interest in the theory of particle acceleration at the Sun lie now at two boundary domains of SCR spectra, namely, in low-energy (non-relativistic) and high-energy (relativistic) ranges. The most important of them are: initial acceleration from the thermal background (e.g. Refs. 384, 225 and 217; see also discussion below), and final stage of acceleration to extremely high energies of $E_p \geq 100$ GeV (e.g. Refs. 279, 271, 224, 226, 228, 230, 146, 147, 239, and references therein; see also Sec. 8).

It would be timely to remind that the problem of initial stage of SEP acceleration is still unresolved and even poor-understood. As a very learning example of existing interesting problems we consider the hypothesis proposed by Miroshnichenko[225] who suggested that the differences ("splitting") between proton (ions) and electron energy spectra are inevitable from the very beginning of the spectrum formation (if both these particle populations are accelerated in the same acceleration process).

Due to possible selectivity of the acceleration mechanisms (e.g. Ref. 228) and different nature of energy losses of electrons and protons, their source spectra should be subject to softening at different rates nearly from the very beginning of the acceleration process. This results in a differentiation of the two spectra initially closely coupled by a common acceleration mechanism.

In this context, it is important to choose the most suitable parameter to compare the quantities of accelerated electrons and protons. In the light of well-known proton hypothesis of Simnett,[325] a convenient parameter would be specific particle energy, i.e. energy per unit of mass. Obviously, the equality of specific energies is possible, provided the condition of $V_p = V_e$ holds. It follows that the momentums (or rigidities) of two particles will obey the ratio of their masses, m_e/m_p. Therefore, it was suggested in Ref. 225 to analyze the spectral differentiation on the condition of normalization of $R_p = 1838 R_e \cong 1.0$ MV, i.e. starting with $V_p \cong V_e$. A proton rigidity of 1 MV approximately corresponds to a thermal energy $E_p \cong 10^3$ eV which would be the initial value for the acceleration of protons, for example, by a DC electric field.

It is natural to suppose that the amount of spectral differentiation will increase with the increase of particle rigidity. An expected picture of such process is shown in Fig. 8. Spectrum curve for protons is in approximate accordance with the observational data from the Proton Source Spectrum catalogue;[238] the normalized curve for electrons illustrates the assumed softening of their spectrum.[225]

To verify the effect under consideration it seems to be reasonable to combine the data of direct measurements of interplanetary electron flux and the observations of different types of wave radiation for the same flare with the results of calculations of electron energy losses. If the source spectrum of the electrons in the entire rigidity range of $R_e = 5.5 \times 10^{-4}$–5.5 MV can be reconstructed from this data set, then the comparison with the source spectrum of protons[238] will yield information of major importance. As far as we know, such a problem has never been considered before.

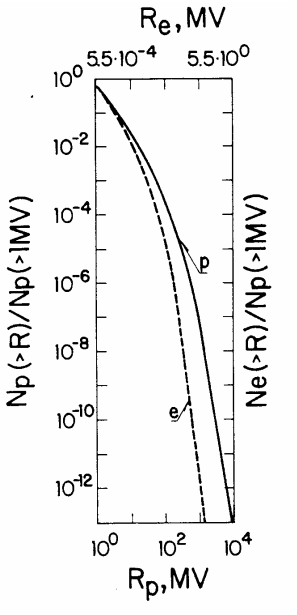

Fig. 8. Expected differentiation of the normalized rigidity spectra of accelerated particles[225] owing to different efficiency of acceleration mechanisms and different pattern of energy losses of electrons and protons (dashed and solid lines, respectively).

Obviously, evaluation of the source spectrum and energy losses of the electrons from data of the wave radiation signature, even for a narrow region of the spectrum, will depend heavily upon model ideas on loss conditions in the source and on mechanisms of emission. Nevertheless, there are good reasons for a possibility of such evaluations. In particular, observations near the Earth show that electron energy spectra from 30 keV to 3.0 MeV have a nonmonotonous decreasing form (see, e.g. Ref. 174), the number of relativistic electrons being several orders less than the number of relativistic protons in the same flare. Such a difference seems to be explainable by electron losses to synchrotron radiation, which under flare conditions falls into the ultraviolet range.[40] In connection with existing difficulties in interpreting of the electron component of solar cosmic rays, it appears to be reasonable to compile an Electron Source Spectrum catalogue, similar to the Proton Source Spectrum catalogue.[238]

6. Gamma Rays and Neutrons from Solar Flares

Measurements of accelerated charged particles near the Earth clearly indicate that such particles are produced in energetic phenomena at/near the Sun. These particles consist of both electrons and nuclei. But until the advent of solar gamma-ray astronomy, observations in the radio and X-ray bands had revealed only the existence of the electronic component in the flare region itself. In the hopes of finding the

properties of accelerated protons and heavier nuclei in flares, a variety of theoretical studies of the possible nuclear reactions of such particles in the flare region have been made (for early references see, e.g. Refs. 284 and 157).

One of the most dramatic manifestations of those reactions is the solar neutral emission (gamma rays and neutrons) produced by accelerated ions interacting with the ambient solar atmosphere. The main components of gamma-ray emission are: electron bremsstrahlung which dominates at energies of the photons of ≤ 1 MeV, and at energies of $\sim$ 10–50 MeV; nuclear gamma-ray line (GRL) emission (of $\sim$ 1–10 MeV) and pion decay emission (> 50 MeV). The experiments on SMM, Yohkoh, GRANAT, Compton Gamma Ray Observatory (CGRO), RHESSI, CORONAS-F and INTEGRAL allowed to accumulate copious data on solar gamma-rays in different energy range, in particular, on annihilation 0.511 MeV line, neutron capture line at 2.223 MeV, nuclear GRL emission of 4–7 MeV, pion decay emission above 50 MeV. There are even some evidences of gamma-ray production at the Sun at energies above 1 GeV.

Notice that an Atlas of all the flares observed in 1980–1989 by the SMM/GRS has been published.[383] About ten years after, a number of spacecraft (RHESSI, CORONAS-F and INTEGRAL) with their large set of detectors have registered several recent energetic solar phenomena, in particular, the flares of 23 July 2002 (e.g. Ref. 342), 28 October and 2 November 2003 (e.g. Ref. 12), and 20 January 2005 (e.g. Refs. 13 and 154).

Gamma rays provide important information on many aspects of the Sun's physics, including the fundamental problem of particle acceleration in the solar atmosphere. Papers by Chupp,[51] Share and Murphy[318] and Murphy and Share[250] give an extended view of the history of the field, its development and its current status, including some physical implications of the gamma-ray data.

6.1. *Recent progress in solar gamma-ray astronomy*

In spite of some limitations, the experiments on SMM, Yohkoh, GRANAT and the Compton Gamma Ray Observatory (CGRO) have already provided data for fundamental discoveries over the past decades relating to particle acceleration, transport and energetics in flares and to the ambient abundance of the corona and chromosphere. These include (e.g. Ref. 318): (1) enhancements in the concentration of low FIP elements where accelerated particles interact; (2) a new line ratio for deriving the spectra of accelerated particles at ≤ 10 MeV; (3) energies in accelerated ions that exceed those in electrons for some flares; (4) a highly variable ion to electron ratio during flares; (5) concentration of ^{3}He in flare-accelerated particles enhanced by a factor of ≥ 1000 over its possible photospheric value; (6) an accelerated α/p ratio > 0.1 in several flares and evidence for high ambient ^{4}He in some flares; (7) measurement of the positronium fraction and a temperature-broadened 511 keV line width; (8) new information on the directionality of electrons, protons, and heavy ions and/or on the homogeneity of the interaction region; and (9) the

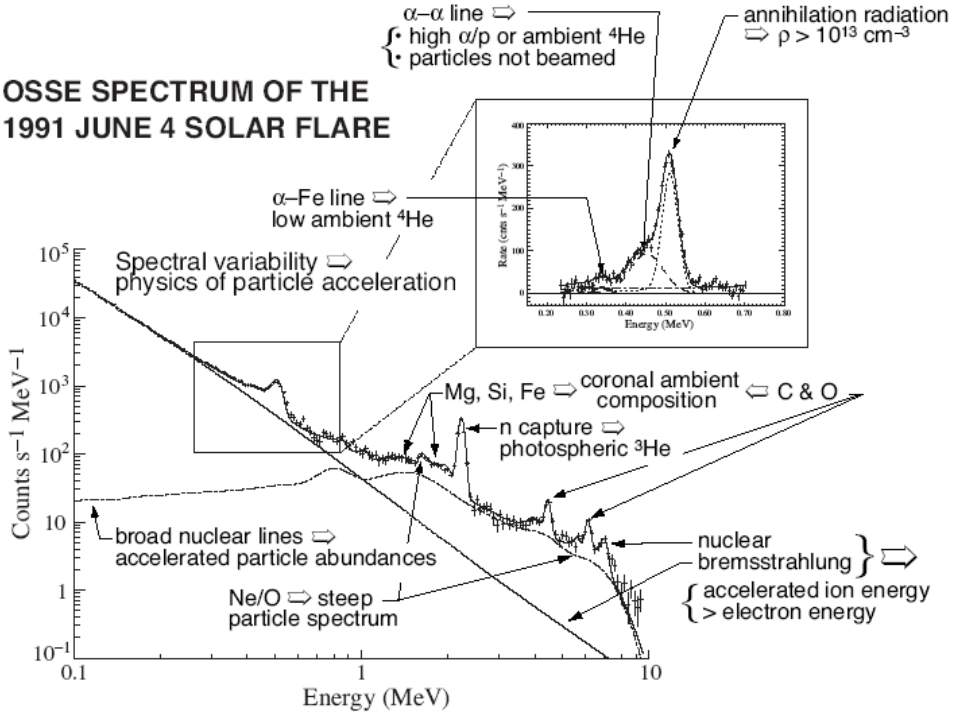

Fig. 9. Energy spectrum of the 4 June 1991 solar flare observed by the CGRO/OSSE instrument, with a summary of the physics to be revealed by gamma-ray spectroscopy.[318]

spectrum of broadened gamma-ray lines emitted by accelerated heavy ions that indicates Fe enhancements consistent with those observed in solar energetic particles.

Share and Murphy[318] summarized some past findings and highlight recent discoveries based primarily on measurements made by SMM/GRS and CGRO/OSSE instruments. The state of our knowledge of high-energy flare emissions is visually demonstrated in Fig. 9 that shows the gamma-ray spectrum of the 4 June 1991 flare observed by the OSSE/CGRO experiment. As one can see, from the gamma ray data may be derived important information about energy spectrum, elemental abundances and other features of accelerated particles, as well as about the properties of the solar atmosphere. Later on, high spectral-resolution measurements of nuclear deexcitation lines and the 2.223 MeV neutron capture line have been carried out with the Reuven Ramaty High Energy Spectroscopic Imager (RHESSI) during the flare of 23 July 2002[342,252]). The data on the time history of the narrow deuterium line at 2.223 MeV turned out to be very informative, in particular, to derive photospheric ^{3}He/H ratio during solar flares.

Due to high resolution spectroscopy of gamma-ray lines from the flare of 23 July 2003 the first gamma-ray images of a solar flare were obtained.[133,134] Two rotating collimators (with 35″ and 183″ resolution) were used to obtain images for the same time interval in four energy bands: the narrow deuterium line at

2.223 MeV formed by the thermalization and capture of neutrons produced in the collisions; the 3.25–6.5 MeV band that includes the prompt de-excitation lines of C and O; and the 0.3–0.5 and 0.7–1.4 MeV bands that are dominated by electron bremsstrahlung. The centroid of the 2.223 MeV image was found to be displaced by $20'' \pm 6''$ from that of the 0.3–0.5 MeV image, implying a difference in acceleration and/or propagation between the accelerated electron and ion populations near the Sun. Note, however, that this discovery is related to the regions of interactions (and emission production) of the electron and protons, respectively, but not to the sources (sites) of their acceleration. Also, we should keep in mind that the 2.223 MeV neutron capture line emission delays for about 100 s relatively to the production of proton above 10 MeV, and this time may be comparable with total duration of the particle acceleration.

As is well known, nuclear deexcitation lines result mainly from bombardment of ambient carbon and oxygen in the solar photosphere by the accelerated protons and alpha-particles (e.g. Ref. 284). Dramatic extensions of experimental possibilities (spacecraft RHESSI, CORONAS-F, INTEGRAL and others) in solar gamma-ray astronomy call for more detailed consideration of a set of physical problems related to the production of gamma-radiation in the processes of interactions of energetic (accelerated) heavy and middle nuclei with that of elements of the solar atmosphere (so-called heavy–heavy or ij-interactions). According to new theoretical estimates,[177] a contribution of these interactions between accelerated and background nuclei in the gamma-ray production in the solar atmosphere may be more important that it was thought earlier. This conclusion is confirmed by a comparison of theoretical estimates and observations during the RHESSI flare of 23 July 2002.[342]

As an example, we note that observed fluences of ^{12}C and ^{24}Mg nuclei[342] turned out to be the same ones (about 28 photons/cm^2), i.e. their ratio is about 1.0 (maximum 1.9). In contrast to this, the calculations for two versions of abundances of these elements in the solar atmosphere ("a" and "b" correspond to Refs. 10 and 42, respectively), give some evidence of that the ratios of fluxes of gamma rays from ^{12}C and from other nuclei in this experiment should be as those given in (Table 11), if we take into account only the processes of pk- and αk-interactions (for more details see Ref. 177).

As it follows from Table 11, to explain the observed ratios we must assume that nuclei of ^{24}Mg and ^{28}Si have been effectively created in the solar active region during the flare due to ij-interactions (for example, the interactions between the nuclei ^{12}C and ^{16}O and ^{16}O with ^{16}O). As for the nucleus of ^{20}Ne, one can see that the contribution of interaction of nuclei C and O into its generation is small, because the initial concentration of this element in the solar atmosphere in amount is comparatively high. The abundance of ^{20}Ne in the solar atmosphere is 5–7 times greater than the abundance of Mg and Si.[10,42] As for the ^{56}Fe, this nucleus cannot be created in the process of C–O and/or O–O interactions mentioned above.

In one of the recent reviews for the standard solar composition, Grevesse and Sauval[125] give for C/Mg and O/Mg the ratios that differ from the values used above

Table 11. Ratios of gamma ray fluxes from ^{12}C to that from other nuclei.

Ratio	Experiment	Calculations	
^{12}C/^{24}Mg	1.01, max 1.90	10.40 (variant "a");	4.40 (variant "b")
^{12}C/^{20}Ne	1.34, max 2.47	2.65 (variant "a");	1.53 (variant "b")
^{12}C/^{28}Si	1.67, max 3.31	31.0 (variant "a");	12.0 (variant "b")
^{12}C/^{56}Fe	3.81, max 8.02	30.0 (variant "a");	2.60 (variant "b")

for about 20–25% and about 2 times in comparison with the data by Cameron[42] and Aller,[10] respectively. Nevertheless, this does not change our main conclusion about important role of ij-interactions in the production of gamma line emission from ^{24}Mg in the flare of 2002 July 23. As to the ratios of C/Si and O/Si, they are even closer to the versions considered by us. Also, conclusions by Kuzhevskij *et al.*[177] concerning the contribution of ij-interactions into the creation of Ne and Fe nuclei become stronger due to the new solar composition results by Grevesse and Sauval.[125]

Another exciting finding of recent flare studies during two past decades turned out to be a registration of high-energy (pion) gamma-rays ($\geq$ 1 GeV) in June 1991.[4,144] In particular, the observations[144] for the flare of 11 June 1991 revealed for the first time the existence of pion radiation as late as 8 hr after the impulsive phase of the flare. We incline to consider such phenomena as serious evidence of multiple acceleration processes at/near the Sun (see Subsec. 6.4).

Quite recently, Murphy and Share[250] present the gamma-ray line-production and loop transport models used in the calculations of high-energy emission. They discussed in detail the calculated interaction time history, the depth distribution, the interacting-particle angular distribution, and fluence ratios of the narrow gamma-ray line. It was shown that the pitch-angle distribution of accelerated particles in the loop model is very important to estimate the GRL fluence.

In conclusion of this section, as a brilliant pattern of general astrophysical associations, we note here gamma-ray line emission from accreting binaries. It is now well admitted that accreting binaries can give rise to electron–positron annihilation line emissions, as observed with SIGMA[118] in the case of X-ray Nova in Musca. This is first clear evidence of gamma-ray line emission from soft X-ray transients. If interpreted as a positron annihilation line, it strongly suggests[118] the X-ray Nova in Musca to be a new black hole candidate.

It has also long been thought that accreting binaries can be the site of nuclear line emission resulting from neutron captures of hydrogen. The gravitational potential energy released through matter accretion onto a compact object could indeed provide ion temperatures more than sufficient to subject heavier nuclei to spallation reactions known to liberate a large number of free neutrons. If released in the vicinity of dense enough media (proton density $n_p > 10^{16}$ cm^{-3}), some of the liberated neutrons might be thermalized and further captured via reactions of the type $_0$n$^1 + {}_1$H$^1 \rightarrow {}_1$D^{2*}, thus producing excited deuterium nuclei whose decay to the ground state releases 2.223 MeV gamma rays.

To search for sites of neutron capture line emissions from celestial objects, McConnell *et al.*[204] have used the database from the COMPTEL experiment on the CGRO. They have obtained all-sky map in the neutron capture line 2.223 MeV. At first glance, the sky at these energies appears relatively featureless, and none of the catalogued bright X-ray sources showed any sign of detectable emission. There is, however, evidence for significant emission from a point-like feature at galactic longitude and latitude, $l \approx 300^\circ$ and $b \approx -30^\circ$, respectively, but without any obvious counterparts (such as an X-ray binary) that are consistent with the emission model discussed above. The authors found a significant signal (at the level of 4σ) at the energy of 2.223 MeV from this point-like source located in the southern part of the sky. This intriguing gamma-ray source has, nevertheless, to stand high on the list of targets to be pointed out by high-resolution gamma-ray spectrometers.

6.2. *Physical implications of the data on neutron capture gamma-ray line*

Elemental abundances and charge states of solar energetic particles are very important sources of astrophysical information. In particular, ^{3}He are thought to be primarily produced by nucleosynthesis in the early Universe, and its abundance is used to place a constraint on cosmological model. Since the photospheric ^{3}He abundance cannot be determined spectroscopically, observations of the neutron capture line at 2.223 MeV from solar flares provide a direct means of determining the photospheric ^{3}He abundance.

Neutrons which are produced simultaneously with prompt gamma-ray lines by interactions of accelerated ions diffuse into the photosphere where the 2.223 MeV line are emitted by neutron capture on hydrogen (see above). Because of the time required for neutrons to slow down and be captured, the 2.223 MeV line is produced about 100 s after the production of the neutrons. The competing capture reaction $^3\mathrm{He}(n,p)^3\mathrm{H}$ affects the delay of the 2.223 MeV line emission.

The 2.223 MeV line flux from instantaneous production of neutron is assumed to fall exponentially in time with a time constant τ given by $1/\tau = 1/\tau_\mathrm{H} + 1/\tau_\mathrm{He} + 1/\tau_d$. Here τ_H is the time constant for capture on H, τ_He is the time constant for capture on ^{3}He and τ_d is the neutron decay time (918 s). The values of τ_H and τ_He are approximated by $1.4 \times 10^{19}/n_\mathrm{H}$ s and $8.5 \times 10^{14}/n_\mathrm{He}$ s, respectively, where n_H and n_He are the number densities of hydrogen and ^{3}He. In a case of the simplified approach (for details see, e.g. Ref. 390) the time profile of the 2.223 MeV line emission $F(t)$ is expressed by

$$F(t) = A \int_{t_0}^{t} \left[\frac{S(t')}{\tau}\right] \exp\left[-\frac{(t-t')}{\tau}\right] dt' \,, \tag{3}$$

where A is the constant, t_0 is the time when the gamma-ray lines are observed and $S(t')$ is the time profile of the neutron production. Temporal dependence of $S(t')$ is assumed to be similar to that of the C + O line emission. Using this formula, we

Table 12. Data of photospheric ^{3}He/H ratio.[390]

^{3}He/H ($\times 10^{-5}$)	Flare	Satellite	References
< 3.8	03 June 1982	SMM/GRS	399
2.3 ± 1.2	03 June 1982	SMM/GRS	400
2–5	11 June 1991	GRANAT/FEBUS	401
2.3	04 June 1991	CGRO/OSSE	402
2.3 ± 1.4	06 Nov 1997	YOHKOH/GRS	391

can obtain τ which gives the best fit for the observed time profile of the 2.223 MeV line emission. The ^{3}He/H ratio is determined from this best fit τ, if $n_{\rm H}$ is assumed.

Yoshimori *et al.*[390] summarized a few data of photospheric ^{3}He/H ratio obtained by different research groups from the gamma-ray line spectroscopy (Table 12). As they noted, in order to advance the understanding of the ^{3}He/H problem, we need more precise gamma-ray observations. Moreover, Share and Murphy[317] suggested the procedure for determining the photospheric ^{4}He/H from the product of the solar wind ^{4}He/^{3}H and the photospheric ^{3}He/H ratio. The ^{3}He/H ratio is related to the ^{4}He/H ratio that is an important parameter for studies of stellar evolution and solar neutrino production.

One of the recent attempts to derive the photospheric ^{3}He/He ratio was undertaken by Murphy *et al.*[251,252] by the RHESSI data on the measured time history of the 2.223 MeV neutron capture line during the flare of 23 July 2002. This ratio, however, was not well-constrained, primarily due to uncertainties of the measured nuclear deexcitation-line flux used to represent the neutron-production time history.

As mentioned above, observed intensity of the neutron capture line of 2.223 MeV is a measure of the concentration of ^{3}He in the photosphere. Moreover, the time history of the 2.223 MeV line fluence may be used to determine the altitude profile of plasma density deeply in the photosphere (e.g. Ref. 357). For the first time such a possibility was demonstrated by the data on the 22 March 1991 flare.

Subsequent analysis of a set of other flares (6 November 1997, 16 December 1988, and 28 October 2003) confirmed an effect of plasma density enhancement (EDE) at the photospheric and subphotospheric levels during those four flares mentioned.[175,176,358] Quite recently it was shown that the 2.223 MeV line data may be used to link the line fluences with a form of the spectrum of accelerated protons in the source.[176,359,360]

Mandzhavidze and Ramaty[197] reviewed the results of gamma-ray investigations that provide information on the solar flare accelerated α/p and ^{3}He/^{4}He ratios, on the ambient He/H, Mg/O, Si/O and Fe/O in subcoronal regions of the solar atmosphere, and on the photospheric ^{3}He/^{4}He ratio. The data on the 2.223 MeV line from five more flares considered here confirms their previous conclusion that the ^{3}He/^{4}He ratio in the photosphere is lower than it is in the corona. These findings have major implications on the understanding of solar atmospheric dynamics, solar wind and solar flare particle acceleration and galactic chemical evolution.

6.3. *High-energy solar neutrons*

The observations at the Earth of solar neutrons generated during powerful solar flares (in combination with X-ray, gamma-ray and other data) allows us to obtain unique information on the Sun's flare processes and particle acceleration mechanisms. The first solar neutrons were observed near the Earth by the GRS/SMM on 21 June 1980 (e.g. Ref. 51). The first simultaneous measurements of solar neutrons by space and ground based detectors were made during prominent event on 3 June 1982.

Table 13 gives a summary of existing data on registration of high-energy neutrons produced in solar flares in 1980–2005. Solar neutrons were registered by different detectors on board the spacecraft, by surface neutron monitors (NM) and solar neutron telescopes (SNT) at the mountains (Alma-Ata, Aragats, Chacaltaya, Gornegrat, Haleakala, Jungfraujoch, Mauna Kea, Norikura, Sierra Negra, and Tibet). In some events also pion decay emission was detected. To compile this table, we used several papers where those data are discussed in more details.[195,101,386,306]

There are also 19 bursts, the most probable candidates for registration of solar neutrons, as they were identified by the data of mountain NM Alma-Ata:[17] 24 July 1979; 7 April 1980; 9 August 1982; 4 September (two bursts), 14 September, and 2 October 1989; 17 September 1990; 1 June, 6 June, 12 June, 15 June, 17 June, 11 July, 14 July, 22 July, 5 August, and 27 October 1991; 8 May 1998.

Five solar neutron events (SNE's) were detected by the ground-based neutron monitors in association with five solar flares with deviations greater than 5σ from the background fluctuations in solar cycle 23:[386] 24 November 2000, 25 August 2001, 28 October, 2 and 4 November 2003 (the authors did not include yet in their analysis the event of 7 September 2005). Also, five SNE's were detected by NM's in previous solar cycles: 3 June 1982, 24 May 1990, 22 March 1991, 4 and 6 June 1991.

Using these data, the authors report on some properties of the SNE's as neutron and proton spectra, flare positions where solar neutron events were produced, and the relation between neutron flux and flare class. An extensive statistical discussion on the properties of SNE's was made. The results of this work can be summarized as follows: (1) the spectral indices of solar neutrons range between -3.0 and -4.0, the corresponding proton index is softer by about -1.0; (2) the numbers of accelerated protons are $10^{30} \sim 10^{33}$, that is 100 to 1000 times more than the neutron flux; (3) there is no correlation between the longitude of solar flares and SNE's. Hence, a solar flare model must account for the acceleration of ions away from the solar surface, or produce neutrons moving away from the solar surface; (4) the class of solar flare is not the main indicator of the magnitude of the ion acceleration.

As a brilliant illustration of the solar neutron registration we present recent data on the SNE from the giant flare of 3B/X17 (S06, E89) on 7 September 2005. The event was registered with high statistical significance's by the Solar Neutron Telescopes located at Mount Chacaltaya (Bolivia) and Mount Sierra Negra (Mexico) as well as by the neutron monitors at Chacaltaya and Mexico City.[306,307] These

Table 13. A summary of solar neutron observations in 1980–2005.

No.	Date	Position	Pions	Neutrons
1	21 Jun 1980	W90 N20	—	SMM/GRS
2	03 Jun 1982	E72 S09	SMM/GRS	SMM/GRS, Decay Protons (ISEE-3) NM, Jungfraujoch
3	24 Apr 1984	E43 S12	SMM/GRS	SMM/GRS, Decay Protons (ISEE-3)
4	16 Dec 1988	E37 N26	SMM/GRS	SMM/GRS, Decay Protons (ISEE-3)
5	06 Mar 1989	E69 N35	SMM/GRS	SMM/GRS
6	19 Oct 1989	E09 S25	—	Several NM's
7	24 May 1990	W75 N33	GRANAT/SIGMA	Several NM's
8	22 Mar 1991	E28 S26	GRANAT/SIGMA	NM, Haleakala
9	04 Jun 1991	E70 N30	—	CGRO/OSSE; SNT, MN, Norikura; EAS, Akeno
10	06 Jun 1991	E54 N32	—	NM, Norikura, Haleakala
11	09 Jun 1991	E04 N34	—	CGRO/COMPTEL, SNT, Norikura
12	11 Jun 1991	W17 N31	CGRO/EGRET	CGRO/COMPTEL, SNT, Norikura
13	15 Jun 1991	W69 N33	GAMMA-1/FEBUS	CGRO/COMPTEL, NM, Alma Ata
14	06 Nov 1997	W43 S16	—	SNT, Chacaltaya
15	17 Aug 1998	Unknown	—	SNT, Mauna Kea
15	18 Aug 1998	E87 N33	—	SNT, Mauna Kea
16	28 Nov 1998	E32 N17	—	SNT, Tibet
17	12 Jul 2000	E27 N17	—	SNT, Gornegrat, Aragats
18	24 Nov 2000	N22 W07	—	NM, Chacaltaya
19	29 Mar 2001	W19 N20	—	SNT, Gornegrat
20	02 Apr 2001	W61 N17	—	SNT, Gornegrat
21	09 Apr 2001	W04 S21	—	SNT, Gornegrat
22	10 Apr 2001	W09 S23	—	SNT, Aragats
23	12 Apr 2001	W04 S21	—	SNT, Gornegrat, Aragats
24	25 Aug 2001	S17 E34	—	NM, Chacaltaya
25	28 Oct 2003	S16 E08	CORONAS/SONG	NM, Tsumeb
26	02 Nov 2003	S14 W56	—	NM, Chacaltaya
27	04 Nov 2003	S19 W83	—	NM, Haleakala
28	07 Sep 2005	S06 E89	—	NM, SNT, Chacaltaya, Mexico, Sierra Negra

Notes: The neutron bursts Nos. 17–24 have been registered at the level of statistical significance from 2.7σ to 4.9σ (see for details in Ref. 101).

observations are illustrated by Fig. 10. The maximum of soft X-ray burst was observed by GOES 11 at 17:40 UT and Type II onset at 17:42 UT. By the GEOTAIL satellite data, the hard X-rays (> 50 keV) peaked at 17:36:40. At the same time an orbiting space laboratory INTEGRAL detected gamma rays in the MeV

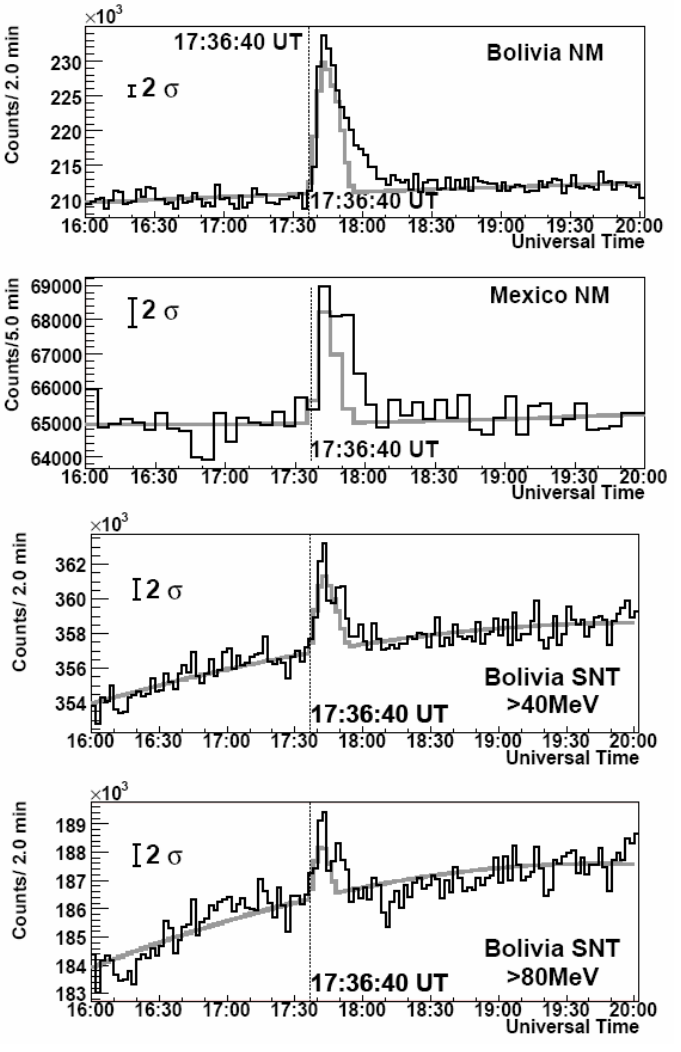

Fig. 10. Solar neutron burst on 7 September 2005:[306] 2-minute counting rate of the Bolivia NM (first, top panel); 5-minute data of the Mexico City NM (second panel); 2-minute data of different channels of the Bolivia SNT (> 40 MeV, third panel, and > 80 MeV, fourth, bottom panel). The moment of 17:36:40 UT is the GEOTAIL hard X-ray peak time. Grey curves show expected counts assuming a neutron flux derived from the Bolivia NM data.

range. Because there was no clear evidence of nuclear lines, high energy radiation is considered to trace the high-energy electrons. Preliminary analysis of the data shows that a model of the impulsive neutron emission at the time of the X-ray/gamma-ray peak can explain the main peaks of all the detected neutron signals, but failed to explain the long tailed decaying phase.

Alternative model that the neutron emission follows the X-ray/gamma-ray profile also failed to explain the long tail. The results by Sako *et al.*[306] indicate that the

ions were accelerated at the same time with electrons but they were continuously accelerated or trapped longer than the electrons in the emission site. The authors also believe that the neutron data observed by multienergy channels of SNT's can constrain the emission models in more detail.

7. Composition and Charge States of Solar Particles

Heavy ions (with atomic number $Z \geq 2$) with a wide range of charge-to-mass ratio (Q/A), isotopic ratios, as ^{3}He/^{4}He and elemental ratios (particularly Fe/C or Fe/O) are useful tools for deciphering the several energy and rigidity processes involved in the injection, acceleration, escape and transport of solar particles.

7.1. *High abundance variability in large SEP events*

In large gradual SEP events (or LGE's, see Table 2), abundances of elements up to Fe at a few MeV/amu are highly variable from event to event. The origin of this variability has been a matter of intense and on going debate. However, it has been argued that when taking their long term averages, it seems they follow a trend similar to the abundances of the solar corona plasma from which ions are accelerated. Observational data on high abundance variability in LGE's are very important, in particular, to substantiate the debating hypothesis: quasiperpendicular shock acceleration of seed suprathermal remnants versus direct flare generation.

Solar abundance of elements with atomic number $Z \geq 34$ decreases drastically by as much as 6–8 orders of magnitude below that of O,[125] however, energetic ions with $Z \geq 34$ often have modest enhancements that follow similar behavior to that of Fe/O and show high-energy spectral rollovers with the same Q/A-dependence as the elements up through Fe.[299] In the case of impulsive SEP events the situation is quite different, where it can be found thousand fold enhancements of ^{3}He/^{4}He, and enhancements in heavier elements that increase with decreasing (Q/A) of the ions at coronal temperatures,[289] resulting also in thousand fold enhancements for ($Z \geq 50$)/O. Intermediate abundances, however, may result when remnant suprathermal ions from impulsive events contribute to the material accelerated in subsequent events, presumably by CME-driven shock waves. Such enhancements in impulsive SEP events are generally attributed to resonant wave–particle interactions in the turbulent plasma (e.g. Ref. 214).

In recent work Tylka *et al.*[369] have extensively described the present status about solar particle abundances and their charge states in LGE's. Above a few tens of MeV per nucleon, large gradual SEP events are highly variable in their spectral characteristics and elemental composition. About one-third of the large SEP events observed by ACE and Wind spacecraft in solar cycle 23 exhibit significant energy dependence in Fe/C ratio, which reflects spectral differences between the two species.

To illustrate the variability from event to event and energy dependence, the authors discuss the events of 21 April and 24 August 2002 (the latter was registered

also as GLE64). Below ~ 10 MeV nucleon^{-1}, the Fe/C ratios are nearly identical in both events, but at higher energies the two events diverge, so that at ~ 60 MeV nucleon^{-1} the ratios differ for more than two orders of magnitude. In the GLE64, the ratio reach a value ~ 7 times the coronal value Fe/C = 0.288, whereas for the 21 April event, values fall as low as 0.05 the coronal value. Fe has a softer spectrum than C at higher energies in the event of 21 April, while in the 24 August event it is harder. The April event is Fe-poor at high energies, while the August GLE is Fe-rich.

Both events were associated with wide CME's, in which the speeds were 2400 km s^{-1} and 1900 km s^{-1} (the fastest during the SOHO period of observation in 1997–2002), and transit times to the Earth for the associated shocks were 51 and 58 hrs, respectively. The associated flares for the two events were also nearly identical in terms of their sizes and solar locations (X1.5/1F at S14, W84; and X3.1/1F at S02, W81, respectively). Thus, the differences cannot be blithely ascribed to factors such as CME speed and source location, which are generally believed to be important for SEP variability.

Events like 24 August 2002, in which Fe/C increases with energy and attains values ≥ 5 times, also tend to have enhanced ^{3}He/^{4}He at the energy above 7 MeV nucleon^{-1}. For a few such events measurements give the mean ionic charge of Fe about 20 above the energy of 30 MeV nucleon^{-1}. Therefore, Fe and C have not too dissimilar Q/A values, and so it is difficult to ascribe Fe/C enhancements only to Q/A effects during acceleration, escape or transport. It has been suggested that the high-charge Fe ions are generated by stripping during acceleration in high-density regions of the corona.[298,20,21] But it is not clear why this process should also lead to enhanced Fe/C. Consequently, the enhanced Fe/C must be a characteristic of the seed population from which the highest energy ions are drawn.

An important fact pointed out by Tylka *et al.*[369] is that such an embryonic population for SEP's likely comprises, at least, two components: the ubiquitous suprathermal tail from the solar wind[117] and suprathermals from previous flare activity.[201,368] Among the distinguishing characteristics of these flare suprathermals are: elevated Fe/C (and Fe/O) ~ 10 times the average coronal and solar-wind values (Fe/O = 1), large enhancements in trans-Fe ions,[293,294,296,203] Fe ions with charge $\langle Q \rangle > 16$,[191] and ^{3}He/^{4}He significantly enhanced above the average solar-wind value of $0.041 \pm 0.003\%$. In contrast, the germ population from the solar wind suprathermal tail has typically values of Fe/O = 0.1 and $\langle Q_{\rm Fe} \rangle = 10$.

As mentioned above, the origin of the overall high-energy variability of the spectral characteristics and elemental composition in large gradual SEP is still a matter of intense debate. To explain such a variability, Tylka *et al.*[369] propose a shock acceleration hypothesis that arises from the interplay of two factors — *shock geometry* and a compound *seed population*, typically comprising both solar-wind and flare suprathermals. Whereas quasiparallel shocks generally draw their seeds from solar-wind suprathermals, quasiperpendicular shocks — by requiring a higher initial speed for effective injection — preferentially accelerate seed particles from flares. These flare suprathermals could be remnants from earlier flare activity.[201,368]

Solar-wind and flare seed particles have distinctive compositional characteristics, which are then reflected in the accelerated particles. Flare suprathermals are more likely to dominate over solar-wind suprathermals as the seed particles in quasi-perpendicular shocks. However, the shock geometry generally evolves as the shock moves out from the Sun, usually from quasiperpendicular toward quasiparallel. Consequently, the nature of the accessible seed population would also change during this evolution. At the same time, as the shock angle decreases, the spectra soften at high energies. The net effect of this evolution is to allow the unique compositional characteristics of flare suprathermals to be reflected preferentially among the higher energy particles. Tylka *et al.*[369] attribute large-fluence events, like that of 21 April, to a predominance of a solar-wind germ population, and GLE's as the 24 August, to a predominance of the seed flare population.

The authors also examine the alternative hypothesis in which a direct flare component (rather than seed flare particles from previous activity subsequently processed through a shock) dominates at high energies, if open field lines connect the associated flare site to the shock front.[295] However, arguments based in timing studies, longitude distributions and spectral characteristics lead them to disregard this alternative. Tylka *et al.*[369] support their shock wave acceleration hypothesis based on a wide correlation analysis. However, they recognize that, although such correlation studies cannot be construed as proof of their shock wave acceleration hypothesis, they certainly confirm its viability. The authors' hypothesis do not considers the low energy component, below 1 MeV nucleon^{-1}. Nevertheless, Tylka *et al.*[369] suggest that the enhanced Fe below 1 MeV nucleon^{-1} (which charge states are characteristic of solar-wind ions, not flare-accelerated ions) may be a transport-induced distortion, due to iron's relatively low Q/A, rather than an attribute of the seed population.

This important summarizing work also contains the results of analysis of the energy dependence of the F/O ratios for 23 events at 1 AU. The authors found that events with rising Fe/O with energy are preferentially associated with large ^{3}He/^{4}He, whereas events with falling Fe/O with energy generally have smaller ^{3}He/^{4}He. However, they note that Fe/O and ^{3}He/^{4}He enhancements in flares are not strictly correlated. So, they argue that enhancements of ^{3}He/^{4}He and Fe/O in flares are produced by distinct mechanisms, so that one can be present in the seed population without the other.

Under the consideration that iron charge states are indicators of seed populations, they infer that the high charge state of Fe, namely, $Q = 15 \pm 3.6$–17.7 ± 3.3, in some events at 0.23–0.30 MeV nucleon^{-1}, tends to support that Fe/O strongly increasing with energy preferentially corresponds to a quasiperpendicular shock operating on a seed population with a significant component of flare suprathermals. Nevertheless, they emphasize that such conditions may be necessary but not sufficient, in addition to statistical limitations of this analysis. Table 14 shows the main properties of the events analyzed by Tylka *et al.*[369] They focus on the oxygen spectrum which is less biased, since, unlike Fe, its interpretation is not potentially complicated by a wide range of Q/A values.

By detailed analysis of the corresponding data for Fe and that of oxygen on basis to the event size (proton fluence) and power-law index (columns 9 and 10 in the Table 14) the authors infer that potential candidates for acceleration by quasiparallel shocks (like the event of 21 April 2002) are larger and have a relatively soft spectrum at the highest energies. At the same time, the candidates for quasiperpendicular shock acceleration (like the event of 24 August) are smaller, but have a relatively hard spectrum. Because quasiperpendicular shocks require higher injection energy, it should be generally expected quasiperpendicular events to have smaller fluences than quasiparallel events. So, quasiperpendicular shocks are more likely to produce GLE's. Tylka *et al.*[369] argue that these differences from the very beginning of events do indeed reflect inherent features of the accelerator while near the Sun. In general, one would expect to see spectral hardening if two distinct acceleration mechanisms were operating, with one mechanism being substantially more prolific at acceleration to high energies.

7.2. *Abundance variability in GLE events*

According to the hypothesis by Tylka *et al.*,[369] one should generally expect GLE's to be Fe-rich at high energies. However, this expectation need not always be true, in that flare Fe might not be available in the seed population of some events. Dietrich and Lopate[69] first reported a tendency for GLE's to have enhanced Fe/O above the energy of 50 MeV nucleon^{-1}. They have reported the spectra and absolute intensity of many of the large SEP events as measured with the CRNC instrument on the IMP-8 satellite. Their instrument responds to ions over the energy range $\sim$ 1–500 MeV/nucleon. It is also able to distinguish the composition of particles, which stop in one of its detector, and can differentiate the isotopes ^{1}H from ^{2}H and ^{3}He from ^{4}He. The authors found that, contrary to earlier analysis, for most of the new events, the largest of the SEP's are iron rich (Fe/O ratio $\sim$ 1), with very hard heavy ion spectra. The spectra were generally power law in energy/nucleon over the energy range mentioned. Also a high correlation between GLE's, observed by NM's, and iron rich SEP events was found.

There has been a general feeling in the past that Fe-rich flares occurred infrequently, and were usually small in their absolute fluence of particles (Fe normal events have a ratio Fe/O $\sim$ 0.075–0.15). The period of 1997–1998 appears to dispute this idea. Using the criterion that a ratio Fe/O $> \sim$1 is an indication of a Fe-rich event, it was found that of the eight large SEP events seen during this period, seven are Fe-rich.

Many researchers have been using a standard set of identifiers for SEP events to categorize these events as "gradual" and "impulsive" (e.g. Refs. 288 and 44). The SEP events seen during 1997–1998 seem to fit many of the criteria for "gradual" events: they are associated with CME's, type II radio bursts, and medium ionic charge state Fe.[70,242,243] However, Dietrich and Lopate[69] have seen that these SEP events are also Fe-rich, a characteristic often associated with "impulsive" events. This may be indicating that Fe/O ratio is not a good quantity for separating the various types of SEP events.

Table 14. Large gradual SEP events of solar cycle 23 (after Ref. 369).

Event no. (a)	Event date (b)	CME speed (c)	Source location (d)	Proton fluence (e)	GLE (f)	Wind/ACE Fe/O/0.134 (g)	Oxygen-Iron index (h)
1 1997	04–06 Nov	785	S14 W33	6.71e+05	Y	4.23/3.03	2.75/3.16–2.37/3.36
2 1997	06–10 Nov	1556	S18 W63	1.22e+07	Y	3.15/5.78	2.53/2.48–1.78/2.43
3 1998	20–26 Apr	1863	S?? W90	2.77e+07	N	2.13/0.019	1.16/6.43–2.64/8.04
4 1998	02–04 May	938	S15 W15	1.50e+06	Y	5.03/4.93	2.36/239–1.78/2.45
5 1998	06–08 May	1099	S11 W65	6.55e+05	Y	4.53/3.99	2.99/3.16–2.44/4.24
6 1998	24–27 Aug	···	N35 E09	3.65e+06	Y	0.406/0.84	3.28/6.27–3.27/2.04
7 1998	30 Sep 03 Oct	···	N19 W85	3.50e+06	N	1.62/1.68	2.55/4.05–2.02/3.77
8 1998	14–17 Nov	···	N? W120	2.51e+06	N	3.70/4.46	2.00/3.85–1.50/3.34
9 1999	01–04 Jun	1772	N? W120	4.20e+05	N	0.83/4.73	2.37/2.69–1.46/2.73
10 1999	04–08 Jun	2230	N17 W69	2.45e+05	N	0.80/2.50	3.81/4.91–3.21/3.45
11 2000	10–13 Jun	1108	N22 W40	2.95e+05	N	5.03/4.56	2.94/4.39–2.31/3.45
12 2000	14–17 Jul	1674	N22 W07	3.42e+08	Y	3.97/0.57	1.08/4.83–1.72/3.73
13 2000	12–16 Sep	1550	S17 W09	9.42e+05	N	0.242/3.10	3.99/4.25–3.39/4.07
14 2000	16–20 Oct	1336	N?? W95	2.02e+05	N	3.36/5.02	2.56/3.36–2.02/3.65
15 2000	08–11 Nov	1345	N10 W75	2.53e+08	N	3.22/0.041	1.63/4.67–1.92/7.16
16[i] 2000	24–28 Nov	994	N22 W07	3.62e+06	N	1.10/0.69	2.72/4.95–2.41/4.19
17 2001	28 Jan 01 Feb	916	S04 W59	2.86e+05	N	1.83/4.36	3.70/3.92–2.64/3.54
18 2001	29 Mar 01 Apr	942	N16 W12	2.83e+05	N	3.35/2.63	2.78/4.13–2.48/4.06
19 2001	02–06 Apr	2505	N17 W87	7.62e+06	N	2.42/1.90	2.12/3.90–2.06/3.64
20 2001	10–12 Apr	2411	S23 W09	1.52e+06	N	0.88/0.76	3.24/4.78–2.68/5.13

Table 14 (*Continued*)

Event no. (a)	Event date (b)	CME speed (c)	Source location (d)	Proton fluence (e)	GLE (f)	Wind/ACE Fe/O/0.134 (g)	Oxygen-Iron index (h)
21 2001	12–14 Apr	1184	S20 W42	5.14e+05	N	0.90/1.58	3.59/4.40–3.24/4.02
22 2001	15–18 Apr	1199	S20 W84	1.16e+07	Y	2.55/4.78	2.61/2.51–2.31/2.20
23 2001	18–22 Apr	2465	S? W120	3.56e+06	Y	1.55/2.50	3.14/2.46–2.46/2.40
24 2001	16–19 Aug	1575	W140, ??	7.37e+06	N	1.33/0.80	1.48/3.63–1.45/3.51
25 2001	24–30 Sep	2402	S16 E23	9.74e+07	N	0.96/0.091	2.06/5.08–2.17/5.69
26 2001	01–05 Oct	1405	S20 W88	6.73e+06	N	0.55/050	1.99/6.91–3.02/3.86
27 2001	22–26 Oct	1336	S21 E18	3.64e+05	N	1.06/5.69	3.57/3.08–2.09/2.43
28 2001	04–09 Nov	1810	N06 W18	2.71e+08	Y	1.80/0.31	1.16/4.16–2.02/3.52
29 2001	22–26 Nov	1443	S15 W34	6.74e+07	N	1.10/0.45	2.16/5.08–2.76/4.13
30 2001	26–29 Dec	1406	N08 W54	6.67e+06	Y	1.49/4.18	2.52/3.01–1.81/2.70
31[j] 2001	30 Dec 04 Jan	?	?	7.62e+05	N	0.68/0.19	2.83/7.61–3.11/6.20
32[k] 2002	10–14 Jan	1794	S18 E79	2.69e+05	N	0.115/···	3.72/···–4.54/···
33 2002	21–24 Apr	2409	S14 W84	5.28e+07	N	1.31/0.14	1.83/5.95–2.15/5.40
34 2002	22–25 May	1494	S22 W53	3.52e+05	N	0.281/0.43	3.59/4.85–2.40/5.53
35[k] 2002	16–19 Jul	1132	N19 W01	2.53e+05	N	0.47/0.88	3.44/5.44–2.58/3.52
36 2002	21–26 Jul	1941	S?? E90	5.13e+05	N	0.62/0.56	2.41/5.69–2.35/3.70
37 2002	22–24 Aug	1005	S07 W62	4.08e+05	N	···/4.64	···/3.98–···/3.55
38 2002	24–27 Aug	1878	S02 W81	3.86e+06	Y	1.17/4.61	2.96/3.33–2.55/2.79
39 2002	09–12 Nov	1838	S12 W29	4.28e+05	N	0.93/0.25	3.00/6.01–3.44/6.01
40 2003	26–28 Oct	1537	N02 W38	1.46e+06	N	1.58/1.21	2.43/3.59–2.51/3.55

Table 14 (*Continued*)

Event no. (a)	Event date (b)	CME speed (c)	Source location (d)	Proton fluence (e)	GLE (f)	Wind/ACE Fe/O/0.134 (g)	Oxygen-Iron index (h)
41 2003	28–29 Oct	2459	S16 E08	2.43e+08	Y	4.36/0.068	0.80/4.82–1.88/3.31
42 2003	29 Oct 2 Nov	2029	S15 W02	4.16e+07	Y	2.50/0.83	1.78/4.05–2.05/3.40
43 2003	02–04 Nov	2598	S14 W56	1.56e+07	Y	1.10/0.57	1.93/4.87–2.58/3.84
44 2003	04–08 Nov	2657	S19 W83	2.58e+06	N	0.598/0.44	3.18/5.42–3.40/3.97

(a) Year and event number as it was registered between 1 November 1997 and 30 April 2004 by Wind/LEMT and ACE/SIS instruments.
(b) Event interval (date of start and stop of the integration interval).
(c) CME speed, km s^{-1}. From one-parameter fits to the LASCO time-height profiles, as given by http://cdaw.gsfc.nasa.gov/CME_list. The measured speeds do not take into account potential projection effects. The Web site does not report error bars on the fitted speeds, but comparisons of results from independent analyses of the LASCO images suggest that the uncertainties are likely to be on the order of 10–20% (M. Andrews, A. Reinhard, S. Kahler, and S. Yashiro 2004, private communications).
(d) Source location (deg). From Cane *et al.*[45,46] whenever possible; later events from Solar Geophysical Data or other sources, as detailed in the text.[369]
(e) Proton fluence > 30 MeV, cm^{-2} sr^{-1}. From GOES-8 or (in 2003) GOES-11. Read "2.00e+07" as 2.00×10^7. The event selection required this fluence to be greater than 2.0×10^5 protons cm^{-2} sr^{-1}.
(f) N = no; Y = reported by least one neutron monitor station.
(g) Fe/O ratio normalized to the nominal coronal value, 0.134,[290] as measured by Wind (LEMT)/ACE(SIS) instruments in the energy ranges 3.2–5.0 MeV $nucleon^{-1}$ and 30–40 MeV $nucleon^{-1}$, respectively (for the error bars see Ref. 369).
(h) Oxygen (first pair) power-law indexes as measured by Wind (LEMT)/ACE(SIS) instruments in the energy ranges 3–10 MeV $nucleon^{-1}$ and 30–100 MeV $nucleon^{-1}$, respectively (first pair), and Iron (second pair) power-law indexes in the energy ranges 3–10 MeV $nucleon^{-1}$ and 21–100 MeV $nucleon^{-1}$, respectively (for the error bars see Ref. 369).
(i) Multiple events.
(j) Solar source not identified.[119]
(k) Delayed onset at 1 AU. Flare and CME associations provided by http://umbra.nascom.nasa/SEP/seps.html.

There are also used enhancements in the $^3He/^4He$ ratio as another indicator of "impulsive" events. In fact, seven of the eight "gradual" events studied by Dietrich and Lopate[69] have $^3He/^4He$ ratio that are well above the solar ratio of $\sim 10^{-4}$. It seems likely that nearly all SEP events have enhancements in the $^3He/^4He$ ratio,[48] perhaps due to resonance of ^3He with lower hybrid waves near the gyrofrequency of protons.[283] Thus, when discussing $^3He/^4He$ enhancements it is important to distinguish between an enhancement above solar values, and enhancements $^3He/^4He > \sim 1$, as is normally considered when describing ^3He-rich events.

The period of 1997–1998 saw two GLE's observed with NM's, one on 6 November 1997 and another on 2 May 1998. The SEP events associated with these two GLE's were Fe-rich. Dietrich and Lopate[69] have found a similar correlation between GLE's and their associated SEP events. Of the 24 GLE's observed in 1973–1998 only one (15 June 1991) does not show this correlation.

One possible explanation for this correlation is that these Fe-rich SEP events have hard enough Fe spectra that high energy Fe precipitating on the atmosphere creates an appreciate "air shower" signal which is observed with the neutron monitors. Estimates by Dietrich and Lopate[69] show that the Fe contribution to the neutron monitor signal is at most 20%. The correlation between the 29 September 1989 GLE and its associated SEP event are discussed in detail by Tylka *et al.*[366] Another explanation for this correlation is that whatever mechanism accelerates large numbers of protons to extremely high energies simultaneously enhances the acceleration of Fe in preference to lower mass elements. But there is no yet a self-consistent explanation for this correlation between GLE's and Fe-rich SEP events.

Table 15 summarizes IMP 8 CRNE observations of high-energy Fe/O for 25 GLE's of solar cycles 21–22.[369] In these events, the Fe/O ratio is compared to the nominal coronal value of 0.134.[290] Setting aside low-statistics GLE's (numbers 34, 35, 37, 40, and 50) in which IMP 8 CRNE collected fewer than 10 oxygen ions, 18 of the remaining 20 GLE's (that is, 90%) have Fe/O that is enhanced relative to the nominal coronal value by a factor of 2 or more.

According to Tylka *et al.*,[369] the dominant role of fast CME-driven shocks in producing particles below 10 MeV nucleon^{-1} should not be in question. They emphasize that what it is still of hypothetical nature are the enhancements of Fe/O at even higher energies. Their assumption is that high-energy particles also come from a shock due to acceleration of a seed population containing remnants flare suprathermals from previous activity. These authors recognize that other assumptions are eventually able to operate for LGE's: for instance, an alternative hypothesis would be two distinct acceleration mechanisms operative in the same event, with a shock producing the lower energy particles while a flare alone directly generates most of the higher energy particles. It is thus difficult to distinguish between the hypotheses using only the composition data. Therefore, in order to support their hypothesis they consider three other lines of evidence against the two-component model related with longitude distribution of Fe-rich-events, spectral characteristics and timing scales of gamma rays together with multi-GeV proton arrival as measured by the neutron monitor world network in GLE events.

To our opinion, it is worth to mention here that our *two-source* model for the GLE events delineated below in Subsec. 8.6 is not completely in contraposition to the hypothesis of Tylka *et al.*[369] In fact, in the two-source model we attribute the so-called *delayed component* (DC) to stochastic acceleration, either associated to a CME-driven shock, or trapped inside a closed expanding structure (magnetic bottle) covering a wide range of heliolongitudes during its expansion, up to a definite height

Table 15. High-energy Fe/O ratio from IMP 8 in GLE's of solar cycles 21–22.[369]

GLE No.[a]	Start date (UT)	Start time (UT)	Source location[b]	Ion acc. time (hr)	Number of Fe ions[c] (47–80 MeV/n)	Number of O ions (43–86 MeV/n)	Fe/O/0.134[d] (47–80 MeV/n)
27[c]	760430	20:00	S08, W46	12.0	9.0	13	$9.0 + 5.4 - 3.6$
28	770919	10:00	N08, W57	30.0	39.0	38	11.0 ± 2.2
29	770924	06:00	N10W120	27.0	123.0	125	9.2 ± 1.0
30	771122	10:00	N24, W40	26.0	28.5	45	6.7 ± 1.5
31	780507	03:00	N23, W72	16.0	7.5	16	$4.9 + 3.3 - 2.1$
32	780923	10:00	N35, W50	30.0	22.5	28	$8.9 + 2.9 - 2.3$
34	810410	16:00	N07, W36	24.0	3.0	4	$10 + 13 - 6$
35	810510	07:00	N03, W75	24.0	1.5	3	$8 + 19 - 7$
36[f]	811012	06:00	S18, E31	50.0	4	13	$4.1 + 3.2 - 1.9$
37	811126	02:00	S12, W87	12.0	4.5	8	$6.2 + 6.0 - 3.3$
38	821207	23:00	S19, W86	32.0	19.5	39	$5.4 + 1.9 - 1.5$
39	840216	09:00	S?−, W130	24.0	10.5	18	$6.3 + 3.4 - 2.3$
40	890725	08:00	N26, W85	24.0	3.0	1	$22 + 110 - 16$
41	890816	01:00	S15, W85	26.0	33.0	87	4.1 ± 0.9
42[f]	890929	11:00	S24,W105	72.0	22	77	3.3 ± 0.7
43[f]	891019	12:00	S25, E09	24.0	48	138	3.6 ± 0.6
44[f]	891022	18:00	S27, W32	36.0	2	19	$1.2 + 1.6 - 0.8$
45[f]	891024	18:00	S29, W37	50.0	27	77	3.9 ± 0.8
46	891115	06:00	N11, W28	17.0	7.5	16	$5.0 + 3.4 - 2.4$
47	900521	22:00	N34, W37	53.0	33.0	21	15.5 ± 3.5
48	900724	20:00	N36, W76	36.0	28.5	34	8.9 ± 2.0
49	900726	21:00	N35W103	32.0	9.0	15	$8.2 + 4.9 - 3.2$
50	900728	04:00	N35W120	84.0	10.5	5	$24 + 18 - 10$
52	910615	08:00	N36, W70	42.0	1.5	52	$0.4 + 0.9 - 0.3$
53	920725	20:00	N09, W69	41.0	24.0	99	2.5 ± 0.6

(a) From the catalog of ground-level events provided by the Australian Antarctic Data Center at http://aadc-maps.aad.gov.au/aadc/gle/index.cfm. Three GLE's have been omitted from this table: No. 33 (21 August 1979; Fe/O dominated by the decay phase of a previous event); No. 51 (11 June 1991; no IMP 8 data coverage); and No. 54 (2 November 1992; no IMP 8 data coverage in the first 12 hr).

(b) From Ref. 322.

(c) Numbers have been corrected for a priority scheme that records only two-thirds of the Fe ions registered in this energy bin. No priority correction is required for the oxygen ions, which come to rest at deeper levels in the detector stack.

(d) Normalized to the nominal coronal value of 0.134 [290] and corrected for priority scheme, galactic and anomalous cosmic-ray oxygen backgrounds, and the difference in oxygen and iron energy intervals.

(e) Combined data from nearly identical instruments on IMP 8 and IMP 7.

(f) These results are from higher energies: Fe ions at 97–175 MeV nucleon^{-1}, O ions at 86–180 MeV nucleon^{-1}, and Fe/O ratio corrected to the common interval 97–175 MeV nucleon^{-1}. Because of the very high count rates in these events, the priority corrections required to evaluate Fe/O at 47–80 MeV nucleon^{-1} are larger than usual. We quote these higher energy values, for which no priority corrections are needed. Fe/O increases with energy in the events of 12 October 1981 and 29 September 1989.[365]

where it connects with open field lines. Particle distribution through heliolongitude has been widely study in the literature (e.g. Ref. 261). Both assumptions imply that the high-energy particles should carry the compositional signatures of flare-acceleration.

The other source in that model, producing the so-called *prompt component* (PC), is associated to a deterministic process by direct electric field acceleration during magnetic merging in a magnetic neutral current sheet high in the corona. The spectral features are then explained in a more direct way because the stochastic process producing the DC leads to a power-law spectra as soon as the steady state is reached (e.g. Ref. 112), whereas the PC acquires an exponential shape spectrum (e.g. Refs. 263 and 264). The high variability in spectral characteristics and composition comes from the differences of sources and from the eventual superposition of accelerated ions from both sources.

At this regard it must be emphasized that modern observations from SOHO, Yohkoh and TRACE invariably associate solar particle acceleration with magnetic merging in Neutral Current Sheets.[16] Also, time profiles and gamma ray timing associated with GeV protons within the frame of the two-source model have been discussed in a series of works (e.g. Refs. 237, 239 and 228). Because stochastic acceleration is associated with large scale structures (a shock or an expanding magnetic bottle) the timing phenomena is not so different from that in the quasiperpendicular shock hypothesis.

7.3. *Theoretical approaches to the study of the charge state of solar ions*

Regarding ion charge states two main hypothesis have been worked out to explain their variability among different events even at the same energy: for one side, the assumption that charges states are indicators of the temperature of the matter in the source, either the flare matter itself or remnant seed suprathermals of previous flares, or even solar-wind suprathermals. On the other hand, there is the assumption of charge interchange during the source acceleration process, when the amount of traversed matter is enough high for the establishment of charge transfer between the accelerated ions and the source matter: $X = \rho v t$ gr cm^{-2}. At a fixed velocity v, the density ρ and the flight time t determine whether charge interchange is established or not. This situation occurs rather when acceleration occurs in a high density region or in a closed magnetic structure where particles spend some time before reaching open field lines. The evolution of ion charge in terms of its velocity during acceleration is described by the so-called effective charge $Q^*(v)$, which evolves according to the balance between the cross-sections of electron capture and electron loss as particles change their velocity during acceleration.

Two different concepts of the charge interchange and evolution of ion charge during the acceleration have been developed.

(1) Original one,[265,266,153] which is mainly based on the fact that charge interchange phenomena occurs between a population which is out of the thermodynamic equilibrium (TE) while it is being accelerated (the "projectile" ions), and a local thermal population which is in TE (the "targets," free electrons and bounded to atoms/ions): both with different energy spectrum, the former

with an inverse power law (or exponential type spectrum) and the later with a Maxwellian distribution. Cross-sections are then those of laboratory and theoretical work for energetic ions out of the TE interacting on different targets, under the concept of Coulomb Electron Capture, Electron Loss and Radiative Capture.

(2) A concept based on charge interchange between the accelerated ions and the components of local thermal matter, where both populations are in Thermodynamic Equilibrium, with Maxwellian distributions. So, the cross-section for thermal matter in TE (radiative and dielectronic recombination, collisional, autoionization, proton impact ionization) are used even for particles accelerated up to very high energies[190] and a series of applications derived from the previous one (e.g. Refs. 173, 149, 152, 150, 151, 259, 162, 163). Wannawichian *et al.*[385] optimized the approach of Luhn and Hovestadt[190] by introducing the so-called kappa distributions for electron velocity that characterize the deviation from a Maxwellian for the high energy tails. A kind of hybrid mixture of thermal with high energy cross-sections has also been developed (e.g. Ref. 67).

Within the frame of concept (1) the criteria for charge interchange during a given acceleration process were derived by Pérez-Peraza *et al.*[267,268,274] and Perez-Peraza and Alvarez-Madrigal.[269] Basically, the interchange is established when the mean free path for electron capture and/or loss is shorter than the mean characteristic length of the acceleration step. In other words, when the mean flight time for charge changing atomic interactions is shorter than the characteristic flight time for acceleration ($\sim \alpha^{-1}$, where α is the acceleration efficiency).

Since the mentioned criteria depend on the source parameters, temperature and density, and on the acceleration parameters, while cross-sections depend on the atomic number, nuclear charge, particle velocity, target velocity, hence, there are situations where both electron loss and capture are established. But there are also situations where none of the charge changing processes is established, in which case the accelerated ions are typical samples of the charge state at the temperature of the source material. This is the case in the high corona when acceleration occurs in open field lines, and in this case one should expect that both low-energy and high-energy ions of the same species have not so dissimilar charge state.

However, there are also situations at the beginning of the acceleration, at low energies, just above the ions thermal energy, that criteria are only satisfied for electron capture. In this case ions during their acceleration only capture electrons, even tending toward neutralization in some cases. Meanwhile, there are situations where only electron losses take place, in which case ions at a given velocity are stripped faster than when charge equilibrium is established. Therefore, the possibilities under this concept of charge evolution are very assorted. This is translated in a high variability of charge states from event to event, and so on processes which are Q/A dependent.

7.4. *Main hypotheses of charge state variability*

Regarding charge states of solar flare ions, two main hypotheses have been worked out to explain their observational variability among different events, even at the same energy.

On one side, the assumption was suggested that charges states are indicators of the temperature of the matter in the source, either the flare matter itself or suprathermal remnant seeds from previous flares, or even solar-wind suprathermals.

On the other hand, there is the assumption that the measured distribution of charge states of solar ions is not representative of the equilibrium charge distribution of thermal plasma defined by the temperature, but rather of the amount of traversed matter in the source and its environment ($X = \rho v t_f$ gr cm^{-2}). At a fixed velocity v, the density ρ and the flight time t_f determine whether charge interchange is established or not; it is established, when the acceleration efficiency is not very high, such that the acceleration is not very fast, or/and acceleration occurs in a relatively high density region, or/and in a closed magnetic structure where particles spend some time before reaching open field lines.

At this level, let us remind here that charge states of energetic ions and their evolution during the passage of ions through matter is a very important factor for the study of particle interaction with matter and electromagnetic fields. The scope of applications was described by Perez-Peraza and Alvarez-Madrigal.[269] It is of particular interest the behavior of charge states in connection with the energy and charge spectra: chemical abundances of the accelerated ions are highly dependent on the charge states during their acceleration and escape from the source, and so it is the emitted radiation when the accelerated ions capture electrons of the medium.[268] The evolution of ion charge in terms of its velocity is described by the so-called "effective charge" $q^*_{\rm eff}$, which evolves according to the balance between the charge interchange processes, during the interaction of the energetic ions with the local source matter or its environment.

The present knowledge of effective charge, $q^*_{\rm eff}$ (or mean equilibrium charge state) is associated with experimental results of stopping power of ions in atomic matter, which can be adequately described by several semiempirical smooth functions of ion velocity and nuclear charge (Z). These kinds of relations refer to experiments of ion deceleration toward stopping in atomic matter, and, in principle, could be applied to the transport of cosmic rays in the interstellar space. However, such expressions do not consider the temperature of the medium (T). Therefore, for astrophysical applications, these kinds of expressions are usually extrapolated by introducing T, commonly by means of a thermal velocity.

All those semiempirical relations, though useful for some purposes, do not give enough information about the underlying physics. Strictly speaking, these kinds of expressions are not valid when ions instead of being stopped are undergoing an acceleration process while interacting with the local matter, as is the case in cosmic ray sources. In fact, because the energy gain rate is of different nature to

the stopping power rate (atomic), the evolution of particle charge as a function of energy must be derived by taking into account the kind of energy change process. Since there is not data of particle charge evolution of ions moving through plasmas, either during stopping or acceleration, a big amount of theoretical works have been done in relation with the charge state evolution of solar flare particles. Therefore, the establishment of charge changing processes is very sensitive to the corresponding cross-sections. Unfortunately, there are no experimental cross-sections of high-energy ions in plasmas, out of ^{2}H and ^{3}H, as it exists in atomic matter. So, one is obliged to do some approximations, among which the two main are the following.

(1) Because the high energy particles interact with the coronal thermal plasma, researchers usually recur to the cross-sections of equilibrium ionization fractions in the coronal plasma (e.g. Refs. 136, 135 and 15). However, such cross-sections are developed for plasma components that are in TE with a well-defined Maxwellian spectrum. Meanwhile, the energetic ions projectiles interacting with the thermal targets are out of the TE, with a power-law or exponential spectrum. Then, it is not clear why such thermal cross-sections may be extrapolated to a high energy population.
(2) Another option was developed by Pérez-Peraza *et al.*,[265–267] based also on a kind of "extrapolation." These authors applied the experimental and theoretical cross-sections of high-energy ions in atomic matter to plasmas, even at energies lower than the thermal energy of electrons. It may be reasonable provided the ions are under an electromagnetic acceleration process, acquiring an exponential or power-law-type spectrum. Such approximation is based on the analogy with experimental interactions of high-energy ions with atomic matter: accelerated solar ions (projectiles) and the source matter (targets).

Figure 11 shows the cross-sections built by Pérez-Peraza *et al.*[265,267] for completely stripped Fe ion ($q = Z$) in atomic hydrogen. The parameters σ_i, σ_{cc} and σ_{cr} are the cross-sections for electron loss, Coulomb capture and radiative capture, respectively (ionization, recombination and radiative recombination in thermal jargon). Then, in order to "extrapolate" them to finite temperature matter, a relative velocity between the projectile and the thermal targets (electrons and protons) was introduced (for details see Ref. 267).

7.5. *Charge interchange of ions during acceleration*

Long ago, Pérez-Peraza *et al.*[265–267] studied the criteria for the establishment of charge changing process of heavy ions with the local matter, when ions are undergoing acceleration and Coulomb energy losses at the source. That was done for several acceleration mechanisms. It was found that depending on the mechanism and its acceleration efficiency, the temperature and density of the medium, either both processes, electron capture and loss, are established, or one of them may be inhibited; electron capture at high energies, or electron loss at low energies, or even do not undergo any charge interchange at all.

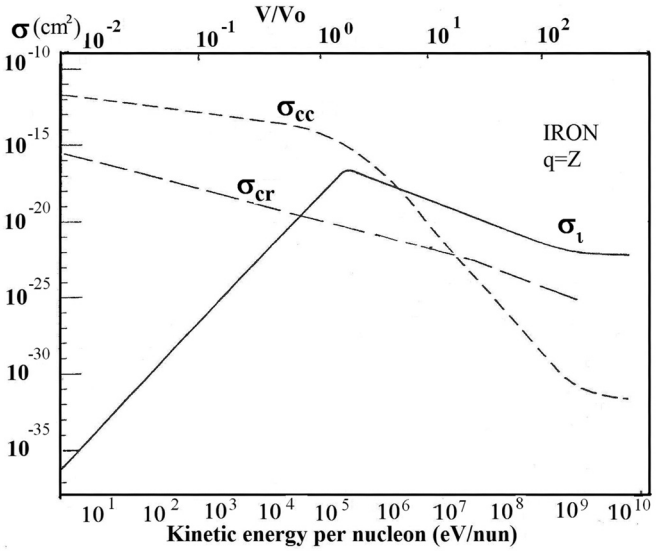

Fig. 11. High-energy cross-sections in atomic matter for a completely stripped Fe ion.[265,267]

Basically, the interchange is established when the mean free path for electron capture and/or loss is shorter than the mean characteristic length of the acceleration step. In other words, when the mean flight time for charge changing atomic interactions is shorter than characteristic flight time for acceleration ($\sim \alpha^{-1}$, where α is the acceleration efficiency). Given the condition $\alpha > \alpha_c$ (where α_c is the critical value of the efficiency where both the acceleration rate and the Coulomb barrier equate), such establishment depends on the relation between their mean flight time for acceleration and the flight time for charge-changing processes, i.e. the mean free path for acceleration λ compared with that of the atomic process λ_c, λ_p. It may occur that $\lambda > \lambda_c$ while $\lambda \ll \lambda_p$ or vice versa, in such a way that in the case that only electron capture is established, ions in a cold plasma may eventually turn into the atomic state and be lost from the accelerated flux. Since $t_a \sim 1/\alpha$, then, if α is small, t_a is enough long for charge changing processes to be established. But if the efficiency is very high, t_a is quite short for such establishment, and then one or two atomic processes could be inhibited.

Therefore, since the mentioned criteria depend on the source parameters (temperature and density) and on the acceleration parameters, while cross-sections depend on the atomic number, nuclear charge, particle velocity, target velocity, hence, there are situations where both electron loss and capture are established. But there are also situations where none of the charge changing processes is established. In this case, the accelerated ions are typical samples of the charge state at the temperature of the source material; this is the case in the high corona when acceleration occurs in open field lines by a highly efficient acceleration process. One should expect in these cases that both low-energy and high-energy ions of the

same species have not so dissimilar charge state since they practically keep the local thermal charge. However, there are also situations at the beginning of the acceleration, at low energies, just above the ions thermal energy, that criteria are only satisfied for electron capture. In this case ions during their acceleration only capture electrons, even tending toward neutralization in some cases. At the same time, there are situations at high energies where only electron loss takes place. In such a case ions, at a given velocity, strip faster than when charge equilibrium is established.

7.6. *Models of charge evolution of solar flare particles*

Two different concepts have been developed, that we can differentiate here on basis to the employed charge-interchange cross-sections: (a) models using High-Energy Cross-Sections hereafter HECSM, and (b) models that use Thermal Cross-Sections, namely THCSM. As stated by Kartavykh *et al.*,[149] the problem was raised for the first time in our work.[265] In other words, historically, the HECSM have been the first to study charge evolution: either during acceleration[265–267,149] or after acceleration[153] in the source environment. In the latter case, it is assumed[153] that the acceleration is so fast that any charge-changing process in cold plasma is out of the acceleration region.

This assumption confirms what we said above, namely, that depending on the acceleration efficiency and the mean free path of the atomic processes, there may be some situations where particles undergo free-flight, with no atomic interactions. Kharchenko and Ostryakov[153] recognized the correctness of the approach by Pérez-Peraza *et al.*[267] to the study of the charge-changing processes. However, there is one essential difference between the approaches by Kharchenko and Ostryakov[153] and Pérez-Peraza *et al.*[266,267] In these later works it is claimed that, if there are not atomic interactions during acceleration, most probably, there will not be during transport in the more diluted coronal plasma while escaping through the magnetic field lines.

Both models[149,153] are numerically solved, whereas the HECSM[266,301,302,67] is analytically solved. The first models[265,266,153] use the temperature-dependent equilibrium charge states given by Jain and Narain,[135] and then move to those of Arnaud and Raymond.[15] The mentioned analytical model uses them only within the frame of the initial charge of ions $q_0(T)$ at the beginning of the acceleration.

The escape high-energy-cross-section model

The original HECSM[269,265,266,274] is mainly based on the fact that charge interchange phenomena occurs between a population, which is out of the TE because it is being accelerated (the "projectile" ions), and a local thermal population, which is in TE (the "targets," free electrons and bounded to atoms and ions). Both populations are presented with different energy spectra, the former with an inverse power-law (or exponential-type) spectrum and the latter with a Maxwellian distribution.

Cross-sections are then those of laboratory and theoretical work for energetic ions out of the TE interacting on different targets, under the concept of Coulomb Electron Capture, Electron Loss and Radiative Capture.

This HECSM currently designed as "Escape"[301,302,67] is a quasianalytical code due that the expression for q_{eff} is an analytical one. It is assumed that "the simplest description of a physical phenomenon is usually the best approach to understand the underlying physics involved in the phenomenon." This is the case of the q^*_{eff} analytical expression which gives information about the acceleration mechanism and its efficiency, the acceleration time, the source parameters, and indirectly the qualitative nature of the charge interchange cross-sections:

$$q^*_{\text{eff}} = q_0 + n_t t_a \Delta q_i \int_0^c [\sigma_l(v)] v f(v) dv - n_t t_a \Delta q_c \int_0^c [\sigma_c(v)] v f(v) dv \,, \qquad (4)$$

where q_0 is the effective charge of the ion at the beginning of each acceleration step (for the first acceleration step $q_0 = q_{\text{th}}(v)$ is the local thermal charge according to the source temperature), Δq_c and Δq_i are the average charge exchange in each capture and loss interaction respectively, $f(v)$ is the Maxwellian plasma electron velocity distribution in the rest frame of the source plasma, σ_i and σ_c are the total cross-section for electron loss and capture, respectively, and t_a is the time spent in each acceleration step.[67] It is just such a simplicity that provokes the annoyance in the papers by Kovaltsov *et al.*[169] and Kocharov *et al.*[164]

In deriving such an analytical and simplified expression the Escape model persecutes several goals: (1) to have a manageable expression for calculation of Coulomb losses while particles are being accelerated, for evaluations of the acceleration rates and for the development of the electron pick-up spectroscopy, as a tool in the field of plasma diagnosis;[269] (2) to study the charge distribution of solar ions and (3) to probe several sets of HECS, as can be found in the literature (e.g. Ref. 36).

It is pretended to infer about the nature of charge-changing cross-sections of high-energy ions in cold and hot plasmas, from the best fitting of our analytical q_{eff} expression to data of solar charge states. Since there are not available data on the energy dependence of charges states for several ions and for a given time in individual solar proton events, up to now no fittings have been made, but only runs of predicting nature have been published, for the particular set of HECS, as given in Refs. 265 and 266.

Among the kindness of this model is that, under its concept, the possibilities of charge evolution are very assorted. This is translated in a high variability of charge states from event to event, and, consequently, leads to the processes that are Q/A-dependent. But perhaps the main kindness is the possibility to be tested when data on charge state of very low-energy ions will be available. In fact, as can be seen in Fig. 11, the capture cross-sections ions at very low energy are several orders of magnitude higher than the electron loss cross-section. Therefore, at the beginning of the acceleration in cold plasmas electron losses can be inhibited, as explained before. As to the ions, some of them will present a fall in q_{eff}, up to a given energy where

both electron capture and loss become comparable, and then $q_{\rm eff}$, begins to increase toward the Z value. These effects can be seen in several figures in Refs. 301, 302 and 67 for the Fermi mechanism. This kind of test is unique to the Escape model; no other model predicts this trend toward neutralization at the beginning of the acceleration.

The thermal cross-section model

Regarding the THCSM, the pioneer work was published by Luhn and Hovestadt.[190] They assumed a charge-changing process after the acceleration, during particle transport in the hot coronal plasma. As emphasized by Kocharov *et al.*,[162] due to the lack of experimental data several assumptions can be made. One of them is precisely the use of thermal cross-sections for thermal matter in TE (radiative and dielectronic recombination, collisional, autoionization) that the authors extrapolate up to high energies of 10 MeV/nucleon as compared with the thermal energy of ions. Calculations are quite complex (see, e.g. Refs. 136, 135 and 15), and so, solved by numerical methods of the Monte-Carlo type.

The work by Luhn and Hovestadt[190] has inspired a subsequent series of works of numerical nature, with all kind of refinements (acceleration of different types, p-impact ionization, photoionization, kappa velocity distributions, etc.) (see, e.g. Refs. 173, 259, 150–152, 163, 385 and 346). Apparently, no fundamental improvement to Ref. 190 was done, but basically the same skeleton is kept. With such refinements it is attempted to obtain the best fit to observational data on charge states, which up to now have so quite error bars, that practically any model can do it.

As discussed in Subsec. 7.5, the concept of charge–interchange after acceleration, during ion transport in the coronal plasma, is quite doubtful, since most probably the plasma is more diluted than in the acceleration volume and magnetic field topologies are rather composed of open field lines. Therefore, the followers of Luhn and Hovestadt[190] refined it by including the acceleration process. What is not clear in these refinements is how thermal cross-sections from Arnaud and Raymond[15] can be used up to near 100 MeV/nucleon?

8. Acceleration and Release of Solar Cosmic Rays

From physical point of view, potential acceleration sites in the Universe need to have the appropriate combinations of sizes, magnetic (electric) fields, shock velocities and other relevant parameters. These criteria have been discussed in general astrophysical context by Hillas[131] and Blandford.[38] As to the particle acceleration at/near the Sun, many existing and/or arising questions are widely discussed in recent reviews (e.g. Refs. 217, 292, 293, 228, 230 and 57). After previous discussion of available observational data and theoretical aspects of SEP acceleration and interaction in the solar atmosphere, we consider below the keenest existing or arising problems in this field in more detail.

8.1. *Current paradigm of acceleration*

In the middle of 1990's the solar physics community seemed to be in a state of transition in its viewpoint regarding energetic solar phenomena. The old traditional view that solar particles must be accelerated by the solar flare arose from the fact that SCR events at sub-relativistic and relativistic energies could be time-associated with solar-flare activity.

Meanwhile, in the MeV energy domain, since the middle of 1970's it was established a certain association of observed particle fluxes with interplanetary shocks. About 15 years ago, this has been advanced as compelling evidence that fast coronal mass ejections (CME's) generate shocks and are a significant, and perhaps the dominant, source of MeV ions observed in space. In recent years it is widely believed that in the large gradual SEP events, acceleration of the particles observed near the Earth's orbit occurs at the CME-driven shock waves and *not* in solar flares (e.g. Refs. 137, 138, 121, 291–293 and 295).

The event-averaged abundances of elements in gradual events, obtained from low-energy measurements, provide a direct measure of element abundances in the corona and solar wind. These abundances are almost entirely independent of the temperature, T, and ionization state, $Q(T)$, of the source plasma. Energetic particles from impulsive flares show element abundances that differ from those in the corona in that elements with $Z > 8$ are strongly enhanced relative to coronal abundances, while He, C, N, or O are not. This pattern of enhancement is consistent with acceleration of the ions from a plasma in the temperature range of $(3\text{–}5) \times 10^6$ K. Elements up to Si are fully ionized and Fe has charge about 20 indicating heating or other ionization of the plasma.

It has been well known for many years that the ratio of coronal and photospheric abundances of elements is a well-organized function of the first ionization potential (FIP) of the element. A summary of abundances is shown in Table 16.[291]

Oetliker *et al.*[403] presented measurements on board the polar orbiting SAMPEX satellite for He, C, N, O, Ne, Na, Mg, Al, Si, S, Ar, Ca, Fe, and Ni in the energy range 0.3–70 MeV/nucleon made in two consecutive large SEP events in October–November 1992. Of all the elements in this data set, Fe has the strongest dependence of $Q(T)$, and thus Fe is the most sensitive indicator of the temperature history of the particles covered in this study. It was found that the particles are highly but not fully ionized in accordance with an equilibrium ionization temperature of 2×10^6 K. For all elements, the mean charge is constant over the observed energy range except for iron where a strong increase from +11 below 3 MeV/nucleon up to +17 at 60 MeV/nucleon was observed.

Contrary to these results, at much higher energies of 200–600 MeV/nucleon, Tylka *et al.*[364] found a mean charge state of Fe ions about $\langle Q_{\mathrm{Fe}} \rangle = 14.1 \pm 1.4$ in a series of very large, historic SPE's during September–November 1989 (Table 17). These ions could not come from the hot plasma in a flare and they would be stripped of electrons in seconds by material at densities of the low corona, so they

Table 16. Solar energetic particle abundances.[291]

Element	Z	FIP, eV	Photosphere	Gradual events	Impulsive events
H	1	13.53	$1.18E+6$	$(1.57 \pm 0.22)E+6$	$(1.57 \pm 0.22)E+6$
He	2	24.46	$1.15E+5$	57000 ± 3000	46000 ± 4000
C	6	11.22	468	465 ± 9	434 ± 30
N	7	14.48	118	124 ± 3	157 ± 18
O	8	13.55	1000	1000 ± 10	1000 ± 45
F	9	17.34	0.0351	< 0.1	< 2
Ne	10	21.47	161	152 ± 4	400 ± 28
Na	11	5.12	2.39	10.4 ± 1.1	34 ± 8
Mg	12	7.61	44.6	196 ± 4	408 ± 29
Al	13	5.96	3.54	15.7 ± 1.6	68 ± 12
Si	14	8.12	41.7	152 ± 4	352 ± 27
P	15	10.9	0.433	0.65 ± 0.17	4 ± 3
S	16	10.3	20.4	31.8 ± 0.7	117 ± 15
Cl	17	12.95	0.218	0.24 ± 0.1	< 2
Ar	18	15.68	4.21	3.3 ± 0.2	30 ± 8
K	19	4.32	0.157	0.55 ± 0.15	2 ± 2
Ca	20	6.09	2.55	10.6 ± 0.4	88 ± 13
Ti	22	6.81	0.10	0.34 ± 0.1	< 2
Cr	24	6.74	0.563	2.1 ± 0.3	12 ± 5
Fe	26	7.83	37.9	134 ± 4	1078 ± 46
Ni	28	7.61	2.05	$6.4 \pm 0.0.6$	42 ± 9
Zn	30	9.36	0.0525	0.11 ± 0.04	6 ± 4

are neither accelerated nor stored in the corona. Moreover, Kahler[138] argued that even particles of GeV energies are accelerated several solar radii out from the Sun at the CME-driven shock waves. Table 17 comprises the basic data on the mean charge of Fe obtained up to 1996.

On the other hand, the energy spectra of Fe in the very large SEP event of 14 July 2000 (Bastille Day event, or BDE) are strikingly different from those of lighter species.[368] The high intensities of the BDE provide an excellent opportunity, in particular, to search for spectral signatures of remnant flare suprathermals. It was shown that this difference can be explained by shock acceleration from a two-component source population, comprising solar wind suprathermals and a small ($\sim$ 5%) admixture of remnant flare particles, as previously proposed to explain enhanced ^{3}He/^{4}He in some gradual SEP events. Flare remnants can also account for several previously unexplained features of high-energy solar heavy ions as well as important aspects of SEP event-to-event variability (see Subsec. 7.1).

8.2. *Open questions in current paradigm of acceleration*

Despite recent progress in understanding the properties of accelerated solar ions using GLE, SEP and gamma-ray observations, when we try to construct a comprehensive, self-consistent picture of that acceleration, we confront more questions

Table 17. Mean ionization states of energetic Fe in large gradual events.[291]

MeV/amu	Q_{Fe}	Events	Spacecraft	References
0.3–2	14.1 ± 0.2	12	ISSE 3	191
0.5–5	11.0 ± 0.2	2	SAMPEX	200
15–70	15.2 ± 0.7	2	SAMPEX	179
200–600	14.1 ± 1.4	3	LDEF	364

than answers (e.g. Refs. 293 and 294): in what magnetic topology does the acceleration take place? At what altitude? Is one mechanism enough? What is the order of acceleration of electrons and ions and is that consistent with the mechanisms of abundance enhancements? Does heating occur before, during, or after acceleration? Are the ions we see at 1 AU the same population as those that produce gamma rays?

From phenomenological point of view, in fact, we should find a certain answer to a question that in recent years arises more and more persistently (e.g. Ref. 43): Are there two classes of solar energetic particle events? Researchers discuss role of flares and shocks in solar energetic particle events very intensively, but, at present, there are no complete clearness in this problem, and even areas of consensus and contention are still not defined distinctly (e.g. Ref. 56). Current views on impulsive and gradual solar particle events have been recently summarized by Kallenrode.[140,141] From observational point of view are still unknown relative contributions of SEP acceleration and interplanetary propagation (e.g. Ref. 57). Some new problems and questions seem to arise from the measurements of Fe ion spectrum.[366–369] It is interesting to note that various Fe charge states contribute in different ways to the overall spectrum. Solar wind charge states dominate at low energies. The remnant flare component becomes more important as energy increase. This modeling implies energy dependence of in $\langle Q_{Fe} \rangle$, which is shown by the solid curve in Fig. 12. This curve is consistent with the measured $\langle Q_{Fe} \rangle$-values from ACE[341] and the Solar, Anomalous, and Magnetospheric Particle Explorer Satellite (SAMPEX)[404] for the Bastille Day event.

For comparison, Fig. 12 also shows observed energy-dependent $\langle Q_{Fe} \rangle$-values for the 1 November 1992 and 6 November 1997 events. The 1992 event shows energy dependence remarkably similar to that derived by Tylka *et al.*[368] for the BDE. The event of 6 November 1997, on the other hand, exhibits stronger energy dependence. Since e-folding energies in this event are large, the two-component model by Tylka *et al.*[368] cannot account for the rapid rise in $\langle Q_{Fe} \rangle$ below 2 MeV/nucleon. The event of 6 November 1997 has been explained by stripping in the low corona during shock acceleration (see Ref. 368, and references therein).

Lest one mistakenly infer that high-energy solar Fe must always be nearly fully stripped, the dashed curve in Fig. 12 shows another calculation, again using the same source mixture but subjected to a shock with e-folding energies an order of magnitude larger. To the opinion by Tylka *et al.*,[368] the event of 29 September 1989 is an example of such a shock: proton e-folding energies exceeded 500 MeV,[187] and

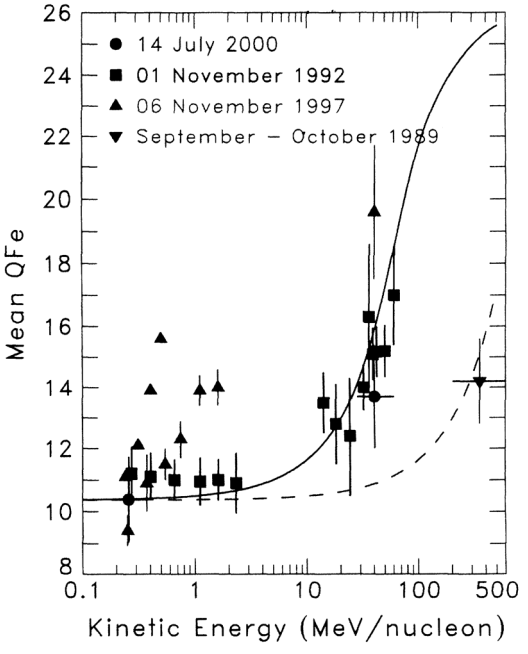

Fig. 12. Energy dependence of the mean ionic charge state of Fe.[368] The solid curve is evaluated from the measured spectra of Fe ions in the Bastille Day solar particle event. The dashed curve is calculated with the same source mixture but subjected to a shock with e-folding energies an order of magnitude larger. Measurements come from various sources.

Fe ions were observed up to nearly 1 GeV/nucleon.[365] In this and other very large events of 1989, Tylka *et al.*[364] measured $\langle Q_{\mathrm{Fe}} \rangle \sim 14$ at 200–600 MeV/nucleon. In this context, it is of great interest that the Fe/C ratio versus energy reveals a distinct minimum at $\sim$ 30 MeV/nucleon. The enhanced Fe/C below $\sim$ 10 MeV/nucleon is probably caused by Q/A-dependent transport, as previously observed in large events.[366]

The increase in Fe/C above $\sim$ 30 MeV/nucleon is due to the remnant flare suprathermal component. The statistical significance of this increase is modest in the BDE case. However, very similar, complicated energy-dependent Fe/O ratios have been previously reported in large SEP events from a wide range of heliolongitudes.[365] Remnant flare suprathermals may also account for the reported association between Fe enhancements above $\sim$ 40 MeV/nucleon and ground-level neutron-monitor events,[69] which almost always occur during periods of high solar activity.

These results offer a new perspective on the enduring controversy over the relative roles of flares and coronal mass ejections (CME's) in producing SEP's. Flare activity clearly makes a unique and critical contribution to the source population. But the predominate accelerator in large gradual SEP events, according to Tylka

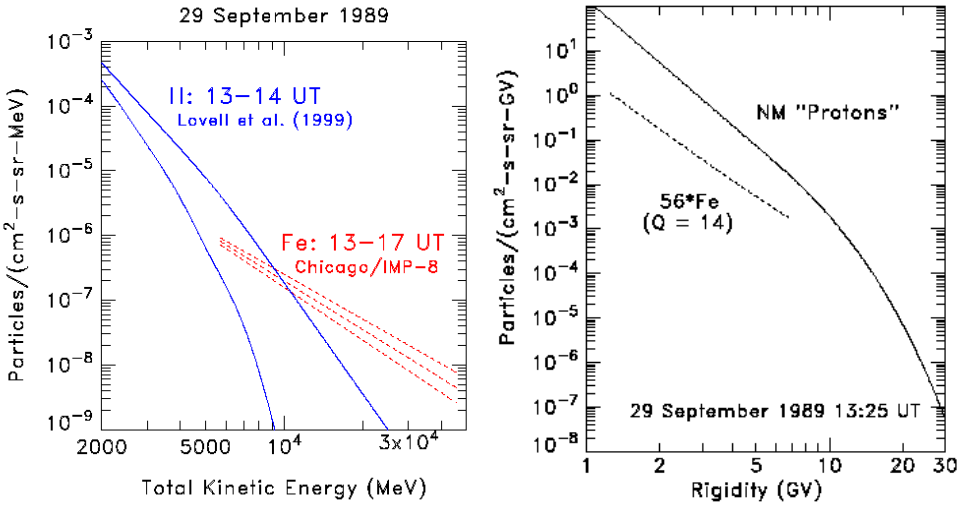

Fig. 13. Energy and rigidity spectra of relativistic solar protons and Fe ions above 100 MeV/nucleon measured in the GLE of 29 September 1989.[366] Left panel: Proton and Fe spectra vs total energy per particle. Solid curves are estimated upper and lower bounds on the protons between 13:00-14:00 UT;[187] dashed curves show Fe, allowing for uncertainty in the fitted spectral index. Right panel: Intensities of Fe ions and protons as functions of rigidity. Fe rigidities are evaluated assuming ionic charge $Q = 14$. The Fe intensity is also multiplied by a factor 56. The solid proton curve is the spectrum at 13:25 UT by Lovell *et al.*[187]

et al.,[369] is the CME-driven shock, and many spectral, compositional, and charge state characteristics of high-energy heavy ions can be understood without invoking other acceleration mechanisms.

In more than 25 years of almost continuous observations, the University Chicago's Cosmic Ray Telescope (CRT) on IMP-8 amassed a unique database on high-energy solar heavy ions (e.g. Refs. 364, 365, 69 and 70). In the very large particle events, IMP-8/CRT has even observed solar Fe ions above the galactic cosmic ray (GCR) background up to the energy of $\sim$ 800 MeV/nucleon. This database allowed to Tylka *et al.*,[366] in particular, to compare the proton spectra above 500 MeV in the GLE of 29 September 1989[187] by NM data to simultaneous measurements of solar Fe ions at $\sim$ 50–1000 MeV/nucleon from the Chicago's Cosmic Ray Nuclear Composition (CRNC) Experiment on IMP-8 (Fig. 13).

These measurements revealed the hardest spectrum of high-energy solar Fe ions ever observed. When examined as a function of rigidity, the Fe nuclei do not appear to be sufficiently numerous to complicate interpretation of the NM results, even after accounting for their partial ionized charge state ($\sim$ 14.0). However, at very high *total* energies, the Fe spectrum is much harder than the proton spectrum, and protons and Fe appear to make comparable contributions to the so-called "all-particle" spectrum.

In this context, Tylka *et al.*[366] discussed a Fe contribution to neutron monitor response. As known, neutron monitors register increases in the atmosphere neutron

flux. These increases are *attributed* to changes in the top-of-the atmosphere *proton* flux above a certain cutoff rigidity, which is determined by the NM location. Given the large Fe/p ratio obtained by Tylka *et al.*,[366] one might worry that neutrons generated by Fe nuclei could be contributing to the NM response. If this were the case, the NM results would have to be reinterpreted and revised.

The authors compared the "proton" (NM) and Fe nuclei (CRNC/IMP-8) intensities as a function of rigidity. For this comparison, the Fe nuclei were assumed to have an ionic charge state of 14, as directly measured by geomagnetic-penetration studies in this event.[364] The Fe intensity was multiplied by a factor 56, to very crudely account for additional neutron production from a Fe projectile. This factor is likely to be an overestimate: the nuclear interaction mean free path of Fe nuclei in air is ~ 10 g/cm^2, and most of the Fe at these energies will slow down or even stop in the atmosphere before they interact. For energies at which CRNC/IMP-8 has measured the Fe spectrum, the Fe contribution is at most $\sim 10\%$ of the proton signal. However, if the Fe spectrum obtained were to continue to higher rigidities without rolling off, the Fe contribution might be significant.[69]

Another intriguing feature in Fig. 13 is the difference in hardness between the proton and Fe rigidity spectra. However, caution is necessary here since propagation effects are not entirely negligible. In particular, Lovell *et al.*[187] also show a proton spectrum at 12:15 UT, *before* arrival of the Fe ions. Although the proton intensities at the highest energies vanish within a few hours, this earlier spectrum is *significantly harder* than the proton spectrum shown here. Such a peculiarity of proton spectrum early in the event of 29 September 1989 was noted by many researchers (for a review see Ref. 239). A fairer comparison between the proton and Fe rigidity spectra would integrate over a longer range of arrival times in order to include the earlier protons. To the opinion by Tylka *et al.*,[366] this integration would reduce — but probably not remove — the difference in hardness between the two spectra.

The authors conclude that CME-driven shock acceleration in this very large SEP event may be producing the same spectral differences and evolution in composition, which are believed to be caused by Supernova-shock acceleration at the "knee" of the galactic cosmic ray (GCR) spectrum. The end-point energy of shock acceleration depends upon several factors, including shock lifetime and particle containment in the shock region and perhaps some larger propagation volume as well. It is generally believed that these factors are involved at the knee of the GCR all-particle spectrum at $\sim 10^{15}$ eV. Available data (e.g. Ref. 49) suggest that the GCR composition (in terms of total energy per particle) in this region evolves towards heavy-ion enrichment and that the heavier ions have harder spectra than protons. In fact, hints of these spectral differences are also seen at energies well below the knee.

The solar proton and Fe comparisons presented by Tylka *et al.*[366] are in some sense trivial, since they are no longer comparing on the more appropriate "energy per nucleon" scale. However, the authors are, nevertheless, examining the composition and spectra near the highest proton energies attained in this CME-driven shock. The similarities between the GCR knee and these SEP observations make it

tempting to speculate that they are due to a common feature of shock acceleration, albeit operating at much lower energies in this case.[292] Note that the CME-driven shock model of particle acceleration cannot explain all observational features of the GLE of 29 September 1989. In particular, observations do not exclude the existence of two sources of relativistic protons separated in space and time.[239] At any rate, a totality of data requires to reconcile all of them in the framework of general self-consistent scenario, as it was suggested earlier (e.g. Refs. 227, 228 and 239).

One examination for the composition changes at the knee is that the finite lifetime of the Supernova-blast-wave shock limits the attainable energy per particle, and that this limit is proportional to the charge.[107] Such finite lifetime effects apply to CME-driven shock, so perhaps there is nothing surprising in the comparisons presented by Tylka *et al.*[366] On the other hand, in the GCR case, one must consider not only the finite shock lifetime and containment in the shock region but also possible distortions introduced by escape from the Galaxy. No analogous escape effect complicates interpretation of the SEP observations. Further study of SEP composition and spectra at the highest possible energies may therefore offer new insights into the physics of shock acceleration, which will complement studies of the GCR knee.

8.3. *Evidence for multiple acceleration processes*

Observation of neutral emission with high-energy and long duration from the flares of 11 and 15 June 1991 have illustrated a long-standing problem concerning the multiple injection and/or or continuous acceleration at/near the Sun (e.g. Refs. 66, 405, 347, 31, 5, 196, 231). The particles can be impulsively accelerated and then trapped in magnetic loops, or they can be continuously accelerated for a long time. It is also possible that the particles are accelerated in several episodes under different physical conditions separated by time intervals, or in different sources separated in space.

It is widely believed that a significant fraction of SEP's following major solar flares are actually accelerated at a CME-driven shock. Thus, the SEP's observed at 1 AU and those that interact at the Sun may represent quite different populations. Evidently, a modern picture of SEP event should include characteristics of the particles escaping into interplanetary space and that of interacting at the Sun to produce gamma-ray emission and neutrons.

Several years ago, Miroshnichenko *et al.*[238] have summarized data on the so-called "source spectra" of solar cosmic rays. By different techniques, the source proton spectra (SPS) have been reconstructed for 80 solar proton events (SPE's) from near-Earth observations of flare particles and gamma-ray emissions in 1949–1991.

Those data open several interesting lines of possible investigations if one identifies the SPS with the proposed source(s). This implies to separate them depending on the source type (flare or/and CME-driven shock, etc.), release mode (escaping or

trapping particles, impulsive or gradual events), energy range (energetic or relativistic particles), conditions of SEP propagation in the interplanetary magnetic field (IMF), etc. Below we present some results[231] of comparative analysis of available estimates of the source spectra for escaping and interacting protons.

From 80 events listed in the SPS catalogue,[238] in 56 cases the source spectra have been estimated only for escaping (interplanetary) protons detected at 1 AU. The rest 24 events were remarkable for considerable neutral emissions (neutron capture line of 2.223 MeV, nuclear deexcitation gamma-ray lines of 4–7 MeV, pion decay gamma-radiation from $\sim$10 MeV to $\sim$ GeV, and high-energy flare neutrons above 50 MeV), and corresponding SPS have been determined for interacting particles.

In three cases (21 June 1980, 3 June and 7 December 1982) it was a possibility to derive the source spectra of interacting particles taking into account observed flux of flare neutrons. Also, in five other events from our list (16 December 1988, 6 March 1989, and 4, 9 and 15 June 1991) solar neutrons were directly detected in space. Unfortunately, in 4 events only available data were plentiful enough to estimate the SPS parameters for both populations of accelerated particles. Note that three of them (4 August 1972, 7 December 1982, and 29 September 1989) were GLE's. The events of 7 December 1982 and 29 September 1989 had the certain CME associations, and the events of 4 August 1972 and 4 June 1991 were followed by interplanetary shocks (IS). In general, strong disturbances in the IMF were observed over all the period between 2 and 11 August 1972.

A summary of different estimates of the source spectra for the four SEP events mentioned is given in Figs. 14(a)–(d) (for details see Ref. 231, and references therein). In this study, in fact, it was attempted for the first time to separate reconstructed spectra depending on their possible sources — impulsive or gradual flares, CME-driven shocks and other energetic solar/interplanetary phenomena. The question of principal interest we addressed here is whether the escaping and interacting particles are distinguishable in impulsive and gradual solar events. As follows from the analysis by Miroshnichenko,[231] the problem of separation of interacting and escaping SEP's cannot be resolved accurately based on available fragmentary data on the SPS only. Nevertheless, conceptually, the SPS data, at least for large proton events, seem to be treated in terms of multiple acceleration processes in large-scale coronal structures (e.g. Refs. 239 and 228).

Some alternative hypotheses suggest that the particles both are accelerated in impulsive regime and then are trapped in magnetic loops, or they are accelerated in continuous regime over a long period of time. Also, it is not excluded that the particles are accelerated at different physical conditions during several episodes separated by certain time intervals, as it was found by Mandzhavidze *et al.*[196] from the event of 11 June 1991. In this last case, the spectra of particles accelerated in different episodes may be essentially different.

Discussion of specific mechanisms for particle acceleration is given in some details in Secs. 7 and 11 of this review paper. Nevertheless, it is timely to note that in many acceleration models an important, if not decisive, role is assigned to a

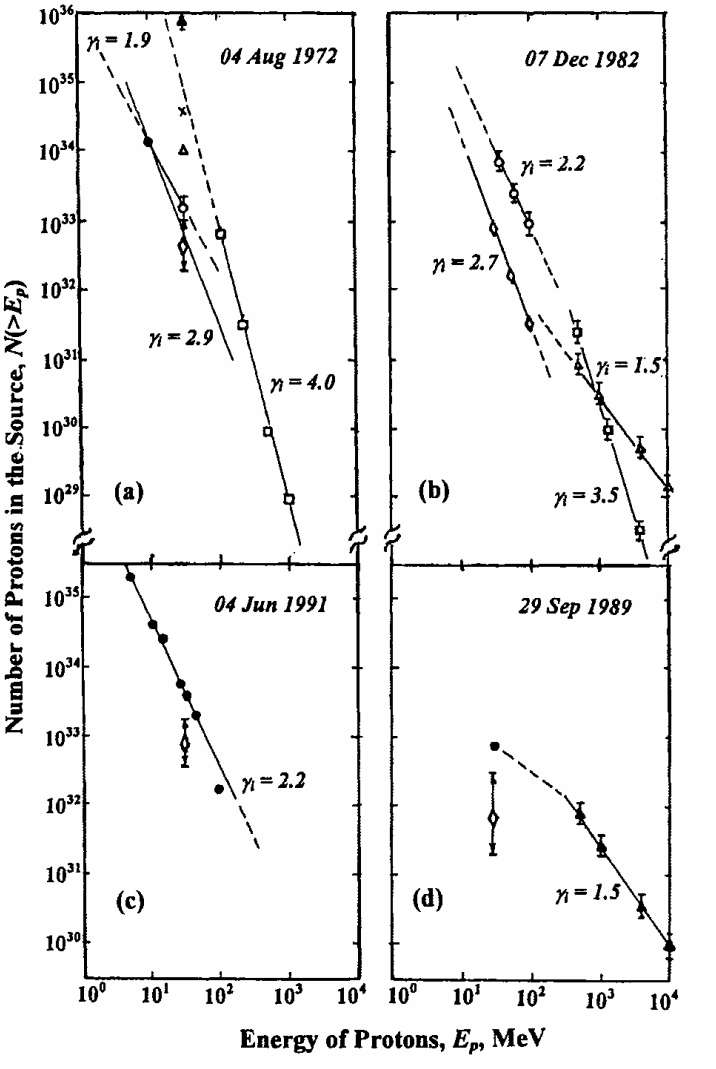

Fig. 14. Integral energy spectra of accelerated solar protons (with the exponent γ_i) in their sources by different estimates for the four SEP events::[229–231] (a) 4 August 1972, interacting (full and open circles, open diamond) and escaping (full and open triangles, cross and squares) protons; (b) 7 December 1982, interacting protons (triangles); prompt (diamonds) and delayed (squares) relativistic components and nonrelativistic escaping particles (circles); (c) 4 June 1991, interacting (diamond) and escaping (circles) particles; (d) 29 September 1989, interacting (diamond) and escaping (circle) protons; prompt relativistic component (triangles).

magnetic reconnection as the energy source and generator of electromagnetic fields necessary for the particle acceleration. For example, some recent studies[293,294,391] include a process of magnetic reconnection as a base for the description of both impulsive[293,294] and gradual[391] solar flares.

In the case of impulsive flares, according to Reames,[293,294] the particles (electrons and ions) are accelerated by stochastic mechanism in resonance regime due to developed wave turbulence produced by reconnection. In more complicated gradual flares[391] magnetic reconnection serves as a connecting link between stochastic acceleration[293,294] and acceleration by a CME-driven shock.

As to acceleration itself at shock waves in the solar corona and/or in the interplanetary space (see, e.g. Refs. 84, 392, 142, 143, 33, 34), its role in complex SEP events, such as the event of 4 August 1972, may be very important.[142,143] However, in spite of well-developed mathematical techniques, existing models are still unable to describe acceleration of solar cosmic rays to extremely high energies of ≥ 100 GeV.[146,147,239,228,230] In our opinion, solar protons may reach such energies due to acceleration by electric fields[185] that are produced at magnetic reconnection in the extended magnetic structures in the Sun's corona. A possible scenario of appropriate acceleration process in the large events of the 29 September 1989 type (e.g. Refs. 239 and 228) should certainly include multiple (at least two) steps.

A new problem evidently arises to incorporate SPS data into a widely discussed paradigm of particle acceleration in different sources at/near the Sun (e.g. Refs. 291–294). It implies using not only recently findings in elemental abundances and ionization states of accelerated particles, but taking into account also the data on solar gamma-ray and neutron emissions. More specifically speaking, to treat the problem of SCR spectrum formation at modern level of the SEP studies, one should examine SPS data in the framework of existing models of particle acceleration and release.

As shown above, the SPS over broad ranges allow fits with different functional forms, including a broken power law that may be indicative of multiple (at least, two-step) acceleration processes. Thus, the incorporation of the SPS data into general picture of energetic solar events allows to insight more deeply into existing problems of particle acceleration at the Sun.

During last decade, the concept of multistep (multiple) acceleration enriched itself of a new content (e.g. Refs. 391 and 228). In particular, several new dynamical models of particle acceleration in the extended coronal structure were proposed and developed: acceleration in presence of a CME;[55] acceleration in rapidly expanding and evolving coronal loops;[5] two-fold ejection of accelerated particles;[354] model of two sources;[270,271,239,228,379–381] two-step acceleration model.[244,207] The main purpose of those models is to give a self-consistent scenario for the entire SEP production process, including a final stage of acceleration to high energies (above 10 GeV). At the same time, we emphasize a great importance of initial stage of acceleration that is still not completely understood (e.g. Refs. 225, 217 and 282).

At present, there is no doubt (e.g. Ref. 228) that the most critical and disputable questions in the SCR physics lie at the opposite ends of their energy spectra (see, for example, Figs. 3 and 8 above). Actually, if initial stage of particle acceleration (up to the energies of $E \leq 10$ MeV, for protons) is closely related to some "intimate" properties of the solar plasma at the "microlevels" (for example,

threshold effects,[225]), energetics of "silent" low-energy protons,[326] etc., then at the final stage (at the energies of $E \gg 10$ GeV) the acceleration process seem to develop in the "macrovolumes" (i.e. in the extended magnetic structures at/near the Sun comparable with a Larmor radius of high-energy particles), in the presence of CME's, shocks and other energetic phenomena. Note that in this case a size of acceleration volume should be much larger than the gyroradius at the maximum energy.

8.4. *Recent developments of shock acceleration*

Shock acceleration in solar flares has been considered previously in many papers. In particular, Ellison and Ramaty[84] have modeled the simultaneous acceleration of protons, alpha particles, and relativistic electrons by first-order Fermi (or diffusive) shock acceleration (for details and references see, e.g. Ref. 282). In all cases examined, Ellison and Ramaty[84] found for any given event that a single shock compression ratio in the range $\sim$1.6–3.0 simultaneously produces reasonably good fits to the observed electron, proton, and alpha-particle spectra. The differential intensity of accelerated particles is given by

$$\frac{dJ}{dE} \propto \left(\frac{dJ}{dE}\right)_0 \exp\left(-\frac{E}{E_0}\right), \tag{5}$$

where E and E_0 are energy for electrons and protons and energy per charge for ions. As energy and gyroradius increase, it becomes less probable that a particle can be contained within the shock region. Ellison and Ramaty[84] suggested that this escape would cause the energy spectra of shock-accelerated particles to roll over more or less exponentially, with e-folding energy E_0 directly proportional to the ion's charge-to-mass (Q/A) ratio.

As noted by Zank *et al.*,[392] there is increasing evidence to suggest that energetic particles observed in "gradual" SEP events are accelerated at shock waves driven out of the corona by coronal mass ejections. Energetic particle abundances suggest, too, that SEP's be accelerated *in situ* solar wind or coronal plasma rather than from high-temperature flare material. In this context, the authors presented a dynamical time-dependent model of particle acceleration at a propagating, evolving interplanetary shock (IP shock). The theoretical model includes the determination of the particle injection energy, the maximum energy of particles accelerated at the shock, energetic particle spectra at all spatial and temporal locations, and the dynamical distribution of particles that escape upstream and downstream from the evolving shock complex. Note that injection here refers to the injection of particles into the diffusive shock acceleration mechanism.

As the shock evolves, energetic particles are trapped downstream of the shock and diffuse slowly away. In the immediate vicinity of the shock, broken power-law spectra are predicted for the energetic particle distribution function. The escaping distribution consists primarily of very energetic particles initially with a very

hard power-law spectrum (harder than that at the shock itself) with a rollover at lower energies. As the shock propagates further into the solar wind, the escaping ion distribution fills in at lower energies, and the overall spectrum remains hard. Downstream of the shock, the shape of the accelerated particle spectrum evolves from a convex, broken power-law shape near the shock to a concave spectrum far downstream of the shock.

Maximum particle energies accelerated at IP shocks result from a competition between the decelerating shock speed, the weakening IMF, and the shock age. Unless a shock is accelerating, the maximum energy to which particles are accelerated at an IP shock decrease monotonically with increasing radial distance. Nonetheless, according to the model by Zank *et al.*,[392] substantial maximum particle energies are possible in the early stages of shock evolution. In particular, energies of order of 1 GeV are possible for young shock waves, and this decreases to $\sim$ 100 MeV at 2 AU. Higher-energy particles tend to escape more easily from the shock complex, but a small number can remain trapped for an extended period.

As noted by Berezhko and Taneev,[34] in both above papers[84,392] the authors have considered a case of plane wave approximation that does not allow to take into account a finite size of the shock wave and its temporal dependence. Such an approximation is applicable to a bulk of accelerated particle in the vicinity of the shock, but it is broken in the range of ultimate energies where the spectrum undergoes to exponential cutoff. In fact, this approach results in significant softening of particle spectrum and decreasing of their maximum energy. To substantiate their model of acceleration of SCR up to relativistic energies by the shock waves produced by CME's, Berezhko and Taneev[34] proposed to use some new observational data.

They used the Alfvén turbulence data at the distances from the Sun above $3R_{\oplus}$ (Ref. 11) and semiempirical model of proton density distribution in the low-latitude corona.[330] Berezhko and Taneev[34] have performed detailed numerical calculations of the spectra for the SCR produced during the propagation of shocks in the solar corona in terms of a model based on the diffusive transfer equation using a realistic set of physical parameters for the corona. The resulting SCR energy spectrum

$$N(E) \propto E^{-\gamma} \exp\left[-\left(\frac{E}{E_{\max}}\right)^{\alpha}\right] \tag{6}$$

is shown to include a power-law portion with an index $\gamma \cong 2$ that ends with an exponential tail with $\alpha \cong 2.3 - \beta$, where β is the spectral index of the background Alfvén turbulence. The maximum SCR energy lies within the range $E_{\max} = 1$–300 MeV, depending on the shock velocity. Because of the soft spectrum of the SCR, their reverse effect on the shock structure is negligible.

The decrease in the Alfvén Mach number of the shock due to the increase in the Alfvén velocity with heliocentric distance r causes the effective SCR acceleration to terminate when the shock reaches a distance of $r = (2 - 3)R_{\oplus}$. In this case, the velocity of diffusive SCR propagation exceeds the shock velocity. As a result, SCR particles intensively escape from the vicinities of the shock. Berezhko and

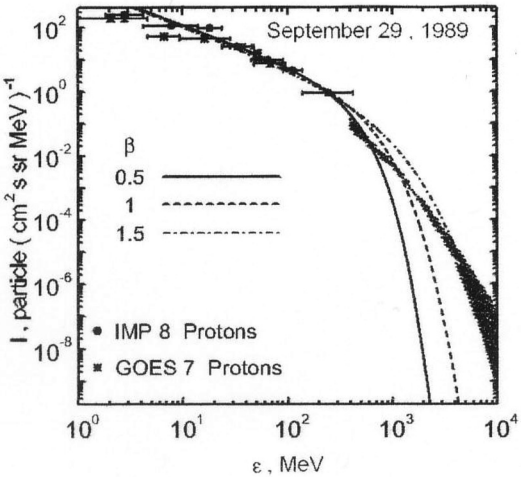

Fig. 15. Proton energy spectrum in the event of 29 September 1989 including data points from IMP 8, GOES 7, the neutron monitor spectrum by Lovell *et al.*[187] (shaded area) and calculated spectra by Berezhko and Taneev[34] for different Alfvén wave spectral index β.

Taneev[34] performed a comparison of the calculated SCR fluxes expected near the Earth's orbit with available observational data (e.g. GLE's of 7 May 1978 and 29 September 1989). Their results indicate that the theory may explain well enough some of the main observed features (absolute intensities, spectrum slopes, etc.) of nonrelativistic solar protons (as an example see Fig. 15 for the GLE's of 29 September 1989).

More deep analysis of their calculations, however, shows that their model still fails in the description of relativistic proton spectrum. In particular, the authors of Ref. 34 applied their model to the observed spectrum[187] related only to rather late period of the GLE of 29 September 1989. Meanwhile, as it was certainly shown,[239] this event distinctly revealed two-component (two-peak) structure with quite different spectra in two peaks. There are also some other methodical disadvantages of this model that requires to examine it more thoroughly. In this respect, a new good opportunity arises from the observations of proton events in October–November 2003 (including three GLE's) and on 20 January 2005. In particular, the fastest shock wave in October has overcome the Sun–Earth distance for 19 h, with a shock speed about 2754 km s^{-1}; estimated CME speeds on 20 January 2005 were from 2500 km s^{-1} (Ref. 327) to 3675 km s^{-1} (Ref. 120). Taking into account, additionally, a temporal evolution of the accompanying CME's, this model may provide a new insight on the problem of separation of the SCR sources (flares or CME-driven shocks).

Alternative numerical model has recently been suggested by Roussev *et al.*[427] for CME-driven shock acceleration. These authors were based on a fully three-dimensional, global MHD code for the initiation and evolution of the coronal mass

ejection which occured on 2 May 1998. This event was followed by rather small GLE56 (see Table 1). In their model, the solar eruption reaches a critical point where a magnetic rope is ejected with a maximum speed in excess of 1000 km s^{-1}. The shock that forms in front of the rope reaches a compression ratio greater than 3 by the time it has traveled a distance of 5 solar radii from the Sun's surface. For such values, diffusive shock acceleration theory predicts a distribution of SEP's with a cutoff energy of about 10 GeV. Whether similar results will be obtained for other events or other assumptions about the initiation mechanism remains to be questionable. However, the authors of Ref. 427 believe that for this event there is no need to introduce an additional mechanism to account for SEP's with energies below 10 GeV.

8.5. *Rogue events*

In distinction of the near-Sun environments, in the inner heliosphere valuable information about the physics and dynamics of the heliospheric plasma can be derived from the studies of the so-called Forbush-decreases in the intensity of galactic cosmic rays, coronal mass ejections and propagation of SCR in the interplanetary magnetic field (IMF). Possible particle acceleration at interplanetary plasma turbulence and shock waves is also of great interest, especially in the case of the so-called "super-events" or "rogue events" (e.g. Refs. 142 and 143), in analogy to rogue ocean waves having unusually large amplitudes.

Rogue events are associated with multiple shocks and CME's. In particular, from observations of two converging shock waves accompanied by an energetic particle event with unusual high and long-lasting intensities in August 1972, it was proposed (see Refs. 142 and 143) the first-order Fermi acceleration between converging interplanetary shocks as a fast and highly efficient acceleration mechanism. Subsequently, time periods with unusually high intensities related to multiple CME-driven shocks as well as other particle events with high intensities between pairs of shocks have been identified. Well-known examples of rogue SEP events at the Earth occurred on 14 July 1959, 4 August 1972, 19 October 1989, and 14 July 2000. Rogue events also have been observed in the inner heliosphere — with Helios 1 on 4 November 1980 at 0.5 AU and with Ulysses in March 1991 at 2.5 AU.

Rogue events cannot result in a simple compression of the medium between two converging shocks: although the distance between converging shocks would decrease with r as the shocks propagate outwards, the cross-section of the flux tube increases $\sim r^2$, leading to a net increase in volume between shocks. Figure 16 shows different geometries for a pair of shocks and the IMF. The left-hand side shows the simplest case: two shocks and a background Archimedean spiral magnetic field. Particles traveling from the upstream region towards the shock partly are reflected at the shock because the magnetic compression across the shock front creates a magnetic mirror. Thus particles can be swept by the shock. However, reflection of particles approaching the shock from its downstream medium cannot be understood because

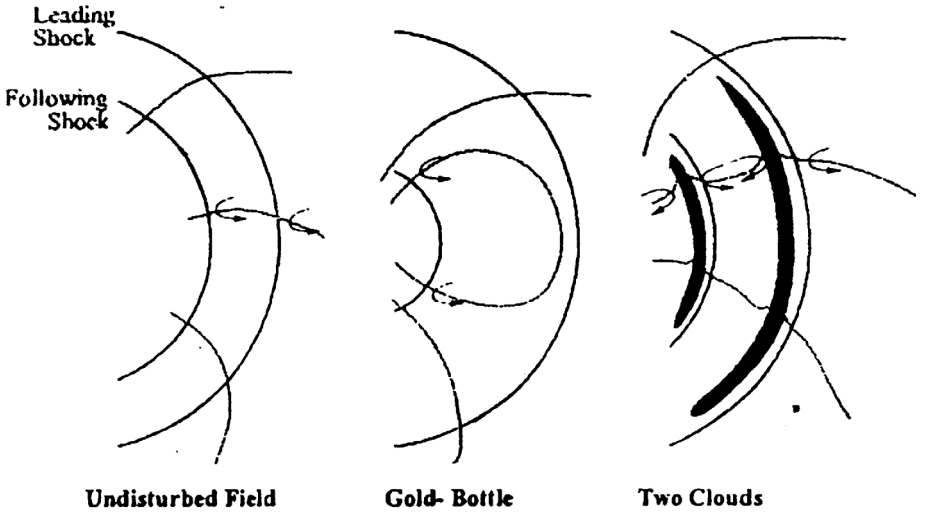

Fig. 16. Possible geometries for the acceleration of energetic particles between two converging shocks produced by the Sun.[142,143]

the particle then experiences a diverging field. Therefore, although the shocks would sweep-up the particles, there would be no particle storage in the volume between them and consequently no first order Fermi acceleration.

To avoid this problem, it was proposed the mechanism of a Gold bottle (middle section of Fig. 16): a large loop extends ahead of the shock and ones in the upstream medium particles have a chance (depending on their pitch angle) of being reflected back and forth along the field line. As the shock expands, the length of the field line in the upstream medium is reduced and the particles are accelerated by a Fermi I process. Although large loops extending beyond 1 AU have been observed, the authors think that this configuration might not be the only one to explain rogue events, in particular, since a typical rogue event has been observed by Ulysses at a distance of 2.5 AU (see Refs. 142 and 143).

Considering the calculations regarding the capability of a magnetic cloud to separate the particle populations upstream and downstream of a magnetic cloud, the authors suggest the scenario depicted on the right-hand side of Fig. 16: particles then are reflected repeatedly between the following shock (particles with small pitch angles passing the shock at the cloud) and the magnetic cloud behind the leading shock. The authors proposed a numerical model that allows simulating the effect of pairs of CME/shock on particle populations. They concluded that (a) the magnetic cloud following the leading shock is of outmost importance for the creation of high particle intensities, (b) the shocks need not to converge to create an intensity enhancement, and (c) the trailing cloud is required to reduce intensities after the passage of the shock pair.

8.6. *New concept of ground level enhancements*

Numerous studies of relativistic solar protons (SCR) allow us to clarify characteristics of the solar accelerators (short acceleration time, upper energy of accelerated particles, etc.) under the extreme conditions. Due to increased statistical accuracy and time resolution of NM data (since the middle of 1960's), it becomes possible, in particular, to study a fine structure of the GLE time histories and pitch-angle distributions (PAD) of relativistic solar protons (RSP).

Since the end of 1980's, systematic differences in the GLE time profiles and other characteristics have been found (e.g. Ref. 234) and treated as a manifestation of possible existence of two different components (prompt and delayed ones, or PC and DC) in some proton events (e.g. Refs. 271, 373, 237 and 239). Also, Shea and Smart[323] noted several events with unusual "spike-like" onsets (22 October and 15 November 1989; 21 May 1990). The only common thread between these three events is that the associated flare activity occurred in a longitude band between 28–37°W. This impelled the authors to examine other GLE's since 1942, and they found 5 similar events. The only event from the previous solar cycles that occurred in this longitude band and for which Shea and Smart[323] could positively identify the spike-like characteristics was on 15 November 1960 (35°W), with an initial spike of 124% followed by a second spike of 154% recorded by the Mawson NM (Antarctic). Type II radio emission was reported associated with this event. The rest four GLE's from this longitude band were too small, so any spike-like profiles would not be easily discerned.

To demonstrate the peculiarities of the GLE's with two components, we discuss in some details the relativistic solar proton increase on 22 October 1989. This event was remarkable for an unusual and complex intensity-time profile. Evidence presented, in particular, by Shea and Smart[324] and Cramp *et al.*[59] indicates that there were two distinct injections of relativistic protons into the interplanetary medium. The first injection resulted in an extremely anisotropic flux at the Earth as it was recorded (with the onset between 17:56–17:58 UT) at Antarctic neutron monitors McMurdo and South Pole, as well as at the Calgary NM, Canada. Most other NM's located at mid and high latitudes recorded an increase approximately 15–20 minutes later, and this second injection resulted in a much smaller anisotropic flux of particles as measured by NM stations viewing in the probable direction of the IMF toward the solar source. A comparison of the timing of the various solar parameters such as CME observations, X-ray and radio emissions with the particle observations shows that the first injections occurred when the inner edge of the CME was between 2 and 2.5 solar radii. The timing is also consistent with the occurrence of the classic flash phase of the solar flare phenomena. The implication of two acceleration processes for this well-connected event is presented.[324,59]

In this context, the measurements reported by Nemzek *et al.*[255] for this event deserve a special attention. These authors analyzed the intensity-time profiles obtained on geosynchronous spacecraft as a function of energy. The "spike" so

prominent in the neutron monitor measurements was preserved down to energies as low as 15 MeV. The time of the maximum intensity at these lower energies is a function of energy since these particles travel with slower velocities.

Thus the particles in the "packet" that was emitted from the Sun between 17:44 and 17:46 UT had energies ranging from 2000 MeV to less than 15 MeV. The spike-like character of this "packet" was retained throughout the event as these particles traversed the same path between the Sun and the Earth being detected at the Earth at times appropriate to their velocity. While the initial lower energy particles (with the spike-like characteristics) were still traversing the interplanetary medium, the higher energy particles associated with the secondary increase were also traversing the same spatial region albeit with broader PAD than the initial higher energy particles. Between 18:15 UT and $\sim$ 19:30 UT the higher energy particles of the secondary injection overtook the lower energy particles of the first injection as determined from the ground-based and satellite measurements. Thus, two separate populations of particles each with identifiable characteristics were traversing the interplanetary medium at the same time.

The authors[324,59] believe that the unique characteristics of the ground-based and satellite measurements during the solar proton event of 22 October 1989 are indicative of a dual acceleration/release scenario. The initial particles (i.e. "spike" feature) left the Sun in time association of an increasing intensity in optical, radio and X-ray emissions (i.e. "classic solar flash phase"). The CME observed at that time was located between 2 and 2.5 solar radii.

The secondary increase, also observed by ground-based and satellite detectors had an initial onset (for GeV energies) 20 minutes after the first increase. The CME would have traveled to $\sim$ 5 solar radii at the time these secondary particles started their transit to the Earth. The secondary event is much longer in time, indicative of particles being accelerated along the advancing shock associated with the coronal mass ejection.

More recent analyses (e.g. Refs. 237, 227, 239, 373, 379–381, 244, 207) of the GLE's observed during the cycles 22–23 allowed to confirm unusual features in the intensity-time profiles, energy spectra and pitch-angle distributions of a number of GLE's. In Table 18 we summarize the results obtained for a number of GLE's[379–381] that have demonstrated distinctly two-component structure of relativistic solar proton populations, namely, Prompt and Delayed ones (PC and DC). The onset time of the type II radio emission corresponds to the start of energy release at the null magnetic point close to the low coronal level and related to its H-alpha eruption and start of the CME.[198] This onset time was also found to be a marker of relativistic proton acceleration.[428]

In every event under study, the authors tried to reveal the prompt and delayed components of relativistic solar protons judging on their spectral forms. The best fits for the PC spectra are provided by exponential form $J = J_0 \exp(-E/E_0)$, where E_0 is characteristic proton energy. As to delayed component, its spectra may be fitted by power-law form $J = J_1 E^{-y}$.

Table 18. Parameters of energy spectra for relativistic solar protons (large GLE's of 1956–2006).

GLE No.	Date of GLE	Type II onset	Flare importance	Helio-coordinates	PC spectrum (exponential)		DC spectrum (power-law)	
					J_0	E_0	J_1	γ
1/05	230256	0331*	3B	N25W85	1.4×10^6	1.30	4.2×10^6	5.2
2/31	070578	0327	1B/X2	N23W82	5.6×10^4	0.71	1.2×10^4	4.1
3/38	071282	2344	1B/X2.8	S19W86	5.7×10^3	0.65	7.2×10^3	4.5
4/39	160284	0858	—/—	S??W132	—	—	5.2×10^4	5.9
5/42	290989	1133	??/X9.8	S24W105	1.9×10^4	1.54	3.5×10^4	4.1
6/44	221089	1805	2B/X2.9	S27W31	7.5×10^4	0.87	1.5×10^4	6.1
7/47	210590	2219	2B/X5.5	N35W36	6.3×10^3	0.83	2.7×10^3	4.1
8/55	061197	1155	2B/X9.4	S18W63	7.3×10^3	1.20	5.0×10^3	4.3
9/59	140700	1020	3B/X5.7	N22W07	3.3×10^5	0.35	2.0×10^4	6.4
10/60	150401	1319	2B/X14.4	S20W85	1.3×10^5	0.53	3.5×10^4	5.3
11/65	281003	1102	4B/X17.2	S16E08	1.4×10^4	0.59	1.5×10^4	4.4
12/67	021103	1703	2B/X8.3	S14W56	5.6×10^4	0.33	2.7×10^3	6.6
13/69	200105	0644	2B/X7.1	N14W61	2.5×10^6	0.49	7.2×10^4	5.6
14/70	131206	0226	2B/X3.4	S06W24	1.1×10^6	0.33	4.4×10^4	5.5

Notes: *Radio emission at 3.3 GHz onset (UT); spectrum constants J_0 and J_1 are given in units of differential particle flux (m^{-2} s^{-1} sr^{-1} GeV^{-1}). Double numeration for GLE's is given in the first left column (e.g. in modern numeration 1/05 means GLE05 of 23 February 1956).

The corresponding parameters of the PC and DC are displayed in the last four columns of Table 18, where characteristic energies E_0 are given in GeV and proton intensities — in units of m^{-2} s^{-1} sr^{-1} GeV^{-1}. Spectra parameters in Table 19 were derived by the authors using the optimization procedure for all events, excepting for the GLE of 19 October 1989. This event consisted of a precursor shot-lived pulse and the basic increase with a wide maximum. Shea *et al.*[321] found that the spectrum of precursor pulse was exponential in rigidity, and the basic increase (near the event maximum) had the power-law spectrum in the rigidity interval between 2 and 3 GV. In Table 18 the parameters of those spectra are presented in energy units.

In their modeling study of the GLE of 7 May 1978, Shea and Smart[319] have obtained a solar particle spectrum in conventional rigidity exponential form. Using the optimization method, Vashenyuk *et al.*[379] come to the conclusion that this spectrum in relativistic range may be described also by exponential function on energy (within the error limits), and the parameters of this revised spectrum are given in Table 18.

The event of 7 May 1978 was unique in the sense that it consisted of a very short-lived and anisotropic increase, and the spectrum during the whole event had an exponential form. Therefore, it is possible that the whole event consisted of the

prompt component only. So, a column for the DC in Table 19 is empty. The contrary situation was observed for the GLE of 16 February 1984. Despite the impulse-like intensity profile is characteristic for PC, the power-law spectrum and great time delay made us to account this to the DC type. Note that estimations by Vashenyuk *et al.*[379] are similar to the values obtained by Debrunner *et al.*[65]

Observationally, PC and DC differ from each other by the form of time profiles (pulse-like and gradual ones), pitch-angle distributions (PAD) (anisotropic and isotropic ones) and spectrum rigidity, namely, by hard (flat) and soft (steep) spectra, respectively. In particular, at the GLE onset the PC is extremely anisotropic. Theoretically, in terms of propagation theory, the DC may be treated as a result of transformation of the PC in the process of interplanetary propagation (SCR scattering at the irregularities of IMF).

In the whole, the results of many studies of the GLE's of the 21–23 solar cycles, as well as retrospective overlook of earlier RSP events (e.g. Refs. 323 and 324), in fact, results in the formulation of a new concept of GLE as a separate (specific) class of solar proton events (see Ref. 228). So, it is timely to consider in more detail two-component model of Ground Level Enhancements from the point of view observational and theoretical grounds and constraints.

This may require significant modifications in today's models describing the occurrence of solar flares, particle acceleration at/near the Sun and the propagation of solar cosmic rays through the interplanetary medium and near-Earth space. In particular, new insight may be expected into the production of high-energy gamma rays and solar flare neutrons. In essence, a matter arises on the formulation of a new paradigm of solar particle acceleration at high rigidity.

As we already mentioned, the GLE of 22 October 1989 displayed an extremely anisotropic onset, with an initial sharp "spike" in intensity. At present, there is no widely accepted model which could convincingly explain all features of this event. At the same time, it provides a good test for the different models of particle acceleration and propagation. In particular, a number of theorists (e.g. Refs. 91, 81, 92, 304, and others) have stated that the scattering conditions for solar particles prior to the establishment of steady state conditions are such that anisotropic (coherent) spikes may be expected early in some events. These spikes are followed by more isotropic particle distributions as the diffusive mode takes over from the coherent mode. As noted by Cramp *et al.*,[59] this scenario is inconsistent with the strong anisotropy of the forward PAD which persisted until quite late in the event of 22 October 1989. It is also expected that such a mechanism would not produce the depression in intensity seen at some stations between the spike and the later enhancement.

An alternative explanation is that there were two individual particle ejections, as it was proposed by Torsti *et al.*[354,355] in their interpretation of the event of 29 September 1989. For the event of 22 October 1989, however, there is no evidence of two phases in the metric radio emission. The soft X-ray emission also exhibits only a single peak. Although there are signatures of structure in the 10-cm radio

emission, Cramp *et al.*[59] found no compelling evidence of that a two-phase source existed at the Sun consistent with the intensity-time profile of relativistic proton flux at the Earth.

In principle, the observed two-peak profiles could have arisen if the particles followed two different paths through the IMF. One possible scenario would be that the magnetic field connection between the particle source and the Earth changed between the time of spike and the subsequent enhancement. This speculative argument[59] could explain the abrupt decrease in intensity from the forward direction between 18:05 and 18:20 UT. It might also account for the change in apparent particle arrival direction between 18:05 and 18:2 UT. However, it is not compatible with an interpretation of the bidirectional particle flow,[59] as the reverse propagating particles could no longer be reflections of the original spike.

As it turned out, the stations which viewed the reverse propagating particles saw a signature of the reflected spike. This was evidenced, for example, by a small but significant (> 10 s) spike at the Deep River neutron monitor, coincident with a sharp rise at the Mawson station. Evidence of the reverse propagating particles is found for all stations having an appreciable portion of their asymptotic cones viewing in the "reverse" direction. Therefore, Cramp *et al.*[59] conclude that the available evidence does not support particle transport along two different IMF paths.

In their opinion, the most logical explanation for this particular event appears to be an impulsive particle ejection followed by continuous shock acceleration over an extended period of time, in agreement with conclusions by Torsti *et al.*[356] Earlier, other authors have reached similar conclusions for different events.[297,372] The changes in the apparent particle arrival direction must be due to changes in the direction of the local IMF line. Unfortunately, there are no measurements of field direction with which to compare the derived arrival directions during the event of 22 October 1989. However, data from preceding and following days indicate that changes in the IMF direction of the same order (e.g. approximately 20°) were present on days either side of this RSP event.

The effects of anisotropy of relativistic SCR during the GLE of 29 September 1989 were studied by Vashenyuk *et al.*[373] on the basis of the hypothesis of the two-component ejection of the particles from the solar atmosphere. The first, prompt component was manifested at the Earth in the single maximum increase at the low latitude cosmic ray stations, high degree of anisotropy and very hard energy spectrum. The axis of the anisotropy in this increase passed through the asymptotic cone of the Thule station, Greenland. The second, delayed component in this event was displayed as a second intensity maximum at many high altitude stations. Very significant temporal variations during the second maximum could be described if one assumes that a large-scale magnetic structure was passing through the Earth at this time and the anisotropy axis was not strongly changing its direction in space during all the event.[407]

As noted by Smart and Shea,[323] the computed position of the maximum flux directions often do not correspond to the quiet time Archimedean-spiral direction.

It was found, in particular, for the GLE's of the 22nd solar cycle, perhaps, because many of these events occurred near the solar-activity maximum. There is often dramatic evolution of the maximum flux direction as the event evolves, for example, during the GLE of 24 May 1990.[245] The major events have sufficient statistics, so that flux contours in space can be derived, along with spectral evolution and rigidity-dependent pitch angle distributions (e.g. Refs. 59, 166, 79 and 80).

As to the general problem of a coherent pulse of solar cosmic rays, the consensus of the solar particle theorists seems to be that this pulse is a natural feature of solar particle propagation. This feature should be expected in the inner heliosphere whenever there are long mean free paths involved. The modeling work of Ruffolo and Khumlumlert[304] indicates, in particular, that diffusion is not really effective at propagation distances less than two mean free paths from the ejection position. Whenever the focusing length, L, dominates the scattering length, $L \gg \Lambda$, at distances not too far from the ejection site, then these coherent pulses, or "flash phase" in the Earl[81] terminology, should be expected at the beginning of an event. The computations by Fedorov *et al.*[92] shows that the time profiles observed during a GLE will depend on the neutron monitor asymptotic viewing direction in space with respect to the particle propagation direction.

On the basis of the Boltzman kinetic equation, Fedorov[89,90] has calculated the particle time profiles, spatial and pitch angle distributions at different regimes of particle ejection from the Sun (anisotropic initial distribution, instantaneous or prolonged ejections, etc.). Such a kinetic approach was applied to several GLE's to estimate the half-width of corresponding ejection time profiles, ΔT, and mean free path Λ (mean transport length). According to estimates by Fedorov,[90] the pairs of these parameters were $\Delta T = 8$ min and $\Lambda = 0.7$ AU, and $\Delta T = 19$ min and $\Lambda = 0.3$ AU, for the events of 16 February 1984 and 29 September 1989, respectively.

A similar approach was used by Fedorov *et al.*[93] to the GLE of 24 May 1990 which displayed a large anisotropy at the event onset and some signatures of two-fold ejection of relativistic protons (see, e.g. Ref. 237). It was postulated a prolonged, energy dependent escape of accelerated particles into interplanetary space. Fedorov *et al.*[93] found that the observed intensity-time profile at the Hobart station corresponds to the ejection profile with a half-width $\Delta T = 19$ min at the value of $\Lambda = 0.6$ AU. Such an approach, however, seems to be insufficient to explain a great time delay between anisotropic peak at several NM stations and a smooth isotropic maximum at the others, until one assumes a second ejection.

In general, the underlying physical circumstances leading to the initial spikes and two-peak structures in some GLE's are not presently understood. Thus, taking into account the above results and their discussion, we do not believe that the hypothesis of "an interplanetary origin" of the features mentioned can resolve alone the problem of RSP events. There are some grounds to accept a two-source model of SCR generation itself at/near the Sun, in the frame of the concept of multiple acceleration processes in the solar atmosphere.

9. Particle Acceleration Mechanisms and Scenarios of Solar Particle Production

Acceleration mechanisms of solar particles were studied well before the first solar proton event was undoubtedly identified at the Earth, on 28 February 1942. That is the case of the so-called betatron mechanism,[349] which was then applied to the study of specific GLE's of 1942–1946.[103,371] Since then, many different acceleration processes have been developed in association with solar energetic particles, and classed in several ways through a number of review papers (e.g. Refs. 311 and 262). One of the recent reviews of the problem, in the context of magnetohydrodynamic theories of reconnection, was given by Priest and Forbes.[282] Let us, hence, proceed for giving a brief glance on the SEP acceleration processes. The consensus about the present status may be summarized as follows.

Particle acceleration is ultimately due to the action of a direct or and induced electric field on charged particles. In terms of the nature of the process as particles gain energy, we can distinguish two kind of acceleration mechanisms:[311] (1) *deterministic* (*secular*) processes, when particles gain energy systematically in a unidirectional form, the accelerating agent is general associated with macroscopical magnetic structures of cosmic plasmas, (2) *stochastic* processes, when particles gain and lose energy in random small changes, but there is statistically a net energy gain, the accelerating agent is associated with wave turbulence. It is also known as "turbulent," "statistical" or even "diffusive" acceleration (at quasilinear order it may be described by a diffusion equation in momentum space). This is the case of the well-known second-order Fermi mechanism.

Particle acceleration in the solar atmosphere is then focused on two *interdependent* aspects, the small-scale and large-scale behaviors (or microscopic and macroscopic processes), associated respectively with particle–wave and wave–wave interactions (stochastic acceleration) and magnetic merging, coalescence, etc. (secular acceleration). Below we give only a brief summary of existing concepts, approaches and models.

9.1. *Deterministic processes*

(I) Direct electric field acceleration
  (1) Acceleration by *perpendicular* electric fields to the local magnetic field: Stationary and time-dependent (1, 2, 3 dimensions) models:
    (a) 1D (magnetic neutral current X-points and lines), 2D (magnetic neutral current sheets) and 3D (magnetic neutral current layers).
    (b) Loop coalescence.
  (2) Acceleration by *parallel* electric fields to the local magnetic field.
    (a) Double layer acceleration.
    (b) Acceleration by current interruption in force-free magnetic flux tubes: inductive circuits as solar twisted loop-like ropes.
    (c) Runway acceleration.

(II) Shock acceleration (first-order Fermi type acceleration)
  (1) DSA — diffusive shock acceleration (turbulent-scattering).
  (2) SDA — shock drift acceleration (scatter-free).

9.2. *Stochastic processes*

Most modern works study stochastic processes within the frame of weak turbulence, in terms of resonant wave–particle or wave–wave-particle interactions by means of the resonant condition: $\omega - S\Omega - kv = 0$.

(I) *Cherenkov* (Landau-damping) acceleration: resonance between the wave phase velocity V_ϕ and the particle velocity v : $k_\parallel v_\parallel/\Omega < 1$; $\omega \ll \Omega$; resonance at $S = 0$.
  (1) Second-order Fermi-type acceleration: damping of the electric field of waves.[408]
  (2) Magnetic pumping (Betatron) acceleration: compression and dilatation of the magnetic field.[172]
  (3) Transit time acceleration (called magnetic Landau-damping): damping of the magnetic field of waves.[408]

(II) *Gyroresonant* acceleration: resonance between the wave frequency and the particle gyrofrequency, $\omega/k_\parallel v_\parallel \ll 1$; $\omega \geq \Omega$; resonance at harmonics $S \geq 1$.

(III) *Nonlinear* Landau-damping and *nonlinear* gyroresonant acceleration.

Acceleration by a collection of weak double layers and DSA by a collection of weak shocks can be treated as stochastic-type acceleration processes.[209]

Stochastic processes have been widely discussed in the literature in connection with the following kinds of "wave turbulence." In cold plasma of hydrogen the most common turbulence can be reduced to two groups (see, for instance, Tables 1 and 2 in Ref. 262):

Electrostatic modes		Electromagnetic modes
— Langmuir waves		MHD turbulence
— Lower hybrid waves		Alfvén waves
— Ion sound waves	$\Longleftrightarrow$	Slow magnetosonic waves
— Ion cyclotron quasiparallel waves		Fast magnetosonic waves
— Ion cyclotron quasiperpendicular waves (Bernstein modes)		Hybrid modes
— Whistler waves		

MHD turbulence is often worked for acceleration of nonrelativistic ions and relativistic electrons within the frame of:

(a) The Cherenkov acceleration ($S = 0$; $p_\perp = \text{const}$) within the frequency regime $\omega \ll \Omega_\text{H}$ ($\lambda \gg r_g$).[1] Landau damping is ineffective for Alfvén waves, affects rather the compressed component (fast mode) of MHD turbulence.[209]

(i) Second-order Fermi acceleration.[172]
(ii) Transit time acceleration.[126,348]
(iii) Magnetic pumping acceleration.[348,97]

(b) The gyroresonant acceleration ($S \geq 1; p_\perp \neq \text{const}$), within the frequency regime $\omega \geq \Omega_{\text{H}}$ ($\lambda \gg r_g$)[19,212] can be highly effective for Alfvén waves.
(c) The nonlinear Landau damping (wave and wave–particle), and the nonlinear gyroresonant wave damping.[361,348]

Low frequency electrostatic waves are usually worked for acceleration of non-relativistic electrons within the frame of:

(a) Landau wave damping.
(b) Gyroresonant wave damping.

It is worth mentioning that, according to Chupp,[51] recent observations indicate that all mechanisms, direct electric field acceleration, shock acceleration and stochastic acceleration, may all be operating in flare phenomena, with ions and electrons being accelerated together even simultaneously during any phase of an event.

9.3. *Turbulent acceleration in solar flare sources*

Particle acceleration by wave–particle scattering in turbulent plasmas is a common process in nature and the most well-known acceleration process in plasma astrophysics. In spite of that the characterization of the physical mechanisms by means of which the turbulence evolves and transfers energy to the plasma particles has been studied for long time (e.g. Refs. 361 and 362), it is a problem that has not been completely solved.[217] Within this context of particle acceleration in a turbulent plasmas, most of acceleration models assume the existence of a turbulent state such that its energetic content remains constant during the acceleration process; however, the condition for the existence of such state requires of a balance between a number of effects to maintain a constant energy flux, from the energy containers of large scale (i.e. large scale turbulent structures) to the small scale energy containers where occurs the dissipation of the turbulent energy and the corresponding energy transfer to the plasma particles.

The study of this two-fold problem leads, for one side, to the establishment of a transport equation of the turbulent energy density $W(r, k, t)$ in the physical space and the wave number space, from the generation region, at large wave lengths, to the spectral regions of dissipation, at short wave lengths, and on the other hand, the establishment of the evolution equation of the number of accelerated particles $N(E, t)$ as a result of the turbulence-particle interaction. Therefore, the equation describing the spectral evolution of the turbulence must be coupled to the equation that determines the energetic evolution of the accelerated particles, however, such a coupling is not a simple one, taking into account that the transport equation of the

turbulence is a nonlinear differential equation. Nevertheless, Miller *et al.*[216] derived numerical solutions for the steady-state case.

Observational constraints regarding time scales, amount of accelerated particles and their energy spectrum impose difficulties that avoid to have at present a general consensus about the operating acceleration mechanism(s). Among the popular mechanisms there is the so-called *turbulent* or *stochastic acceleration* where particles gain energy at the expense of damped waves. As stated in last section, two main approaches are distinguished in these kind of mechanisms, the so-called Cherenkov or Landau-damping acceleration (resonance at the harmonic $S = 0$, $\omega \ll \Omega_p$), and gyroresonant acceleration ($S \geq 1, \omega \geq \Omega_p$). This kind of acceleration needs an appropriate source of waves providing a wave spectrum with high enough energy content to produce efficient acceleration in times ≤ 1 s, and so a suitable wave–particle energy exchange process for particles to draw energy from those waves, producing hence their damping.

There is also the need of a preheating mechanism to supply enough amounts of particles of energy higher than the threshold injection value for efficient resonant wave–particle interactions (e.g. nonlinear Landau damping, see Ref. 340). Under these conditions, resonant wave–particle interactions, nonresonant wave damping and nonlinear wave interactions, play the main role in determining the efficiency of particle acceleration by the turbulence waves.

9.4. *Acceleration efficiency from different wave modes*

Though several kinds of turbulence waves are susceptible of coexistence in the flare plasma their plausible energy source is still a controversial matter. Nevertheless, for the case of MHD turbulence it is known that its generation may occur when a macroscopic magnetized system supported by magnetic stress becomes unstable. Besides, due to mass motions, merging processes in reconnecting current sheets, the presence of MHD in solar flare sources seems highly probable.[273] So, it is expected that its presence is widely spread in the solar atmosphere.

The relative efficiency for turbulent acceleration among different wave modes, that presumably could develop and subsist for some time in the turbulent flare plasma, has been studied in a series of works[109–111,114,112,113,273,276,277] to determine whether or not the nonresonant damping processes and Coulomb collisions allow for efficient stochastic acceleration of the type Landau damping under conditions of the flare plasma. The efficiency of such kind of turbulence has been delimited on basis to their survival time to dissipation processes and their ability to reproduce the observed SEP energy spectra. The main nonresonant damping processes of magnetosonic waves in flare regions are viscosity and thermal conduction. The results allow to determine the feasibility of particle acceleration at different levels of the flare body.

The study of acceleration efficiencies shows that acceleration by short wave turbulence (Bernstein modes) may be higher than other longitudinal waves as

Langmuir turbulence: this is a promising acceleration process in the nonrelativistic particle domain but not for relativistic solar particles.[111] MHD turbulence is characterized by three modes, the fast and slow magnetosonic modes and Alfvén waves; the slow magnetosonic mode of MHD turbulence may be an interesting option to accelerate particles from the thermal background at deep chromospheric levels,[110] but in the coronal flare plasma requires of a continuous source of turbulence at a rate $\geq 10^3$ erg cm^{-3}.

Alfvén waves have a longer mean life time than the other two MHD modes, because they are more resistant to the several dissipation processes that affect them in the turbulent regions of solar flares. Since Alfvén waves are scarcely damped in the resonance $S = 0$, their contribution is rather associated to gyroresonant particle acceleration, but in this case the acceleration is only efficient for particles with initial velocities much higher than the local hydromagnetic velocity.[110] Besides, Miller *et al.*[212] show that gyroresonant acceleration by Alfvén waves in the solar corona requires about five times the energy density required by Cherenkov acceleration with fast magnetosonic waves.

The less restricted type of turbulence to accelerate solar particles and to fit observational constraints seems to be the fast MHD mode. A relevant discussion was given in Gallegos-Cruz *et al.*[110] and Gallegos-Cruz and Pérez-Peraza.[112] Though particle acceleration by wave–particle processes may occurs when the acceleration time is shorter than the damping time for nonresonant interactions, $t_{\rm acc} < t_{\rm dam}$, however, that does not assure that particles escape from the thermal distribution to produce an acceleration energy spectrum. Even if particle energization may occurs under the previously mentioned condition between acceleration and damping times that does not assure that particles escape from the thermal distribution to produce an acceleration energy spectrum. They also need to overpass the barrier of energy losses, which in the case of flare regions the most relevant is collisional Coulomb losses. So, an additional condition must be fulfilled, $t_{\rm acc} < t_{\rm Coul}$, where $t_{\rm Coul}$ is the time taken for a particle of energy E to cede its energy excess over thermal energy ($\Delta E = E - 1.5kT$) to the medium.

An approach to this problem of turbulent energy supply, ignoring nonlinear wave–wave interactions and cascade effects, and assuming a constant and steady injection rate of turbulence with a mean life time of about 1 s was carried out in Ref. 113 with consideration of wave energy dissipation and Coulomb particle energy losses. The study was extended to other assumptions on the energy density injection different to the constant a stationary rate.[114] It was found that protons can be accelerated up to energies > 1 GeV in a time < 1 s. The steady situation of the acceleration process is reached after 5–60 s,[112,114] which explains the invariability of spectra slope in gradual particle events after some time.

Such an approach of the real possibilities of stochastic acceleration in solar flare plasmas leads to conclude, that under conditions of continuous injection of fast magnetosonic turbulence, protons and electrons may be accelerated according to observational energies and time scales values, in the bottom part of the coronal

flare body and the top of the chromospheric flare. However, the number of accelerated protons is many orders of magnitude smaller than the observational intensity. Also, since the injection energy is higher than the mean thermal particle energy the requirement of a particle preheating step cannot be avoided if one needs to reproduce the observational amount of accelerated particles.

To fit the observed amount of accelerated particles it must be assumed an injection to the process with a supra-Alfvénic energy E_0, though a nonlinear analysis including cascade effects[180] leads to an increase of the acceleration efficiency, allowing particles to be accelerated from the thermal background. To overcome the deficit of accelerated protons it is assumed that the injection energy can be reduced to $E \leq 1.5kT$, on basis to the nonlinear and cascade effects discussed by Miller and Roberts,[215] Smith and Miller,[340] Miller *et al.*,[216,217] Lenters and Miller.[180] In Gallegos-Cruz and Pérez-Peraza[113] it is delimitated the turbulence levels and time scales under which such a kind of acceleration by the fast mode can overcome nonresonant thermal dissipation processes and Coulomb collisional losses in the solar corona in order that acceleration be efficient.

It was shown in Pérez-Peraza *et al.*[273] that for some specific conditions of magnetic field strength, density and temperature of the flare plasma, even protons of energy as low as 6 keV may reach energies $\cong$ 1 GeV in times of $\cong$ 1 s. Since in that energy interval $t_{\rm acc} < t_{\rm Coul}$, the accelerated protons never turn back to the thermal background, forming thus an acceleration spectrum of energetic protons. The relative efficiency for turbulent acceleration among different wave modes that presumably could develop and subsist for some time in the turbulent flare plasma has been summarized in Ref. 262.

9.5. *Constraints for solar particle acceleration*

Whatever the involved acceleration mechanism, models of solar particle generation must be able to t explain, at least, the observational data on:

(1) time scales of acceleration (rise time and duration);
(2) particle energy spectra of different events;
(3) number of accelerated particles (10^{32}–10^{41});
(4) selectivity to describe the variability of electron/proton ratios and that of ions and isotopic abundances.

If acceleration is by wave turbulence, it is additionally required:

(5) a plausible source for such turbulence;
(6) stability of turbulence energy density (with values in then range $\sim$ 1–10 ergs cm^{-3};
(7) enough number of particle with a minimum energy above an "injection threshold" value (which may be a thermal or suprathermal one according the kind of involved turbulence).

9.6. *Limitations of acceleration mechanisms in the solar atmosphere*

In spite that most of *direct electric field acceleration* processes do act efficiently at laboratory scale (mainly in linear and toroidal confinement experiments), and that *plasma turbulence* and *shock waves* are common features of nature and can be reproduced at laboratory scale, all the proposed acceleration processes are still a matter of polemic work, and most of them has been objected on theoretical grounds:

- Arguments against *shock acceleration* in connection with flares are for instance: Scatter free-shock drift acceleration (SDA) in a single crossing of the shock front can only increase the particle energy by at most a factor of 2.5. While Diffusive Shock acceleration (DSA) by scattering of particles in the turbulent upstream and downstream lead to a large energy increase because every shock crossing leads to an energy gain, however, DSA is efficient only for those gradual events where the shock can develop in a time < 0.1 s, provided that particles have velocities higher than the mean square velocity of the turbulent scatters.[105] Also, DSA may be no effective in the low corona because of the high hydromagnetic velocity (low Mach number). Nevertheless, since gradual events are associated with CME's (which drive the coronal shocks) and DSA can reproduce the single power law-rigidity spectra observed with low energy electrons in gradual events, DSA remain a very promising process in the high corona: to know the real accelerating efficiency, the energy density level of the scattering turbulence needs to be determined.
- *Direct electric field acceleration* depends strongly in the existence of anomalous resistivity during the time scale of the phenomenon, while Runway acceleration is strongly inhibited by self-inductance. It is argued that due to current interruption (necessary for developing anomalous resistivity) the number of accelerated electrons falls below observational values. In particular, reconnection in neutral current sheets (NCS) is often objected in connection with a poor particle escape into the interplanetary space. However, it should be noted that in Ref. 249 it has been calculated the trajectories of particles in NCS and shown that most of the particles are able to escape, though the degree of escape depends on the magnetic field topology of the sheet. Further arguments supporting NCS has been widely discussed by Somov[344,345] and Litvinenko and Somov.[185]
- The biggest problem that *stochastic acceleration* confronts is that, there is no direct observational evidence of the level of turbulence and mean-life of both, low frequency electrostatic waves and MHD turbulence, during the flare phenomena. By the moment, what we can do is to derive the conditions that need to be satisfied in order for stochastic acceleration to be effective. Though physical concepts date from more of five decades, big advances are continuously reached in the task of delimiting the efficiency conditions for stochastic acceleration.

10. Source Energy Spectrum and Scenarios of Solar Particle Production

Sounding space sources of particle acceleration can be made through the analysis of the emitted radiation from the interaction of accelerated particles with matter and electromagnetic fields, or by the study of the properties of the accelerated particles themselves. The distribution of particles according to their energies (energy spectrum), is one of those properties. The study of such spectra in the sources allows inferring about the kinds of acceleration mechanisms, involved of turbulence, parameters of the acceleration process and local physical parameters (magnetic field strength, plasma density and temperature).

10.1. *Formalism of stochastic acceleration*

The formalism of stochastic acceleration is based on the very well-known quasilinear kinetic approach of a momentum–diffusion equation in the phase space for the pitch angle-averaged particle density (e.g. Ref. 313). Under a variable change, it can be transformed to a generalized Fokker–Planck-type equation. A particular case of that equation, for Cherenkov-type acceleration, with a constant and steady rate of Kolmogorov-type turbulence was solved by Gallegos and Pérez-Peraza,[112] Pérez-Peraza and Gallegos.[272] By means of the WKBJ method the authors derived time-dependent and stationary analytical solutions for the particle energy spectra through the whole energy range, from nonrelativistic to ultrarelativistic energies, including the transrelativistic domain that up to then had been only worked out by numerical methods: energy spectra and time scales for acceleration do agree with the numerical results of others authors.

Since particle sources in solar flares are often imbedded in expanding plasma that drives the CME a rate of energy loss by adiabatic cooling has been introduced in the transport equation. The time-dependent solution, assuming a monoenergetic continuous injection, has a form:[276,277]

$$N(E,t) = \frac{kq_0}{2}\left(\frac{3}{4\pi a}\right)^{1/2} \frac{\varepsilon^{3/4}[\varepsilon^2 - m^2c^4]^{\frac{3\rho}{2\alpha}}}{(\varepsilon^2 - m^2c^4)^{1/8}} \times \left\{[\mathrm{erf}(z_1) - 1]e^{(3a/\alpha)^{1/2}J} + [\mathrm{erf}(z_2) + 1]e^{-(3a/\alpha)^{1/2}J}\right\} \tag{7}$$

which determines the instantaneous distribution of the accelerated particles per energy interval. The parameters α and ρ are the acceleration and adiabatic cooling efficiencies respectively, and

$$k = \frac{[\varepsilon_0 + \sqrt{\varepsilon_0^2 - m^2c^4}\,]^{3\rho/2\alpha}}{\varepsilon_0^{1/4}(\varepsilon_0^2 - m^2c^4)^{5/8}}\,,$$

$$Z_{1,2} = (at)^{1/2} \pm R_2 t^{-1/2}\,, \qquad R_2 = \frac{1}{2}\,J(E)\,,$$

$$J(E) = \left(\frac{3}{\alpha}\right)^{1/2} \left\{ \tan^{-1}\beta^{1/2} - \tan^{-1}\beta_0^{1/2} + 0.5 \ln\left[\frac{(1+\beta^{1/2})(1-\beta_0^{1/2})}{(1-\beta^{1/2})(1+\beta_0^{1/2})}\right]\right\},$$

$$a(E,\tau) = \tau^{-1} + 0.5[F(\beta_0) + F(\beta)]\,,$$

$$F(\beta) = \frac{\alpha}{3}\,(\beta^{-1} + 3\beta - 2\beta^3) - \rho(2-\beta^2)\,, \tag{8}$$

β_0 is the value of $\beta = v/c$ at the injection energy E_0 and is the total energy. For the solution reduces to Eq. (41),[112] and this same spectrum tend to a power-law form in the high-energy range as the time elapses toward the steady state situation. If instead of a supra-Alfvénic monoenergetic injection energy E_0, it is assumed a more realistic injection by pre-acceleration in a Magnetic Neutral Current Sheet, with a well-defined spectrum of the type of Eq. (9) here below, the solution is then given by Gallegos-Cruz and Pérez-Peraza[112] [Eqs. (50) and (51)].

By coupling the solutions of the transport equation of turbulence to the equation of particle energy evolution, Gallegos and Pérez-Peraza (2002) show that under more realistic spectral distribution of the turbulence energy density (with dissipation effects) than those obtained with the idealized $W(r,k,t) = \text{const}$ (no dissipation effects) there is a notorious diminution of the amount of particles per energy interval, in both cases the steady-state and the time-dependent spectra, which becomes more notorious as the wave propagation angle increases. This fact imposes an additional constraint on acceleration models with regard to the amount of accelerated particles.

For the case of deterministic processes, direct electric field acceleration in a magnetic neutral current sheet (MNCS) has been widely discussed and reviewed in the literature since the pioneer works of Giovanelli and Dungey (e.g. Refs. 281 and 16). In order to discriminate between the wide variety of NCS topologies proposed for solar flares, Pérez-Peraza *et al.*[263,264] derived the energy spectrum of particles which is produced in each of the proposed MNCS topologies. The authors found that the best one to reproduce observational spectra from thermal energies up to some GeV, in realistic conditions of anomalous conductivity of the flare plasma, is the topology proposed in the work of Priest.[280] On this basis they derived the following steady-state acceleration spectrum:

$$N(E) = N_0\left(\frac{E}{E_c}\right)^{-1/4} \exp\left[-1.12\left(\frac{E}{E_c}\right)^{3/4}\right], \tag{9}$$

where $N_0 = 8.25 \times 10^5 (nL^2/B)(1/E_c)$ (protons/MeV), B, L and n are the magnetic field strength, the length of the sheet diffusion region and number density, respectively, and $E_c = 1.792 \times 10^3 (B^2 L/n)^{2/3}$ MeV.

10.2. *Fitting observational spectra with theoretical source spectra*

As it was said in the previous section, particle source spectra furnish information not only about the acceleration process but also about the source parameters.

However, source spectra may be modulated either during interplanetary propagation or during coronal azimuthal transport (e.g. Ref. 261). Therefore, the direct confrontation carried out by many authors of theoretical source spectra to observational spectra, ignoring transport effects on the particle fluxes, is mainly based on the following arguments:

- Many flares events occur in the well-connected Sun–Earth coordinates.
- Most of time one is dealing with GLE which relativistic protons practically do not feel interplanetary magnetic structures.
- Fluxes are considered at the time t_m of maximum intensity.
- For the events which are far from the Sun–Earth connection heliolongitude, a model dependent assumption is considered: a closed expanding coronal magnetic structure connect particle fluxes with the well-connected region of 60°W heliolongitude (e.g. Ref. 228, Fig. 7.25).
- Additionally, as was previously stated, the integral spectra observed near the Earth's orbit are a proxy of source spectra at the ejection into the interplanetary medium (e.g. Refs. 222 and 106), at least, for well-connected events.

It is under such a direct confrontation where the best fits of theoretical and observational spectra determine the plausible source and acceleration parameters, that acceleration efficiencies, time scales of acceleration, density, temperature and magnetic field strength in the source of some GLE's of the 22–23 solar cycles were derived in Pérez-Peraza *et al.*[270,271,275,277,278] The kind of phenomenology taking place at the source may also be inferred: for instance, that adiabatic cooling becomes negligible even for expansion velocities higher than 3500 km/s when the acceleration efficiency is relatively high ($\alpha > 0.1$ s^{-1}), and in cases where at low values of α the best fit is with the spectrum without adiabatic losses, it can be inferred that the acceleration does not occur in an expanding structure. Besides, it has also established that MNCS injection to a MHD turbulence environment in solar fare regions reproduces better the observational spectrum that under the idealized conventional assumption of a monoenergetic injection into the stochastic process.[277,278]

It should be emphasized that in the fitting process of observational spectra, the derived source parameters and the parameter of acceleration efficiency are within the realistic values expected in the coronal flare, as determined from electromagnetic emissions. Results of the mentioned methodology are illustrated in Figs. 17(a)–(d) for the so-called Delayed Component of SRP events and Figs. 18(a) and 18(b) for the Prompt Component, both of them described in Subsec. 10.4.

10.3. *Scenarios of acceleration with different mechanisms*

Modeling of SEP production is generally done for individual events, so that a huge amount of scenarios can be found in the literature taking into account peculiarities of events and the behavior of the associated emissions. According to the *Amount of*

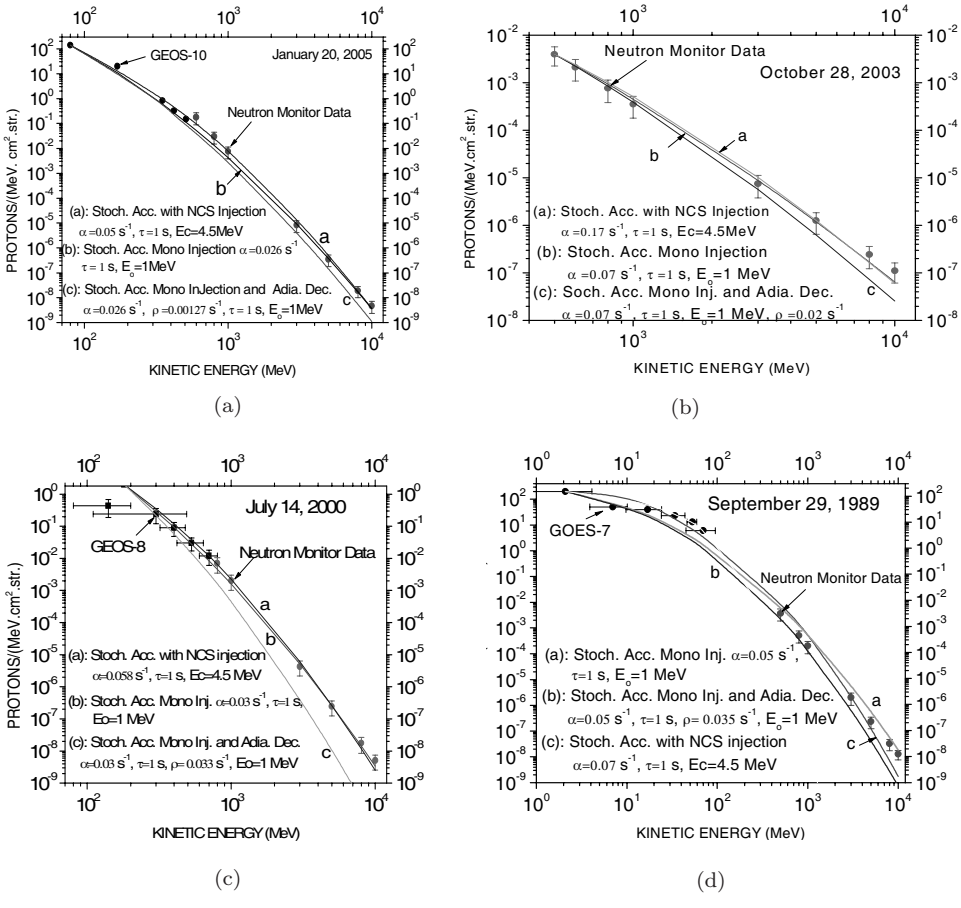

Fig. 17. Fitting of the theoretical spectrum (Eq. (6)) to observational data of satellite and neutron monitors, under the assumptions of monoenergetic injection into a stochastic process in a fast magnetosonic wave environment, with/without adiabatic cooling, and injection from a pre-acceleration step in a magnetic neutral current sheet (Eq. (8)).

Traversed Matter X (g cm^{-2}) $= \rho v t$ (ρ, v, t are the density, particle velocity and confinement time, respectively), possible scenarios are based on:

Thick target models (when ρ and/or t are relatively high): particle trapping in closed topologies with strong converging magnetic fields and/or low corona (or chromospheric) densities, ρ can be low, but t can be very long (closed magnetic topologies), the energy spectrum is modified by collisions.
Thin target models (when ρ and t are relatively low): acceleration in the high corona and free particle escape (open magnetic field topology) and energy spectrum is not altered.

To account for the abundance ratios, charge states and the associated radio, X-ray and γ-ray emissions, a vast amount of scenarios, postulating combinations of

thick and thin target models have been developed, either with continuous acceleration in 1-phase, or *episodically* in 2- and 3-acceleration phases with trapping between them, as mentioned above (e.g. Refs. 51, 287 and 16).

- Often, acceleration phases are associated with a thin target, followed by precipitation into an interaction region associated with a thick target. However, full scenarios have also been proposed within the frame of one of them, either the thick or the thin target geometry.
- One-phase acceleration is frequently associated to direct electric field acceleration, while 2- and 3-acceleration phases are rather associated with stochastic and shock wave acceleration.
- On the previous basis, impulsive events are better described in terms of acceleration by stochastic turbulence, whereas gradual events may be explained also by stochastic acceleration as well as by shock wave acceleration or a DC-field acceleration process. In the next subsection we present a scenario for a specific kind of ground level events which data (mostly during solar cycles 22–23) indicate the presence of two independent relativistic proton components.

10.4. *Two-source scenario for SPE with various relativistic components*

Following Subsec. 8.6, the existence of two different components in RSP has been proven in a number of works.[373–378,380,223,235–237,227,228,262,271,273,275,277,244,207] The authors intensively analyzed a number of large GLE's of the 22–23 solar cycles (in particular, 29 September, 19 and 22 October 1989, 24 May 1990, 14 July 2000, 15 April 2001, 28 October and 2 November 2003, 20 January 2005). Analysis of dynamical changes of the spectrum, pitch-angle distributions (PAD) and anisotropy in successive moments of time, together with their time profile reveals the existence of two distinct RSP populations, a prompt component (PC) characterized by an impulse-like intensity increase, rigid spectrum and high anisotropy, followed by a delayed component (DC) presenting a gradual increase, soft spectrum and low anisotropy. In general, spectra at the early stage of the events are very hard, just at the time when the PAD's in both events are the narrowest. As the PAD widen with time the spectra becomes softer.

The observational spectra at the initial time shows a very peculiar exponential energy dependence, but as time elapses the spectrum gets gradually steeper without drastic changes up to certain time when only the high energy portion of the spectrum has a fast intensity drop. To discriminate among the PC and the DC components data must be chosen at times where the spectrum is clearly different from the PC at the early phase of the event, and the profile shows a clear fall in intensity of the first impulsive peak, what can be done at the time t_m when the flux intensity reaches its maximum. For the interpretation of these observational data a plausible scenario has been developed in a series of works (e.g. Refs. 223, 235–237, 227, 228, 373–378, 380, 262, 271, 273, 275, 277) in terms of two different sources given below.

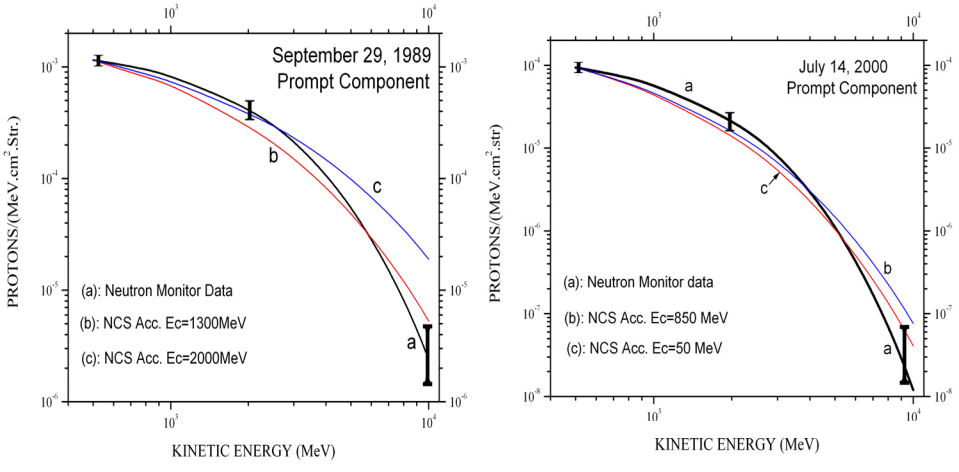

(a) (b)

Fig. 18. Fitting of the theoretical spectrum (Eq. (8)) to observational data of the PC from neutron monitors, assuming direct electric field acceleration in a magnetic neutral current sheet.

Delayed Component. It is proposed that the DC is produced during the impulsive flare phase in the flare body, within an expanding closed magnetic structure in the low corona, where the bulk of particles are stochastically accelerated in the turbulent plasma, while eventually loosing energy by adiabatic cooling in the expanding bottle. This population is injected into the interplanetary space at the time of about 0.5–2 hrs as a consequence of an opening of the closed structure due to a plasma instability (tearing or Raleigh–Taylor), or because they are carried off by a lifting CME. The invariability of the energy spectrum of the DC during times of ~ 2 hrs supports this mechanism.

Prompt Component. The PC is produced afterward in an anisotropic source located in a region of open field lines, higher in the corona, allowing particles to drift azimuthally and reach the Earth's environment before the bulk of the accelerated particles of the DC. The acceleration of the PC is attributed to impulsive electric fields generated in a reconnection process in extended coronal structures of opposite magnetic field lines, as for instance the trailing part of coronal transients (CME or eruptive filaments), or in the MNCS which can be formed when a flare expanding magnetic structure get in touch with magnetic lines of opposite polarity from neighboring loops, arcades or new emerging magnetic fluxes. Local particles of the nonadiabatic region of the neutral current sheet may be accelerated to relativistic energies by the intense electric fields generated in the merging process.

Energy spectra of the PC can be adequately reproduced by an exponential-type spectrum from neutral current sheet acceleration, even in its 2D-stationary version, as it is illustrated in Figs. 18(a) and 18(b). This is not the case for the DC which

data may represent the superposition of at least two different sources, since the presence of CME indicates the possible production of RSP in a shock acceleration process, as has been suggested by other authors (e.g. Ref. 187), in particular, for the 29 September 1989 event. Besides, energy spectra of the DC can be nicely reproduced in a straight way by spectra from stochastic acceleration, as illustrated in Figs. 17(a)–(d), whereas the so-called prompt component cannot be explained by stochastic acceleration. This result effectively points toward the confirmation of two components of different origin.

In the case of the 28 October 2003 event, the development under the proposed scenario should have undergone the following sequence.[278] According to the type II radio onset of the 4 B/X17.2/S16E08 flare, the magnetic loop associated to the flare begins to expand around 11:02 UT. The stroke to the collateral loop should occur at $\sim 11:10$ UT, since particles of the PC which has been accelerated by direct electric field in a developed MNCS are seen at earth at 11:20 UT. Meanwhile the "population in the expansion bottle" has been about half an hour undergoing adiabatic cooling, competing with stochastic acceleration up to the moment that efficiency reach the value α_1 to overcome the loss barriers and begin to escape with an average escape time of about 1 s.

Taking into account that relativistic particle last about 8 min to reach the Earth, the first bunch measured at $\sim$11:40 UT should have been generated before $\sim$11:32 UT, when the acceleration efficiency $\alpha(t)$ has reached a value enough high to overcome the energy loss barrier, say $\alpha_1 \approx 0.9\ \mathrm{s}^{-1}$ (efficiency under which the observed particles spend ~ 4 s). Later, after 10 s the stochastic process efficiency decreases to a value $\alpha_2 \approx 0.7\ \mathrm{s}^{-1}$, such that particles measured at 12:00 UT have been accelerated under this efficiency regime. Finally, after 20 s of acceleration, the efficiency decreases to $\alpha_3 \approx 0.65\ \mathrm{s}^{-1}$, where the steady state ($\alpha = \mathrm{const}$) is practically being reached, the magnetic structure is open and turbulence is dissipated (particles under this regime are observed at about 12:10 UT).

Figures 19(a) and 19(b) shows the evolution of DC spectrum, up to the steady-state situation, fitted with Eq. (6), and Fig. 19(c) illustrates the fitting of the PC spectrum with Eq. (8). The previous two-source model has been recently reviewed[351] in a survey of different options for solar particle acceleration.

10.5. *Ground-basis supporting the two-source model*

A synthesis of recent observations and theoretical concepts on solar flares and particle acceleration[16] shows that present high-precision timing measurements (down to a few microseconds) combined with high-resolution imaging (down to a few arc-seconds) of solar flares provide the required physical parameters to conduct quantitative data analysis on the kinematics of SEP. This new information imposes several constraints on the time-dependent location and geometry of acceleration regions, as well as the dynamics of the acceleration processes, *limiting the role of speculative models.*

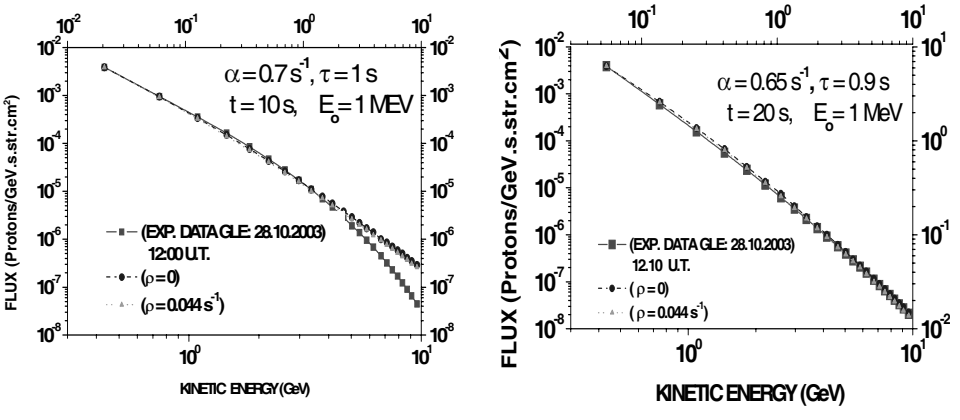

(a) (b)

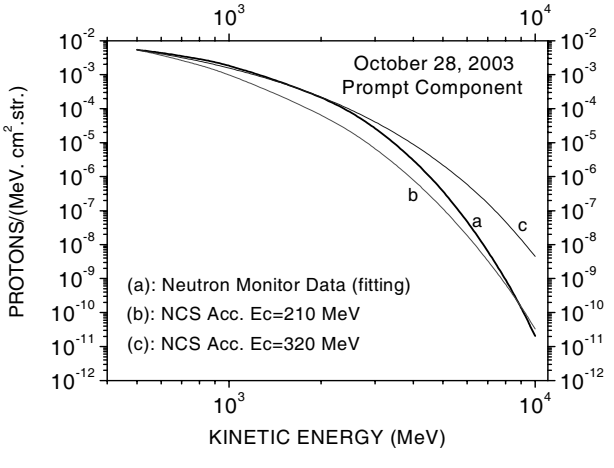

(c)

Fig. 19. Evolution of the DC spectrum Eq. (6) of the 28 October 2003 event as it seen (a) at the Earth at 12:00 UT, after having been accelerated during 10 s at the source under a efficiency of 0.7 s^{-1}; and (b) at 12:10 UT after 20 s of acceleration with an efficiency of 0.65 s^{-1} when the steady state situation is reached; (c) PC spectrum at 11:20 UT at the Earth after 1–2 min of acceleration in a MNCS high in the solar corona (9).

The scenario discussed in the last section, in connection with GLE presenting two-relativistic-components, has been developed in terms of stochastic (turbulent) acceleration and neutral current sheet acceleration on basis to the following arguments: it has been previously mentioned that MHD turbulence may be generated when a macroscopic system supported by magnetic stress becomes unstable, as well as during merging processes in reconnecting current sheets. This is the case in Gradual Events that are often associated with CME's driving coronal shocks, and thus setting up: reconnection; turbulence and opening of magnetic field lines. Under

this context, since gyroresonant acceleration by Alfvén waves is marginally less efficient than Cherenkov acceleration by the fast mode wave (e.g. Ref. 409), hence, for the stochastic acceleration stage of the two-step-scenario discussed in the last section, it is usually evoked acceleration by Landau damping of the fast MHD mode. Besides, according to data reported in Ref. 16 *most of flare events are associated with magnetic reconnection in bipolar, tripolar or quadrupolar magnetic topologies between open–closed and closed–closed field lines*, involving magnetic arcades or loops.

The geometry of acceleration regions inferred from magnetic topology constraints is illustrated by Aschwanden[16] (see Fig. 7), where the presence of two distinct acceleration regions in the flare body can be appreciated, one of which in some cases is associated with open magnetic field lines. This kind of X-type reconnection geometry seems to be the case for the particular flare of 14 July 2000 (the well-known Bastille Day event, or BDE), as schematized in Fig. 46 of the mentioned work. It was a very complex SPE, where even the neutral line was a curved one (Figs. 36 and 46 in Ref. 16), with several acceleration sites in space–time according to the dynamical evolution of magnetic geometry. Furthermore, since for a simply static neutral sheet acceleration efficiency decreases with the distance to the adiabatic region of the sheet, this may perhaps explain the rapid change of the spectral shape of the PC in some events, in particular in the case of BDE.

Therefore, the two-source scenario seems to be reinforced in the light of modern observations. Observational evidences of the opening of field lines in the evolution process of the magnetic merging and reconnection in closed–open structures, and the time evolution of spectral data reproduced with time-dependent spectra, speaks in favor of the origin of the PC and DC as proposed in such a scenario.

10.6. *Stochastic versus shock wave acceleration*

As described in Subsec. 8.4, shock wave acceleration is a promising mechanism, not only for particle acceleration in the interplanetary space but also in solar flare regions, due to the occurrence of CME in most of gradual SPE. Though recently many authors tend to favor this process, mainly in connection with the behavior of solar particle abundances from event to event, one should not ignore the constraints in its efficiency, as described in Subsec. 9.6. Here we will only mention the present status relative to the reproduction of the energy spectra for both, stochastic and shock acceleration.

Quite recently, Bombardieri *et al.*[39] studied the GLE of 14 July 2000 on basis to the shock wave acceleration model of Ellison and Ramaty[84] and stochastic acceleration according to the spectral formulation given in Gallegos and Pérez-Peraza.[112] They found that the spectra corresponding to the peak of intensity and the declining phase is better reproduced by stochastic acceleration, though the rise phase was better reproduced with shock acceleration. They even identified a change in spectral form, attributed to a new source and claimed that this should be reproduced by

MNCS acceleration. Such a new source corresponds to the PC in the two-source model which spectra is reproduced precisely by MNCS acceleration (9) as illustrated in Fig. 17(a).

Earlier on, Berezhko and Taneev[33,34] have studied the GLE of 29 September 1989 on basis to diffusive shock acceleration and they are able to reproduce spectral data at low energies but fail at relativistic energies (see Fig. 15). In both cases, the spectrum of shock acceleration is not time-dependent but corresponds to the steady-state, so their application to different times of the events is not justified. As a matter of fact, it should be expected from the analysis of Bombardieri *et al.*,[39] that shock acceleration should fit better the declining phase of the event, when there is a tendency toward a stationary situation.

In contrast, stochastic acceleration allows time-dependent descriptions of the spectrum time evolution[112] as illustrated with the GLE of 28 October 2003 above in Figs. 19(a)–(c). Therefore, though shock acceleration is undoubtedly a process that is present, it seems that its contribution is mainly to the low energy part of the spectrum, which probably mixes with the bulk of particles of the DC population stochastically accelerated in a MHD environment. Ultimately, the flare phenomenon seems to be characterized by a multistep acceleration behavior. Finally, it is worth mentioning that no shock acceleration model has attempted to explain the PC, that up to now has only been interpreted in terms of MNCS acceleration.

The 20 January 2005 event provides several new challenges to models of SEP events at the Sun and in the heliosphere (e.g. Refs. 210, 211, 178, 120, 379, 381, 277, 278, 244 and 207). The CME from this event was first observed by SOHO/LASCO at 06:54 UT. Unfortunately, subsequent LASCO images were totally obscured by high-intensity solar-particle "snow," so CME velocity measurements were not possible from SOHO alone. Using other data,[327] in particular, estimated a CME velocity of $\sim$ 2500 km s^{-1}. Figure 20 shows the height of the CME leading edge versus time for a constant velocity of 2500 km s^{-1}.

At the time the first high-energy particles were (apparently) released from the Sun, the CME was below 1.5 solar radii, having left the Sun $\sim$ 7 mins earlier. A challenge to shock acceleration models is to form a shock very low in the corona ($\leq 1.5R_s$) and accelerate particles to GeV energies within minutes (for details and references see Refs. 210 and 211). Ionic charge state measurements place further restrictions.[178] If the first high-energy particles left the Sun when the CME shock was at $\sim 1.5R_s$ above the solar surface, then the charge-equilibration calculations for this height and the observed mean charge state of +12 for Fe imply that ≤ 90 second were available to accelerate and release the particles. The calculations combine charge equilibration for Fe ions in hot plasma[168] with a model of electron density in the solar corona.[330]

On the other hand, if the first LASCO data point are combined with the EIT/SOHO data, one finds a velocity of 3242 km s^{-1} (Ref. 120) when the CME first appeared in the LASCO field of view. These authors estimated, finally, that the CME had the largest sky-plane velocity of 3675 km s^{-1}. In their opinion, the

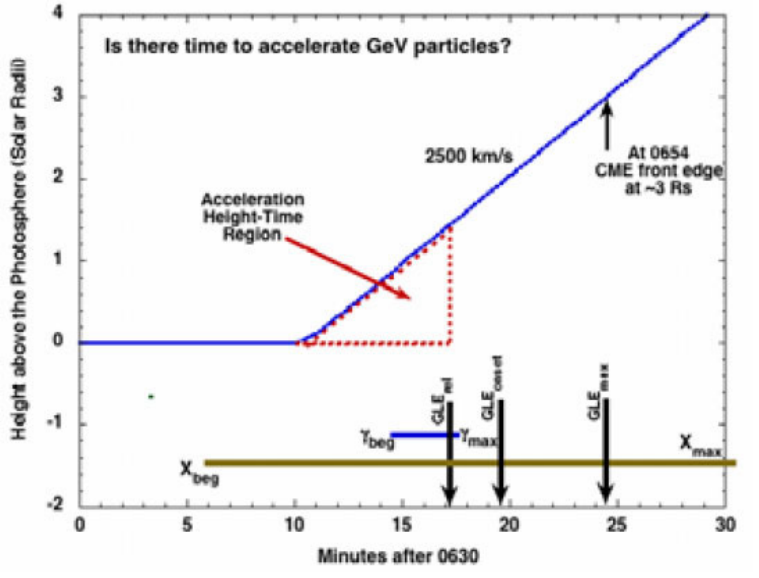

Fig. 20. Estimated height of the CME leading edge versus time for a constant velocity of ~ 2500 km s^{-1} on 20 January 2005.[210,211] If this SEP event was caused by a CME-driven shock, it formed low in the corona and reached GeV energies in minutes.

average height of CME leading edge was $\sim 4.5R_s$ at the time when the GLE proton injection started. Moreover, Vashenyuk *et al.*[379] have found that relativistic protons in the GLE of 20 January 2005 were presented by two components, prompt and delayed ones, with different times, spectral and anisotropy characteristics. Quite recently, Moraal *et al.*[244] confirmed that there were two distinctly different populations in this GLE (P1 and P2 pulses). Two similar pulses were also observed in 10 other GLE's from Tables 2, 5, 8, 11, 31, 44–48. McCracken and Moraal[207] propose an explanation of these two pulses by two separate acceleration episodes in the typical GLE: (a) acceleration directly associated with the flare in the lower corona, and (b) acceleration by a supercritical shock driven by the associated CME, at $\sim 2.5R_s$.

Note that in the shock model of acceleration proposed recently by Berezhko and Taneev[33,34] the effective SCR acceleration terminates when the shock reaches a distance of 2–3R_s. Though this model seems to be more compatible with the results of Mewaldt *et al.*,[210,211] Labrador *et al.*,[178] and McCracken and Moraal,[207] a new complex analysis of the event under consideration would be very promising.

11. Magnetic Reconnection in Acceleration Scenarios

As mentioned above, a concept of magnetic reconnection in astrophysical objects is one of the foundations to explain and to describe particle acceleration and energy release in energetic plasma phenomena (e.g. Ref. 282). According to modern model

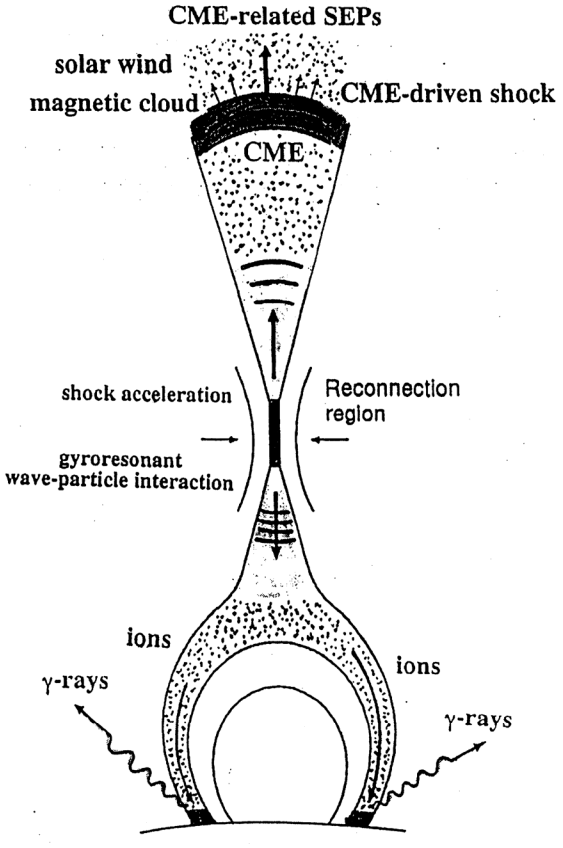

Fig. 21. High-energy particle production processes in the solar atmosphere.[391]

assumptions (e.g. Ref. 391), the magnetic reconnection in the solar atmosphere takes place above the top of flaring loop, producing strong Alfvén waves or fast shocks. The latter case is illustrated in Fig. 21.

11.1. *Fast reconnection and particle acceleration*

From the above considerations (see Subsecs. 5.1, 10.3–10.6) it follows that the majority of the proposed models of the SEP events are based, partially or completely, on the concept of magnetic reconnection in the solar corona. In order to complete the reconnection (acceleration) scenario for the event of the 29 September 1989 type,[239] we estimate the time, t_f, required for the formation of the reconnecting current sheet (RCS) in the source region, and the time for acceleration of protons by an electric field, $t_{\rm ac}$, to energies $\geq$ 10–100 GeV. First we will introduce the corresponding estimates of Ref. 185 for RCS which is supposed to form during the rise of a CME at the posteruptive stage of the flare.

A typical CME velocity of upward motion equals the Alfvén speed in the corona $V_A \cong 1000$ km s^{-1} under characteristic values of the coronal magnetic field $B \cong 100$ G and plasma density $n \cong 10^{11}$ cm^{-3}. Assuming the speed of plasma inflow into the RCS to be $u = 0.1V_A$ (fast reconnection under high, but finite conductivity) we obtain $t_f = L/u = 10^2$–10^3 s, where $L = 10^9$–10^{10} cm is the characteristic scale for width and length of the sheet. Further, it should be taken into account the effect of transverse electric field outside the RCS. It was shown[185] that this field efficiently locks the nonthermal ions inside the sheet. Such a confinement allows the particles to be accelerated with a characteristic time $t_{\rm ac} \cong 0.03\ (E_p/1\ {\rm GeV})$ s. It follows that the proton requires only 3 s to be accelerated up to energy $E_p \sim 100$ GeV.[185,5,345]

11.2. *Estimates of source parameters*

On the other hand, under derived conditions for the PC generation at the source II in Pérez-Peraza *et al.*,[271] for the event of 23 February 1956 ($B = 30$ G, $n = 2 \times 10^7$ cm^{-3}, $L = 10^{10}$ cm); one can estimate the Alfvén speed $V_A = 1.5 \times 10^9$ cm s^{-1}. If we take $u = 0.1V_A$, then the time for formation of the RCS will be $t_f \cong 66.7$ s. This is close to the lower estimate of Ref. 185. For the event of 29 September 1989 ($B = 91$ G, $n = 1.2 \times 10^7$ cm^{-3}, $L = 10^9$ cm);[376] the time for formation of the RCS is considerably less, $t_f \cong 1.74$ s. However, we should bear in mind that if the magnetic bottle (with an expansion velocity $V_c \sim 300$ cm s^{-1}) interacts with a coronal arch, there will probably be stimulated (explosive) reconnection. As shown by Yokoyama and Shibata,[410] its rate is determined not only by the parameters of the stimulating (driving) process, but also strongly depends on the plasma resistivity (uniform or anomalous) near the neutral point. It appears that the formation of magnetic islands (plasmoids) and their subsequent ejection from the current sheet is a key physical process leading to fast reconnection.[410] Anyway, and this is important, the problems of magnetic reconnection and coronal mass ejections are closely related.[343,345,411]

Overall, it is fair to say that the two-source model is consistent with modern theories of magnetic reconnection in the solar corona, including the possible acceleration of protons to energies $\sim$ 10–100 GeV. We note that if the reconnection speed is $u = 0.1V_A$, instead of accepted earlier $u = V_A/18$,[412] the calculated number of accelerated particles changes considerably.[271] For example, for $E_p = 25$ MeV, the number of accelerated protons increases by a factor of 2.4.

From these estimates it is concluded that the acceleration of the prompt component of relativistic protons in the 29 September 1989 event may be understood in the framework of reconnection models of Martens and Kuin[199] and Litvinenko and Somov.[185] Here the particle acceleration proceeds in the electric field that is produced between reconnecting magnetic field lines in the trailing part of coronal transient behind the eruptive filament. On the other hand, while gaining energy in the electric field, particles may accomplish an azimuthal drift in the neutral sheet carrying them to the visible side of the Sun from the behind-the-limb flare. So,

the prompt arrival of particles and gamma ray emission from the behind-the-limb flare[413] may be easily explained as well.

11.3. *Observational constraints*

However, the two-source model cannot yet answer, of course, all the questions involved. At least, three important problems remain unresolved theoretically, namely, the drift effects of relativistic particles in expanding bottle (loop), possible adiabatic loss of particle energy as the volume of the bottle increases, and maximum rigidity of accelerated particles. Though the first two problems were treated in several works (e.g. Refs. 414, 194, 415, 416), many questions remain unclear (for example, the escape of the *first* relativistic protons from expanding magnetic structures).

As to the maximum rigidity of accelerated particles, available acceleration models do not exclude large values of R_m (or E_m), and the problem seems to reduce to the search for adequate magnetic configurations (structures) in the solar corona. For example, the model of two SCR sources[271] gives a value of $E_m \sim 250$ GeV for the flare of 23 February 1956 type; in the electromagnetic model of solar flare[279] maximum proton energy may be as large as 10^6 GeV. On the whole, however, all such estimations depend heavily on the choice of acceleration model.

Moreover, to compare the estimated values with observational results it is not only important to calculate E_m, but also to resolve a more difficult problem, namely, to determine the SCR spectrum shape at the source and the number of accelerated particles of extremely high energy. In this respect, the results of the generalization of the SCR spectrum data[224,226,228–230] for the most powerful SPE's (see Fig. 3) impose certain upper limitations. In the range of energies from several units to several tens GeV, the data point to a steepening behavior of the SCR spectrum (e.g. Ref. 239). At any rate, they do not give convincing grounds for its extrapolation[417,165] by the power-law function with unchanging slope to the higher energies.

As to the BUST muon burst during the event of 29 September 1989 (see Ref. 146), it is difficult to explain, first of all, its delay for a time > 1 h relative to the first intensity peak at the surface muon telescopes. At the same time, it is obviously impossible to accept a hypothesis about the trapping and prolonged containment of relativistic protons in magnetic loops of the solar corona during certain SPE's (e.g. Ref. 194). The presence of the acceleration source high in the corona[237,227,373–375,381,382] would be a possible explanation of above fact.

Such a suggestion, however, comes in collision with the fact that the proton intensity corresponding to the BUST burst does not agree with the spectrum of relativistic protons at the early stage of this GLE.[146] It becomes clear that in application to the BUST effect the existing two-source model must be modified to take into account either possible additional acceleration of solar particles at the shock front far from the site of the proper flare, or eventual modulation of galactic cosmic rays at the energies above 500 GeV.[146,147]

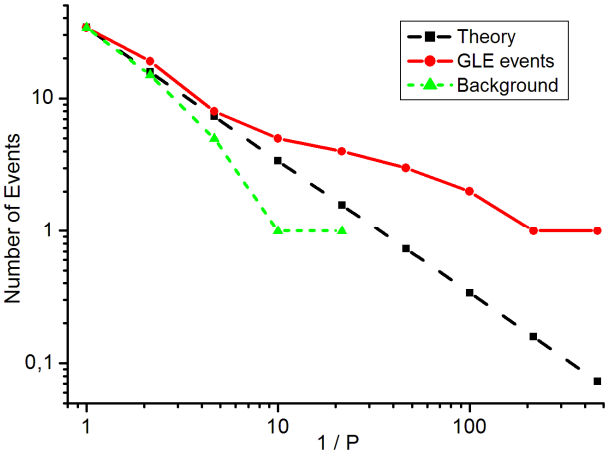

Fig. 22. Integral distributions, $N(1/P)$, of the muon bursts by the BUST data during GLE's of 21–23 solar activity cycles (1981–2005). The circles represent the distribution for the bursts observed during GLE's, squares correspond to theoretically expected distribution, and the triangles are related to the distribution for the bursts from the background intervals.[147]

Quite recently, statistical analysis of the muon bursts with energy ≥ 200 GeV recorded at the BUST during the GLE's was extended on the 23rd cycle of solar activity.[147] As it was noted above, the data of muon registration with energy ≥ 200 GeV at the BUST are used in searching for SCR with energy > 500 GeV. The 35 GLE events have occurred during the BUST operation since April 1981 up to now. The data of the muon registration at the BUST are available in 34 cases. The 19 GLE events of the 22nd solar activity cycle and of the end of 21st one have been investigated earlier. The 15 new GLE events, which occurred from 1997 to 2005, are added now. The temporal evolution of the newly occurred bursts shows the asymmetry found earlier: the delay of the bursts relative to maximum of corresponding X-ray flare is equal to about 1–2 hours. The ecliptic longitude distribution of the bursts shows surplus in the interval of 0°–60° to the west from the Sun–Earth direction which possibly indicates the link with the IMF.

Integral distribution of the bursts number versus $1/P(3\text{h})$ is depicted in Fig. 22 where $P(3\text{h})$ is a probability of random realization of a burst due to fluctuations in any of 680 angular cells of during 3 hours. The total number of the bursts having probability not exceeding a given $P(3\text{h})$ (integration from $1/P$ up to $+\infty$) is shown in each point. The 3-hour intervals distanced on 1 day up to or after corresponding flare were used as the background intervals. Selection of the bursts within those intervals was made by the same method as during GLE events. The integral distribution of events $N(1/P)$ for a purely random process (Poisson, Gauss, etc.) in double logarithmic scale presents a direct line with a slope $k = -1$ (as a corollary of the law of big numbers). The probability distribution for the bursts recorded during GLE events significantly differs from theoretically expected distribution and from the distribution for background intervals.

The observed surplus of bursts of large amplitude possibly indicates that an additional muon flux exists. For control intervals there is a good agreement of experiment with theoretically expected distribution. Figure 22 also demonstrates distinctly that distribution of muon bursts during GLE differs from the Poisson one. Therefore, the absolute value of the burst probability $P(3h)$ is less important than the probability where differences of experiment from background and from theory are beginning, i.e. the probability P is approximately 0.1 in our case. Considerable growth of statistics has given an opportunity to select confidently four muon bursts, which cannot be explained by the background fluctuations. From this position it is possible to regard as significant four bursts only: 29 September 1989, 28 October 2003, 15 June 1991 and 12 October 1981. Moreover, by using new presentation of observational data in the form of integral distribution $N(1/P)$, the authors[147] are visually and quantitatively able to determine the difference in numbers of registered bursts and theoretically expected ones. Observational characteristics of four most significant bursts are similar; in particular, they have the same spatial and temporal properties. As to physical interpretation of the obtained results, it is a rather difficult task and should be a subject of separate study (see also Subsec. 3.3).

Recently, Karpov and Miroshnichenko[148] suggested new statistical method of additional fluctuations for search of weak signals of various natures. This method may be applied, when average value of a signal does not give statistically significant excess over an average background of the device (detector). The method uses property of statistical distributions to increase number of the large fluctuations far from mean value and, hence, provides extraction of such deviations caused by a weak signal. Examples of such signals are high-energy gamma-ray bursts[339] and muon bursts at the Baksan Underground Scintillation Telescope. The authors apply this method to obtain and interpret some peculiarities of muon bursts observed at the BUST in close correlation with a number of GLE events. One of the preliminary conclusions is that the SCR flux magnitude estimated by new method may be about 10 times lesser than that obtained before, for example, for the event of 29 September 1989[146] using the full burst amplitude of 5.5σ. This conclusion seems to allow one to reconciliate the BUST data on the GLE of 29 September 1989 with integral spectrum for other GLE's in the range of energies above 10 GeV (see Fig. 3).

The method of additional fluctuations may be useful mostly in the search experiments working near to a limit of accuracy of the device. Probably, it may also be applied to interpret some effects in the solar-terrestrial system when a weak "solar signal" superposes on fluctuating "geophysical background."

12. Occurrence Probability of Giant Flares

How large an event can the Sun produce? Notice that the ULS model (see Subsec. 3.2) deals with the largest proton fluxes observed (or expected) near the Earth's orbit at the moment t_m, but not with the fluences (event-integrated fluxes). Therefore, the ULS seems to be not very representative as to determining largest

particle fluences. For example, based on the limit intensity $I_p(\geq 10\ \text{MeV}) = 10^6\ \text{cm}^{-2}\ \text{s}^{-1}\ \text{sr}^{-1}$ (see Table 3) one can obtain a limit fluence, $F_s(\geq 10\ \text{MeV}) = 1.25 \times 10^7 \Delta t\ \text{cm}^{-2}$, where Δt is the integration time interval. Hence, to obtain the fluence values of $\geq 10^{10}\ \text{cm}^{-2}$ it is necessary to integrate the peak proton intensity over $\Delta t \geq 10^3$ s. On the other hand, proceeding from the largest fluence $F_s(\geq 10\ \text{MeV}) = 3.2 \times 10^{10}\ \text{cm}^{-2}$, estimated for the single event of 12 November 1960,[94,95] our model gives $\Delta t = 2.5 \times 10^3$ s. Although both estimations of Δt are very similar it should be emphasized that the ULS model is hardly able to characterize thoroughly a single proton event because of rather complicated relations between its time profile, peak intensity and duration.

12.1. *Cosmic rays and ancient catastrophes*

In this context the estimates of Sakurai[309] for occurrence probability of extremely large flares are of great interest. The occurrence rate of the flares during solar cycle 19 at the Wolf number $W > 100$ turned out to be approximately proportional to the value of W, independent of flare importance. A number of flares for this cycle diminished exponentially with increasing of flare importance from 2 to 4. The extrapolation of such dependence indicates that during the cycle 19 one gigantic flare of hypothetical importance 5 could occur. The most realistic candidate for such a case is the flare of 23 February 1956, though this event turned out to be not an extreme one as regards, for example, the fluence of ≥ 30 MeV protons.[387]

According to the estimates of Sakurai[309] the flares of importance 4 or more release about 50% of their total energy in the form of SCR with energy $E_p \geq 10$ MeV which in turn is expected to result in very large enhancement of proton energy density near the Earth. However, the SCR data already obtained for more than 60 years of observations still give no grounds for such expectations (see, e.g. Fig. 4 for the late phase of the 23 February 1956 event). Moreover, according to our estimates,[220,221] the contribution of protons with $E_p \geq 10$ MeV to the flare energetics seems to be $\leq 10\%$ for the most powerful SPE's, this portion being slowly increased at $E_p < 10$ MeV.

The occurrence rate of giant flares can also be estimated from some circumstantial data. For example, it is suggested[30] that the recently discovered four cases of extinction of Radiolaria for the last 2.5 million years were due to the occurrence of such giant flares with a frequency $\sim 10^{-4}\ \text{y}^{-1}$ coinciding with the geomagnetic inversion period. As to the SEP event distribution in terms of proton fluence, F_s, per single event the observation data are controversial. On the one hand, Lingenfelter and Hudson[182] have revealed an abrupt cutoff in the distribution of proton events, $\sim F^{-1.5}$, at $F_s > 10^{10}\ \text{cm}^{-2}$. This result was also confirmed by McGuire *et al.*[193] On the other hand, more recently Feynman *et al.*[94–96] showed that the fluence for events in solar cycles 19–22 all fitted in one continuous log–normal distribution. Anyway, at the present level of solar activity the largest fluence is apparently confined to the value of 10^{11}–$10^{11}\ \text{cm}^{-2}$ (see also Ref. 320).

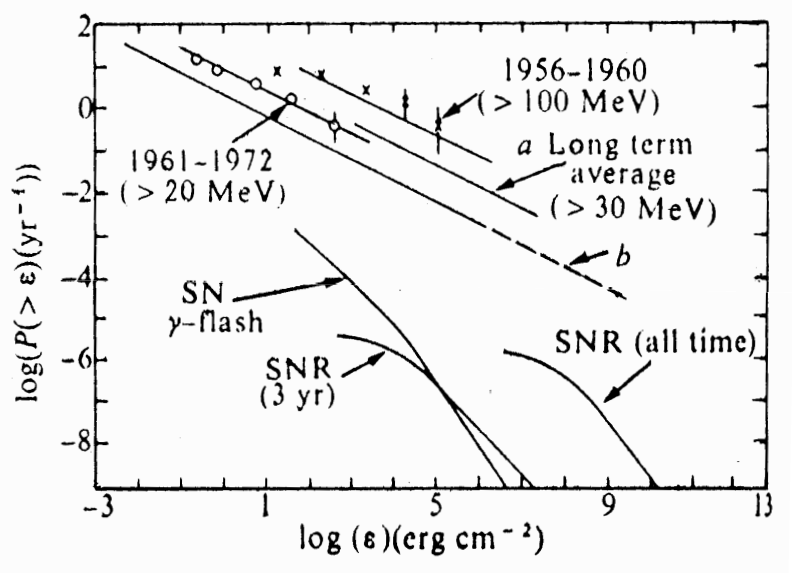

Fig. 23. Integral frequencies of solar cosmic-ray events at the Earth[418] (for details see text).

A detailed study of expected catastrophic effects from cosmic rays (primarily the depletion of atmospheric ozone layer) was undertaken by Wdowczyk and Wolfendale.[418] In terms of the energy density ε of cosmic ray particles (in erg cm^{-2}) received at the top of the atmosphere, they endeavored to estimate, in particular, the likely frequency of solar flares of sufficient strength to have significant effect. The frequency distributions were constructed for two periods, 1956–1960 and 1961–1972, with different average levels of solar activity. The results obtained for SEP's are summarized in Fig. 23, together with the corresponding estimates for the frequency of gamma flashes from the Supernovae.

The abscissa in Fig. 23 is the energy density in the event and relates to the top of the atmosphere. Line *a* is a rough estimate of the long-period average event frequency (for energies above $\sim$ 30 MeV) and derived from measurements made on protons during the very active period 1956–1960 and during the most recent solar cycle 1961–1972, the latter being of apparently rather average solar activity as judged by the mean sunspot numbers. Most of the particles under consideration normally arrive in the polar regions. Line *b* represents the frequency distribution when the event energy density is averaged over the Earth's surface; SN γ-flash denotes the frequency distribution of energy deposition from the gamma-ray flash from Supernovae at 10 pc. SNR (3 yr) and SNR (all time) represent energy deposition over a 3-year period, and integrated over the whole time, respectively, from protons when the Earth is immersed in a Supernova remnant. P is a probability and ε the energy density.

As it has been shown by Crutzen *et al.*,[61] a prominent effect is a destruction of the ozone layer by nitrogen oxide NO produced after ionization of the stratosphere, and the incident proton energy necessary to reach the appropriate levels in the stratosphere is about 30 MeV. Thus, an energy threshold of 20 MeV in Fig. 23 is only a little low for the necessary limit. In spite of an evident disparity in the absolute frequencies, $P(>\varepsilon)$, the slopes of the variations are very similar in the two periods. There seems to be evidence for an empirical power law for $P(>\varepsilon)$ over seven orders of magnitude. The authors suggested that such a distribution can probably be extended by at least several magnitudes more. Anyhow, one can clearly see that among the bursts at a given energy density, solar energetic particles in the range of 20–100 MeV drastically exceed in occurrence rate such an exotic source of radiation as a Supernova remnant.

These conclusions, however, have been seriously questioned by Mullan and Kent.[248] They argued against the proposed extrapolation[418] of the frequency distribution function of solar flares to time intervals of the order of 10 years. Mullan and Kent[248] proposed that the power-law spectra, which have been fitted by Wdowczyk and Wolfendale[418] to the SCR data, in fact, could not be extended to arbitrarily high energies. Instead of this, the spectra fall off rapidly beyond the last data point. In their discussion, Mullan and Kent[248] refer to certain similarities in the energy distribution functions obtained by Rosner and Vaiana[303] for three different classes of flaring objects: solar X-ray bursts, optical flares in dwarf M stars of spectral class dMe, and X-ray bursts from a cosmic X-ray source (burster) MXB 1730–335. In all three cases, there seems to be a range of flare energies, E, in which the flare frequency, $f(>E)$, can be fitted by a power law in E.

Rosner and Vaiana[303] developed a general model for flaring in which stored energy is built up in a short time scale, and the rate of energy storage, dE/dt, is assumed to be proportional to the energy already stored, $dE/dt = aE$. The release of the stored energy is thought to constitute the flare event. In this context, Mullan and Kent[248] proposed the following physical argument for a rapid cutoff of the flare frequency distribution for the Sun at about 11 years.

The point is that solar flares energies are derived, ultimately, from the toroidal magnetic field which is created inside the Sun by the action of solar differential rotation on the poloidal field. It is known, however, that after 11 years elapsed, the poloidal and toroidal fields reverse sign, the toroidal field having been decreased to zero. From this point of view, each 11-year cycle begins with an emptying out of the energy reservoir.

This suggests that the equation derived by Rosner and Vaiana[303] for the amount of stored energy $E(t) = E_0[\exp(at) - 1]$ is applicable only up to a maximum time of approximately 11 years. Hence, the frequency distribution $f(E) \sim E^{-\gamma}$ applies as long as f^{-1} does not exceed 11 years. Therefore, in the opinion of Mullan and Kent,[248] extrapolation of the power law behavior beyond 11 years is not valid, and ancient catastrophes should not on this account be related to extremely high level of solar activity.

12.2. *Long-term variations of solar particle fluences*

Solar activity follows a somewhat irregular 11-year cycle. There are indications both for longer cycles and for long quiescent periods (such as Maunder minimum from about 1640 to 1710). Most of the solar and interplanetary energetic particles are produced intermittently, either in solar flares or in coronal mass ejections (CME's) followed by fast interplanetary shocks. In fact, most of the large particle events are due to the latter process (see, e.g. Ref. 121). Interrelationships among the processes associated with flares and CME's have recently been reviewed by Cane.[419] Proton fluxes at MeV energies at 1 AU vary by at least 7 orders of magnitude. With increasing energy, the events become rarer and shorter and the relatively quite periods longer, but the extreme variability remains.

Many years ago, Wdowczyk and Wolfendale[418] addressed the question on the long-term frequency of large solar energy releases and their possible effects, compared with other catastrophic events. The main body of their evidence appears still valid, although some details have changed. The very flat integral power-law fits (logarithmic slope around -0.5) suggest that several dramatic solar energy releases should be expected in geologically short times, if the trend continues. One has to take into account, however, that events with low-energy fluences are identified less efficiently. And that the slope might become steeper with increasing fluence (energy fluence is the energy flux integrated over the duration of an event). The long-term extrapolation depends critically on the functional form chosen. One possibility is the log–normal model of Feynman *et al.*,[96] which has been widely used for short-term risk analysis of manned and unmanned space missions. They based their interplanetary fluence engineering model "JPL 1991" on IMP and OGO fluence data measured between 1963 and 1991 for proton fluences above five limiting energies.

Extrapolating their highest energies (> 60 MeV) fit to long time scales, Kiraly and Wolfendale[155] obtained some new interesting estimates. It turns out that while the highest fluence measured up to now (in about 30 years) was 3×10^9 cm^{-2}, one would expect in 1 My a few events above 10^{12} cm^{-2}, and in 100 My a few above 10^{13} cm^{-2}. This is far less than one would expect from flat slopes found by Wdowczyk and Wolfendale,[418] but probably more realistic. Thus, the largest solar particle events in geological history should have been not more than 10^3 to 10^4 times larger than those detected so far, giving rise to only moderate "energetic particle catastrophes." One might suspect that the time dependence in the efficiency of the magnetospheric protective shield considerably enhances the dangers. This might be the case if the fluence distribution decreases very fast on the high end (faster than the log–normal fit). If, however, the decrease is consistent with the above model, then the shorter periods, when the strength of magnetosphere is anomalously low, probably do not allow sufficiently large particle enhancements to occur with high enough probability.

12.3. *Cosmic rays in terrestrial radiation environment*

Short-term SEP observations, of course, cannot give an exhaustive answer to the important question on long-term particle fluence distributions in the near-Earth radiation environments. In this context, Kiraly and Wolfendale,[155] in addition to solar particle effects, considered also a long-standing and intriguing problem of the Supernova explosions. A Supernova explosion should occur very rarely close enough to the Earth (e.g. once in about 10^8 years at a distance of 10 pc or less) to have a substantial effect on terrestrial life. A prompt optical and UV flash would increase atmospheric ionization even from larger distances, but that first flash is unlikely to cause a lasting effect. X- and gamma-ray radiations, arriving somewhat later, would be mostly absorbed in the atmosphere, and very little would penetrate to ground level.

Although very energetic cosmic rays might arrive within a few years after the light-flash, their energy content would be small, and an important effect on life is unlikely. The main component of cosmic rays would arrive thousands or tens of thousands of years later, probably together with the shock. The shock might push back the solar wind and set the Earth more open for direct effects, but the atmosphere would still effectively protect life against direct radiation increases — even if cosmic ray fluxes at ground level increased by a factor of ten or so for a few hundred or thousand years. Indirect effects through atmospheric chemistry and ozone destruction, followed by some ecological chain reactions, might be more important.

Very large fluctuations in solar activity, mainly if combined with a reduction of terrestrial magnetic field, might perhaps give an equally or even more plausible explanation for some of the mass extinctions.[418] However, as suggested by Clark *et al.*,[52] the Supernova scenario is certainly one of the possibilities. A recent, detailed discussion of the expansion of the Supernova ejecta and shock, and possible isotopic signatures in terrestrial geological archives was given by Ellis *et al.*[83] One important point is that Supernova explosions might contribute not only to radiation and energetic particles, but also to dust grains, which may or may not survive atmospheric entry. If they do and are preserved as spherules, their isotopic composition might be checked for Supernova signatures.

Apart from Supernovae of the distant past, a search from recent nearby Supernovae is also of considerable interest. Cosmic rays might hold the key for such discoveries. Although at present cosmic rays are surprisingly isotropic and their energy spectra are smooth up to about 10^{14} eV, some increase of anisotropies and a rather peculiar spectral behavior is experienced in the spectral "knee" region at above 10^{15} eV, where the spectrum becomes steeper. Erlykin and Wolfendale[87] have analyzed the situation, and found some evidence for a substantial single-supernova contribution over and above the smooth background due to a large number of earlier and more distant Supernovae.

13. Archaeology of Solar Cosmic Rays

As known, the understanding of climate oscillations or trends in the past and their prediction for the future require the long-term sets of various astrophysical and geophysical data. In this context, as one can conclude from the above considerations, there are of a certain interest also the data on long-term trends and cyclic variations in the SPE occurrence rate, spectra and SCR fluxes as a function of the level of solar activity. Direct methods, however, do not permit one to establish the characteristics of the cosmophysical and ecological processes over a large time scale, excepting, probably, for the sunspot number variations observed since 1749. To solve these problems one has to use indirect methods of extracting the data from the physical "eyewitnesses" of the past which were capable not only of recording phenomena, but of retaining the relevant information in their memory in its original form.

13.1. *Cosmogenic isotopes in extraterrestrial objects*

One of the "eyewitnesses" of such kind are cosmogenic isotopes, produced in galactic and solar cosmic ray interactions with the material of the Moon and planets, meteorites, cosmic dust and the Earth's atmosphere. In particular, isotopic studies of early Solar system objects in primitive meteorites have revealed the presence of about a dozen short-lived nuclides with half-life ranging from 10^5 to 10^8 years at the time of formation of these objects (see, e.g. Ref. 122, and references therein). The nuclides with relatively short half-life (in millions of years, or Ma), such as ^{41}Ca (0.1 Ma), ^{26}Al (1.5 Ma) and ^{10}Be (1.5 Ma), must have been produced shortly before or during the very early stages of the formation of the Solar system. Two plausible sources are proposed for these nuclides; they could be freshly synthesized stellar material injected into the protosolar cloud at the time of its collapse or they are products of interactions of SEP's with gas and dust in the solar nebula.

Cosmic ray sources and mechanisms of cosmogenic isotope production in the Earth's environment are represented schematically in Fig. 24. The most detailed data available presently on the variations of the cosmic ray flux in the past were obtained by studying the ^{14}C and ^{10}Be isotopes produced in the Earth's atmosphere (see, e.g. Ref. 160). They are the radioisotopes with the highest atmospheric production rate (2.2 and 0.02 atoms cm^{-2} s^{-1}, respectively) of all long-lived isotopes (with a half-life $T_{1/2} \geq 100$ years).

The major source for the radiocarbon is the reaction of the capture of thermal neutrons released in cosmic ray interactions in the atmosphere by nitrogen, $^{14}\mathrm{N}(n,p)^{14}\mathrm{C}$. Beryllium-10 is produced in spallation reactions of nitrogen and oxygen by cosmic rays. These isotopes are rapidly oxidized to form CO_2 and BeO and enter subsequently into various geochemical and geophysical processes. Carbon dioxide distributes itself throughout the global carbon exchange system while beryllium oxide becomes attached to atmospheric aerosols and precipitates onto the Earth's surface with them. Thus, the samples used to study these isotopes are essentially different, namely, radiocarbon measurements which are primarily carried

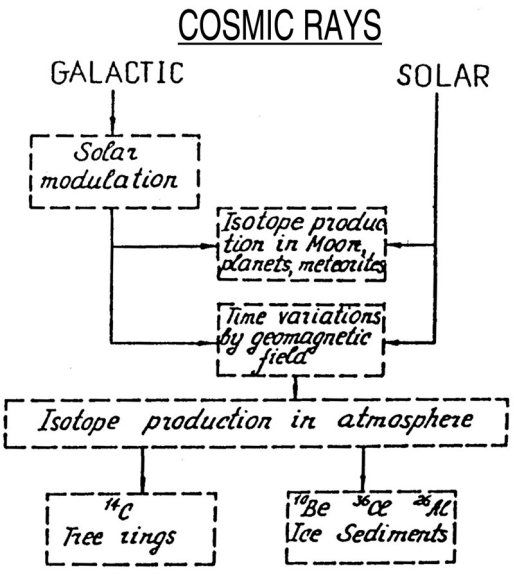

Fig. 24. Schematic representation of cosmic ray sources and cosmogenic isotope production mechanisms (after Ref. 160).

out on tree rings, whereas the ^{10}Be content is determined in polar ices and oceanic sediments (e.g. Ref. 29).

The high rate of ^{14}C production and comparatively short half-life time ($\sim$ 5730 years) permit one to use well-developed radiometric techniques (see, e.g. Ref. 68). The use of such techniques to measure ^{10}Be content in samples would involve formidable difficulties because of its low production rate and long life ($T_{1/2} \sim 1.5 \times 10^6$ y). Therefore, in this case one employs a more sophisticated and expensive method of accelerator mass-spectroscopy. Besides, one can use another possibility, for example, to choose different radionuclides in the analysis of long-term processes in the heliosphere, at the Sun, etc.

The most reliable series of data are compiled for the radiocarbon concentration over the last $\sim$ 10,000 years (e.g. Ref. 68). An essential difference in energy spectra makes it possible to discriminate between SCR and GCR effects in the production of radioactive isotopes of ^{14}C, ^{81}Kr, ^{26}Al, and ^{53}Mn in meteorites and lunar rocks, as well as to estimate average SCR fluxes and to determine their spectral form as far as $\sim 10^7$ years back. Thus, Bhandari and Bhattacharaya[37] used the data on the ^{26}Al content in lunar rocks to show that the spectrum of solar protons $\sim 1.5 \times 10^6$ years ago can be represented in the form $\sim \exp(-R/R_0)$, where $R_0 = 150$ MV is the characteristic spectrum rigidity. Then, the average proton flux with $E_p > 10$ MeV ($R > 143$ MV) is $\langle F \rangle = 150$–180 cm^{-2} s^{-1}, with an accuracy within 25%.

On the other hand, the values of $\langle F\,(> 10$ MeV$)\rangle$ in the same units obtained by Goswami *et al.*[123] using a large amount of data on the content of cosmogenic

isotopes in lunar rock are as follows: $\sim 2 \times 10^2$ (for $\sim 2 \times 10^5$ years, ^{81}Kr); ~ 125 (for $\sim 10^6$ years, ^{26}Al); ~ 70 (for $\sim 10^7$ years, ^{53}Mn). Similar estimates have been obtained for $\langle F\,(> 10\ \text{MeV})\rangle$ from solar flares in the last three solar cycles: 4×10^2 (cycle 19), ~ 90 (cycle 20), and ~ 65 (cycle 21). The SCR rigidity spectrum also varies significantly. If the spectrum is represented in the form $\sim \exp(-R/R_0)$, then $R_0 = 100 \pm 20$ MV for the last $\sim 10^6$ years and $R_0 = 48 \pm 22$ MV for the years 1965–1982.

The data obtained suggest considerable long-term variations of SCR flux and its effective rigidity. Thus, the average SCR flux was steadily increasing for the last 10^7–10^4 years (approximately by a factor 3), whereas the value of $\langle F\rangle$ for the last three solar cycles, on the contrary, became nearly 6.5 times smaller. Goswami *et al.*[123] believe that these variations of SCR parameters may be caused by two factors: (1) long-term variations of solar activity with characteristic periods of $\sim 10^5$–10^6 years; (2) giant flares that produce SPE with the proton fluence of $F_s \sim 10^{13}$ cm^{-2} (e.g. flares of the 23 February 1956 type).

Both causes are plausible, though hypothetical (see Ref. 228). For example, the concentration of cosmogenic isotopes, ^{10}Be, ^{26}Al, and ^{53}Mn in ocean and lake sediments cores, in meteorites and lunar rocks shows that 2–4 million years ago their production rate was 4 times as high as nowadays.[156] On the one hand, this might be due to an increased GCR flux as a result of Supernova outburst,[406] to the geomagnetic field inversion[68] and/or to an extremely low GCR modulation during the inversion of the global magnetic field of the Sun.[370] In turn, a weak GCR modulation may be indicative of a lowered solar activity. On the other hand, the effect noted by Kocharov[156] might as well be the result of increased solar activity that is characterized by growing flare production and SPE intensity. In other words, the level of solar activity in the ancient times might have been quite different from the present-day situation.

In this context, it is of great interest to study the "ancient" acceleration processes which took place during the early evolution stage of the Sun when it was an active young star of the T-Tauri type, with a strong solar wind and a flare activity 10^3–10^5 times as high as at present. With this purpose, Caffee *et al.*[41] used a high-sensitivity mass-spectrometer to measure the content of spallogenic noble gases (^{21}Ne and ^{38}Ar) in individual grains from the gas-rich meteorites. The grains containing the track of solar flare-generated heavy ions proved to be enriched with ^{21}Ne and ^{38}Ar compared with the grains without the tracks. The data on meteorites Murchison (the carbonaceous chondrite), Weston and Fayeteville (H-chondrites), and Kapoeta (achondrite) were analyzed. The contents found of the stable ^{21}Ne and ^{38}Ar imply a (100–200) $\times 10^6$-year exposure to galactic cosmic rays near the surface. From other data it follows, however, that the exposure did not exceed 10^6 years. The authors have concluded that the > 10 MeV proton fluence had to be some 10^{16}–10^{18} cm^{-2}, which correspond to a $\sim 10^3$ times as high irradiation by SCR flux for $\sim 10^5$ years during the T-Tauri stage as the irradiation during the last 10^6 years.

As noted by Goswami and Marhas,[122] up to now there was a general consensus for a stellar source for the short-lived nuclides present in the early Solar system. But recent discovery of ^{10}Be in the early solar system objects revived the energetic particle production model because ^{10}Be is not a product of stellar nucleosynthesis. These authors have found evidence of the presence of ^{10}Be in the early solar system from studies of primitive meteorites. Interaction of SEP's (in the range of tens to hundreds of MeV) from the active early Sun with gas and dust present in the solar nebula is considered to be the most plausible source of this nuclide. On the other hand, the presence of ^{10}Be in meteorite samples is often accompanied by other short-lived nuclides (e.g. ^{26}Al) for which a stellar origin is generally favored. The studies by Goswami and Marhas[122] show that ^{10}Be is also present in the samples in which ^{26}Al is below detection level. This suggests that the primary source of these two nuclides cannot be the same. Their results place limits on the spectral shape and flux of energetic particles from the proto-Sun, such that production of ^{10}Be is not accompanied by significant production of ^{26}Al. Finally, they concluded that the SEP's from the early Sun were characterized by a hard spectrum and the particle flux was more than 10^3 times the average flux from contemporary Sun.

13.2. *Proton events and nitrate abundance in the polar ice*

Thus, one can see that radiochemical methods, alongside a new "nitrate method" noted in Subsec. 3.1, are very effective tool for solar cosmic ray research. Although the analysis of tree rings, meteorites, returned lunar samples, oceanic sediments, etc. is a more mature technology than the more recent analysis of polar ice cores[76] for the determination of historical proton events, each of these technique can be used to improve our knowledge of SPE occurrence prior to the middle of 20th century and of some important features of solar cosmic rays. In the whole, this branch of space physics may be called "archaeology of solar cosmic rays" (see also Ref. 320).

As an interesting example, it is worth to mention a possibility to obtain upper limit of total energy induced by solar flare protons relying upon the data of nitrate abundance in the polar ice. Crucial point of such an approach is a quantitative correlation between the abundance of the nitrate NO_3 and total energy delivered to solar protons in each solar flare in the past. Figure 25 shows distribution of SEP events for solar cycles 19–21 on the > 10 MeV proton energy fluences ε.[420]

The circles in Fig. 25 represent the occurrence rate of SEP events with proton energy fluence above ε estimated by available observational data since 1955 (dotted–dashed line). In turn, the crosses indicate the distribution of energy fluences averaged over the 3-month periods by the nitrate data of Dreschhoff and Zeller[76] from Kansas University (dashed line). According to the data on cosmogenic isotope abundances in lunar samples,[421] average flux of the > 10 MeV solar protons for the past million years is 100 ± 25 cm^{-2} s^{-1} that is close to the value obtained for the last several solar cycles. Therefore, Gladysheva *et al.*[420] concluded that dotted–dashed line does not correspond to a real distribution of SEP events in the past.

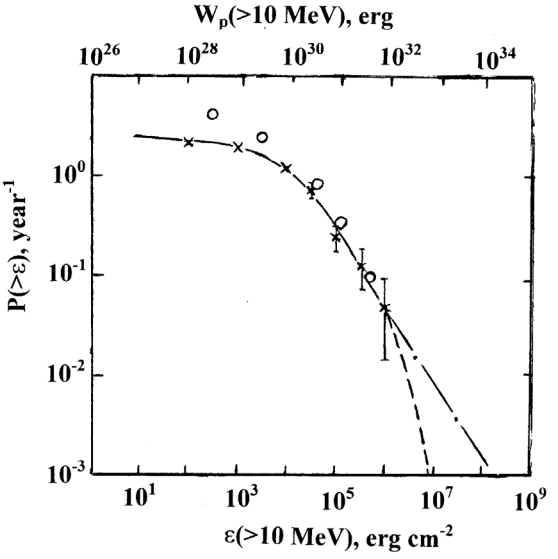

Fig. 25. Integral distribution of solar proton events in solar cycles 19–21 as a function of the > 10 MeV proton energy fluence ε.[420] The circles represent the occurrence rate of proton events with total energy flux greater than ε (dotted–dashed line); the crosses correspond to the seasonal distribution of energy fluence (averaged over the 3-month period, dashed line). The dashed line only could be in agreement with available data on the nitrate content in the polar ices.

On the contrary, the dashed line only could be in agreement with available data on the nitrate content in the polar ices.

The abundance of the nitrate can be measured with the time resolution of about three months which is better than in the case of radiocarbon measurements. As one can see from Fig. 24, averaging for 3 months practically does not change the distribution of the most powerful events. The measurements of the nitrate content for the last cycles of solar activity show that the threshold of sensitivity of this method is at the level of $\varepsilon = 3 \times 10^5$ erg cm^{-2}.

13.3. *Restrictions for proton fluence in the past*

More recently, Peristykh and Damon[422] presented evidence of intense solar proton events in the last decade of the 19th century (solar cycle 13) based on diverse solar and geophysical data. One of those events (15 July 1892) was observed as remarkable solar disturbance (white-light flare). Besides white-light flares, there were numerous storm sudden commencements (SSC) of high amplitude (> 40 nT), noticeable enhanced annual sums of the *aa*-index, and more frequent observations of very bright auroras in North America. The event of 15 July 1892 is also revealed from data on nitrates in polar ice and cosmogenic isotopes in terrestrial archives. Up-to-date data on the rate of giant flare occurrences over long time scale and maximum fluences of solar protons are presented in Sec. 12.

On the other hand, as noted by Dreschhoff and Laird,[77] in the past decades considerable attention of researchers has been directed to toward the delineation of a signal of discrete ionization episodes from energetic solar proton events (SPE) inducing large impulsive nitrate anomalies as indicated by a short-term rise in nitrate concentration in the ice (e.g. Ref. 76). The injection of highly energetic protons into the polar stratosphere and their ability to ionize nitrogen and oxygen will generate oxides of nitrogen. Nitrate ions (NO_3^-) from these events superimposed on a nitrate "background" from terrestrial sources, ultimately will be deposited in thin layers in polar ice. There is also some evidence for stratigraphic record of Supernovae (SNe) in polar ice. In particular, early data from a South Pole led to the suggestion of a correlative signal between nitrate anomalies of about 1 year duration and the dates of historical, nearby Supernovae: SN 1006 (30 April 1006), Crab (4 July 1054), SN 1181 (6 August 1181), Near Vela ($\sim$ 1300), Tycho (6–11 November 1572), Kepler (1 November 1604), and Cassiopeia A ($\sim$ 1700, or 1680, or 1667?).

Large stratospheric ionization events can occur from the energy deposition of gamma-rays from SNe. The gamma-rays are capable of penetrating the Earth's atmosphere to an altitude of 27–32 km before Compton scattering begins to convert their energy to that of ionizing electrons, which ultimately contribute to the production of nitrate. However, one interesting problem arises to distinguish prehistoric SNe-induced nitrate anomalies from those generated by large solar proton events. And this task may be difficult one.

In fact, it has been shown that nitrate anomalies with amplitudes of several standard deviations above the mean, which are superimposed on a seasonal background, originate from major high-fluence solar proton events (e.g. Ref. 76). A total of 125 large fluence (> 30 MeV, $> 1.0 \times 10^9$ sm^{-2}) SPE's have been identified in the 430-year nitrate record from the Greenland ice sheet.[205,206] Although the more frequently occurring SPE complicate identification of occasional SNe in ice cores, nevertheless, there is a significant probability that three enhancements in the 430-year, high resolution nitrate record do have their origin in large stratospheric ionization events from SNe. Of particular interest is in this strictly observational study, is the detection of the closely occurring SNe of Tycho (1572) and Kepler (1604) with the correct time separation. Our attempt to associate these two events within the population of impulsive nitrate events with the SN origin of Kepler and Tycho is mostly based on the time association.

The nitrate enhancement dated 1700 may very well represent the signal of Cassiopeia A (Cas A), although previously it has been interpreted as part of a series of solar proton events close to the termination of the Maunder minimum.[206] This observational study[77] made use of the best available to date, two independent data sets from Antarctica (South Pole and Vostok stations) for the last 1200 years and, in particular, the data set from Greenland (Summit station) covering the last 430 years (Fig. 26).

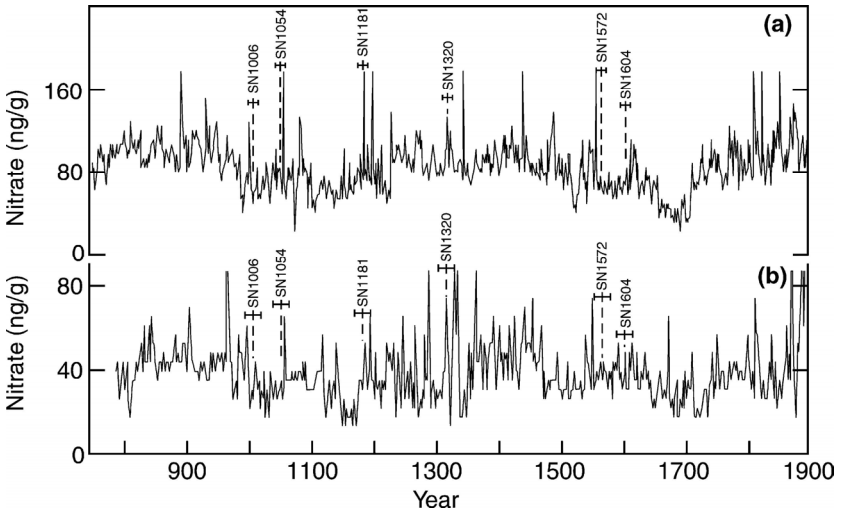

Fig. 26. Nitrate concentration in the South Pole core representing $\sim$ 1200 years (a), and the time equivalent upper part of the Vostok core (b). Historical SNe are indicated for the respective nitrate anomalies. Minimum estimated errors ($\sim$ 10 years for South Pole record; $\sim$ 30 years for Vostok record) are indicated by error bars.[77]

The latter ultrahigh resolution, continuous nitrate sequence from very thin layer of ice provides highly detailed information about the ionization history of the polar stratosphere, induced by energetic solar protons and/or X-rays and by gamma-rays from SN remnants. If longer time sequences can be obtained, statistical significance will be increased, especially if some SNe events to occur within the periods of extended low solar activity. Furthermore, separating this type of signal will greatly be helped by high resolution data of cosmogenic isotopes, i.e. ^{10}Be in ice cores (e.g. Ref. 29) and ^{14}C from single-year tree rings (e.g. Ref. 62).

Probable interference from SPE complicates the interpretation of SNe frequency in ice cores, however, it may be possible to separate these two sources of nitrate in future studies. It is estimated that the historical SNe make up only the small fraction ($\sim$ 20%) of those occurred in this time frame, because the rest are simply obscured by the dust which pervades our Galaxy. Nevertheless, as pointed by Gaisser *et al.*,[108] energetic photons, produced in powerful astrophysical processes outside our Solar system, impinge on the Earth's atmosphere and produce showers and cascades of secondary radiation capable of ionizing the neutral atmosphere at lower layers. The probability of contributions to the ionization signal from other, but less well understood sources such as γ-ray bursts will have to be considered in the future, particularly since some unusual lower-energy γ-ray bursts may be more abundant than previously thought. In summary Dreschhoff and Laird[77] believed that the data presented here can contribute to the important astrophysical question of whether photon-induced ionization from SNe exist at detectable levels in the Earth's geochemical records.

14. Summary and Conclusions

As noted by John Simpson,[329] ground-level monitoring of the neutron and muon components of GCR and SCR for several decades have played and important role in developing concepts of the physics of near-Earth space, theory of solar wind and interplanetary electrodynamics. In particular, continuous surface observations have led to discovery of the heliosphere; set constraints on solar flare particle acceleration models and flare energetics; established the concepts and tests of solar modulation of GCR.

In addition, surface observations of galactic and solar cosmic rays, when combined with spacecraft measurements, have discovered traveling collisionless shocks as the origin of Forbush-decreases; demonstrated the heliocentric origin of the 11-year solar modulation cycle; contributed to an understanding of the active Sun. As to solar activity and SCR themselves, it should be noted that in solar physics the observational restrictions (constraints) are more certain and rigid than in stellar physics as a whole.

In the above sections we reviewed the data on main temporal, spectral and pitch-angle characteristics of relativistic SCR at the Earth's orbit and near the Sun over the period of 1942–2006. Several key features of different acceleration mechanisms in solar flares (particle energy gain and release rates in the form of SCR, maximum energy of accelerated particles and their source(s) location in the solar atmosphere, SCR spectrum peculiarities, etc.) are analyzed. Copious observational data on solar gamma rays, high-energy flare neutrons, charge states and element abundances of accelerated SEP's, together with some involved problems of solar physics (e.g. production of the neutrinos in solar flares), are considered in general context of fundamental problem of acceleration of charged particles in space (astrophysical) conditions.

Based on recent observational and statistical findings, the problems of initial acceleration of SCR and their high-energy limits are discussed in the framework of reconnection theory of the flare. It is shown that the distribution functions of solar flare events on various parameters (peak fluxes and/or energy fluences in X-ray and radio wave bursts, in proton and electron emissions, etc.) allow the interpretation of some scale and time flare parameters in terms of expected threshold effects. However, these functions are still deficient to evaluate the relative share of different emissions in global energy budget of the flare.

In this context, a more promising attempt is to derive a direct ratio between the quantity of accelerated protons and total flare energy within the framework of a certain acceleration model. It is argued that an absolute threshold for proton production does not exist, however, the flux and threshold energy of accelerated protons overcoming Coulomb loss maximum ($\sim$ 1–10 MeV), in fact, may depend heavily on the global output of flare energy.

Due to the lack of trustable data on charge state distribution of solar energetic ions in a given solar event, at a given time, and for different ions, several models

have been developed to predict their charge evolutions. Main differences among the models are the kind of cross-sections employed, and whether charge interchange, if occurs, takes place, during or after acceleration. Though, in some events the observed charges can be representatives of local matter, there exist some inferences indicating that this cannot be a systematic situation. The advantages of the high-energy cross-section model (HECSM), namely "escape," among others, are following: (1) it provides a test of the model that could be done when data at very low energies will be available, that is, charge state should be lower than the local thermal charge of the ion of the presumably source (determined by other means, γ, X-rays, etc); (2) it is an analytical model with the subsequent computational economy and direct physics content, that in contrast with other models, it is within the context of the dictum, that the simplest description of a physical phenomenon is often the best approach to understand the underlying physics involved in the phenomenon.

A concept of multiple accelerations processes at/near the Sun turned out to be very promising and fruitful for understanding some peculiarities of SEP's production. In particular, a number of evidences were obtained that two relativistic components (prompt and delayed ones, PC and DC) may exist in certain solar proton events (SPE). What is the physical reason for the formation of two particle populations? We consider two possibilities: (1) a magnetic bottle (and/or coronal shock) interacting with extended magnetic arcade (or streamer) at high level in the corona, and (2) a combination of two acceleration processes, namely, (a) acceleration directly associated with the flare in the lower corona, and (b) acceleration by a supercritical shock driven by the associated CME. The particle acceleration is realized by direct electric fields produced in the processes of magnetic reconnection (source I), and/or by stochastic or diffusive shock mechanisms in the extended coronal structures (source II).

A model of two acceleration sources is suggested to interpret the results of observations for several largest relativistic SPE's, 23 February 1956, 20 January 2005, 29 September 1989 and some others. In the first case, maximum energy of solar protons about 65 GeV was recorded, meanwhile a pertinent theoretical estimate is about 250 GeV. During the event of 29 September 1989, solar flare protons with the energies above 100 GeV seem to be observed (for the first time) by underground muon telescopes. Some evidences exist and imply that relativistic protons with the energies of several hundreds GeV can be produced in the extended coronal structures. Very low intensity of the multi-GeV protons, significant steepening of their spectrum at extremely high energies, and galactic cosmic ray background, all three factors together prevent a strict determination of the upper capacities of solar accelerators. Muon measurements with a high angle resolution by nonstandard surface and underground detectors are needed to advance in the range of extremely high-energy solar cosmic rays.

In general, we emphasize the close relations, common features, similarities and/or analogies between particle acceleration processes at the Sun and other stars, in different spaces and astrophysical plasmas, between the processes in the heliosphere

and beyond, between magnetic fields, astroparticles, MHD and shock waves in different astrophysical objects. Also, there are many common research methods and theoretical models applied in solar physics and astrophysics. The authors believe that the information accumulated from 65 years of the studies of solar energetic particles will be very useful in all mentioned fields of space physics.

Acknowledgments

The authors are very indebted to all researchers whose data, figures and other materials have been used in this paper. We also thank many colleagues from international cosmic ray and solar physics communities for hot discussions, impartial criticism and valuable comments that help us to improve the text. Our special thanks are to the editors and editorial staff of the International Journal of Modern Physics A for their kind attention, thorough examination of the manuscript and invaluable technical help. This work has been supported in part by the CONACyT, Mexico (project 45822 PERPJ10332), Russian Foundation for Basic Research (projects 02-02-39032, 03-02-96026, 04-02-26806, 05-02-39011, 07-02-01405), Federal Purpose Scientific and Technical Program (Section I, Project 4), Program of the Russian Academy of Sciences "Non-Stationary Phenomena in Astronomy" (project of IZMIRAN "Non-Stationary Phenomena at the Sun"), and by two President's Grants of Russian Federation (project SS-1145.2003.2 and SS-8499.2006.2).

References

1. A. Achterberg, *Astron. Astrophys.* **97**, 259 (1981).
2. J. H. Adams and A. Gelman, *IEEE Trans. Nucl. Sci.* **31**, 1212 (1984).
3. M. Aglietta *et al.*, Search for neutrinos from solar flares with the Mont Blanc detector, in *Proc. 22nd Int. Cosmic Ray Conf.*, Dublin, Ireland (1991), Vol. 3, pp. 728–731.
4. V. V. Akimov *et al.*, Observation of high energy gamma-rays from the Sun, *Proc. 22nd Int. Cosmic Ray Conf.*, Dublin, Ireland (1991), Vol. 3, pp. 73–76.
5. V. V. Akimov *et al.*, *Solar Phys.* **166**, 107 (1996).
6. S. T. Akinyan *et al.*, *Catalogue of Solar Proton Events 1970–1979*, ed. Yu. I. Logachev (Nauka, Moscow, 1983).
7. V. V. Alexeenko, A. B. Chernyaev, A. E. Chudakov, N. S. Khaerdinov, A. M. Semenov, J. Szabelski and A. V. Voevodsky, 29 September 1989 GLE (Ground Level Enhancement) at Baksan Air Shower Array (BASA), *Proc. 23rd Int. Cosmic Ray Conf.*, Calgary, Canada (1993), Vol. 3, pp. 163–166.
8. E. N. Alexeyev, V. N. Zakidyshev and S. N. Karpov, *Geomagn. Aeronomy* **32**, 189 (1992).
9. E. N. Alexeyev and S. N. Karpov, *Geomagn. Aeronomy* **34**, 143 (1994).
10. L. H. Aller, *Abundance of the Elements* (Interscience Publ., New York, 1961).
11. A. I. Andreev, L. N. Efimov, L. N. Samoznaev, I. V. Chashei and M. K. Bird, *Solar Phys.* **176**, 387 (1997).
12. I. V. Arkhangelskaya, A. I. Arkhangelskij, Yu. D. Kotov, S. N. Kuznetsov and A. S. Glyanenko, The flare catalogue in low-energy gamma-ray range based on the AVS-F instrument data onboard the Coronas-F satellite in 2001–2005, *Astronomicheskii Vestnik* (*Astronomy Herald*), Vol. 40, No. 2 (Nauka, Moscow, 2006), pp. 150–159 (in Russian).

13. I. V. Arkhangelskaya, A. I. Arkhangelskij, Yu. D. Kotov, S. N. Kuznetsov and A. S. Glyanenko, Gamma-ray radiation of solar flares in October–November 2003 according to the data obtained with the AVS-F instrument onboard the CORONAS-F satellite, *Astronomicheskii Vestnik* (*Astronomy Herald*), Vol. 40, No. 4 (Nauka, Moscow, 2006), pp. 331–343 (in Russian).
14. T. Armstrong, National Space Science Data Centre (NASA/GSFC), Data Set 73-078A-08G-IMP8 H and J (1993).
15. M. Arnaud and J. Raymond, *Astrophys. J.* **398**, 394 (1992).
16. M. J. Aschwanden, *Space Sci. Rev.* **101**, 1 (2002) [Also published by Kluwer Academic Publishers (2002) (ISBN 1-4020-0725-6)].
17. V. Aushev, V. Antonova, A. Belov, E. Eroshenko, O. Kryakunova and A. Struminsky, Search for solar neutron events in Alma-Ata NM data, *Proc. 26th Int. Cosmic Ray Conf.*, Salt Lake City, USA (1999), Vol. 6, pp. 50–53.
18. J. N. Bahcall, *Neutrino Astrophysics* (Cambridge University Press, Cambridge, 1990).
19. D. B. Barbosa, *Astrophys. J.* **233**, 383 (1979).
20. A. F. Barghouty and R. A. Mewaldt, *Astropys. J. Lett.* **520**, L127 (1999).
21. A. F. Barghouty and R. A. Mewaldt, *AIP Conf. Proc.* **528**, 71 (2000).
22. G. A. Bazilevskaya, *Adv. Space Res.* **35**, 458 (2005).
23. G. A. Bazilevskaya and V. S. Makhmutov, *Geomagn. Aeronomy* **28**, 169 (1988).
24. G. A. Bazilevskaya and A. K. Svirzhevskaya, *Space Sci. Rev.* **85**, 432 (1998).
25. G. A. Bazilevskaya, Yu. I. Stozhkov and T. N. Charakhchyan, *J. Exp. Theor. Phys. Lett.* **35**, 273 (1982) (in Russian).
26. G. A. Bazilevskaya *et al.*, *Catalogue of Energetic Spectra of Solar Proton Events 1970-1979*, ed. Yu. I. Logachev (Nauka, Moscow, 1986), p. 235.
27. G. A. Bazilevskaya *et al.*, *Catalogue of Solar Proton Events 1980-1986*, ed. Yu. I. Logachev (World Data Center B-2, Moscow, 1990), Part I, p. 160, Part II, p. 204.
28. G. A. Bazilevskaya *et al.*, *Geomagn. Aeronomy* **43**, 442 (2003) (in Russian).
29. J. Beer, J. M. Raisbeck and F. Yiou, Time variations of ^{10}Be and solar activity, in *The Sun in Time*, eds. C. P. Sonnett, M. S. Giampapa and M. S. Mathews (The University of Arizona Press, Tucson, 1991), pp. 343–359.
30. P. Beland and D. A. Russel, *Nature* **263**, 259 (1976).
31. A. Belov, I. Chertok and A. Struminsky, Time evolution of solar proton energy spectra at the Earth's orbit and possibility of multi-step particle acceleration, *Proc. 24th Int. Cosmic Ray Conf.*, Rome, Italy (1995), Vol. 4, pp. 127–130.
32. E. G. Berezhko, S. I. Petukhov and S. N. Taneev, *Izvestiya RAN, Phys. Ser.* **64**, 339 (2001).
33. E. G. Berezhko and S. N. Taneev, Solar energetic particle spectra produced by shocks in solar corona, *Proc. 28th Int. Cosmic Ray Conf.*, Tsukuba, Japan (2003), Vol. 6, pp. 3343–3346.
34. E. G. Berezhko and S. N. Taneev, *Astron. Lett. Russia* **29**, 601 (2003).
35. V. S. Berezinsky, S. V. Bulanov, V. A. Dogel, V. L. Ginzburg and V. S. Ptuskin, *Astrophysics of Cosmic Rays* (Elsevier Science Publishers, Amsterdam, 1990).
36. H. D. Betz, *Rev. Mod. Phys.* **44**, 465 (1972).
37. N. Bhandari and S. Bhattacharaya, Shape of the solar flare proton spectrum in 10–100 MeV region in the past, *Proc. 14th Int. Cosmic Ray Conf.*, München, Germany (1975), Vol. 12, pp. 4245–4246.
38. R. D. Blandford, *Astrophys. J. Suppl.* **90**, 515 (1994).
39. D. J. Bombardieri, M. L. Duldig, K. J. Michael and J. E. Humble, *Astrophys. J.* **643**, 565 (2006).

40. S. V. Bulanov, L. V. Kurnosova, Ya. Yu. Ogulchansky, L. A. Razorenov and M. I. Fradkin, *Astron. Lett. Russia* **11**, 383 (1985).
41. M. Caffee, J. N. Goswami, C. M. Hohenberg and T. W. Swindle, Solar flare irradiation in meteorites provides evidence for an early active Sun, *Proc. 20th Int. Cosmic Ray Conf.*, Moscow, USSR (1987), Vol. 4, pp. 299–302.
42. A. G. W. Cameron, *Space Sci. Rev.* **15**, 121 (1973).
43. H. V. Cane, Are there two classes of solar energetic particle events?, *Proc. 27th Int. Cosmic Ray Conf.*, Hamburg, Germany (2001), pp. 311–314.
44. H. V. Cane, D. V. Reames and T. T. von Rosenvinge, *Astrophys. J.* **373**, 675 (1991).
45. H. V. Cane, W. C. Erickson and N. P. Presage, *J. Geophys. Res.* **107**, 1315 (2002).
46. H. V. Cane, T. T. von Rosenvinge, C. M. S. Cohen and R. A. Mewaldt, *Geophys. Res. Lett.* **30**, 8017 (2003).
47. H. Carmichael, Cosmic rays (instruments), *Annals of the IQSY*, Vol. 1 (MIT Press, Cambridge, MA, 1968), pp. 178–197.
48. J. Chen, T. G. Guzik and J. P. Wefel, *Astrophys. J.* **442**, 875 (1995).
49. M. L. Cherry *et al.*, Multiplicities and angular distributions of nucleus–nucleus interactions at SPS energies: Protons to lead, in *Proc. Sixth Conf. on the Intersections of Particle and Nuclear Physics*, Big Sky, Montana, AIP Conf. Proc., Vol. 412, ed. T. Donnelly (1997), pp. 253–258.
50. I. M. Chertok, Post-eruption particle acceleration in the corona: A possible contribution to solar cosmic rays, *Proc. 24th Int. Cosmic Ray Conf.*, Rome, Italy (1995), Vol. 4, pp. 62–65.
51. E. L. Chupp, Evolution of our understanding of solar flare particle acceleration: (1942–1995), in *High Energy Solar Physics*, AIP Conf. Proc., Vol. 374, eds. R. Ramaty, N. Mandzhavidze and X.-M. Hua (AIP, New York, 1996), pp. 3–31.
52. D. H. Clark, W. H. McCrea and F. R. Stephenson, *Nature* **265**, 318 (1977).
53. E. W. Cliver, Solar flare gamma-ray emission and energetic particles in space, in *High Energy Solar Physics*, AIP Conf. Proc., Vol. 374, eds. R. Ramaty, N. Mandzhavidze and X.-M. Hua (AIP, New York, 1996), pp. 45–60.
54. E. W. Cliver, D. J. Forrest, H. V. Cane, D. V. Reames, R. E. McGuire, T. T. von Rosenvinge, S. R. Kane and R. J. MacDowall, *Astrophys. J.* **343**, 953 (1989).
55. E. W. Cliver, S. W. Kahler and W. T. Vestrand, On the origin of gamma-ray emission from the behind-the-limb flare on 29 September 1989, *Proc. 23rd Int. Cosmic Ray Conf.*, Calgary, Canada (1993), Vol. 3, pp. 91–94.
56. E. Cliver, B. Klecker, M.-B. Kallenrode and H. Cane, *EOS Trans., AGU* **83**, 132 (2002).
57. C. M. S. Cohen, Solar energetic particle acceleration and interplanetary propagation, in *Proc. 28th Int. Cosmic Ray Conf., Invited, Rapporteur, and Highlight Papers*, Japan, Tsukuba (2003), Vol. 8, pp. 113–133.
58. A. H. Compton, E. O. Wollan and R. D. Bennet, *Rev. Scientific Instruments* **5**, 415 (1934).
59. J. L. Cramp, M. L. Duldig, E. O. Flückiger, J. E. Humble, M. A. Shea and D. F. Smart, *J. Geophys. Res.* **102**, 24237 (1997).
60. N. B. Crosby, M. J. Aschwanden and B. R. Dennis, *Solar Phys.* **143**, 275 (1993).
61. P. J. Crutzen, I. S. A. Isaksen and G. C. Reid, *Science* **189**, 457 (1975).
62. P. E. Damon, D. Kaimei, G. E. Kocharov, I. B. Mikheeva and A. N. Peristykh, *Radiocarbon* **37**, 599 (1995).
63. C. D'Andrea and J. Poirier, *Geophys. Res. Lett.* **32**, L14102 (2005).
64. R. Davis, Jr., in *Proc. 7th Workshop on Grand Unification* (*ICOBAN-86*), Toyama, Japan, ed. J. Arafune (World Scientific, Singapore, 1987), p. 237.

65. H. Debrunner, E. O. Fluckiger, E. Gradel, J. A. Lockwood and R. E. McGuire, *J. Geophys. Res.* **93**, 7206 (1988).
66. H. Debrunner, J. A. Lockwood and J. M. Ryan, *Astrophys. J.* **409**, 822 (1993).
67. L. Del Peral, M. D. Rodríguez-Frías, R. Gómez-Herrero, J. Rodríguez-Pacheco and J. Gutiérrez, *Astropart. Phys.* **17**, 415 (2002).
68. V. A. Dergachev, *Geomagn. Aeronomy* **34**, 433 (1994).
69. W. Dietrich and C. Lopate, Measurements of iron reach SEP events using the University of Chicago IMP-8 instrument, *Proc. 26th Int. Cosmic Ray Conf.*, Salt Lake City, USA (1999), Vol. 6, pp. 71–74.
70. W. Dietrich and C. Lopate, Determination of the ionic charge states of SEP's using the University of Chicago IMP-8 instrument, *Proc. 26th Int. Cosmic Ray Conf.*, Salt Lake City, USA (1999), Vol. 6, pp. 91–94.
71. H. W. Dodson *et al.*, *Catalogue of Solar Proton Events 1955–1969*, eds. Z. Svestka and P. Simon (D. Reidel Publ., Dordrecht, 1975).
72. L. I. Dorman, *Cosmic Ray Variations* (Gostekhteorizdat, Moscow, 1957) (in Russian) [English version: Transl. Techn. Doc. Liaison Office, Wright-Patterson Airforce Base, USA, 1958].
73. L. I. Dorman, Geophysical and astrophysical aspects of cosmic radiation, in *Progress in Elementary Particles and Cosmic Ray Physics*, Vol. 7, eds. J. G. Wilson and S. A. Wouthuysen (North-Holland, Amsterdam, 1963), p. 358.
74. L. I. Dorman and L. I. Miroshnichenko, *Solar Cosmic Rays* (Nauka (Fizmatgiz), Moscow, 1968), p. 468 (in Russian) [English edition for NASA by Indian National Scientific Documentation Center, Delhi, 1976].
75. L. I. Dorman and D. Venkatesan, *Space Sci. Rev.* **64**, 183 (1993).
76. G. A. M. Dreschhoff and E. J. Zeller, *Solar Phys.* **127**, 333 (1990).
77. G. A. M. Dreschhoff and C. M. Laird, *Adv. Space Res.* **38**, 1307 (2006).
78. S. P. Duggal, *Rev. Geophys. Space Res.* **17**, 1021 (1979).
79. V. M. Dvornikov and V. E. Sdobnov, *J. Geophys. Res.* **102**, 24209 (1997).
80. V. M. Dvornikov and V. E. Sdobnov, *Solar Phys.* **178**, 405 (1998).
81. J. A. Earl, Propagation of charged particle pulses immediately after injection, *Proc. 24th Int. Cosmic Ray Conf.*, Rome, Italy (1995), Vol. 4, pp. 293–296.
82. H. Elliot, The variations of cosmic ray intensity, in *Progress in Cosmic Ray Physics*, Vol. 1, eds. J. G. Wilson and S. A. Wouthuysen (North-Holland, Amsterdam, 1952), pp. 453–514.
83. J. Ellis, B. D. Fields and D. N. Schramm, *Astrophys. J.* **470**, 1227 (1996).
84. D. C. Ellison and R. Ramaty, *Astrophys. J.* **298**, 400 (1985).
85. A. G. Emslie, H. Kucharek, B. R. Dennis, N. Gopalswamy, G. D. Holman, G. H. Share, A. Vourlidas, T. G. Forbes, P. T. Gallagher, G. M. Mason, R. A. Metcalf, R. A. Mewaldt, R. J. Murphy, R. A. Schwartz and T. H. Zurbuchen, *J. Geophys. Res.* **109**, A10104 (2004).
86. A. G. Emslie *et al.*, *J. Geophys. Res.* **110**, A11103 (2005).
87. A. D. Erlykin and A. W. Wolfendale, *Astropart. Phys.* **8**, 265 (1998).
88. I. N. Erofeeva, E. V. Kolomeets, V. S. Murzin and V. N. Sevost'yanov, Neutrino generation during the flares at visible and invisible sides of the solar disk, in *Study of Muons and Neutrino in Large Water Volumes*, eds. E. V. Kolomeets, G. A. Gonchar, A. Kh. Lyakhova, A. A. Petrukhin and E. A. Chebakova (Kazakh State University, Alma-Ata, 1983), pp. 24–33.
89. Yu. I. Fedorov, *Kinematics and Physics of Celestial Bodies, Kiev* **11**, 34 (1995).
90. Yu. I. Fedorov, *Geomagn. Aeronomy* **37**, 1 (1997).

91. Yu. I. Fedorov and B. A. Shakhov, Solar cosmic rays in homogeneous regular magnetic field, *Proc. 23rd Int. Cosmic Ray Conf.*, Calgary, Canada (1993), Vol. 3, pp. 215–218.
92. Yu. I. Fedorov, Yu. V. Kyzhyurov, S. F. Nosov and B. A. Shakhov, Solar cosmic ray transport under anisotropic injection, *Proc. 24th Int. Cosmic Ray Conf.*, Rome, Italy (1995), Vol. 4, pp. 297–300.
93. Yu. I. Fedorov, M. Stehlik, K. Kudela and J. Kassovicova, The GLE of May 24, 1990: Kinetic approach to anisotropic event, *Proc. 25th Int. Cosmic Ray Conf.*, Durban, South Africa (1997), Vol. 1, pp. 193–196.
94. J. Feynman, T. P. Armstrong, L. Dao-Gibner and S. Silverman, *J. Spacecraft and Rockets* **27**, 403 (1990).
95. J. Feynman, T. P. Armstrong, L. Dao-Gibner and S. Silverman, *Solar Phys.* **126**, 385 (1990).
96. J. Feynman, G. Spitale, J. Wang and S. Gabriel, *J. Geophys. Res.* **98**, 13281 (1993).
97. L. A. Fisk, *J. Geophys. Res.* **81**, 4633 (1976).
98. C. E. Fichtel, D. E. Guss and K. W. Ogilvie, Details of individual solar particle events, in *Solar Proton Manual*, ed. F. B. McDonald (NASA, Washington, D.C., 1963), pp. 29–55 [NASA Rept. TR-169, September 1963, p. 117].
99. A. T. Filippov, P. A. Krivoshapkin, I. A. Transky, A. I. Kuz'min, G. F. Krymsky, A. S. Niskovskikh and E. G. Berezhko, Solar cosmic ray flare on September 29, 1989 by data of the Yakutsk Array Complex, in *Proc. 22nd Int. Cosmic Ray Conf.*, Dublin, Ireland (1991), Vol. 3, pp. 113–116.
100. E. O. Flückiger, R. Butikofer, Y. Muraki, Y. Matsubara, T. Koi, H. Tsuchiya, T. Hoshida, T. Sako and T. Sakai, A new solar neutron telescope at Gornergrat, in *Rayos Cosmicos-98 — Proc. 16th European Cosmic Ray Symp.*, ed. J. Medina (Alcala University Press, Spain, 1998), pp. 219–222.
101. E. O. Flueckiger *et al.*, Search for solar neutrons in association with the July 12 and July 14, 2000, solar flares, *Proc. 27th Int. Cosmic Ray Conf.*, Hamburg, Germany (2001), Vol. 6, pp. 3044–3047.
102. S. E. Forbush, *Phys. Rev.* **70**, 771 (1946).
103. S. E. Forbush, P. S. Gill and S. M. Vallarta, *Rev. Mod. Phys.* **21**, 44 (1949).
104. S. E. Forbush, T. D. Stinchcomb and M. Schein, *Phys. Rev.* **79**, 501 (1950).
105. M.A. Forman and G.M. Webb, Acceleration of energetic particles, in *Collisionless Shocks in the Heliosphere*: *A Tutorial Review* (A87-2532609-92) (AGU, Washington, D.C., 1985), pp. 91–114.
106. M. A. Forman, R. Ramaty and E. G. Zweibel, The acceleration and propagation of solar flare energetic particles, in *Physics of the Sun*, ed. P. A. Sturrock (D. Reidel Publ. Co., Dordrecht, 1986), Chap. II, pp. 249–289.
107. T. K. Gaisser, *Cosmic Rays and Particle Physics* (Cambridge University Press, 1990), pp. 157–160.
108. T. K. Gaisser, D. Martello and T. C. Miller, *Antarct. J. US* **30**, 344 (1995).
109. A. Gallegos-Cruz, J. Pérez-Peraza and A. Alvarez-Madrigal, Efficiency of particle acceleration by magnetosonic waves, *Proc. 22nd Int. Cosmic Ray Conf.*, Dublin, Ireland (1991), Vol. 3, pp. 1–4.
110. A. Gallegos-Cruz, J. Pérez-Peraza, L. I. Miroshnichenko and E. V. Vashenyuk, *Adv. Space. Res.* **13**, 187 (1993).
111. A. Gallegos-Cruz, J. Pérez-Peraza, L. I. Miroshnichenko, D. Rodríguez-Frías, G. L. del Peral and E. V. Vashenyuk, Solar particle acceleration by short wavelength turbulence, *Proc. 24th Int. Cosmic Ray Conf.*, Rome, Italy (1995), Vol. 4, pp. 14–17.
112. A. Gallegos-Cruz and J. Pérez-Peraza, *Astrophys. J.* **446**, 400 (1995).

113. A. Gallegos-Cruz and J. Pérez-Peraza, On the amount of thermal particles accelerated in the solar corona, *Proc. 16th European Cosmic Ray Symp.*, Alcalá de Henares, Madrid, Spain, ed. J. Medina (Universidad de Alcalá, Madrid, 1998), pp. 141–144.
114. A. Gallegos-Cruz, J. Pérez-Peraza, M. D. Rodríguez-Frías and L. del Peral-Gochicoa, Supply of turbulent energy for particle acceleration in astrophysical plasmas, *Proc. 6th World Multiconference on Systemics, Cybernetics and Informatics*, Orlando, USA, 2002, eds. N. Callaos, Y. He and J. A. Pérez-Peraza (The International Institute of Informatics on Systemics, 2003), Vol. 17, pp. 426–431.
115. L. C. Gentile, *J. Geophys. Res.* **98**, 21107 (1993).
116. I. V. Getselev, N. N. Kontor and N. N. Pavlov, *Radiation Measurements* **26**, 457 (1996).
117. G. Gloeckler, L. A. Fisk, T. H. Zurbuchen and N. A. Schwadron, Sources, injection and acceleration of heliospheric ion populations, in *Acceleration and Transport of Energetic Particles in the Heliosphere*, AIP Conf. Proc., Vol. 528, eds. R. A. Mewaldt, J. R. Jokipii, M. A. Lee, E. Möbius and T. H. Zurbuchen (AIP, 2000), pp. 221–228.
118. A. Goldwurm *et al.*, *Astrophys. J. Lett.* **389**, L79 (1992).
119. N. Gopalswamy, *Geophys. Res. Lett.* **30**, 8013 (2003).
120. N. Gopalswamy, H. Hie, S. Yashiro and I. Usoskin, Coronal mass ejections and ground level enhancements, *Proc. 29th Int. Cosmic Ray Conf.*, Pune, India (2005), Vol. 1, pp. 169–172.
121. J. T. Gosling, *J. Geophys. Res.* **98**, 18937 (1993).
122. J. N. Goswami and K. K. Marhas, Limits on the spectral shape and flux of energetic charged particles from the proto-Sun, *Proc. 29th Int. Cosmic Ray Conf.*, Pune, India (2005), Vol. 1, pp. 79–82.
123. J. N. Goswami, R. Jha, D. Lal, R. C. Reedy and R. E. McGuire, Secular variations in solar flare proton fluxes, *Proc. 18th Int. Cosmic Ray Conf.*, Bangalore, India (1983), Vol. 2, pp. 373–376.
124. J. N. Goswami, R. E. McGuire, R. C. Reedy, D. Lal and J. Jha, *J. Geophys. Res.* **93**, 7195 (1988).
125. N. Grevesse and A. J. Sauval, *Space Sci. Rev.* **85**, 161 (1998).
126. D. E. Hall and P. A. Sturrock, *Phys. Fluids* **10**, 1593 (1967).
127. D. E. Hall and P. A. Sturrock, *Phys. Fluids* **10**, 2620 (1967).
128. B. M. Haisch, *Solar Phys.* **121**, 3 (1989).
129. B. Haisch, K. T. Strong and M. Rodonö, *Ann. Rev. Astron. Astrophys.* **29**, 275 (1991).
130. Dj. Heristchi, G. Trottet and J. Pérez-Peraza, *Solar Phys.* **49**, 151 (1976).
131. A. M. Hillas, *Ann. Rev. Astron. Astrophys.* **22**, 425 (1984).
132. J. E. Humble, M. L. Duldig, D. F. Smart and M. A. Shea, *Geophys. Res. Lett.* **18**, 737 (1991).
133. G. J. Hurford, R. A. Schwartz, S. Krucker, R. P. Lin, D. M. Smith and N. Vilmer, First gamma-ray images of a solar flare, in *Proc 28th Int. Cosmic Ray Conf.*, Japan, Tsukuba (2003), Vol. 6, pp. 3203–3206.
134. G. J. Hurford, R. A. Schwartz, S. Krucker, R. P. Lin, D. M. Smith and N. Vilmer, *Astrophys. J. Lett.* **595**, L77 (2003).
135. N. K. Jain and V. Narain, *Astron. Astrophys. Suppl.* **31**, 1 (1978).
136. C. Jordan, *Mon. Not. R. Astron. Soc.* **142**, 501 (1969).
137. S. W. Kahler, *Ann. Rev. Astron. Astrophys.* **30**, 113 (1992).
138. S. Kahler, *Astrophys. J.* **428**, 837 (1994).

139. S. W. Kahler, M. A. Shea, D. F. Smart and E. W. Cliver, Ground level events from impulsive flares, *Proc. 22nd Int. Cosmic Ray Conf.*, Dublin, Ireland (1991), Vol. 3, pp. 21–24.
140. M.-B. Kallenrode, Charged particles, neutrals and neutrons, in *Solar Encounter*: *The First Solar Orbiter Workshop*, Puerto de la Cruz, Tenerife, Spain, 14–18 May 2001, ESA SP-493, September 2001, pp. 23–34.
141. M.-B. Kallenrode, *J. Phys. G*: *Nucl. Part. Phys.* **29**, 1 (2003).
142. M.-B. Kallenrode and E. W. Cliver, Rogue SEP events: Observational aspects, *Proc. 27th Int. Cosmic Ray Conf.*, Hamburg, Germany (2001), Vol. 8, pp. 3314–3317.
143. M.-B. Kallenrode and E. W. Cliver, Rogue SEP events: Modeling, *Proc. 27th Int. Cosmic Ray Conf.*, Hamburg, Germany (2001), Vol. 8, pp. 3318–3321.
144. G. Kanbach *et al.*, *Astron. Astrophys. Suppl.* **97**, 349 (1993).
145. S. R. Kane, K. Hurley, J. M. McTiernan, M. Sommer, M. Boer and N. Niel, *Astrophys. J. Lett.* **446**, L47 (1995).
146. S. N. Karpov, L. I. Miroshnichenko and E. V. Vashenyuk, *Nuovo Cimento C* **21**, 551 (1998).
147. S. N. Karpov, L. I. Miroshnichenko and E. V. Vashenyuk, The muon bursts with energy $\geq$ 200 GeV during GLE events of 21–23 solar activity cycles, *Proc. 29th Int. Cosmic Ray Conf.*, India, Pune (2005), Vol. 1, pp. 197–200.
148. S. N. Karpov and L. I. Miroshnichenko, Method of additional fluctuations for search of weak signals, *Proc. 30th Int. Cosmic Ray Conf.*, Merida, Yucatan, Mexico (2007), Vol. 6, pp. 413–416.
149. Yu. Yu. Kartavykh, V. M. Ostryakov and I. Yu. Stepanov, Heavy ion acceleration with account of charge transfer processes, *Proc. 24th Int. Cosmic Ray Conf.*, Rome, Italy (1995), Vol. 4, pp. 30–33.
150. Yu. Yu. Kartavykh and V. M. Ostryakov, Plasma diagnostics by the charge distributions of heavy ions in impulsive solar flares, *Proc. 26th Int. Cosmic Ray Conf.*, Salt Lake City, USA (1999), Vol. 6, pp. 272–275.
151. Yu. Yu. Kartavykh and V. M. Ostryakov, The influence of non-thermal electrons on the charge state of heavy ions, *Proc. 27th Int. Cosmic Ray Conf.*, Hamburg, Germany (2001), Vol. 8, pp. 3165–3168.
152. Yu. Yu. Kartavykh, S. Wannawichian, D. Ruffolo and V. M. Ostryakov, *Adv. Space Res.* **30**, 119 (2002).
153. A. A. Kharchenko and V. M. Ostryakov, On the charge state of solar energetic particles, *Proc. 20th Int. Cosmic Ray Conf.* (1987), Vol. 3, pp. 248–251.
154. J. Kiener, M. Gros, V. Tatischeff and G. Weidenspointner, *Astron. Astrophys.* **445**, 725 (2006).
155. P. Kiraly and A. W. Wolfendale, Long-term particle fluence distributions and short-term observations, *Proc. 26th Int. Cosmic Ray Conf.*, USA, Salt Lake City (1999), Vol. 6, pp. 163–166.
156. G. E. Kocharov, *Izvestiya AN SSSR, Ser. Phys.* **42**, 898 (1978).
157. G. E. Kocharov, *Nuclear Astrophysics of the Sun*, Taschenbucher-Band 89 ((Verlag Karl Thiemig, Munchen, 1980).
158. G. E. Kocharov, *Izvestiya AN SSSR, Ser. Phys.* **47**, 1716 (1983).
159. G. E. Kocharov, G. A. Kovaltsov and I. G. Usoskin, Solar thermonuclear and flare neutrinos, in *Neutrino Astrophysics*, ed. G. E. Kocharov (Physical and Technical Institute, Leningrad, 1990), pp. 5–44.
160. G. E. Kocharov, Cosmogenic nuclei, solar neutrinos, neutrons and gamma rays, *Proc. 22nd Int. Cosmic Ray Conf.*, Dublin, Ireland (1991), Vol. 5, pp. 344–347.

161. G. E. Kocharov, G. A. Kovaltsov and I. G. Usoskin, Solar flare neutrinos, *Proc. 22nd Int. Cosmic Ray Conf.*, Dublin, Ireland (1991), Vol. 3, pp. 752–755.
162. L. Kocharov, G. A. Kovaltsov, J. Torsti and V. M. Ostryakov, *Astron. Astrophys.* **357**, 716 (2000).
163. L. Kocharov, G. A. Kovaltsov and J. Torsti, *Astrophys. J.* **556**, 919 (2001).
164. L. Kocharov, G. A. Kovaltsov and J. Torsti, *J. Phys. G*: *Nucl. Part. Phys.* **28**, 1511 (2002) [Comment on *Particle Charge Evolution During Acceleration Processes in Solar Flares*, by M. D. Rodríguez-Frías, L. del Peral and J. Pérez-Peraza].
165. E. V. Kolomeets, E. A. Chebakova and L. E. Kolomeets, High-energy particle generation during the solar flares, *Proc. 24th Int. Cosmic Ray Conf.*, Rome, Italy (1995), Vol. 4, pp. 240–243.
166. C. A. De Koning and T. Mathews, *Canadian J. Phys.* **74**, 290 (1996).
167. G. A. Kovaltsov, *Izvestiya AN SSSR, Phys. Ser.* **43**, 1151 (1981).
168. G. A. Kovaltsov, A. F. Barghouty, L. Kocharov, V. M. Ostryakov and J. Torsti, *Astron. Astrophys.* **375**, 1075 (2001).
169. G. A. Kovaltsov, Y. Y. Kartavykh, L. Kocharov, V. M. Ostryakov and J. Torsti, *J. Geophys. Res.* **107**(A10), 1276 (2002).
170. G. F. Krymsky, Cosmic rays and near-Earth space, in *Solar-Terrestrial Physics*, Vol. 2 (Russian Academy of Sciences, Irkutsk, 2002), pp. 42–45.
171. G. F. Krymsky, A. I. Kuzmin, P. A. Krivoshapkin, S. A. Starodubtsev, I. A. Transky and A. T. Filippov, *Trans.* (*Doklady*) *USSR Acad. Sci.* **314**, 20 (1990).
172. R. M. Kulsrud and A. Ferrari, *Astrophys. Space Sci.* **12**, 302 (1971).
173. I. G. Kurganov and V. M. Ostryakov, *Sov. Astron. Lett.* **17**, 77 (1991).
174. V. G. Kurt, Yu. I. Logachev, V. G. Stolpovsky and E. I. Daibog, Energetic solar particle spectra according to Venera-11, 12 and Prognoz-5, 6 observations, *Proc. 17th Int. Cosmic Ray Conf.*, Paris, France (1981), Vol. 3, pp. 69–72.
175. B. M. Kuzhevskij, L. I. Miroshnichenko and E. V. Troitskaia, Derivation of density profiles in the solar atmosphere by the 2.223 MeV line data for the 6 November 1997 flare, *Proc. 27th Int. Cosmic Ray Conf., Invited, Rapporteur, and Highlight Papers*, Germany, Hamburg (2001), pp. 285–288.
176. B. M. Kuzhevskij, L. I. Miroshnichenko and E. V. Troitskaia, *Astron. Rep.* **49**, 566 (2005).
177. B. M. Kuzhevskij, W. Q. Gan and L. I. Miroshnichenko, *Chin. J. Astron. Astrophys.* **5**, 295 (2005).
178. A. W. Labrador, R. A. Leske, R. A. Mewaldt, E. C. Stone and T. T. von Rosenvinge, High energy ionic charge state composition in the October/November 2003 and January 20, 2005 SEP events, *Proc. 29th Int. Cosmic Ray Conf.*, India, Pune (2005), Vol. 1, pp. 99–102.
179. R. A. Leske, J. R. Cummings, R. A. Mewaldt, E. C. Stone and T. T. von Rosenvinge, *Astrophys. J. Lett.* **452**, L149 (1995).
180. G. T. Lenters and J. A. Miller, *Astrophys. J.* **493**, 451 (1998).
181. R. P. Lin, R. A. Mewaldt and M. A. I. van Hollebeke, *Astrophys. J.* **253**, 949 (1982).
182. R. E. Lingenfelter and H. S. Hudson, Solar particle fluxes and the ancient Sun, in *Ancient Sun. Foss. Res. Earth, Moon and Meteorit. Proc. Conf.*, Boulder, Colorado, 16–19 October 1979–New York, 1980 (Pergamon Press, 1980), pp. 69–79.
183. R. E. Lingenfelter, R. Ramaty, R. J. Murphy and B. Kozlovsky, in *Solar Neutrinos and Neutrino Astronomy*, AIP Conf. Proc., Vol. 126, eds. M. L. Cherry, W. A. Fowler and K. Lande (AIP, New York, 1985), p. 121.

184. C. G. Little and H. Leinbach, The riometer — A device for the continuous measurements of ionospheric absorption, *Proc. of the Inst. of Radio Engineers* **47**(2), 315–320 (1959).
185. Yu. E. Litvinenko and B. V. Somov, *Solar Phys.* **158**, 317 (1995).
186. J. A. Lockwood, W. R. Webber and L. Hsieh, *J. Geophys. Res.* **79**, 4149 (1974).
187. J. L. Lovell, M. L. Duldig and J. E. Humble, *J. Geophys. Res.* **103**, 23733 (1998).
188. E. W. Lu and R. J. Hamilton, *Astrophys. J. Lett.* **380**, L89 (1991).
189. E. W. Lu, R. J. Hamilton, J. McTiernan and K. Bromund, *Astrophys. J.* **412**, 841 (1993).
190. A. Luhn and D. Hovestadt, *Astrophys. J.* **317**, 852 (1987).
191. A. Luhn, B. Klecker, D. Hovestadt and E. Möbius, *Astrophys. J.* **317**, 951 (1987).
192. V. S. Makhmutov, Investigation of energy spectra of solar cosmic rays at the energies above 100 MeV in the 21st cycle of solar activity, Candidate dissertation, Moscow State University, Institute of Nuclear Physics, Moscow (1983).
193. R. E. McGuire, J. N. Goswami, R. Jha, D. Lal and R. C. Reedy, Solar flare particle fluences during solar cycles 19, 20 and 21, *Proc. 18th Int. Cosmic Ray Conf.*, Bangalore, India (1983), Vol. 4, pp. 66–69.
194. N. Mandzhavidze and R. Ramaty, *Astrophys. J. Lett.* **396**, L111 (1992).
195. N. Mandzhavidze and R. Ramaty, *Nucl. Phys. B* (*Proc. Suppl.*) **33**, 141 (1993).
196. N. Mandzhavidze, R. Ramaty, D. L. Bertsch and E. J. Schneid, Pion decay and nuclear line emissions from the 1991 June 11 flare, in *High Energy Solar Physics*, AIP Conference Proceedings, Vol. 374, eds. R. Ramaty, N. Mandzhavidze and X.-M. Hua (AIP, New York, 1996), pp. 225–236.
197. N. Mandzhavidze and R. Ramaty, Particle acceleration from gamma-ray line spectroscopy, in *High Energy Solar Physics — Anticipating HESSI*, ASP Conf. Series, Vol. 206, eds. R. Ramaty and N. Mandzhavidze (Astronomical Society of the Pacific, 2000), pp. 64–70.
198. P. K. Manoharan and M. R. Kundu, *Astrophys. J.* **592**, 597 (2003).
199. P. C. H. Martens and N. P. M. Kuin, *Solar Phys.* **122**, 263 (1989).
200. G. M. Mason, J. E. Mazur, M. D. Looper and R. A. Mewaldt, *Astrophys. J.* **452**, 901 (1995).
201. G. M. Mason, J. E. Mazur and J. R. Dwyer, *Astrophys. J. Lett.* **525**, L133 (1999).
202. G. M. Mason, C. M. S. Cohen, A. C. Cummings, J. R. Dwyer, R. E. Gold, S. M. Krimigis, R. A. Leske, J. E. Mazur, R. A. Mewaldt, E. Möbius, M. Popecki, E. C. Stone, T. T. von Rosenvinge and M. E. Wiedenbeck, *Geophys. Res. Lett.* **26**, 141 (1999).
203. G. M. Mason, J. E. Mazur, J. R. Dwyer, J. R. Jokipii, R. E. Gold and S. M. Krimigis, *Astrophys. J.* **606**, 555 (2004).
204. M. McConnell *et al.*, COMPTEL all-sky imaging at 2.2 MeV, *Proc. 25th Int. Cosmic Ray Conf.*, Durban, South Africa (1997), Vol. 3, pp. 93–96.
205. K. G. McCracken, G. A. M. Dreschhoff, E. J. Zeller, D. F. Smart and M. A. Shea, *J. Geophys. Res.* **106**, 21585 (2001).
206. K. G. McCracken, G. A. M. Dreschhoff, D. F. Smart and M. A. Shea, *J. Geophys. Res.* **106**, 21599 (2001).
207. K. G. McCracken and H. Moraal, Two acceleration mechanisms for ground level enhancements, *Proc. 30th Int. Cosmic Ray Conf.*, Merida, Yucatan, Mexico (2007), Vol. 6, pp. 409–412.
208. F. B. McDonald (ed.), Solar Proton Manual, NASA TR R-169, September 1963, National Aeronautics and Space Administration, Washington, D.C. (1963).

209. D. B. Melrose and M. H. Pope, Diffusive shock acceleration by multiple shocks, *Astron. Soc. Australia Proc.* **10**, 222 (1993).
210. R. A. Mewaldt *et al.*, *J. Geophys. Res.* **110**, A09S18 (2005).
211. R. A. Mewaldt *et al.*, Solar-particle energy spectra during the large events of October-November 2003 and January 2005, *Proc. 29th Int. Cosmic Ray Conf.*, India, Pune (2005), Vol. 1, pp. 111–114.
212. J. A. Miller, N. Guessoum and R. Ramaty, *Astrophys. J.* **361**, 701 (1990).
213. J. A. Miller and R. Ramaty, Stochastic acceleration in impulsive solar flares, in *Particle Acceleration in Cosmic Plasmas*, AIP Conference Proceedings, Vol. 264, eds. G. P. Zank and T. K. Gaisser (AIP, New York, 1992), pp. 223–228.
214. J. A. Miller and A. F. Viñas, *Astrophys. J.* **412**, 386 (1993).
215. J. A. Miller and D. A. Roberts, *Astrophys. J.* **452**, 912 (1995).
216. J. A. Miller, T. N. La Rosa and R. L. Moore, *Astrophys. J.* **461**, 445 (1996).
217. J. A. Miller, P. J. Cargill, A. G. Emslie, G. D. Holman, B. R. Dennis, T. N. LaRosa, R. M. Winglee, S. G. Benka and S. Tsuneta, *J. Geophys. Res.* **102**, 14631 (1997).
218. L. I. Miroshnichenko, *Geomagn. Aeronomy* **10**, 898 (1970).
219. L. I. Miroshnichenko, *Izvestiya AN SSSR, Phys. Ser.* **43**, 2535 (1979).
220. L. I. Miroshnichenko, *Izvestiya AN SSSR, Phys. Ser.* **45**, 588 (1981).
221. L. I. Miroshnichenko, Dynamics and prediction of radiation characteristics of solar cosmic rays, Doctoral Dissertation, IZMIRAN, Moscow (1990).
222. L. I. Miroshnichenko, V. M. Nesterov, V. M. Petrov and A. P. Tibanov, *Kosmicheskiye Issledovaniya* (*Space Research*) **12**, 892 (1974).
223. L. I. Miroshnichenko, J. Pérez-Peraza, O. M. Sorokin, E. V. Vashenyuk, M. Alvarez-Madrigal and C. Gallegos, Two relativistic solar proton components in some SPE's, *Proc. 21st Int. Cosmic Ray Conf.*, Australia, Adelaide (1990), Vol. 5, pp. 5–8.
224. L. I. Miroshnichenko, *Geomagn. Aeronomy* **34**, 29 (1994).
225. L. I. Miroshnichenko, *Solar Phys.* **156**, 119 (1995).
226. L. I. Miroshnichenko, *Radiation Measurements* **26**, 421 (1996).
227. L. I. Miroshnichenko, *J. Moscow Phys. Soc.* **7**, 17 (1997).
228. L. I. Miroshnichenko, *Solar Cosmic Rays* (Kluwer Academic Publishers, Dordrecht, 2001).
229. L. I. Miroshnichenko, *Radiation Hazard in Space* (Kluwer Academic Publishers, Dordrecht, 2003).
230. L. I. Miroshnichenko, *Izvestiya RAN, Ser. Phys.* **67**, 463 (2003).
231. L. I. Miroshnichenko, Multiple acceleration at the Sun: New approach to separation of the sources, in *Proc. ISCS 2003 Symp. on Solar Variability as an Input to the Earth's Environment*, Tatranska Lomnica, Slovakia, 23–28 June 2003 (European Space Agency, 2003), ESA SP-535, September 2003, pp. 625–630.
232. L. I. Miroshnichenko, High-energy cutoff for solar cosmic rays by the data of large non-standard detectors, in *Proc. XII Int. School on Particles and Cosmology*, eds. V. A. Matveev, V. A. Rubakov and Kh. S. Nirov (INR of RAS, Moscow, 2004), pp. 96–100.
233. L. I. Miroshnichenko, V. M. Petrov and A. P. Tibanov, *Izvestiya AN SSR, Phys. Ser.* **37**, 1174 (1973).
234. L. I. Miroshnichenko, M. O. Sorokin, J. Pérez-Peraza, M. Alvarez-Madrigal, A. Gallegos-Cruz and E. V. Vashenyuk, Two relativistic solar proton components in some SPE's, *Proc. 21st Int. Cosmic Ray Conf.*, Adelaide, Australia (1990), Vol. 5, pp. 5–8.
235. L. I. Miroshnichenko, J. Pérez-Peraza, E. V. Vashenyuk, M. D. Rodriguez-Frías, L. del Peral and A. Gallegos-Cruz, On the formation of relativistic particle beams

in extended coronal structures: Two source model for solar cosmic rays, *Proc. 24th Int. Cosmic Ray Conf.*, Rome, Italy (1995), Vol. 4, pp. 34–41.
236. L. I. Miroshnichenko, M. D. Rodriguez-Frías, L. del Peral, J. Pérez-Peraza and E. V. Vashenyuk, Absolute proton fluxes from the Sun at rigidity above 1 GV by ground-based data, in *Proc. 24th Int. Cosmic Ray Conf.*, Rome, Italy (1995), Vol. 4, pp. 54–57.
237. L. I. Miroshnichenko, J. Pérez-Peraza, E. V. Vashenyuk, M. D. Rodríguez-Frias, L. del Peral and A. Gallegos-Cruz, On the formation of relativistic particle fluxes in extended coronal structures, in *High Energy Solar Physics*, AIP Conf. Proc., Vol. 374, eds. R. Ramaty, N. Mandzhavidze and X.-M. Xua (AIP, New York, 1996), pp. 140–149.
238. L. I. Miroshnichenko, B. Mendoza and R. Pérez-Enriquez, *Solar Phys.* **186**, 381 (1999).
239. L. I. Miroshnichenko, C. A. de Koning and R. Pérez-Enriquez, *Space Sci. Rev.* **91**, 615 (2000).
240. L. I. Miroshnichenko, B. Mendoza and R. Pérez-Enriquez, *Solar Phys.* **202**(1), 151 (2001).
241. E. Möbius, L. M. Kistler, M. A. Popecki, K. N. Crocker, M. Granoff, E. J. Lund, S. Turco, D. Hovestadt, B. Klecker and E. Kunneth, *EOS Trans. Supplement, AGU* **79**, F694 (1998).
242. E. Möbius *et al.*, *Space Sci. Rev.* **86**, 449 (1998).
243. E. Möbius, M. Popecki, B. Klecker, L. M. Kistler, A. Bogdanov, A. B. Galvin, D. Heirtzler, D. Hovestadt, E. J. Lund and D. Morris, *Geophys. Res. Lett.* **26**, 145 (1999).
244. H. Moraal, K. G. McCracken and P. Stocker, Analysis of the 20 January 2005 cosmic ray ground level enhancement, *Proc. 30th Int. Cosmic Ray Conf.*, Merida, Yucatan, Mexico (2007), Vol. 6, pp. 405–408.
245. I. Morishita, S. Sakakibara, Z. Fujii, Y. Muraki, K. Koi and K. Takahashi, Anisotropic space distribution of solar particles of the GLE observed on 24 May 1990, *Proc. 24th Int. Cosmic Ray Conf.*, Rome, Italy (1995), Vol. 4, pp. 220–223.
246. D. Moses, W. Dröge, P. Meyer and P. Evenson, *Astrophys. J.* **346**, 523 (1989).
247. D. J. Mullan, *Astrophys. J.* **269**, 765 (1983).
248. D. J. Mullan and D. W. Kent, Can solar flares be the cause of ancient catastrophes?, *Proc. 16th Int. Cosmic Ray Conf.*, Kyoto, Japan (1979), Vol. 5, pp. 323–326.
249. D. J. Mullan, J. Pérez-Peraza and M. Alvarez-Madrigal, *Adv. Space Res.* **4**, 157 (1984).
250. R. J. Murphy and G. H. Share, *Adv. Space Res.* **35**, 1825 (2005).
251. R. J. Murphy, G. H. Share, X.-M. Hua, R. P. Lin, D. M. Smith and R. A. Schwartz, Physical implications of RHESSI neutron capture-line measurements, *Proc. 28th Int. Cosmic Ray Conf.*, Tsukuba, Japan (2003), Vol. 6, pp. 3195–3198.
252. R. J. Murphy, G. H. Share, X.-M. Hua, R. P. Lin, D. M. Smith and R. A. Schwartz, *Astrophys. J. Lett.* **595**, L93 (2003).
253. K. Nagashima, S. Sakakibara and I. Morishita, Quiescence of GLE-producible solar proton eruptions during the transition phase of heliomagnetic polarity reversal near the solar-activity-maximum period, *Proc. 22nd Int. Cosmic Ray Conf.*, Dublin, Ireland (1991), Vol. 3, pp. 29–32.
254. M. N. Nazarova, N. K. Pereyaslova and I. E. Petrenko, *Geomagn. Aeronomy* **32**, 23 (1992).
255. R. J. Nemzek, R. D. Belian, T. E. Cayton and G. D. Reeves, *J. Geophys. Res.* **99**, 4221 (1994).

256. R. A. Nymmik, *Radiation Measurements* **26**, 421 (1996).
257. R. A. Nymmik, SEP Event distribution function as inferred from spaceborne measurements and lunar rock isotopic data, *Proc. 26th Int. Cosmic Ray Conf.*, Salt Lake City, USA (1999), Vol. 6, pp. 268–270.
258. R. A. Nymmik, Relationships among solar activity, SEP occurrence frequency, and solar energetic particle event distribution function, *Proc. 26th Int. Cosmic Ray Conf.*, Salt Lake City, USA (1999), Vol. 6, pp. 280–283.
259. V. M. Ostryakov, Yu. Yu. Kartavykh, D. Ruffolo and G. A. Kovaltsov, *J. Geophys. Res.* **105**, 315 (2000).
260. J. Pérez-Peraza, *J. Geophys. Res.* **80**, 3535 (1975).
261. J. Pérez-Peraza, *Space Sci. Rev.* **44**, 91 (1986).
262. J. Pérez-Peraza, Acceleration of solar particles during cycle 22, Invited talk, *16th ECRS*, Alcalá de Henares, Madrid, España (1998), pp. 97–112.
263. J. Pérez-Peraza, M. Gálvez and R. Lara, Energy spectrum of flare particles from an impulsive acceleration processes, *Proc. 15th Int. Cosmic Ray Conf.*, Plovdiv, Bulgaria (1977), Vol. 5, pp. 23–28.
264. J. Pérez-Peraza, M. Gálvez and R. Lara, *Adv. Space Res.* **18**, 365 (1978).
265. J. Pérez-Peraza, J. Martinell and A. Villarreal, *Adv. Space Res.* **2**, 197 (1982).
266. J. Pérez-Peraza, J. Martinell and A. Villarreal, Particle charge behavior during acceleration and implications on mass and charge spectra, *Proc. 18th Int. Cosmic Ray Conf.*, Bangalore, India (1983), Vol. 9, pp. 309–312.
267. J. Pérez-Peraza, M. Álvarez, A. Laville and A. Gallegos, Temperature-dependent cross-sections for charge changing processes: Delimitation of conditions for charge transfer establishment and photo production from electron capture, *Proc. 19th Int. Cosmic Ray Conf.*, La Jolla, USA (1985), Vol. 4, pp. 18–29.
268. J. Pérez-Peraza, M. Álvarez-Madrigal and A. Gallegos-Cruz, *Adv. Space Res.* **9**, 97 (1989).
269. J. Pérez-Peraza and M. Álvarez-Madrigal, Evolution of effective charge of accelerated ions, *Proc. 21st Int. Cosmic Ray Conf.*, Adelaide, Australia (1990), Vol. 5, pp. 382–385.
270. J. Pérez-Peraza, A. Gallegos-Cruz, E. V. Vashenyuk and L. I. Miroshnichenko, Spectrum of accelerated particles in solar proton events with a prompt component, *Proc. 22nd Int. Cosmic Ray Conf.*, Ireland, Dublin (1991), Vol. 3, pp. 5–8.
271. J. Pérez-Peraza, A. Gallegos-Cruz, E. V. Vashenyuk and L. I. Miroshnichenko, *Geomagn. Aeronomy* **32**, 1 (1992).
272. J. Pérez-Peraza and A. Gallegos-Cruz, *Astrophys. J. Suppl. Series* **90**, 669 (1994).
273. J. Pérez-Peraza, A. Gallegos-Cruz and E. V. Vashenyuk, Solar particle acceleration by high energy density MHD turbulence, *Proc. 25th Int. Cosmic Ray Conf.*, Durban, South Africa (1997), Vol. 1, pp. 177–181.
274. J. Pérez-Peraza, A. Gallegos-Cruz, A. Álvarez-Madrigal and A. Sánchez-Hertz, Equilibrium charge of energetic ions from the balance of electron capture and loss cross-sections, *Proc. 26th Int. Cosmic Ray Conf.*, Salt Lake City, USA (1999), Vol. 6, pp. 95–98.
275. J. Pérez-Peraza, A. Gallegos-Cruz, E. V. Vashenyuk and L. I. Miroshnichenko, Efficiency for RSP acceleration in the 14.07.2000 and 15.04.2001 events, *Proc. 28th Int. Cosmic Ray Conf.* (2003), Vol. 6, pp. 3327–3330.
276. J. Pérez-Peraza, A. Gallegos-Cruz, E. V. Vashenyuk, Yu. V. Balabin and L. I. Miroshnichenko, *Adv. Space Res.* **38**, 18 (2006).
277. J. Pérez-Peraza, L. I. Miroshnichenko, E. V. Vashenyuk, Yu. V. Balabin and A. Gallegos-Cruz, Different types of plasma turbulence in the process of solar

particle acceleration, in *Plasma and Fusion Science*, AIP Conference Proceedings, Vol. 875, ed. J. Julio E. Herrera-Velazquez (AIP, Melville, New York, 2006), pp. 312–315.
278. J. Pérez-Peraza, A. Gallegos-Cruz, E. V. Vashenyuk, Yu. V. Balabin and L. I. Miroshnichenko, Relativistic proton production at the Sun in the 20 January 2005 solar event, *Adv. Space Res.* (2007), in press.
279. A. I. Podgorny and I. M. Podgorny, An electromagnetic model of solar flare, in *Physics of Magnetic Flux Ropes*, Geophysical Monograph 58, eds. C. T. Russel, E. R. Priest and L. C. Lee (AGU, Washington, D.C., 1990), pp. 279–283.
280. E. R. Priest, *Astrophys. J.* **181**, 227 (1973).
281. E. R. Priest, *Solar Flare Magnetohydrodynamics* (Gordon & Breach, 1981).
282. E. Priest and T. Forbes, *Magnetic Field Reconnection* (MHD Theory and Applications) (Cambridge University Press, 2000).
283. S. Ramadurai and G. Thejappa, *Adv. Space Res.* **6**, 281 (1986).
284. R. Ramaty, B. Kozlovsky and R. E. Lingenfelter, *Space Sci. Rev.* **18**, 341 (1975).
285. R. Ramaty and R. J. Murphy, *Space Sci. Rev.* **45**, 213 (1987).
286. R. Ramaty, N. Mandzhavidze, B. Kozlovsky and J. G. Skibo, *Adv. Space. Res.* **13**, 275 (1993).
287. R. Ramaty and N. Mandzhavidze, Implications of solar flare charged particle, gamma ray and neutron observations: Rapporteur Paper II, in *High Energy Solar Physics*, AIP Conference Proceedings, Vol. 374, eds. R. Ramaty, N. Mandzhavidze and X.-M. Hua (AIP, New York, 1996), pp. 533–543.
288. D. V. Reames, *Astrophys. J. Suppl.* **73**, 235 (1990).
289. D. V. Reames, J. P. Meyer and T. T. von Rosenvinge, *Astrophys. J. Suppl.* **90**, 649 (1994).
290. D. V. Reames, *Adv. Space Res.* **15**, 41 (1995).
291. D. V. Reames, Energetic particles from solar flares and coronal mass ejections, in *High Energy Solar Physics*, AIP Conference Proceedings, Vol. 374, eds. R. Ramaty, N. Mandzhavidze and X.-M. Hua (AIP, New York, 1996), pp. 35–44.
292. D. V. Reames, *Space Sci. Rev.* **90**, 413 (1999).
293. D. V. Reames, What we don't understand about ion acceleration in flares, in *High Energy Solar Physics — Anticipating HESSI*, ASP Conference Series, Vol. 206, eds. R. Ramaty and N. Mandzhavidze (Astronomical Society of the Pacific, 2000), pp. 102–111.
294. D. V. Reames, *Astrophys. J.* **540**, L111 (2000).
295. D. V. Reames, *Astrophys. J. Lett.* **571**, L63 (2002).
296. D. V. Reames and C. K. Ng, *Astrophys. J.* **610**, 510 (2004).
297. D. V. Reames, H. V. Cane and T. T. von Rosenvinge, *Astrophys. J.* **357**, 259 (1990).
298. D. V. Reames, C. K. Ng and A. J. Tylka, *Geophys. Res. Lett.* **26**, 3585 (1999).
299. D. V. Reames, C. K. Ng and A. J. Tylka, *Astrophys. J. Lett.* **548**, L233 (2001).
300. R. C. Reedy, Recent solar energetic particles: Updates and trends, in *Lunar and Planetary Science XXXIII* (2002), p. 2.
301. M. D. Rodríguez-Frías, L. del Peral and J. Pérez-Peraza, *J. Phys. G.*: *Nuc. Part. Phys.* **26**, 259 (2000).
302. M. D. Rodríguez-Frías, L. del Peral and J. Pérez-Peraza, *J. Geophys. Res.* **106**, 15,657 (2001).
303. R. Rosner and G. S. Vaiana, *Astrophys. J.* **222**, 1104 (1978).
304. D. Ruffolo and T. Khumlumlert, Propagation of coherent pulses of solar cosmic rays, *Proc. 24th Int. Cosmic Ray Conf.*, Rome, Italy (1995), Vol. 4, pp. 277–280.

305. O. G. Ryazhskaya, L. V. Volkova and G. T. Zatsepin, *Nucl. Phys. B* (*Proc. Suppl.*) **110**, 358 (2002).
306. T. Sako, K. Watanabe, Y. Muraki, Y. Matsubara, H. Tsujihara, M. Yamashita, T. Sakai, S. Shibata, J. F. Valdés-Galicia, L. X. González, A. Hurtado, O. Musalem, P. Miranda, N. Martinic, R. Ticona, A. Velarde, F. Kakimoto, S. Ogio, Y. Tsunesada, H. Tokuno, Y. T. Tanaka, I. Yoshikawa, T. Terasawa, Y. Saito, T. Mukai and M. Gros, *Astrophys. J. Lett.* **651**, L69 (2006).
307. T. Sako, K. Watanabe, J. F. Valdes-Galicia, L. X. Gonzalez, A. Hurtado, O. Musalem, P. P. Miranda, N. Martinic, R. Ticona, A. Velarde, Y. Muraki, Y. Matsubara, T. Sakai, S. Shibata, F. Kakimoto, Y. Tsunesada, H. Tokuno and S. Ogio, Emission profile of solar neutrons obtained from the ground based observations for the 7 September 2005 event, *Proc. 30th Int. Cosmic Ray Conf.*, Merida, Yucatan, Mexico (2007), Vol. 6, pp. 25–28.
308. K. Sakurai, *Physics of Solar Cosmic Rays* (Tokyo University Press, Tokyo, 1974).
309. K. Sakurai, *Astrophys. Space Phys.* **63**, 369 (1979).
310. V. Sarabhai, S. P. Duggal, H. Razdan and F. S. G. Sastry, *Proc. Ind. Acad. Sci.* **43**, 309 (1956).
311. E. Schatzman, in *Summer School of Theoretical Physics* (Gordon and Breach, Les Houches, 1966), p. 229.
312. S. M. Schindler and P. D. Kearney, Evidence for very high-energy solar particle production, *Proc. 13th Int. Cosmic Ray Conf.*, Denver, Co., USA (1973), Vol. 2, pp. 1554–1559.
313. R. Schlickeiser, *Astrophys. J. Suppl.* **90**, 929 (1994).
314. N. I. Shakhovskaya, *Solar Phys.* **121**, 375 (1989).
315. G. H. Share and R. J. Murphy, *Astrophys. J.* **452**, 933 (1995).
316. G. H. Share, R. J. Murphy and J. G. Skibo, Gamma-ray line measurements and ambient solar abundances, in *High Energy Solar Physics*, AIP Conference Proceedings, Vol. 374, eds. R. Ramaty, N. Mandzhavidze and X.-M. Hua (AIP, New York, 1996), pp. 162–171.
317. G. H. Share and R. J. Murphy, *Astrophys. J.* **484**, L165 (1997).
318. G. H. Share and R. J. Murphy, Gamma ray spectroscopy in the pre-HESSI era, in *High Energy Solar Physics — Anticipating HESSI*, ASP Conference Series, Vol. 206, eds. R. Ramaty and N. Mandzhavidze (Astronomical Society of the Pacific, 2000), pp. 377–386.
319. M. A. Shea and D. F. Smart, *Space Sci. Rev.* **32**, 251 (1982).
320. M. A. Shea and D. F. Smart, *Solar Phys.* **127**, 297 (1990).
321. M. A. Shea, D. F. Smart, M. D. Wilson and E. O. Fluckiger, *Geophys. Res. Lett.* **18**, 829 (1991).
322. M. A. Shea and D. F. Smart, Solar proton events: History, statistics and predictions, in *Solar-Terrestrial Prediction-IV*: *Proc. of a Workshop*, Ottawa, Canada, May 18–22, 1992 (U.S. Department of Commerce, NOAA, SEL, Boulder, Colorado, Vol. 2, pp. 48–70.
323. M. A. Shea and D. F. Smart, Unusual intensity-time profiles of ground-level solar proton events, in *High Energy Solar Physics, High Energy Solar Physics*, AIP Conference Proceedings, Vol. 374, eds. R. Ramaty, N. Mandzhavidze and X.-M. Hua (AIP, New York, 1996), pp. 131–139.
324. M. A. Shea and D. F. Smart, Dual acceleration and/or release of relativistic solar cosmic rays, *Proc. 25th Int. Cosmic Ray Conf.*, Durban, South Africa (1997), Vol. 1, pp. 129–132.
325. G. M. Simnett, *Solar Phys.* **106**, 165 (1986).

326. G. M. Simnett, *Space Sci. Rev.* **73**, 387 (1995).
327. G. M. Simnett and E. C. Roelof, Timing of the relativistic proton acceleration responsible for the GLE on 20 January, 2005, *Proc. 29th Int. Cosmic Ray Conf.*, Pune, India (2005), Vol. 1, pp. 233–236.
328. J. A. Simpson, Cosmic-radiation neutron intensity monitor, *Annals of the IGY*, Vol. 4 (Pergamon Press, London, 1957), pp. 351–373.
329. J. A. Simpson, Astrophysical phenomena discovered by cosmic rays and solar flare Ground Level Events: The early years, *Proc. 21st Int. Cosmic Ray Conf., Invited Papers, Highlight Papers, Miscellaneous*, Adelaide, Australia (1990), Vol. 12, pp. 187–195.
330. E. C. J. Sittler and M. Guhathakurta, *Astrophys. J.* **523**, 812 (1999).
331. A. I. Sladkova, *Radiation Measurements* **26**, 447 (1996).
332. A. I. Sladkova *et al.*, in *Catalogue of Solar Proton Events 1987–1996*, ed. Yu. I. Logachev (Moscow University Press, Moscow, 1998).
333. D. F. Smart and M. A. Shea, *Solar Phys.* **16**, 484 (1971).
334. D. F. Smart and M. A. Shea, *J. Spacecraft and Rockets* **26**, 403 (1989).
335. D. F. Smart and M. A. Shea, Probable pitch angle distribution and spectra of the 23 February 1956 solar cosmic ray event, *Proc. 21st Int. Cosmic Ray Conf.*, Adelaide, Australia (1990), Vol. 5, pp. 257–260.
336. D. F. Smart and M. A. Shea, A comparison of the magnitude of the 29 September 1989 high energy event with solar cycle 17, 18 and 19 events, *Proc. 22nd Int. Cosmic Ray Conf.*, Dublin, Ireland (1991), Vol. 3, pp. 101–104.
337. D. F. Smart and M. A. Shea, *Adv. Space Res.* **17**, 113 (1996).
338. D. F. Smart, M. A. Shea, M. D. Wilson and L. C. Gentile, Solar cosmic rays on 29 September 1989: An analysis using the worldwide network of cosmic ray stations, *Proc. 22nd Int. Cosmic Ray Conf.*, Dublin, Ireland (1991), Vol. 3, pp. 97–100.
339. D. V. Smirnov, V. B. Petkov and S. N. Karpov, *Astron. Lett.* **32**, 1 (2006).
340. D. F. Smith and J. A. Miller, *Astrophys. J.* **446**, 390 (1995).
341. C. W. Smith, N. F. Ness, L. F. Burlaga, R. M. Skoug, D. J. McComas, T. H. Zurbuchen, G. Gloeckler, D. K. Haggerty, R. E. Gold, M. I. Desai, G. M. Mason, J. R. Dwyer, M. A. Popecki, E. Mobius, C. M. S. Cohen and R. A. Leske, *Solar Phys.* **204**, 227 (2001).
342. D. M. Smith, G. H. Share, R. J. Murphy, R. A. Schwartz, A. Y. Shin and R. P. Lin, *Astrophys. J. Lett.* **595**, L81 (2003).
343. B. V. Somov, *Physical Processes in Solar Flares* (Kluwer Academic Publishers, 1992).
344. B. V. Somov, *Fundamental of Cosmic Electrodynamics* (Kluwer Academic Publishers, Dordrecht, 1994).
345. B. V. Somov, Reconnection and acceleration to high energies in flares, in *High Energy Solar Physics, High Energy Solar Physics*, AIP Conference Proceedings, Vol. 374, eds. R. Ramaty, N. Mandzhavidze and X.-M. Hua (AIP, New York, 1996), pp. 493–497.
346. M. F. Stovpyuk and V. M. Ostryakov, *Solar Phys.* **198**, 163 (2001).
347. A. Struminsky, M. Matsuoka and K. Takahashi, *Astrophys. J.* **429**, 400 (1994).
348. T. H. Stix, *Phys. Fluids B* **2**, 1729 (1990).
349. W. F. G. Swann, *Phys. Rev.* **43**, 217 (1933).
350. D. B. Swinson and M. A. Shea, *Geophys. Res. Lett.* **17**, 1073 (1990).
351. T. Terasawa, Particle acceleration at solar flares/interplanetary shocks, Invited Lecture at the *36th COSPAR Scientific Assembly*, Beijing, China (2006), p. 50.
352. O. V. Terekhov, A. G. Kuzmin, R. A. Sunyaev, A. Yu. Tkachenko, D. V. Denisenko, C. Barat, R. Talon and G. Vedrenne, *Astron. Lett.* (*Russia*) **22**, 362 (1996).

353. M. Teshima, Origin of Cosmic Rays Above 10^{14} eV, in *Proc. 23rd Int. Cosmic Ray Conf., Invited, Rapporteur, and Highlight Papers*, eds. D. A. Leahy, R. B. Hicks and D. Venkatesan (World Scientific, Singapore, 1994), pp. 257–278.
354. J. Torsti, T. Eronen, M. Mahonen, E. Riihonen, C. G. Schultz, K. Kudela and H. Kananen, Search of peculiarities in the flux profiles of GLE's in 1989, *Proc. 22nd Int. Cosmic Ray Conf.*, Dublin, Ireland (1991), Vol. 3, pp. 141–144.
355. J. J. Torsti, T. Eronen, M. Mahonen, E. Riihonen, C. G. Schultz, K. Kudela and H. Kananen, Estimation of high-energy solar particle transport parameters during the GLE's in 1989, in *Solar Wind Seven*, eds. E. Marsch and R. Schwenn (Pergamon Press, Oxford, 1992), pp. 545–548.
356. J. Torsti, L. G. Kocharov, R. Vainio, A. Anttila and G. A. Kovaltsov, *Solar Phys.* **166**, 135 (1996).
357. E. V. Troitskaia and B. M. Kuzhevskij, Absorption of 2.22 MeV solar flare gamma rays and determining of the solar plasma density altitude profile, *Proc. 26th Int. Cosmic Ray Conf.*, Salt Lake City, USA (1999), Vol. 6, pp. 17–20.
358. E. V. Troitskaia, W. Q. Gan, B. M. Kuzhevskij and L. I. Miroshnichenko, Vertical profile of plasma density in the solar atmosphere by the data on the 2.223 MeV line for the flare of 16 December 1988, *Proc. 28th Int. Cosmic Ray Conf.*, Japan, Tsukuba (2003), Vol. 6, pp. 3219–3222.
359. E. V Troitskaia, W. Q. Gan, B. M. Kuzhevskij and L. I. Miroshnichenko, *Solar Phys.* **242**, 87 (2007).
360. E. V. Troitskaia and L. I. Miroshnichenko, Study of the 28 October 2003 solar flare by means of 2.223 MeV gamma-emission, *Proc. 30th Int. Cosmic Ray Conf.*, Merida, Yucatan, Mexico (2007), Vol. 5, pp. 17–20.
361. V. N. Tsytovich, *Soviet Phys. Uspekhi* **9**, 370 (1966).
362. V. N. Tsytovich, *Non-Linear Effects in Plasma* (Plenum, New York, 1970).
363. L. V. Tverskaya, M. V. Teltsov and V. I. Shumshurov, *Geomagn. Aeronomy* **31**, 928 (1991).
364. A. J. Tylka, P. R. Boberg, J. H. Adams, Jr., L. P. Beahm, W. F. Dietrich and T. Kleis, *Astrophys. J. Lett.* **444**, L109 (1995).
365. A. J. Tylka and W. F. Dietrich, *Radiation Measurements* **30**, 345 (1999).
366. A. J. Tylka, W. F. Dietrich, C. Lopate and D. Reames, High-energy solar Fe ions in the 29 September 1989 Ground Level Event, *Proc. 26th Int. Cosmic Ray Conf.*, Salt Lake City, USA (1999), Vol. 6, pp. 67–70.
367. A. J. Tylka, D. V. Reames and C. K. Ng, *Geophys. Res. Lett.* **26**, 2141 (1999).
368. A. J. Tylka, C. M. S. Cohen, W. F. Dietrich, C. G. Maclennan, R. E. McGuire, C. K. Ng and D. V. Reames, *Astrophys. J. Lett.* **558**, L59 (2001).
369. A. J. Tylka, C. M. S. Cohen, W. F. Dietrich, M. A. Lee, C. G. Maclennan, R. A. Mewaldt, C. K. Ng and D. V. Reames, *Astrophys. J.* **625**, 474 (2005).
370. G. K. Ustinova and A. K. Lavrukhina, The features of modulation mechanism over a long-time scale, *Proc. 20th Int. Cosmic Ray Conf.*, Moscow, USSR (1987), Vol. 4, pp. 307–310.
371. S. M. Vallarta, Primary radiation, in *Proc. Echo Lake Cosmic Ray Symp.*, Echo Lake, Colorado, USA, June 23–28, 1949 (Office of Naval Research, Washington, D.C., 1949), Vol. 1, pp 163–170.
372. M. A. I. Van Hollebeke, F. B. McDonald and J.-P. Meyer, *Astrophys. J. Suppl.* **73**, 285 (1990).
373. E. V. Vashenyuk, L. I. Miroshnichenko, M. O. Sorokin, J. Pérez-Peraza and A. Gallegos-Cruz, *Geomagn. Aeronomy* **33**, 1 (1993).

374. E. V. Vashenyuk, L. I. Miroshnichenko, M. O. Sorokin, J. Pérez-Peraza and A. Gallegos-Cruz, *Adv. Space Res.* **14**, 711 (1994).
375. E. V. Vashenyuk, L. I. Miroshnichenko, J. Pérez-Peraza, H. Kananen and P. Tanskanen, Generation and propagation characteristics of relativistic solar protons during the GLE of September 29, 1989, *Proc. 25th Int. Cosmic Ray Conf.*, Durban, South Africa (1997), Vol. 1, pp. 161–164.
376. E. V. Vashenyuk, L. I. Miroshnichenko and B. B. Gvozdevsky, *Nuovo Cimento* **23**, 285 (2000).
377. E. V. Vashenyuk, V. V. Pchelkin, B. B. Gvozdevsky and J. Pérez-Peraza, Relativistic solar cosmic rays and their importance for astroparticle physics, *Proc. 6th World Multiconference on Systemics, Cybernetics and Informatics*, Orlando, USA, 2002, eds. N. Callaos, Y. He and J. A. Pérez-Peraza (The International Institute of Informatics on Systemics, 2003), Vol. 17, pp. 443–446.
378. E. V. Vashenyuk, Yu. V. Balabin and B. B. Gvozdevsky, Relativistic solar proton dynamics in large GLE's of 23rd cycle, *Proc. 28th Int. Cosmic Ray Conf.*, Tsukuba, Japan (2003), Vol. 6, pp. 3401–3404.
379. E. V. Vashenyuk, Yu. V. Balabin, B. B. Gvozdevsky, S. N. Karpov, V. G. Yanke, E. A. Eroshenko, A. V. Belov and R. T. Gushchina, Relativistic solar cosmic rays in January 20, 2005 event on the ground based observations, *Proc. 29th Int. Cosmic Ray Conf.*, Pune, India (2005), Vol. 1, pp. 209–212.
380. E. V. Vashenyuk, Yu. V. Balabin, J. Pérez-Peraza, A. Gallegos-Cruz and L. I. Miroshnichenko, *Adv. Space Res.* **38**, 411 (2006).
381. E. V. Vashenyuk, Yu. V. Balabin and L. I. Miroshnichenko, Relativistic solar protons in the GLE of 23 February 1956: New study, *Adv. Space Res.* (2007) (in press).
382. E. V. Vashenyuk, L. I. Miroshnichenko, J. Pérez-Peraza, Yu. V. Balabin and A. Gallegos-Cruz, Two-component features of the two largest GLE's: 23 February 1956 and 20 January 2005, *Proc. 30th Int. Cosmic Ray Conf.*, Merida, Yucatan, Mexico (2007), Vol. 6, pp. 401–404.
383. W. T. Vestrand, G. H. Share, R. J. Murphy, D. J. Forrest, E. Rieger, E. L. Chupp and G. Kanbach, *Astrophys. J. Suppl.* **120**, 409 (1999).
384. L. Vlahos *et al.*, Particle acceleration, in *Energetic Phenomena on the Sun*, eds. M. Kundu, B. Woodgate and E. J. Schmahl (Kluwer Academic Publishers, Dordrecht/Boston/London, 1989), pp. 131–224.
385. S. Wannawichian, D. Ruffolo and Yu. Yu. Kartavykh, *Astrophys. J. Suppl.* **146**, 443 (2003).
386. K. Watanabe *et al.*, Solar neutron events associated with large solar flares in solar cycle 23, *Proc. 29th Int. Cosmic Ray Conf.*, India, Pune (2005), Vol. 1, pp. 37–40.
387. W. R. Webber, A review of solar cosmic ray events, in *AAS-NASA Symposium on the Physics of Solar Flares*, ed. W. N. Hess (NASA, Washington, D.C., 1964), pp. 215–255.
388. D. C. Wilkinson, GOES Space Environment Monitor, Format Description for 1- and 5-Minute Averaged Data, GOES Data Distribution Disk (1992).
389. B. E. Woodgate, R. D. Robinson, K. G. Carpenter, S. P. Maran and S. N. Shore, *Astrophys. J. Lett.* **397**, L95 (1992).
390. M. Yoshimori, A. Shiozawa and K. Suga, Photospheric ^{3}He to H abundance ratio derived from gamma-ray line observations, *Proc. 26th Int. Cosmic Ray Conf.*, Salt Lake City, USA (1999), Vol. 6, pp. 5–8.
391. M. Yoshimori, K. Suga, A. Shiozawa, S. Nakayama and H. Takeda, High energy particles of the 1997 November 6 solar event, in *High Energy Solar Physics — Anticipat-*

ing HESSI, ASP Conference Series, Vol. 206, eds. R. Ramaty and N. Mandzhavidze (Astronomical Society of the Pacific, San Francisco, 2000), pp. 393–399.
392. G. P. Zank, W. K. M. Rice and C. C. Wu, *J. Geophys. Res.* **105**, 25,079 (2000).
393. A. G. Zusmanovich and Ya. E. Shvartsman, *Geomagn. Aeronomy* **29**, 353 (1989).
394. J. H. King, *J. Spacecraft and Rockets* **11**, 401 (1974).
395. I. V. Getselev, private communication (2002).
396. L. I. Dorman and E. V. Kolomeets, *Geomagn. Aeronomy* **1**, 1015 (1961).
397. N. J. Martinic *et al.*, Search for solar neutrons using NM-64 equipment, *Proc. 19th Int. Cosmic Ray Conf.*, La Jolla, USA (1985), Vol. 4, pp. 138–141.
398. V. A. Bondarenko *et al.*, *Spectra of Solar Proton Events in Solar Activity Cycles 20 and 22* (World Data Center B-2, Moscow, 1986), p. 46.
399. T. A. Prince *et al.*, The time history of 2.22 MeV line emission in solar flares, in *Proc. 18th Int. Cosmic Ray Conf.*, Bangalore, India (1983), Vol. 4, pp. 79–82.
400. X.-M. Hua and R. E. Lingenfelter, *Astrophys. J.* **319**, 555 (1987).
401. G. Trottet *et al.*, *Astron. Astrophys. Suppl.* **97**, 337 (1993).
402. R. J. Murphy *et al.*, *Astrophys. J.* **490**, 883 (1997).
403. M. Oetliker *et al.*, Charge states of heavy solar energetic particles: Observations with the HILT sensor on SAMPEX, *Proc. 24th Int. Cosmic Ray Conf.*, Rome, Italy (1995), Vol. 4, pp. 470–473.
404. R. A. Leske *et al.*, Isotopic abundances in the solar corona as inferred from ACE measurements of solar energetic particles, in *Proc. Joint SOHO-ACE Workshop 2001*, Switzerland, 6–9 March 2001, AIP Conf. Proc., Vol. 598, ed. R. F. Wimmer-Schweingruber (AIP, New York, 2001), pp. 405–410, in press.
405. G. E. Kocharov *et al.*, Evidence for extended neutron and gamma-ray generation during two solar flares, *Proc. 23rd Int. Cosmic Ray Conf.*, Calgary, Canada (1993), Vol. 3, pp. 107–110.
406. G. E. Kocharov, Cosmic radiation bursts and cosmogenic isotopes, *The 12th Seminar on Cosmophysics in Leningrad* (1982), pp. 203–207.
407. E. V. Vashenyuk and L. I. Miroshnichenko, *Geomagn. Aeronomy* **38**(2), 129 (1998).
408. T. H. Stix, *Waves in Plasmas* (AIP Press, New York, 1992).
409. E. Schatzman, *Space Res.* **3**, 709 (1963).
410. T. Yokoyama and K. Shibata, *Astrophys. J.* **436**, L197 (1994).
411. A. I. Verneta, *Solar Phys.* **170**, 357 (1997).
412. E. R. Priest, *Solar Magnetohydrodynamics*, Geophysics and Astrophysics Monographs, Vol. 21 (D. Reidel Publishing Company, Dordrecht, The Netherlands, 1982).
413. W. T. Vestrand and D. J. Forrest, *Astrophys. J.* **409**, L69 (1993).
414. D. J. Mullan and K. H. Schatten, *Solar Phys.* **63**, 153 (1979).
415. R. Ramaty and N. Mandzhavidze, Theoretical models for high energy solar flare emissions, in *High Energy Solar Phenomena — A New Era of Spacecraft Measurements*, AIP Conference Proceedings, Vol. 294, eds. J. M. Ryan and W. T. Vestrand (AIP, New York, 1994), pp. 26–44.
416. R. Ramaty and N. Mandzhavidze, On the origin of long lasting gamma ray emission from solar flares, in *Proc. of Kofu Symposium*, NRO Report No. 360, Japan, July 1994, (1994), pp. 275–278.
417. E. V. Kolomeets, T. V. Pokudina and E. A. Chebakova, *Izvestiya AN Russia, Ser. Phys.* **57**, 19 (1993).
418. J. Wdowczyk and A. W. Wolfendale, *Nature* **26**, 510 (1977).
419. H. V. Cane, Energetic particles in the solar wind: Propagation, acceleration and modulation, *Proc. 25th Int. Cosmic Ray Conf.*: *Invited, Rapporteur, and*

Highlight Papers, eds. M. S. Potgieter, B. S. Raubenheimer and D. J. van der Walt (World Scientific, Singapore–New Jersey–London–Hong Kong, 1998), Vol. 8, pp. 135–150.
420. O. G. Gladysheva, Y. Iwasaka, G. E. Kocharov and Y. Muraki, Unique possibility to obtain upper limit of total energy induced by solar flare protons, *Proc. 24th Int. Cosmic Ray Conf.*, Rome, Italy (1995), Vol. 4, pp. 1129–1131.
421. R. C. Reedy, Lunar radionuclide records of average solar cosmic ray fluxes over the last ten million years, in *Proc. Conf. Ancient Sun*, eds. R. O. Pepin, J. A. Eddy and R. B. Merril (Pergamon Press, New York, 1980), pp. 365–386.
422. A. N. Peristykh and P. E. Damon, Multiple evidence of intense solar proton events during solar cycle 13, *Proc. 26th Int. Cosmic Ray Conf.*, Salt Lake City, USA (1999), Vol. 6, pp. 264–267.
423. L. I. Dorman and L. I. Miroshnichenko, *Geomagn. Aeronomy* **6**, 215 (1966).
424. L. I. Miroshnichenko, Acceleration parameters and particle spectrum dynamics in solar flares, *Proc. 23rd Int. Cosmic Ray Conf.*, Calgary, Canada (1993), Vol. 3, pp. 25–28.
425. S. B. Gabriel and J. Feynman, *Solar Physics* **165**, 337 (1996).
426. R. C. Reedy, Constraints on solar particle events from comparisons of recent events and million-year averages, *Proc. 16th Int. Workshop on Solar Drivers of the Interplanetary and Terrestrial Disturbances*, New Mexico, USA, 16–20 October 1995, ASP Conference Series, Vol. CS-95, eds. K. S. Balasubramaniam, S. L. Keil and R. N. Smartt (Astronomical Society of the Pacific, 1996), pp. 429–436.
427. I. I. Roussev *et al.*, *Astrophys. J.* **605**, L73 (2004).
428. E. W. Cliver *et al.*, *Astrophys. J.* **260**, 362 (1982).
429. A. I. Podgorny and I. M. Podgorny, *Solar Physics* **139**, 125 (1992).
430. Yu. V. Balabin *et al.*, *Astron. Rep.* **49**, 837 (2005).